Biomedical Engineering Aspects of Infant Thermoregulation and Respiration

A thesis submitted in fulfilment
of the requirements of the degree of
Doctor of Philosophy
in Electrical and Electronic Engineering
from the
University of Canterbury
Christchurch, New Zealand

by

Craig Simon Tuffnell
B.E. (Hons)

December, 1993

RJ
320
.S93
.T914
1993

Abstract

Analysis of infant body temperature, environmental temperature and respiratory behaviour has become an important aspect of Sudden Infant Death Syndrome research. The application of engineering techniques as a means of providing research tools has been found to be beneficial for medical research.

Signal processing techniques have been developed and applied to the analysis of physiological signals that have been collected from infants in the home environment. These techniques allow physiological signals to be analysed and correlated with the use of both time and frequency domain algorithms. Signals of several days duration are manipulated so they may be easily viewed and studied without the loss of significant information. Parameter evaluation of the fundamental frequencies of periodic signals and statistical parameter estimation of random signals have been employed to tease out trends from within the data.

Analysis of physiological signals from sleeping infants has revealed hourly oscillations in their body temperatures that are highly correlated with their breathing rate and breathing rate interquartile range (variability). The oscillations appear to have the highest magnitude when the infant rectal temperatures are near to the mean rectal temperature value. Although some form of relationship between temperature and respiration is evident, insufficient information has been yielded by these signal processing techniques to divulge exactly what the relationship is.

A mathematical model of the human thermoregulatory control system has been developed to investigate the behaviour of temperature regulation in infants. The model has been used to test the hypothesis that infant thermal control is inherently unstable. In this model, heat flow through the body tissues is calculated and the effect of bedding on heat loss is also considered. Automatic temperature regulation is achieved by negative feedback control of the metabolic rate, sweat rate and blood flow distribution in the model. Under physiologically normal conditions, the model shows oscillatory behaviour with a period of approximately one hour. Therefore, the model indicates that the temperature oscillations that have been observed in infants in the home environment, may be a direct result of a marginally stable or unstable thermoregulatory control system. The oscillations occurred when the model was operating just below the thermoneutral point. If the mean infant rectal temperature is assumed to be close to the thermoneutral point, then the model behaviour agrees closely with the data collected from infants.

Evidence gathered from the behaviour of the thermoregulation model and from the signals collected from infants suggests that thermoregulation may be a dominant control system within the body, therefore, temperature may directly influence respiration. A mathematical model of the human infant respiratory control system has been developed to investigate the effect of body temperature on respiratory system behaviour during sleep and to test the hypothesis that the respiratory system is influenced directly by temperature and indirectly by thermoregulation. A multi-compartment model configuration is used to represent

the carbon dioxide and oxygen stores within the body and a controller, sensitive to carbon dioxide and oxygen, adjusts the ventilation rate to complete a negative feedback control loop. Small changes in body temperatures were found to affect the steady state response of the respiratory model while the stability remained relatively unaffected. However, the respiratory model is highly sensitive to small amounts of noise added to blood flows, metabolic rate and arterial gas partial pressures. Therefore, the observed oscillations in infant breathing rate may be a direct effect of thermoregulation while the infant breathing rate interquartile range oscillations are probably induced by another mechanism.

Acknowledgements

Undoubtedly, this thesis would not have come to fruition without the support of numerous people. Firstly, I would like to convey my sincerest thanks to my supervisor, Dr Kathy Garden. Her guidance and encouragement have proved invaluable for my research. I am also deeply grateful to Dr Rodney Ford for providing me with a medical research environment and the financial assistance necessary to complete this thesis. His dedication to cot death research in Canterbury is a model example of how research should be accomplished. I have thoroughly enjoyed the countless hours of professional and personal interaction with both Kathy and Rodney.

Throughout my research I have enjoyed numerous stimulating discussions with many medical and biomedical engineering research colleagues. In particular, I would like to thank Dr Jeff Brown, Richard Dove and Dr Richard Fright, without whom I would not have attained sufficient understanding of many areas of this research. Many thanks also go to Paul Macey for helping to guide my research and coax my thesis into shape and to Brent Price for countless hours of technical assistance.

I would particularly like to convey my sincerest appreciation to Brenda Satherley for support and encouragement and providing much input into the readability of this thesis. I would also like to thank Brenda and other close friends for the wonderful adventures ("team trips") we have had.

I gratefully acknowledge the financial support of Cardinal Community Laboratories and travelling assistance from the Cot Death Division of the National Childrens Health Research Foundation, the Canterbury Cot Death Society and the Canterbury Branch of the Royal Society of New Zealand.

Last, but by no means least, I wish to thank my parents for the opportunity, support and encouragement to complete this thesis.

Preface

The research presented in this thesis is concerned with the development and application of engineering techniques to another discipline, namely medical research. The particular medical field of interest is the investigation of Sudden Infant Death Syndrome (SIDS or Cot Death).

During 1985, Dr Rodney Ford, a community paediatrician, became interested in SIDS research in Canterbury. Dr Ford recognised the need for the application of engineering techniques to help study infant physiology and clinical aspects of SIDS. Thus, Dr Ford, the late Professor R. H. T. Bates, Dr Richard Fright and my supervisor, Dr Kathy Garden, began a collaborative research effort between the Christchurch hospital and the Department of Electrical and Electronic Engineering at the University of Canterbury. To assist in the study of infant physiology, a masters project was undertaken in 1987, by Mr Richard Dove, with the aim of constructing a system to collect and store infant physiological signals using a personal computer. The system has become known as *BabyLog* [Dove, 1988]. It was as a continuation of this project that the heart of my research has evolved.

I was introduced to biomedical research late in 1989 when I began a three month summer studentship at Christchurch hospital, supported by the South Australian SIDS Association. During this time I continued the development of the software for *BabyLog*. Following this I began my postgraduate studies at the University of Canterbury, concentrating on signal processing of respiratory and temperature signals collected from infants with *BabyLog*. This soon lead to mathematical modelling of the thermoregulatory and respiratory control systems of infants in an attempt to explain the behaviour observed from studies of infants using *BabyLog*. The general research area has been coined *thermo-respiratory* research. The research group now includes a number of engineering students in addition to medical and technical staff.

The following paragraphs outline the structure of this thesis and identify original aspects of my research. An important part of some areas of this research has been the collaboration with other researchers. Collaborative efforts have been made clear where appropriate. Conclusions are drawn in relevant sections of some chapters in order to give the motivation for chapters which follow.

Chapter 1 provides the motivation and introduction to thermo-respiratory research. The problem of SIDS is introduced and briefly reviewed. The relevance of infant thermo-respiratory research to SIDS is highlighted. The physiology of the human thermoregulatory and respiratory control systems is reviewed. No original material is presented in this chapter.

Chapter 2 introduces two complementary methods of investigating physiological control systems; signal processing and mathematical modelling. The necessary background to the development of signal processing, system modelling and simulation is provided as a basis for the work presented in the following chapters. Emphasis has been placed on frequency domain transforms since the frequency components of the signals and systems discussed in the following chapters are of great interest. The two research approaches are tied together both mathematically and as subsequent steps of an iterative research scheme. Once again, no original work is presented.

The physiological signal collection, analysis procedures and results of the analysis of infant temperature and respiratory signals are presented in Chapter 3. The polygraph system (*BabyLog*) is discussed since physiological signals collected on this system form the focus of this research. *BabyLog* has been developed through a collaborative effort where my input has been as part of a team of people developing the signal collection software. The statistical analysis of respiratory waveforms is also presented. I have derived equivalent frequency domain characteristics of the statistical estimates in order to show their validity and so that they may be optimally calculated. Finally, the quantitative analysis of temperature and respiratory signals is discussed and results of the analyses are presented. The results show interesting and previously unreported behaviour along with typical behaviour that has been reported by other researchers. My discussions on the thermo-respiratory behaviour result from my engineering experience and reflect the similarity of the systems with which the engineer deals and physiological control systems. The work contained in this chapter is the first formal mathematical analysis of the relationships between infant temperature and respiration recorded in the home environment. Many co-workers have been involved with the collection and study of the physiological signals, however, both the development and application of the analysis techniques are entirely my own work.

Chapter 4 describes a mathematical model of infant thermoregulation which I have developed to investigate the temperature behaviour of infants. The model is based on adult models proposed by other researchers. However, I have modified their models in order to account for the considerably different thermoregulation characteristics of infants and the insulating properties of the bed clothes. The numerical values for the parameters of the model are also included.

The behaviour of the infant thermoregulation model is presented in Chapter 5. The steady state response and stability of the model are illustrated graphically for a range of environmental temperatures and insulation thicknesses. Comparison is made between the model characteristics and the temperature and respiratory behaviour observed in infants (Chapter 3). The striking similarity validates the model and gives evidence towards the cause of the temperature and respiratory oscillations which have been observed in infants.

Chapter 6 describes a mathematical model of infant respiration. The model is based on models proposed by other researchers. I have developed the model to include temperature sensitive parameters so that the effect of temperature and thermoregulation on infant respiration may be investigated. I have placed considerable emphasis on reducing inaccurate aspects which are inherent in other respiratory models. In particular, I have included precise mathematical descriptions of the temperature sensitive carbon dioxide and oxygen dissociation curves. Numerical values for the parameters of the respiratory models are also presented.

It is in Chapter 7 that the behaviour of the infant respiratory model is presented. The steady state and dynamic response of the model are shown for a range of temperatures and thermoregulation states. The temperature sensitivity of the model yields a possible explanation to the observed relationship between infant rectal temperature oscillations and oscillations in breathing rate, however, breathing rate interquartile range oscillations are not satisfactorily explained.

Chapter 8 presents conclusions regarding the original medical and biomedical engineering research content of this thesis. The applicability of signal processing and mathematical modelling techniques to cot death research is discussed. Suggestions on aspects of future research are also included.

The following publications and presentations have been prepared during the course of my PhD research:

Tuffnell C, Dove R, Brown J, Ford R. Collection and analysis of physiological signals from infants in the home. *Proceedings of the 14th Annual International Conference of the IEEE Engineering in Medicine and Biology Society*, 1992.

Tuffnell C, Garden K, Ford R. The influence of body temperature on a model of the human respiratory system. *Proceedings of the 14th Annual International Conference of the IEEE Engineering in Medicine and Biology Society*, 1992.

Brown J, Dove R, Tuffnell C, Ford R. Oscillations of body temperature at night. *Archives of Disease in Childhood*, 67: 1255-1258, 1992.

Ford R, Brown J, Dove R, Tuffnell C, Macey P. HomeLog: long term recording of infant temperature, respiratory, and cardiac signals in the home environment. *Journal of Paediatrics and Child Health*, 28 Supplement 1: S26-S32, 1992.

Tuffnell C, Dove R, Ford R, Brown J, Fright R. SIDS studies using a polygraphic assessment system. *New Zealand Branch Meeting of the Australasian College of Physical Scientists and Engineers in Medicine*, Christchurch, November 1990.

Dove R, Brown J, Fright R, Tuffnell C, Ford R. Computer polygraphic system for infants at risk for sudden infant death syndrome. *Australasian Physical & Engineering Sciences in Medicine*, 13(4): 188-191, 1990.

Dove R, Fright R, Ford R, Tuffnell C, Brown J. Polygraphic assessment system for infants at risk from SIDS. *Proceedings of the 12th Annual International Conference of the IEEE Engineering in Medicine and Biology Society*, 12(5): 2031-32, 1990.

Work in Preparation:

Tuffnell C, Brown J, Ford R. The relationship between rectal temperature and thermoregulation stability.

Tuffnell C, Garden K, Ford R. Respiratory system modelling: The effect of temperature on model behaviour.

Contents

Glossary

Unless otherwise stated, the abbreviations and symbols used in this thesis have the following definitions:

Abbreviations

ALTE	apparent life threatening event
BPM	breaths per minute
BR	breathing rate
CNS	central nervous system
CO_2	carbon dioxide
DFT	discrete Fourier transform
ECG	electrocardiogram
EEG	electroencephalogram
FFT	fast Fourier transform
FRC	functional residual capacity of the lung
IQBR	breathing rate interquartile range
IQR	interquartile range
MBR	median breathing rate
MRR	metabolic rate ratio
O_2	oxygen
PDF	probability density function
REM	rapid eye movement (sleep state)
SIDS	sudden infant death syndrome (cot death)

Terminology

apnoea	temporary cessation of breathing
afferent	towards a centre (the brain)
efferent	away from a centre (the brain)
multifactorial etiology	multiple causal factors for a disease
thermo-respiratory	combined study of thermoregulation and respiration
thermoneutral	optimal temperature environment
in vitro	within a test tube or artificial environment
in vivo	within the living body

Thermoregulation Symbols

r	radius	m
l	length	m
A	area	m^2
K	specific thermal conductivity	$W \cdot cm/m^2/°C$
α	counter current heat exchange	N.A.
ρ	density of blood	Kg/l
C	specific thermal capacity	W/°C/Kg
T	temperature	°C
I	total effective insulation thickness	mm
Q, $\dot{Q}$	blood volume, blood flow	ml, ml/min
R	resistance to heat flow	°C/W
E	Evaporation rate	$g/hr/m^2$
m	mass	Kg
ϕ	heat	W
L	latent heat of vaporisation	$W/m^2/g$
MRR	metabolic rate ratio	N.A.
G	gain	N.A.

Subscripts

i, j, k	compartments i, j, k
Cond	conduction between coaxial compartments
Bl	blood
DHT	dry heat transfer
MR	metabolic rate
Evap	evaporative
Resp	respiratory
S, $\bar{S}$	skin, skin area weighted average
Env	environmental
Set	set point
HC	head core compartment
HS	head skin compartment
TS	trunk skin compartment
TM	trunk muscle compartment
TC	trunk core compartment
CB	central blood compartment
t	tissue compartment
I	insulation
Ins	insensible
Sw	sweat

Respiration Symbols

P	partial pressure	mmHg
P_{50}	P_{O2} at which haemoglobin is half saturated	mmHg
C	content of gas	ml/100ml
V, $\dot{V}$	gas volume, minute ventilation rate	l, l/min
MR	metabolic rate (oxygen consumption)	ml/min
S	saturation	%
T	temperature	°C
m	mass	Kg
t	time	s
τ	circulation delay	s
RQ	respiratory quotient	N.A.
Q, $\dot{Q}$	blood volume, blood flow	ml, ml/min
Hb	haemoglobin	ml/100ml
Hct	Haematocrit	%

Secondary letters

r	lung functional residual capacity
a	arterial
A	alveoli
I	inspired
B	barometric
v, $\bar{v}$	venous, mixed venous
E	respiratory end (at the mouth)
D	respiratory dead space

Subscripts

i	compartment i
b	brain compartment
o	other compartment
CO_2	carbon dioxide
O_2	oxygen
c	cardiac
$Virt$	virtual
C	central (within the brain compartment)
P	peripheral (within the arterial blood)
Thn	thermoneutral (37°C)
Bl	blood

Chapter 1

Infant Thermo-respiratory Research

Of all things in life, there should be nothing so preventable,
as there is nothing on the face of it so unnatural,
as the death of a little child.

Charles Dickens

Throughout history, a common goal of humans has been to strive to improve the quality and duration of our lives by manipulating our environment to suit our needs. This not only includes making the most of our physical world, but improving the care of the unhealthy. In order to progress in this direction, we must first begin to understand the processes which we are attempting to manipulate. The science of understanding the functioning of these processes in living organisms is known as physiology. Physicians, engineers and other scientists have enhanced our knowledge of human physiology for many thousands of years. However, for every question they answer, there are a multitude of questions generated, of which the answers to many prove to be elusive. One example of such a problem, to which much attention has been focused in recent years, is the study of Sudden Infant Death Syndrome (SIDS), more commonly known as Cot Death. SIDS is the sudden and unexpected death of an infant that appeared to be perfectly healthy. Evidence from clinical studies indicates that SIDS is somehow related to temperature and possibly the cardiorespiratory system. Therefore, the study and clinical investigation of infant thermoregulatory and respiratory (thermo-respiratory) physiology has become an avenue of great interest for SIDS research.

This thesis investigates the behaviour of infant thermoregulation and how it influences respiration. This chapter deals with the clinical background to this research. Section 1.1 gives a brief overview of SIDS including current research issues, highlighting the importance of thermo-respiratory investigations. The effect of temperature and thermal control as an underlying factor in many aspects of physiological behaviour, and in particular for SIDS, is introduced in section 1.2. Respiratory control is discussed in section 1.3, including the important consequences of temperature on respiration.

Chapter 2 provides the necessary background for the signal processing and mathematical modelling aspects of infant thermo-respiratory research presented in chapters 3 through 8. A system for physiological signal collection and analysis and the results of a clinical investigation of infant temperature and respiration using this system are presented in Chapter 3. A mathematical model of infant thermoregulation is developed and simulated in Chapters 4 and 5 respectively. The thermoregulation model has been designed to provide a possible explanation for the infant body temperature behaviour observed in the clinical experiment presented in Chapter 3. Similarly, a model of infant respiration, which is sensitive to temperature, is developed and simulated in chapters 6 and 7 respectively in order to investigate the infant respiratory behaviour presented in Chapter 3. Conclusions and suggestions for further research are presented in Chapter 8.

1.1 Sudden Infant Death Syndrome

SIDS is probably one of the most devastating events that can happen to the parents of an infant. Consider the response of the parents of an infant when they discover to their horror that their young infant, who appeared perfectly healthy when put to bed, has died in its sleep. The first response is to blame themselves as no alternative reason for the death can be established, even after a thorough postmortem examination. This is not a rare scenario, but is in fact common throughout the western world.

The infant mortality rate attributable to SIDS varies considerably between countries, ranging from approximately 0.5 to 5 for every 1000 live births [Engleberts, 1991, p3]. The SIDS mortality rate is relatively small in comparison to the number of live births. However, SIDS remains the single most common cause of death of infants between one week and one year of age in the western world. The incidence of SIDS in New Zealand since 1970 has remained at approximately 4 deaths per 1000 live births [Ford et al., 1991]. In Canterbury the cot death rate has exceeded 6 per 1000 live births [Ford et al., 1991]. Thus, in New Zealand and in particular Canterbury, the mortality rate due to SIDS remains one of the highest in the world. For this reason, much attention has been centred on SIDS research in New Zealand and other western countries.

Although SIDS has probably occurred throughout history, it was not until relatively recently that significant media and research attention focused on SIDS. This probably reflects the previously high mortality rates of infants resulting from infectious diseases and malnutrition that we are now able to prevent, and until recently overshadowed mortality due to SIDS.

Numerous clinical studies have been carried out over the past two decades and have provided us with many clues to causes of the problem [Hunt & Brouillette, 1987]. No single risk factor is universally present and most researchers agree that there is no single cause of SIDS. It is assumed that many factors simultaneously come together in a particular baby to cause death. This is known as *multifactorial etiology* and is highlighted by the considerable number and variety of risk factors for SIDS. Recent epidemiological studies have isolated numerous risk factors, however, the underlying mechanisms that cause SIDS have proved to be elusive.

1.1.1 Diagnosis of SIDS

There are two key characteristics which assist in the diagnosis of SIDS victims [Engleberts, 1991, p3]. Firstly, SIDS normally occurs while the infant is unattended and assumed to be asleep. Secondly, it is very rare for SIDS to occur during the first week of life, or after one year, and the peak incidence occurs around the second and third months of life. A recent definition for SIDS is as follows [Zylke, 1989]:

> The sudden death of an infant under one year of age which remains unexplained after a complete postmortem examination, including an investigation of the death scene and a review of case history. Cases failing to meet this definition, including those without postmortem examinations, should not be diagnosed as SIDS.

Unexplained infant deaths failing to meet all the criteria of this definition may be referred to as cot death. However, for many practical purposes, SIDS and cot death can be considered as the same. From the above definition, SIDS is diagnosed through a process of elimination. Once all plausible causes of death have been completely discounted, and if the infant is of the appropriate age, the death is labelled as SIDS. This is a somewhat less than ideal definition but is the only tenable one given the current level of knowledge about SIDS. It is worth noting that SIDS may include subgroups of deaths from differing causes and the above definition does take this heterogeneity of SIDS into account. The large majority of SIDS cases are not caused by mechanical suffocation, however, this forms one possible subgroup of SIDS. During death scene investigations, suffocation must be considered and if possible eliminated as a cause of death.

Although there is no discernable evidence for a cause of death, SIDS has been recognised as a disease in its own right by the majority of paediatricians and researchers from throughout the world. In 1979 the World Health Organisation created a category in the International Classifications of Diseases: ICD 798.0, Cot Death or SIDS.

1.1.2 Epidemiological risk factors

Much of the research into SIDS has involved epidemiological studies designed to identify risk factors. Infants who have any of these risk factors are at increased risk for SIDS and it has been suggested that careful physiological monitoring of these infants should occur. However, this remains controversial as there is no evidence that SIDS rates have been reduced as a result of monitoring [Hunt & Brouillette, 1987]. Numerous epidemiological studies from throughout the world have repeatedly identified a large number of SIDS risk factors. Studies have shown that maternal smoking, bed sharing, not breast feeding and young mothers are all risk factors [Mitchell et al., 1992b]. Prone sleeping has recently been identified as a major risk factor in New Zealand [Mitchell et al., 1992a]. Low socioeconomic conditions have been identified as a risk factor [Mitchell et al., 1992b; Borman et al., 1988], but they may be related to other factors such as ethnicity, siblings of SIDS and maternal drug use. Male infants, low birth weight and premature infants are also at a higher risk [Borman et al., 1988]. The significance of temperature on SIDS is highlighted by the increased risk in winter months and in cooler regions of temperate countries [Borman et al., 1988]. Also, overheating has been identified in some cases of SIDS in Australia [Ponsonby et al., 1992].

1.1.3 Clinical research

Many hypotheses have been proposed to clinically account for the epidemiological risk factors for SIDS. However, it has proven difficult for researchers to contrive useful clinical experiments which are ethically acceptable. Much of the research is limited to polygraphic sleep studies of physiological variables that are able to be measured relatively non-invasively.

Postmortem examination reveals no pathological evidence for death in SIDS, indicating some form of functional failure. A review of SIDS research [Hunt & Brouillette, 1987] has highlighted the following points regarding functional failure. The hypothesis that SIDS is related to respiratory control appears to carry the most credence. However, short apnoea episodes (the temporary cessation of breathing) are no longer considered an important respiratory factor. Studies of respiratory control have revealed the following abnormalities in infants who have been considered at risk for SIDS: prolonged sleep apnoea, increased frequency of brief inspiratory pauses, excessive periodic breathing, diminished ventilatory sensitivity to *hypercapnia* (excess blood carbon dioxide levels) or *hypoxia* (low blood oxygen levels) and impaired arousal response to hypercapnia and hypoxia. Brain-stem abnormalities, which may influence respiratory control, have also been found in some SIDS victims.

Investigations have revealed that environmental temperature is highly correlated with SIDS [Ponsonby et al., 1992]. The development of thermoregulation in infants with regards to SIDS is also of interest to researchers [Flemming et al., 1992]. It is not known what this relationship is or if there is even a direct influence of temperature on SIDS. Respiration and temperature are both highly significant for SIDS, but this is hardly surprising when the importance of temperature and respiratory control for sustaining human life is considered.

1.2 Temperature: The Common Denominator

The common thread, woven through every aspect of this thesis, is the significance of temperature. When the influence of temperature is taken to the extreme, we can see that every process in our physical universe is dependent on temperature. Without a doubt, every physical action or chemical reaction that occurs either consumes or liberates energy, some of which is normally in the form of heat. Therefore, temperature is critical in all biological processes and it significantly influences many of the processes within the human body. It comes as no surprise that the incidence of SIDS is also correlated with environmental temperature and much research into SIDS revolves around attempting to deduce the role of temperature. Mathematical expressions that describe many of the ways in which temperature affects metabolic and circulatory processes in the human body are explored in Chapter 4 as part of a mathematical model of human infant thermoregulation.

The influence of temperature on biological processes is highlighted by the surprisingly narrow thermal tolerance of the core body temperatures of humans and many other living organisms. The normal core body temperature for humans is approximately 37°C and generally varies between individuals [Hensel, 1981, Chapter 14; Jessen, 1990, p3]. If the core body temperature increases by more than a few degrees Celsius then irreversible denaturing of protein begins to occur within the body. Conversely, if the body core is cooled then body processes begin to slow. Either of these situations can be fatal. It has become quite clear that the human core body temperatures must be maintained at a relatively constant temperature, for a wide range of environmental conditions, in order to sustain life.

1.2.1 Thermoregulation

The maintenance of a constant core body temperature under changing environmental conditions, known as *homeothermy*, is achieved in humans through two mechanisms, *behavioural* and *autonomic thermoregulation*. Behavioural thermoregulation is the conscious adjustment of the thermal environment in order to maintain comfort. This is achieved by altering the level of body insulation (clothing) or the environmental temperature. Autonomic thermoregulation is the process by which mechanisms within the body subconsciously and precisely control internal body temperatures through the autonomic nervous system. Autonomic thermoregulation occurs at all times, even during sleep when behavioural control does not generally occur. A third mechanism, which may be considered as part of behavioural thermoregulation, is technical thermoregulation. This is the use of a system for maintaining a constant environmental temperature. An example of this is air conditioning or central heating which monitor the temperature of a room and adjust the heat flow into the room to maintain a constant temperature. Figure 1.1 shows the features of human thermoregulation.

Autonomic, behavioural and technical thermoregulation are all negative feedback control systems (see section 2.2.5). The temperature is measured or sensed and if the temperature deviates from normal, an error signal, the magnitude of which is directly related to the temperature deviation, is generated. The regulator then adjusts heat production or heat loss to minimise the error, thus maintaining a constant temperature.

Disturbances to body temperatures have two main sources, internal heat generation and environmental heating or cooling. All organs produce metabolic heat due to exothermic chemical reactions even when the body is resting. Heat produced in the muscles during exercise can be many times greater than that produced while at rest. Heat is lost to the environment from the skin when the skin surface temperature is higher than the environmental temperature, otherwise heat is absorbed by the skin. For core body temperatures to be constant, the heat produced within the body must equal the heat lost to the environment. This is known as heat balance or equilibrium heat flow.

An intricate mechanism regulates the production and loss of heat required to achieve homeothermy in humans [Hensel, 1981; Jessen, 1990]. Thermo-receptors in the skin, head core and possibly in other areas of the body sense the temperature and rapidly transfer the information to the central nervous system through afferent pathways. The hypothalamus then integrates the thermal drives and regulates body temperatures by adjustment of several of the processes that occur in the body. When the core of the body is cool, additional heat production is achieved through increasing muscle activity (shivering or non shivering thermogenesis). The circulatory system transports heat around the body and tends to equalise temperatures within the central core. It also assists the flow of heat to the skin surface where it is lost to the environment. There is also a

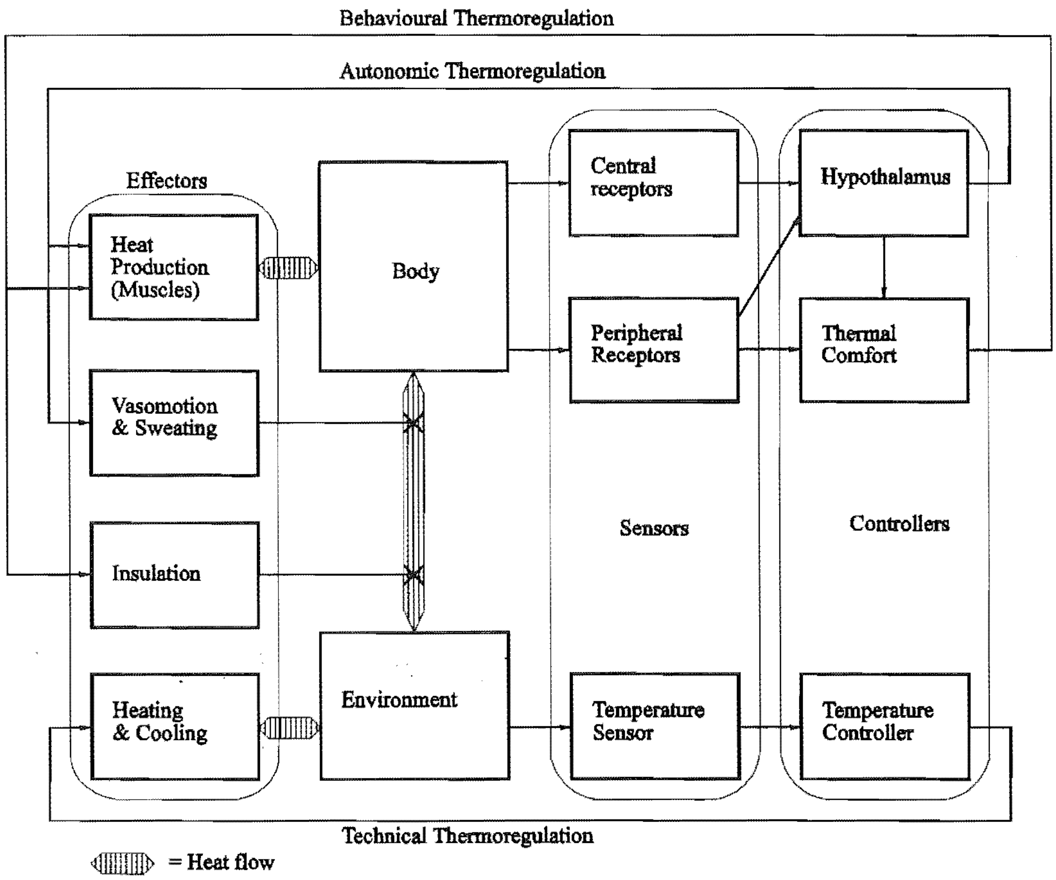

Figure 1.1 Schematic diagram of technical, behavioural and autonomic thermoregulation in humans. All three are negative feedback control systems and each system comprises sensors, a controller and effectors.

considerable increase in cardiac output associated with the rapid blood flow through dilated cutaneous vessels. If the body is hot, the peripheral circulation increases (vasomotor activity), thus raising skin temperatures and increasing the rate at which heat is lost to the environment. Sweat production (sudomotor activity) also helps cool the body through vaporisation of water on the skin surface. This process consumes energy known as the latent heat of vaporisation. Human adults can produce up to 23 litres of sweat per hour for short periods of time [Jessen, 1990, p3]. However, for effective heat loss, the sweat must evaporate. This is not possible in humid conditions for high sweat rates. Air movement assists both evaporative and convective heat loss from the body.

Thermal control is achieved by integration of the central and average skin temperatures. Control responses are elicited when skin and core temperatures deviate from threshold temperatures (set points). For adult humans, the skin temperature threshold is approximately 2-3°C lower than the core temperature set point [Jessen, 1990, Chapter 7]. Temperatures below the set points induce a cold defence response while temperatures above the thresholds induce a hot defence response. There is much debate concerning the integration of the central and peripheral thermal drives. Many researchers believe they are multiplicative while others believe they are additive [Jessen, 1990, p155-157]. Regardless of the exact nature of thermal drive integration, the mid range response can be explained by either mathematical operator [Jessen, 1990, p155]. This is further examined in section 5.2.

Thermoregulation processes allow the core of the body to be maintained at a constant temperature. However, the peripheral temperatures depend on the particular state of the body and the environmental conditions. Figure 1.2 illustrates two possible temperature distributions for the body. Under conditions where no hot or cold defence response is elicited and equilibrium heat flow occurs, the body is considered to be in an ideal thermal environment. The body is said to be at the *thermoneutral point*. The effective volume of the body core which has a temperature close to 37°C is larger in a warmer environment. Note also that in both hot and cold conditions, the temperature of the head and trunk core are maintained relatively constant, while the temperatures of the extremities change dramatically.

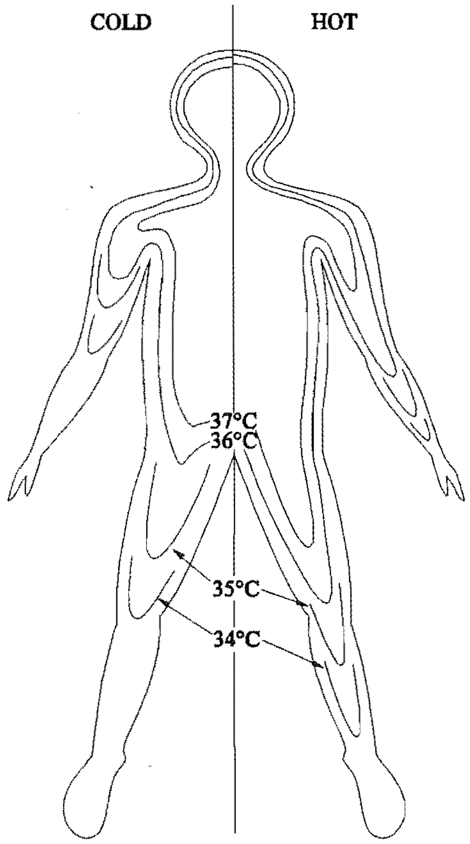

Figure 1.2 Isothermal lines within the body for two temperature extremes. The left and right halves of the figure indicate cold and hot environments respectively.

1.2.2 Infant thermoregulation

The human neonate, with the exception of during the first few hours of life, maintains approximately the same average core body temperature as that found in adults [Brück, 1961]. The infant has principally the same thermal control system as adults but with a different sensitivity of the control system to account for the effect of the physical size difference.

Unquestionably, the neonate and infant have a large body surface area to volume ratio in comparison to the adult and decreased body shell insulation [Hensel, 1981, p241]. The full term neonate has a surface area to volume ratio that is approximately 2.7 times that of the adult. Therefore, for a given mass, the infant loses considerably more heat to the environment. Heat production per body mass required for equilibrium heat flow in the infant would need to be nearly five times that of the adult [Hensel, 1981, p242]. However the metabolic rate per unit body mass is only 1.5 to 2 times greater than that of the adult [Hill & Rahimtulla, 1965]. In cool environments, the remaining heat flow is generated through increased muscle activity and non-shivering thermogenesis. Consequently, it is possible for the infant thermal control system to be producing additional heat while that of the adult, under the same environmental conditions, is attempting to increase heat loss.

To maintain constant core body temperatures in a cool environment, similar to that of an adult in the same environment, the core temperatures of the infant would be expected to deviate from normal by a larger extent than in the adult. This would produce a larger load error signal which is necessary to produce the extra heat per unit body mass required for equilibrium heat flow in the infant. This, however, is not the case. The small load error is accounted for by the fact that the cold defence and heat loss mechanisms in the infant are elicited at a higher mean skin temperature (≈36°C) compared to the adult (≈34°C) [Ryser & Jéquier, 1972; Brück, 1961]. Also, the increment in metabolism in relation to average skin temperatures is approximately six times that of the adult [Brück, 1961]. Non-shivering thermogenesis of the brown adipose tissue plays an important role as a source of cold-induced heat production, particularly in human neonates [Jessen, 1990, Chapter 14].

1.3 Respiration

Respiration is the exchange of oxygen and carbon dioxide between the atmosphere and the body cells. In humans, this process includes inspiration and expiration, diffusion of oxygen from alveoli to the blood and of carbon dioxide from the blood to the alveoli, and the transport of oxygen to and carbon dioxide from the body cells by means of the circulatory system. Respiration is fundamental to life as it supplies fuel (including oxygen) and removes waste products (including carbon dioxide) from the cells. The body has relatively little capacity for storage of the respiratory gases so the respiratory control system must attempt to supply oxygen and remove carbon dioxide at the rate at which the cells require. This section deals with the basic principles involved in respiratory control, infant respiration and the impact that changing body temperatures and thermal control have on respiratory control. A mathematical model which includes mathematical expressions for the respiratory functions outlined in this section is described in Chapter 7. A novel aspect of this model is the inclusion of mathematical expressions which describe the effect of temperature on respiratory processes.

1.3.1 Respiratory control

Similar in concept to thermoregulation, respiratory control is a negative feedback control system [Talbot & Gessner, 1973, Chapter 18]. Figure 1.3 illustrates the basic principles of the respiratory control system. Oxygen in the air is brought to, and carbon dioxide is removed from the body cells through the lungs and the circulatory system. The higher the ventilation rate of the lungs, the greater the quantity of gas that is pumped into and out of the circulating blood.

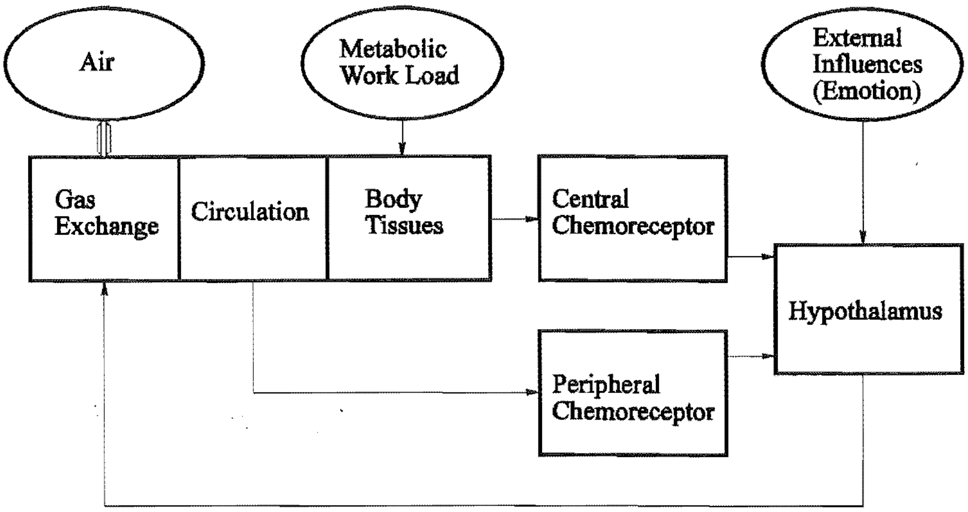

Figure 1.3 Schematic diagram of the human respiratory control system.

The body cells alter the gas partial pressures in the blood as they consume oxygen and produce carbon dioxide at a rate proportional to the cellular metabolic rate. This is dependent on factors such as exercise or heat production requirements of the body. Chemoreceptor structures provide information on the oxygen and carbon dioxide partial pressures in the blood and the carbon dioxide gas partial pressure in the cerebrospinal fluid (CSF) of the brain. This information is conveyed by afferent neural pathways to the respiratory control centre in the hypothalamus of the brain, which adjusts the ventilation of the lungs to maintain gas partial pressures at normal values.

To a limited extent respiratory gases are stored in the body. This provides a buffer to sudden disturbances to the gas partial pressures in the body which may occur, for example, as a result of rapid changes in the levels of exercise. Carbon dioxide is primarily stored in the body tissues and only a small quantity is stored in solution in the blood [Farhi & Rahn, 1960]. Conversely, little oxygen is stored in the body tissues but significant quantities are stored in chemical combination with haemoglobin in the blood.

Although respiratory control forms a complete system, it cannot be considered independent of other systems within the body. One system that has a major bearing on respiration is the cardiovascular system. Should the metabolic rate of a particular organ increase then, in order to facilitate the additional demands placed on the transport of metabolites to and from that organ, an increase in blood flow to that organ must also occur. This change in blood flow alters the dynamics of the respiratory system.

1.3.2 Infant respiration

Respiratory control in the human infant is fundamentally the same as in the adult. However, certain system parameters have a significantly different value in the infant compared with the adult.

There are three system parameters which are significantly different in the infant. Firstly, because of the small size of the infant, the tissue carbon dioxide and blood oxygen storage capacities are significantly reduced, thus reducing the disturbance buffering capability of the system. This is countered for by the smaller total metabolism of the infant, placing less demand on the respiratory system. However, because the basal metabolism per unit mass is larger in the infant compared to the adult [Hill & Rahimtulla, 1965], a loss of buffering remains. Secondly, the oxygen carrying capacity of the blood changes dramatically over the first few months of life [Delivoria-Papadopoulos et al., 1971]. The infant begins life with blood that has increased affinity for oxygen. It is not until the fourth to sixth months, after considerable changes to the blood, that the oxygen affinity of infant blood is similar to that of the adult. Finally, the system controller characteristics alter as the infant matures because the peripheral chemoresponse has been found to be minimally functional for several weeks after birth [Wilkie et al., 1987].

1.3.3 The effects of temperature on respiration

The involvement of temperature in processes that occur within the human body has already been alluded to and the respiratory system is no exception. Temperature may affect the respiratory system either directly or indirectly through the thermoregulatory system.

Even when core body temperatures are maintained at normal values, the consequences of thermoregulation during temperature extremes alter the behaviour of human respiration. Thermoregulation alters the metabolism and blood flow distribution within the body. These changes considerably alter the characteristics and behaviour of the respiratory control system. Both the steady state and the response of the system to a sudden disturbance may be altered by temperature variations.

Altering the temperatures within the body has a direct bearing on respiration. The oxygen storage capacity of the blood and the carbon dioxide storage capacity of the tissues change with temperature [West & Wagner, 1977, Chapter 5]. The central nervous system and the chemoreceptors are also directly affected by temperature [Kiley et al., 1985; Paintal, 1971].

1.4 Summary

SIDS is the most common cause of death of infants aged between one week and one year in the western world. Some form of functional failure appears to be an important causal factor. In particular, SIDS has been shown to be related to respiratory control and temperature. This thesis investigates aspects of infant respiration and thermoregulation through signal processing and mathematical modelling techniques. The aim is to contribute to human respiration and thermoregulation knowledge and therefore assist in aspects of SIDS research.

Chapter 2

Physiological Signal Processing and System Modelling: Complementary Methodologies

The human body can be considered to comprise a large number of highly coupled systems. These systems perform the precise control of a number of specialised tasks necessary for our survival. The form and function of these systems can usefully be thought of as conceptually and mathematically similar to systems with which engineers deal. The similarity is such that control theory is often used to explain physiological problems to students of the medical profession. Consequently, it comes as no surprise that engineering techniques can be applied to the investigation of physiological systems.

This chapter gives an overview of the complementary biomedical engineering techniques of signal processing and system modelling which are used in the investigation of infant thermo-respiratory behaviour. Background to the techniques employed in the research which is presented in the following chapters is discussed. Section 2.1 is an overview of the application of signal processing to physiological signals. Methods by which feedback control systems within the body may be modelled and analysed are introduced in section 2.2. A summary is included in section 2.3.

2.1 Physiological Signal Processing

A polygraph is a system which graphically displays electrical signals. Although the polygraph is often associated with the somewhat controversial field of lie detection, this is only one of its numerous applications. Polygraphs are commonly used for recording and displaying physiological signals in areas of clinical research, diagnosis and critical care monitoring. Modern medical polygraph systems often employ digital computers to record, analyse and process the signals. The polygraph is the basis by which many physiological experiments have been developed.

The number and nature of polygraphic experiments that can be performed on humans, particularly infants, is limited by ethical issues. Therefore, to increase our understanding of human physiological systems, one has to gather as much information as possible from non-invasive experimentation and perform a detailed analysis of the resulting data. To achieve the best possible results from physiological signal analysis techniques, it is necessary to obtain signals with a minimum of noise. Any noise introduced into the signal may be impossible to remove by analysis procedures and may cloud the useful information contained in the signal. Considering this, it is necessary to tailor the polygraphic recording equipment, clinical instrumentation and experimental procedures to the requirements of the analysis procedures. For example, experiments performed in the infant's home, with non-invasive instrumentation, will allow normal behaviour of the subject in a comfortable environment, thus minimising the artifact noise input into the collected data.

The information gathered from just one physiological signal carries significant information about the physiological behaviour of many of the systems within the body. This is a result of the dynamic interaction (or coupling) that occurs between each of the systems within the body. An example of this is respiratory sinus arrythmia where the heart rate is modulated by the respiratory rate. Analysing this type of information is no simple task, particularly when there are large amounts of data involved. However, signal processing techniques allow trends or behaviour that is beyond the reach of our senses to be quickly enhanced and analysed. The analysis of many long duration physiological signals may yield considerable information that would otherwise be impractical to obtain by simple observations of the signals. Comparison of two or more signals and quantification of the behaviour or trends of signals is also achievable through signal processing. The techniques available for analysis of physiological signals are wide and varied and are invaluable for clinical research.

This section provides the background to the implementation of signal processing techniques for interpretation of infant physiological signals. The practical application of signal processing of infant respiratory and temperature behaviour is discussed in Chapter 3.

2.1.1 Signals

There are a large number of signal sources which provide information on the behaviour of a physical process. This information can be converted by a transducer from its original form (e.g. temperature, pressure etc.) into a convenient quantity (such as electrical potential or current) which is known as a signal. Thus, the behaviour of the signal represents some aspect of the behaviour of the original physical process. The signal transfers the information from the source to instrumentation or analysis systems.

The signal is commonly a function of time, as is the case with the signals discussed in this thesis. Thus, time is the independent variable. However, many other independent variables for signals are possible. For example, the measure of the deflection of a loaded steel beam along its length has distance as the independent variable. A signal is said to be continuous if the independent variable takes on all values. When the independent variable is only known for a sub-set of all possible values, comprising of separated samples, the signal is said to be discrete. Also, for many practical analysis purposes, the signal is often of finite length.

Signals may be classified as *deterministic* or *random*. Deterministic signals may be periodic or contain transients. Regardless of signal content, deterministic signals are always predictable at any future time if the history of the signal is known. On the other hand, random signals are unpredictable and only the probability of the signal having a certain value at any point in the future can be found from the history of the signal. The approaches taken to analyse deterministic and random signals are quite different (see section 3.2).

2.1.1.1 The Fourier transform

Any signal, including physiological signals, can be considered to be the sum of many sinusoidal signals, each with a different frequency, phase and amplitude. A representation of a signal in terms of frequency and phase is known as a spectrum. The *Fourier transform* constitutes the formal connection between a signal (normally in the time domain) and its spectrum (frequency domain). Frequency domain representation of a signal may illuminate aspects of the signal structure that are not obvious in the time domain and, in some cases, it may simplify analysis algorithms.

Consider a complex, non-periodic function of one variable, $g(t)$. The one-dimensional continuous Fourier transform, $G(f)$, of $g(t)$ [Bracewell, 1978, p7] is defined by

$$G(f) = \int_{-\infty}^{\infty} g(t) e^{-j2\pi ft} dt, \tag{2.1}$$

where j is the imaginary operator such that $j = \sqrt{-1}$. The inverse Fourier transform is defined as

$$g(t) = \int_{-\infty}^{\infty} G(f) e^{j2\pi ft} df. \tag{2.2}$$

A lower-case letter is used to represent a function of time, while an upper-case letter represents the transform of the function in the frequency domain. Although the Fourier transform is presented here as a function of *time* and *frequency*, it is also applicable to other pairs of variables, such as *spatial position* and *spatial frequency* which are used in image processing. The notation $G(f) = \mathcal{F}\{g(t)\}$ or $G(f) \leftrightarrow g(t)$ defines a Fourier transform pair such that $G(f)$ is the Fourier transform of $g(t)$ and $g(t)$ is the inverse Fourier transform of $G(f)$. In general, $G(f)$ is complex, such that it has magnitude $|G(f)|$ and phase $\angle\{G(f)\}$ where

$$G(f) = |G(f)| e^{j\angle\{G(f)\}}. \tag{2.3}$$

A signal is defined completely in the frequency domain by $G(f)$ as it is in the time domain by $g(t)$.

There are a number of properties of the Fourier transform that make it particularly useful for signal analysis [Bracewell, 1978, Chapter 6]. Of particular importance to this chapter is the convolution theorem. The application of the convolution theorem is incorporated in the discussion of linear filtering (section 2.1.1.3), sampled signals (section 2.1.2) and statistical analysis (section 3.2.2). When a signal, $g(t)$, is passed through a linear system, having an impulse response $h(t)$, the output, $c(t)$, is modified according to the response of the system via convolution. This is defined by

$$c(t) = g(t) \odot h(t) = \int_{-\infty}^{\infty} g(\tau)h(t-\tau)d\tau, \tag{2.4}$$

where $\odot$ denotes the one-dimensional convolution operator [Bracewell, 1978, Chapter 3]. The Fourier transform of (2.4) becomes a product [Bracewell, 1978, p110] such that

$$g(t) \odot h(t) \Leftrightarrow G(f)H(f). \tag{2.5}$$

Similarly, multiplication in the time domain transforms to convolution in the frequency domain. Convolution is commutative, associative and distributive [Bracewell, 1978, p110].

2.1.1.2 Signal properties

This subsection describes a number of properties of signals which, once measured, are useful for describing the behaviour of a signal under investigation. It is not intended to cover the whole topic, but to present a useful subset of properties that have been used in the signal analysis techniques described in Chapter 3. A detailed discussion of the properties of signals is included in many excellent books [Haykin, 1983; Bracewell, 1978].

The *autocorrelation function* gives a measure of the periodic behaviour of a signal. It is obtained by making measurements of the signal amplitude at two instants of time, separated by a delay τ, finding their product, and averaging over the total record. The autocorrelation function, $R_g(\tau)$, is written mathematically as

$$R_g(\tau) = \lim_{T\to\infty} \frac{1}{T}\int_0^T g(t)\cdot g(t+\tau)dt. \tag{2.6}$$

where T is the length of the signal. It is important to note that the autocorrelation function is symmetrical about T = 0. Auto-correlation has the ability to determine the presence of periodicity in an apparently random signal. This is demonstrated for random noise and a sine wave in figure 2.1. The autocorrelation of random noise, 2.1(a), is an impulse function, 2.1(b), while the autocorrelation of a sinusoid, 2.1(c), produces another sinusoid, 2.1(d). An example of the practical application of the autocorrelation function is the detection of a weak periodic signal imbedded in noise. Figure 2.1(f) is the autocorrelation of the sinusoid, 2.1(c), imbedded in noise, 2.1(a), where the noise has twice the power of the sinusoid. The presence of the sinusoid is clearly evident in 2.1(f).

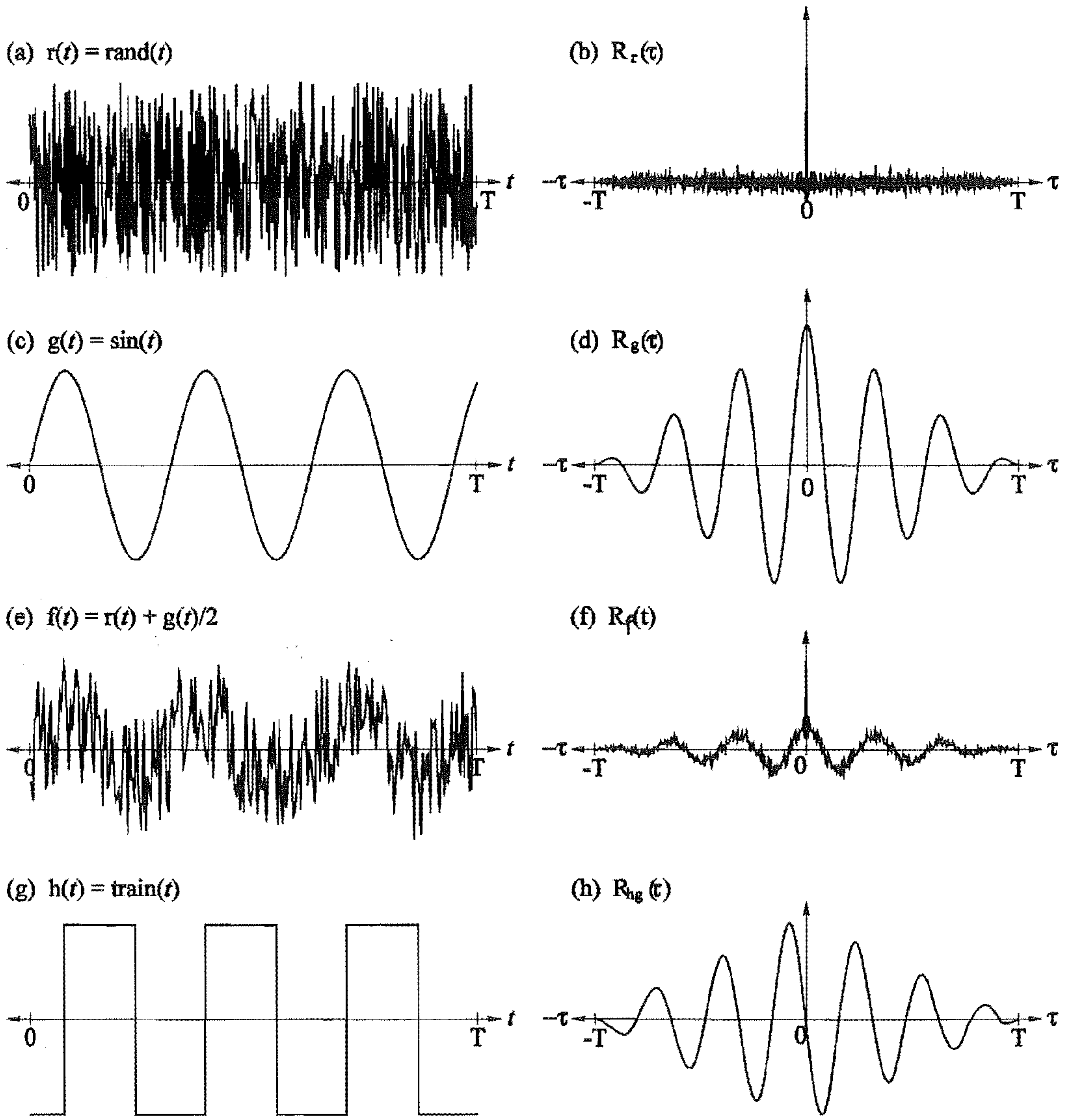

Figure 2.1 (a) A random signal, (b) its autocorrelation. (c) A sinusoid, (d) its autocorrelation. (e) Noisy sinusoid, (f) its autocorrelation. (g) A pulse train, (h) cross-correlation of sinusoid and pulse train.

Evaluating the autocorrelation function for zero delay ($\tau = 0$) yields

$$R_g(0) = \lim_{T\to\infty} \frac{1}{T}\int_0^T g^2(t)dt\,, \tag{2.7}$$

which is the mean square value of the signal.

The *cross-correlation function* is similar to the auto-correlation function, but is used to compare two different signals. The cross-correlation function, $R_{gh}(\tau)$ is expressed as

$$R_{gh}(\tau) = \lim_{T \to \infty} \frac{1}{T} \int_{-T}^{T} g(t) \cdot h(t+\tau) dt, \tag{2.8}$$

which is a measure of the joint properties which the two signals, g(t) and h(t), may share. The notation g(t) $\otimes$ h(t) defines the cross-correlation function, $R_{gh}(\tau)$, between the two signals g(t) and h(t). Figure 2.1(h) is the cross-correlation of a sine wave, 2.1(c), and a pulse train, 2.1(g), The phase difference between the sine wave and the pulse train is evident in 2.1(h) from the value of τ at which the peak nearest $\tau = 0$ occurs.

The linear decay of the correlation functions as τ approaches $\pm$T (see figure 2.1) is produced because of the finite signal lengths. As τ approaches $\pm$T, the correlation coefficient, $R(\tau)$, is evaluated over fewer points, (T - τ), producing a smaller value. To eliminate this effect, the term 1/T can be substituted with the function 1/(T - τ). However, this does not correct for the reduced accuracy resulting from the smaller evaluation period at larger delays.

The power spectral density of a signal gives a measure of the average power or mean square of every frequency component of the signal. It can be calculated from the Fourier transform of the signal as

$$S(f) = |G(f)|^2 = G(f) \cdot G^*(f), \tag{2.9}$$

where the superscript * denotes the complex conjugate. The total mean square value of the signal can therefore be calculated from the sum of the mean square value of each frequency component as

$$\mu^2 = \int_{-\infty}^{\infty} |G(f)|^2 df. \tag{2.10}$$

Therefore, combining (2.7) and (2.10) yields

$$R_x(0) = \int_{-\infty}^{\infty} S(f) df. \tag{2.11}$$

The Fourier transform relationship between the correlation function and the power spectral density function is known as the *Weiner-Khintchine theorem* [Haykin, 1983, p58]. For real values at positive frequencies they can be shown to be

$$\begin{aligned} S(f) &= \int_{0}^{\infty} R(\tau) \cos\omega\tau \, d\tau, \\ R(\tau) &= \int_{0}^{\infty} S(f) \cos\omega\tau \, df. \end{aligned} \tag{2.12}$$

2.1.1.3 Ideal linear filtering

In ordinary usage, a filter is a device for separating an aggregate of two classes, those that *pass* and those that are *stopped*. In the context of signal processing, a filter separates the frequency components of a signal. In this thesis, the separation of frequency components of signals is required for the analysis of infant physiological signals (see section 3.3).

Frequency domain analysis is useful for filter design and implementation since an ideal low pass linear filter is characterised in the frequency domain by the simple expression

$$|\mathrm{H}(f)| = \begin{bmatrix} 1, & |f| \leq f_c \text{ (passband)} \\ 0, & |f| > f_c \text{ (stopband)} \end{bmatrix} \tag{2.13}$$

and has zero phase, that is

$$\angle\{\mathrm{H}(f)\} = 0. \tag{2.14}$$

The impulse response of the ideal filter, derived from the inverse Fourier transform of H(f) is thus

$$\mathrm{h}(t) = 2f_c \mathrm{sinc}(2\pi f_c t) \quad \text{for } -\infty < t < \infty, \tag{2.15}$$

where $\mathrm{sinc}(x) = \sin(x)/x$. The impulse and frequency responses of the ideal low pass filter are shown in figure 2.2(a) and 2.2(b) respectively.

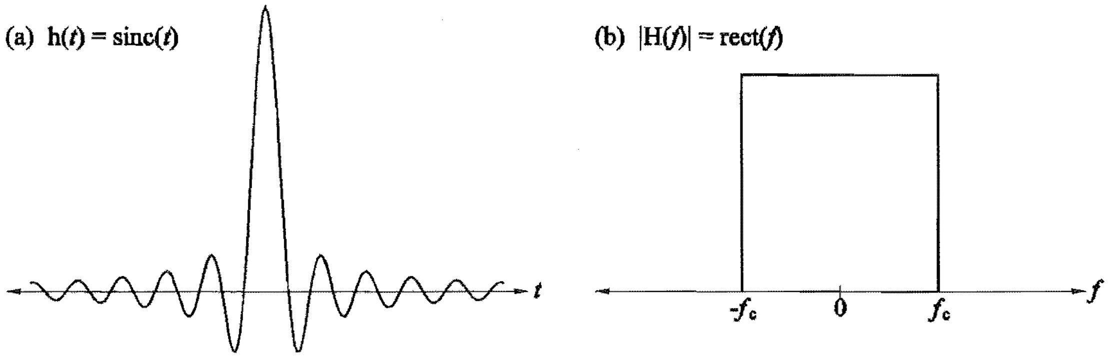

Figure 2.2 Ideal low-pass filter characteristics: (a) Impulse response, (b) frequency response.

Mathematically, the application of a filter consists of multiplying the frequency response of the signal by the filter's frequency response. In the time domain, the process becomes a convolution of the signal with the filter impulse response (see section 2.1.1.1).

In practice, the ideal filter is impossible to achieve because h(t) does not vanish for t < 0 (i.e. it is not possible to construct a filter with an infinitely long impulse response as suggested in (2.15)). However, in many applications an ideal filter can be approximated by a filter which has characteristics which closely, but not exactly, match those of the ideal filter. There are numerous techniques for designing and applying analog and digital filters, however, detailed introduction into these techniques is beyond the scope of this thesis. The interested reader is recommended to peruse some of the numerous excellent works on the topic [Ludeman, 1987, Chapters 4 & 5].

2.1.2 Sampled Signals

The advent of digital computers has enabled powerful and flexible analysis procedures to be carried out automatically and at great speed on sampled signals. Sampling is a process by which a continuous signal is converted into a series of discrete numbers or samples. Sampling is necessary for the recording, storage and analysis of signals on a digital computer. Aspects of sampling are considered in the design of the signal collection and analysis systems presented in Chapter 3. All signals discussed in this thesis are real, one dimensional, sampled data sets of finite length.

The ideal function for obtaining a single sample is a unit area impulse [Bracewell, 1978, Chapter 5]. Its' properties are

$$\begin{aligned} \delta(t) &= 0 \quad \text{for } t \neq 0, \\ \int_{-\infty}^{\infty} \delta(t)dt &= 1. \end{aligned} \tag{2.16}$$

The ideal sampling function is comprised of equally spaced unit area impulse functions, forming what is known as an *impulse train*. The impulse train, $\Delta(t)$, and it's frequency spectrum, $\Delta(f)$, are given by

$$\Delta(t) = \sum_{n=-\infty}^{\infty} \delta(t - n\mathrm{T}_s) \leftrightarrow \Delta(f) = \frac{1}{\mathrm{T}_s} \sum_{n=-\infty}^{\infty} \delta(f - \frac{n}{\mathrm{T}_s}). \tag{2.17}$$

where T_s is the time spacing between adjacent impulses in the time domain impulse train (i.e. the sampling period). In practice, the sampling process is of finite duration, therefore the sampling is not ideal.

The continuous signal, $g(t)$, is identified by curved brackets, while the same signal after sampling, denoted $g[n]$, is identified by square brackets. The independent variable n is an integer.

The sampling theorem [Bracewell, 1978, p189] states that a signal which is band limited to a maximum frequency, f_c, is uniquely determined by its samples, provided the sampling frequency, f_s, is greater than $2f_c$. Before a signal is sampled, it is critical to determine that the highest frequency component of the signal is less than half the sampling frequency in order to prevent aliasing.

Figure 2.3 illustrates the sampling process and the effect of aliasing. A signal, $g(t)$, and its magnitude spectrum, $|G(f)|$, are presented in figure 2.3(a) and 2.3(b) respectively. An ideal low pass filter spectrum, with a cut off frequency at f_c, is shown in 2.3(d). The impulse response of the filter, shown in 2.3(c), is convolved with $g(t)$ to produce the filtered signal, 2.3(e), and its magnitude spectrum 2.3(f). An ideal sampling function $\Delta(t)$, illustrated in 2.3(g), is multiplied by the filtered

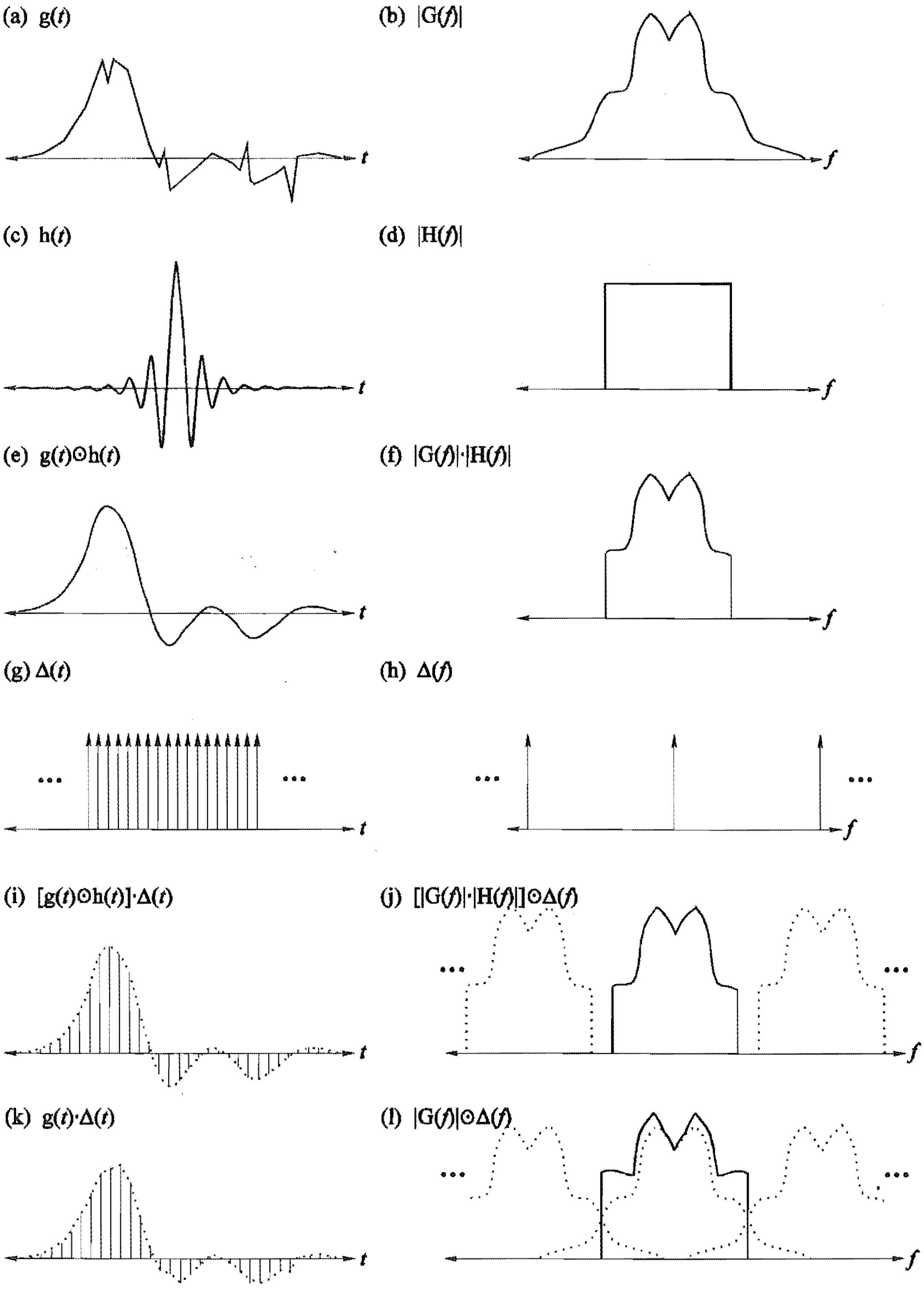

Figure 2.3 An illustration of the sampling theorem: (a) A signal, (c) an anti-aliasing filter impulse response, (e) the filtered signal, (g) and ideal sampling signal, (i) the sampled filtered signal, (k) the sampled <u>unfiltered</u> signal which is corrupted due to aliasing. (b), (d), (f), (h), (j) and (l) show the frequency domain representations. The effect of aliasing is shown clearly in the frequency domain in part (l) by the overlapping repetitions of the spectrum (dotted lines) which add together to produce the recovered spectrum (solid line).

signal to produce a band-limited sampled signal, 2.3(i). Note that the spectrum of the sampling function, 2.3(h), is also an impulse train in which the impulses are spaced at intervals of f_c. The repetitions in the spectrum of the sampled signal are a result of the convolution of the signal spectrum with the sampling function. Figure 2.3(k) is the sampling function, 2.3(g), multiplied by the unfiltered signal, 2.3(a). Note that the magnitude spectrum of this, 2.3(l), is corrupted because high frequency components of the spectrum overlap (and superimpose) with adjacent repetitions of the spectrum. This distortion is known as *frequency aliasing* and results from undersampling in the time domain.

2.1.2.1 The discrete Fourier transform

Digital computers are unable to calculate, store and process the continuous Fourier transform of a signal. The *discrete Fourier transform* (DFT) [Bracewell, 1978, Chapter 18] allows discrete frequency domain transformation of sampled data sets to be carried out. Calculation of the DFT requires the Fourier transform of a signal to be sampled. This is equivalent to multiplying the spectrum of the signal by an impulse train. The impulse train, $\Delta(f)$, and its inverse Fourier transform, $\Delta(t)$, are thus

$$\Delta(f) = \sum_{k=-\infty}^{\infty} \delta(f-k\mathrm{F_s}) \Leftrightarrow \Delta(t) = \frac{1}{\mathrm{F_s}} \sum_{k=-\infty}^{\infty} \delta(t-\frac{k}{\mathrm{F_s}}), \tag{2.18}$$

where F_s is the frequency spacing between adjacent impulses in the frequency domain sampling function. Thus, the impulse train transforms to another impulse train in the time domain which comprises of impulses spaced by $1/F_s$. Figure 2.4 illustrates the frequency domain sampling process. A signal and its spectrum are illustrated in 2.4(a) and 2.4(b) respectively. The signal spectrum is multiplied by the sampling function, 2.4(d), to produce the sampled spectrum, 2.4(f). In the time domain, the signal, 2.4(a), is convolved with the inverse Fourier transform of the sampling function, 2.4(c). This produces repetitions of the signal, occurring at a period of $1/F_s$. *Time aliasing* will occur if the length of the signal is longer then $1/F_s$ (i.e. when undersampling in the frequency domain occurs).

The discrete Fourier transform directly calculates the sampled spectrum from a sampled signal. Consider a sampled signal which is band-limited to $1/(2T_s)$ and has N samples. The length of the signal is thus NT_s. If the spectrum of the signal is sampled at frequency components spaced by F_s then the maximum length of the signal which avoids time domain aliasing is $1/F_s$, therefore

$$\frac{1}{\mathrm{F_s}} = \mathrm{NT_s}. \tag{2.19}$$

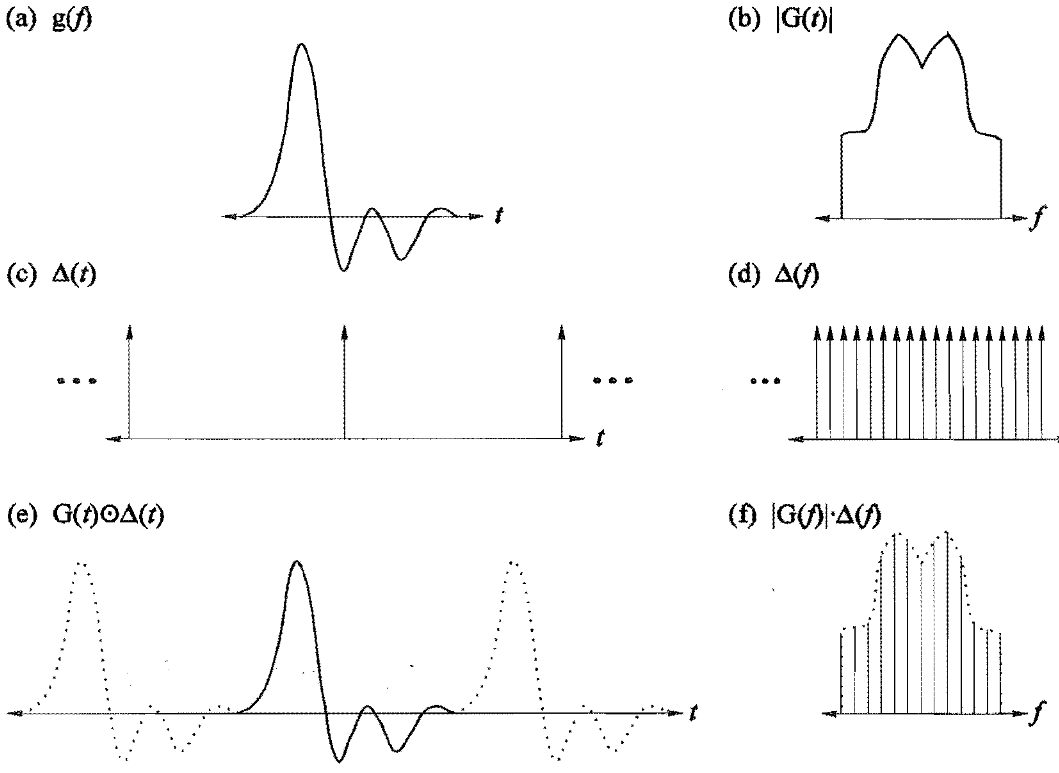

Figure 2.4 Frequency domain sampling: (a) A signal, (b) its spectrum, (d) an ideal sampling function, (c) its impulse response, (f) the sampled spectrum, (e) the sampled spectrum impulse response.

Similarly, a sampled spectrum has a bandwidth of $1/(2KF_s)$, thus

$$\frac{1}{2KF_s} = \frac{1}{2T_s}. \tag{2.20}$$

Substitution of (2.19) into (2.20) yields N = K. Therefore, the minimum number of samples of the frequency spectrum required to fully describe a signal which is band-limited to $1/(2T_s)$ is equal to the number of samples of the signal.

The one-dimensional DFT [Ludeman, 1987, Chapter 6] for a sequence of N samples is defined by

$$\begin{aligned} G[k] &= \sum_{n=0}^{N-1} g[n] e^{-j2\pi nk/N} \\ g[n] &= \sum_{k=0}^{N-1} G[k] e^{j2\pi nk/N}, \end{aligned} \tag{2.21}$$

where k and n are integers. The spectrum of g[n], denoted G[k], contains spectral components spaced at discrete frequencies in the range of $-T_s/2$ to $T_s/2$, where T_s is the sampling period. The spacing between adjacent spectral components is

$1/(NT_s)$ Hz. The properties of the continuous Fourier transform are valid for the DFT [Bracewell, 1978, Chapter 18].

Spectral estimates obtained via the DFT are subject to unavoidable limitations. As already stated, the frequency resolution is limited to the reciprocal of the duration of the sampled data (equations (2.19) and (2.20)). In order to increase the frequency resolution it is necessary to take a longer sequence of samples. However, a longer sequence of samples is more likely to include changes in the spectral content of the signal as time progresses (non-stationary behaviour). Thus, there is a trade off between frequency resolution and time resolution of a time-varying spectrum.

The DFT operates on a finite number of samples and as such the signal may be considered to have an infinite length which is multiplied by a window that has zero magnitude outside of an interval representing the number of samples in the signal. The calculated spectrum is therefore the ideal spectrum convolved with the spectrum of the windowing function [Harris, 1978]. The power of a signal, at any given frequency, will be spread by the convolution of the signal spectrum with the window spectrum into adjacent frequency regions. This is known as leakage [Harris, 1978]. Choice of an appropriate windowing function may help to reduce the effect of leakage at the expense of reduced spectral resolution. This is due to the effective reduction of sequence length if the window is not rectangular. The ideal, but unobtainable, window function is a single unit area impulse in the frequency domain which requires the signal to have infinite length. Figure 2.5 illustrates the rectangular and Hanning (cosine) window shapes and their Fourier transforms. The spectral side lobes are larger for the rectangular window, but the width of the main lobe is larger for the Hanning window. This clearly demonstrates the trade off between spectral resolution and side lobe leakage effects. Thus, the choice of window, from the numerous windows types that are commonly used in signal processing [Harris, 1978], is dependent on the application requirements.

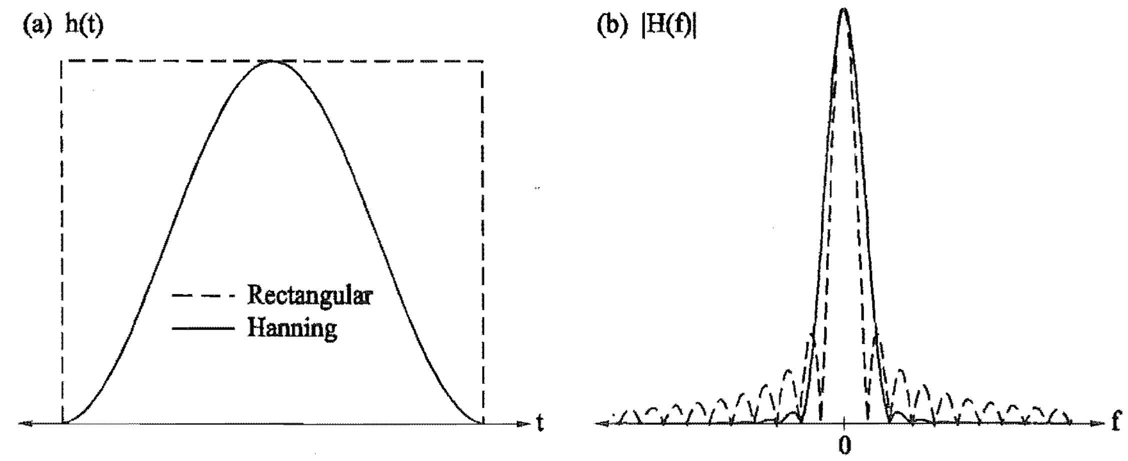

Figure 2.5 The effect of windowing: (a) Rectangular and Hanning windows, (b) their frequency spectrums showing the trade-off between main lobe width and side lobe magnitude.

Many algorithms exist for evaluating the DFT, the most common of which is the *Fast Fourier Transform* (FFT) [Bracewell, 1978, p370]. The FFT is a computationally efficient algorithm which reduces the number of operations required to calculate the DFT by manipulating odd and even samples of g[k] separately, thus making use of the cyclic nature of $e^{-j2\pi nk/N}$. For a one-dimensional data set of N samples, where N is a power of 2, the FFT requires $2NLog_2N$ complex operations, compared with the N^2 necessary for the direct DFT. Due to the computational efficiency of the FFT, the frequency domain analysis procedures outlined in this thesis employ the FFT.

It is important to recognise that all of the useful properties of the continuous Fourier transform remain valid for both the DFT and FFT [Bracewell, 1978, Chapter 18].

2.2 Human Control Systems Modelling

Many of the systems within the body act to regulate some variable, such as temperature, carbon dioxide and oxygen gas partial pressures, sugar levels, motor functions and circulation. These systems are termed control systems and are difficult to analyse because of their cross-coupled nature. Mathematical modelling techniques can be employed to aid such investigations.

There are numerous reasons why a modelling approach to systems analysis forms a practical investigative tool. Modelling is particularly appropriate for the analysis of human control systems because simulations may be performed using the model where it would be unethical to perform similar in vivo experiments on humans. A simple model of any system may produce a wealth of information about the optimal working conditions of the system, extremes where the system fails, and gives an indication of the sensitivity of the system to changes in parameter values. The model may also be used for the purposes of prediction. Insights into the behaviour of systems that may have been swamped with noise may become obvious in model simulations. For example, noise generated by cross-coupling effects in the system may be avoided in model simulations.

There is little point developing a model if everything is known about the system under investigation. However, analysis of the behaviour of a model that represents the system allows for validation of the assumptions and hypotheses and increases understanding of the system. If the model behaviour is considerably different from experimental results, within the bounds of the design of the model, then the assumptions and possibly the structure of the model may be incorrect. Finally, a simple model of a complicated system may highlight certain areas where useful experiments could be performed on the original system, thus limiting the total number of clinical experiments necessary for a more complete understanding of the system.

2.2.1 Hierarchy of systems organisation

A system is a set of interconnected entities which form an organised whole. In the context of engineering or medicine, the entities act together to produce results which for each entity alone would be impossible to achieve. However, each entity is in fact a subsystem in its own right, comprising a lower level of entities or subsystems. For example, the human thermoregulatory system is the interconnection of thermo-receptors, control centres of the hypothalamus, circulation, effectors and body tissues. The subsystem of circulation also consists of receptors, a controller and an effector. Each of these entities may be further divided. Alternatively, thermoregulation may be considered to be a subsystem of the human. In this manner, all systems can be considered as coupled. Figure 2.6 illustrates the hierarchy of systems for thermoregulation. These levels of organisation have a complicated structure because any system may be a subsystem for more than one parent system. This is illustrated in figure 2.6 by the inclusion of the respiratory and circulatory systems which are coupled to the thermoregulatory system.

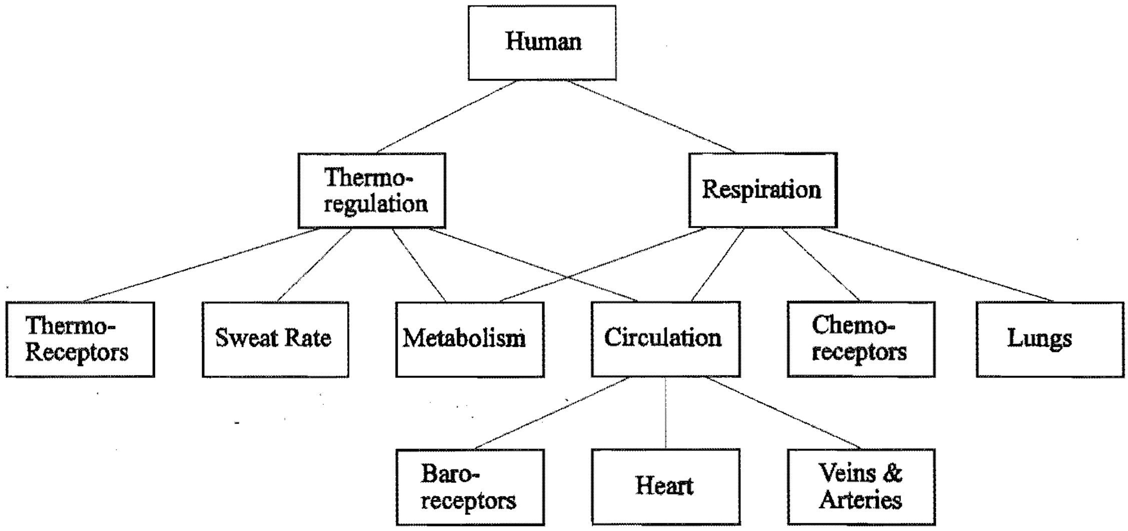

Figure 2.6 Hierarchy of systems organisation for thermoregulation showing the coupling to the respiratory and circulatory systems.

2.2.2 Systems modelling

The formal discussion of a system implies some form of conceptual representation. A simple flow diagram or a complicated mathematical expression are both representations of a system and as such are models. The *functional* representation of a system attempts to describe what the system does while the *structural* representation describes how the system works.

Mathematical modelling, in its crudest sense, is a process of fitting a mathematical expression to experimental data that represents an input/output relationship for the system. Many different mathematical expressions may fit adequately for a specific set of circumstances. However, it is unlikely that any of the expressions will describe the system for all possible circumstances. Generally, the more complicated the expression, the better the fit. If the number of variables in the expression is increased, the model will normally fit for a larger number of circumstances.

The process of curve fitting contributes little to the understanding of the system and is limited to a particular set of circumstances. It is however, a useful functional representation of the input/output relationship of the system. The limitation of curve fitting to many human systems is that there are often wide variations between individuals. Also, it is often impossible or unethical to experimentally measure the input/output relationship of many human systems.

When constructing a model for performance analysis of a system, similar behaviour of the model to experimental results is necessary but not sufficient. Structural similarity is also necessary. In order to improve the accuracy of the model and gain greater insight into the structure of the system, it is necessary to divide the system into a group or series of subsystems which describe lower level processes. The model is now a structural representation and is intrinsically similar to the parent system. In this manner, the circulatory system can be divided into receptors, the nervous system, blood vessels, the brain (controller) and the heart (effector). The dilemma now is how to deal with each subsystem. The simplest and often most practical solution is to model each subsystem by curve fitting. However, one is tempted to repeatedly reduce each subsystem to structural blocks of lower level subsystems. In some circumstances this may be beneficial but often will produce little increase in accuracy of the model and only serve to increase complexity and confuse. Indeed, a loss of accuracy may result due to the flow of errors through complicated computations in model simulations. More importantly, such a detailed representation is redundant. For example, it is meaningless to express the circulatory system in sub-cellular terms. In all cases, the lowest level subsystems must be functional representations which are derived by curve fitting.

Mathematical expressions which represent systems may include a multitude of mathematical operators. Addition, subtraction, multiplication, logarithm, exponential, piece-wise functions and time delays are all typical examples. Many systems can be represented by differential equations. For example, the rate of change of temperature, T, with respect to time, of a body of mass, is proportional to the heat entering the body, ϕ_{IN}, minus the heat leaving, ϕ_{OUT}, viz

$$\frac{dT}{dt} = \alpha(\phi_{IN} - \phi_{OUT}), \tag{2.22}$$

where α is a constant. Heat leaving the body by means of conduction and radiation to the environment is proportional to the difference between the temperature of the body and the environmental temperature, T_{ENV}, such that

$$\phi_{OUT} = \beta(T - T_{ENV}), \tag{2.23}$$

where β is a constant. Combining (2.22) and (2.23) yields

$$\frac{dT}{dt} = -\mathrm{A}T + \mathrm{B}, \tag{2.24}$$

where $\mathrm{A} = \alpha\beta$ and $\mathrm{B} = \phi_{IN} - \beta T_{ENV}$. Equation (2.24) is a first order linear ordinary differential equation.

One model will not suffice for all possible system tasks, for that would require a model as complicated as the system itself. There would be little point attempting to develop such a model since one of the goals of modelling is to increase system understanding, yet the development of such a model requires a complete understanding of the system. Thus, no physical system can be represented in full detail, therefore, idealising assumptions must be made for analysis and modelling purposes. Such approximations limit the use of the model to applications where the approximations are valid.

In many circumstances, approximations may be advantageous to the practical application of a model. A typical example is when a system is fitted with an equation that does not include the effect of cross-coupling with a second system. The model is then capable of being analysed without the noise that would be introduced from the secondary system. In addition, it is often impossible to isolate a system during in vivo experimentation. Approximations also improve the simplicity of the model allowing faster, simpler solutions. Often an analytical solution is impossible without many approximations.

The development and implementation of mathematical models of two human physiological control systems are discussed in this thesis. A model of thermoregulation of infants is discussed in Chapter 4 and a model of the temperature dependence of the respiratory system of infants is discussed in Chapter 6.

2.2.3 Linear systems analysis

A mathematical model is linear if it obeys the principle of superposition [Nagrath & Gopal, 1986, p14]. This implies that the application of the sum of two inputs to a linear system produces an output which is equal to the sum of the outputs which would be obtained if the inputs were applied separately.

Mathematical models described by differential equations are linear if the coefficients of the differential equations are either functions of the independent variable only, or are constants [Nagrath & Gopal, 1986, p14]. If the coefficients are functions of the independent variable, then the model is linear time-varying, otherwise it is linear time-invariant.

2.2.3.1 The Laplace transform

The study of systems involves the interplay of functional (input/output relationships) and structural (system/subsystem relationships) system descriptions. For linear systems, the time domain functional representation is often in terms of linear differential equations, but the frequency domain functional representation leads to linear algebraic equations that are much simpler to manipulate. The *Laplace transform* [Bracewell, 1978, Chapter 11] is a powerful tool for evaluating the frequency domain functional representation of a system, known as the *system function* or *transfer function*. The system function describes the gain of the system for every complex frequency and can be used to describe the frequency domain characteristics of the system. The Laplace transform, similar to the Fourier transform, is a convenient method of mapping the mathematical expression that describes a system, from the time domain to the complex frequency domain, thus determining the system function. Given a time domain function $g(t)$, the integral

$$G(s) = \int_0^\infty g(t)e^{-st}dt \tag{2.25}$$

defines a function of the complex frequency variable s, where $s = \alpha + j\omega$. The function $G(s)$ is the *unilateral* Laplace transform of $g(t)$. The notation $G(s) = \mathcal{L}\{g(t)\}$ or $G(s) \Leftrightarrow g(t)$ defines a Laplace transform pair such that $G(s)$ is the Laplace transform of $g(t)$ and $g(t)$ is the inverse Laplace transform of $G(s)$. For physical systems $s = j\omega$, where $\omega = 2\pi f$ is the frequency in radians per second. Thus (2.25) becomes equivalent to (2.1) which is the Fourier transform.

Obtaining the Laplace transform of many functions is simplified by the use of a table of the properties of the Laplace transform [Siebert, 1986, Chapter2]. For example, the Laplace transform of a differentiation operator is

$$\frac{dg(t)}{dt} \Leftrightarrow sG(s) - g(0)\,. \tag{2.26}$$

Thus, the Laplace transform of the linear thermal system described by equation (2.24) is

$$sG(s) - T_0 = A \cdot G(s) + \frac{B}{s}, \tag{2.27}$$

where T_0 is the initial temperature. Rearrangement of (2.27) yields

$$G(s) = \frac{T_0}{s + A} + \frac{B}{s(s + A)}\,. \tag{2.28}$$

For low frequencies, as $s \to 0$, $G(s)$ approaches T_0/A, while at very high frequencies, as $s \to \infty$, $G(s)$ reduces to 0. The system can therefore be considered to be a low-pass linear filter (i.e. high frequency thermal loads will not significantly alter the temperature of the body of mass).

2.2.3.2 Dynamic behaviour of second order systems

For a linear second order system, a step input can be used to investigate the dynamic behaviour of the system. The step response can be calculated from the transfer function of the system or directly measured from the system after a step input. The transfer function of a second order system with a step input can be expressed as

$$C(s) = \frac{\omega_n^2}{s^2 + 2\zeta\omega_n s + \omega_n^2}, \tag{2.29}$$

where ζ is the damping factor and ω_n is the undamped natural frequency [Nagrath & Gopal, 1986, p139]. Figure 2.7 shows the responses of a second order system to a unit step input for a range of damping factors. For $\zeta = 0$, the system is unstable and continuous oscillations occur. Where $0 \leq \zeta < 1$, oscillations occur which decay and the system is said to be *under-damped* or *marginally stable*. For $\zeta \geq 1$, oscillatory behaviour is not present and the system is said to be *over-damped*. *Critical damping* occurs where $\zeta = 1$. The damping factor may be used to give a measure of the stability or oscillatory behaviour of the system.

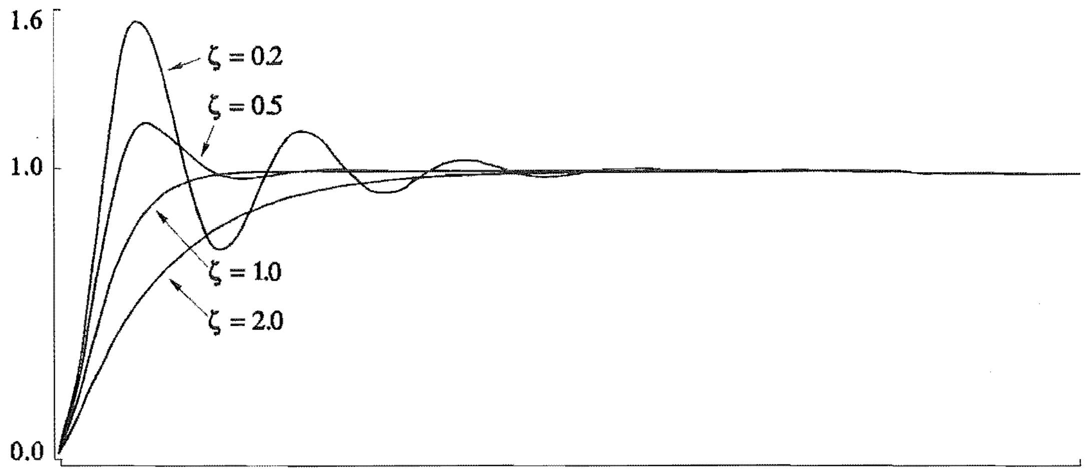

Figure 2.7 Time response of a second order system with a unit step input for different damping factors ζ.

For under-damped systems, the damping factor can be directly measured from the peak overshoot which occurs after a step input [Nagrath & Gopal, 1986, p144]. The peak overshoot, P_{MAX}, is related to the damping factor by

$$P_{MAX} = e^{-\pi\zeta/\sqrt{1-\zeta^2}} . \tag{2.30}$$

Therefore, the peak overshoot is also a measure of stability. For over-damped systems, no overshoot occurs and therefore, P_{MAX} cannot be measured. This is of no concern because over-damped systems are inherently stable. That is, the system does not overshoot the steady state value and the output converges towards the steady state value asymptotically.

Only second and higher order systems are capable of producing oscillatory behaviour. First order linear systems are asymptotically stable under all circumstances. However, in practice there are few control applications where a first order system is capable of responding to a step input with the desired speed.

Although this discussion has centred on linear systems, the peak overshoot to a step input at an equilibrium point of a non-linear system can be useful for investigating relative stability. However, the step size must be fixed because the ratio of the step size to the overshoot may vary with the step size. The study of the behaviour of the non-linear mathematical model of infant thermoregulation, presented in Chapters 4 and 5, incorporates step response analysis.

2.2.4 System simulation

Unfortunately, no natural physical system is perfectly linear. Therefore, assumptions about the system under investigation are necessary in order to obtain a linear model. However, it is not always possible to obtain a valid linear model in the presence of a strong non-linearity because the linearisation assumptions may considerably distort the behaviour of the model. Analysis of such a model may be performed through a number of graphical or mathematical techniques.

Many non-linear analysis techniques attempt to graphically represent the dynamics of the model [Nagrath & Gopal, 1986, Chapter 14]. Regions of stability, limit cycles (sustained oscillations) and attractors (regions where the behaviour tends towards a certain region) may all be visually presented. Graphical representation is effective for simple systems but becomes difficult to apply and interpret for large multivariant systems that require graphs of more than two dimensions to represent them.

An alternative approach is to linearise and analytically analyse the model for a small perturbation. The stability of the model at one equilibrium state can be found using linear analysis techniques. Unfortunately, this method becomes cumbersome for large systems with large non-linearities.

A practical method of analysing a system is through numerical simulation of a model of a system. Linear or non-linear models consisting of a set of differential equations may be easily simulated on a computer by employing a numerical integration algorithm [Press et al., 1986, Chapter 15]. The simulation produces a time varying output in response to a set of initial conditions. In this manner, the simulation follows the behaviour of the in vivo system response to the same input. This facilitates the use of signal processing techniques to analyse the simulation results and correlate them directly with the behaviour of the in vivo system.

2.2.4.1 Runge-Kutta numerical integration

Problems involving *ordinary differential equations* of Nth order can always be reduced to the study of sets of N first order ordinary differential equations having the form

$$\frac{dy_i}{dx} = f_i(x,y_1,\ldots,y_N) \qquad i = 1,\ldots,N. \tag{2.31}$$

The simplest problem of this nature is an *initial value problem* where all the y_i are given at a starting value x_s and it is desired to find the y_i's at some final point x_f, or at some discrete list of points. This is the nature of the problem associated with simulations of the mathematical models presented in this thesis.

Numerical integration is achieved by considering the *dy*'s and *dx*'s in (2.31) as finite steps Δy and Δx respectively, and multiplying the equation by Δx [Press et al., 1986, p548], giving

$$\Delta y_i = f_i(x,y_1,\ldots,y_N)\Delta x \qquad i = 1,\ldots,N. \tag{2.32}$$

This gives the algebraic formulas for the change in the functions when the independent variable is stepped by Δx and is a good approximation to the underlying differential equation when Δx is very small.

Runge-Kutta methods of numerical integration [Press et al., 1986, p550] propagate a solution over an interval, h, by evaluating Δy_i over several sub-intervals of h and using the results obtained to match a Taylor series expansion up to some higher order. The *fourth order Runge-Kutta* algorithm is thus

$$
\begin{aligned}
k_1 &= hf(x_n, y_n) \\
k_2 &= hf(x_n + h/2, y_n + k_1/2) \\
k_3 &= hf(x_n + h/2, y_n + k_2/2) \\
k_4 &= hf(x_n + h, y_n + k_3) \\
y_{n+1} &= y_n + \frac{k_1}{6} + \frac{k_2}{3} + \frac{k_3}{3} + \frac{k_4}{6} + \mathrm{O}(h^5),
\end{aligned}
\tag{2.33}
$$

where $\mathrm{O}(h^5)$ is the error term. Runge-Kutta virtually always succeeds but is not the most computationally efficient method [Press et al., 1986, p551]. Fourth order Runge-Kutta is generally superior to both higher and lower order Runge-Kutta schemes [Press et al., 1986, p552].

Adaptive step size algorithms are possible, which increase the step size when the error term is very small, thus reducing the number of iterations required to complete the integration to the desired accuracy. However, these schemes are not considered here since equidistant spaced samples are required for subsequent analysis of the data and computational efficiency is of no great concern.

Numerical integration is a viable method of solving sets of first order ordinary differential equations, regardless of the type or linearity of the equations. For the simulations of the mathematical models of infant thermoregulation and respiration described in this thesis, fourth order Runge-Kutta numerical integration has been used.

2.2.5 Negative feedback control

Feedback is a means of automatic regulation and is inherent in many natural physical and biological systems. Thermoregulation, respiration, hormonal control, motor functions and circulation are all examples of negative feedback control systems present in the human body.

The principle of *negative feedback* is to supervise the output of a system and to compensate at the input of the system for errors which may have occurred. Compensation is achieved by subtracting a function of the output from the input signal. Figure 2.8 is a representation of a simple negative feedback control system. The process output, $\mathrm{C}(s)$, is measured by the sensor, $\mathrm{H}(s)$, which produces a feedback signal, $\mathrm{B}(s)$. The comparator then generates an error signal $\mathrm{E}(s)$ from the difference between the input signal, $\mathrm{R}(s)$, and the feedback signal, $\mathrm{B}(s)$, thus a closed loop in the signal path of the system is formed. The error signal is applied to the process $\mathrm{G}(s)$ to influence the output in a manner which tends to reduce the error signal. The process $\mathrm{G}(s)$ is the *open loop system function*. The overall system function is easily derived using convolution theory discussed in section 2.1.1.1 and is written

$$
\mathrm{F}(s) = \frac{\mathrm{G}(s)}{1 + \mathrm{G}(s)\mathrm{H}(s)}. \tag{2.34}
$$

Equation (2.34) is termed the *closed loop system function*.

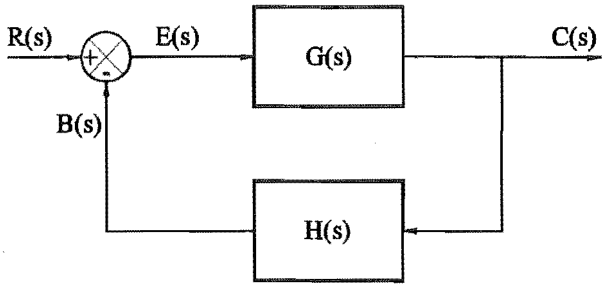

Figure 2.8 Simple negative feedback control of the process G(s). C(s), H(s) and R(s) are the output, sensor and input respectively.

The input to many control systems is known as the set point, because the output is required to be regulated as close as possible to the set point for a range of environmental temperatures. For example, the input or set point for thermoregulation of the human core body temperature is approximately 36.6°C.

The sensitivity to parameter variations within the process G(s) is low in negative feedback control systems. For example, human thermoregulation maintains a relatively constant body temperature for changes in the environmental temperature parameter. The sensitivity of a linear system with respect to variations in the process G(s) can be shown to be reduced by a factor of $(1+G(s)H(s))$ compared to that of an open loop (i.e. no feedback) system [Sedra & Smith, 1982, Chapter 12]. This reduction in parameter sensitivity is paid for by a loss of system gain. Thus, the use of feedback has reduced the system gain by the same factor that system sensitivity to parameter variations is reduced.

Negative feedback systems that are frequency dependent are not necessarily stable, that is, they may produce an oscillatory output when the input is constant or zero. It is the manner in which the loop gain varies with frequency that determines if a feedback system is stable or unstable. For physical frequencies $s = j\omega$, thus the loop gain of the system illustrated by figure 2.8 is

$$L(j\omega) = G(j\omega)H(j\omega)\,, \tag{2.35}$$

and can be represented in terms of magnitude and phase as

$$L(j\omega) = |G(j\omega)H(j\omega)|e^{j\phi(\omega)}. \tag{2.36}$$

Consider the frequency at which the phase angle, $\phi(\omega)$, becomes 180°. At this frequency, ω_{180}, the loop gain, $L(j\omega)$, will be a real number with a negative sign. Thus, the feedback signal behaves as if it is being added to the input rather than subtracted. When a small signal of frequency ω_{180} is input into the system for a finite period of time and then removed, the signal will repeatedly circulate around the feedback loop. The magnitude of the signal will be multiplied by the loop gain during each circulation. If the loop gain is less than unity then the signal will decay. If the loop gain is equal to unity then the signal will be sustained. This means the system produces an output for zero subsequent input, which by definition is an oscillator. If the loop gain is greater than unity then the oscillations will increase in magnitude until some non-linearity forces the loop gain back to unity. The sustained oscillations produced by the combination of a high loop gain and a non-linear term which restricts their amplitude form what is known as a *limit cycle*. Noise is normally sufficient to produce a signal in the system which may initiate oscillations if the system is unstable.

When the loop gain is less than but close to unity, the oscillations may take a considerable period of time to decay. From equation (2.34) the closed loop gain, F(s), will be greater than the open loop gain, G(s), since the denominator will be smaller than unity. Thus, the output will be larger for inputs at ω_{180} than at other frequencies.

From this analysis, it is evident that the stability of the system is dependent on the loop gain and phase of the feedback system. The higher the loop gain, the greater the likelihood of the system being unstable. Also, if there is no delay in the system then there is no phase change where the feedback signal is subtracted from the input signal and in this case the system must be stable.

2.3 Summary

The complementary methodologies of physiological signal processing of data collected from clinical experiments and mathematical modelling of the physiological systems under investigation form a powerful tool for biomedical research. Clinical experimentation produces data which may assist in the development of a functional model of such systems. Signal processing of the data is necessary to retrieve as much information from the data collected from the physiological systems. Mathematical modelling and simulation of the systems may be used to help validate any hypothesis about the systems, while reducing the need for invasive experimentation. This chapter has presented the mathematical background to aspects of physiological signal processing and physiological system modelling. The following chapters of this thesis, which provide an investigation into aspects of infant thermo-respiratory behaviour, are based on the details presented in this chapter.

Chapter 3

Analysis and Interpretation of Infant Thermo-respiratory Signals

Researchers throughout the world have performed numerous clinical experiments on infants in recent decades, resulting in the collection of large amounts of physiological data. Each new experiment, which may have been only subtly different from its predecessors, has yielded new and valuable information. The development of technologically innovative and non-invasive clinical instrumentation and recording apparatus now allows the collection of physiological information from infants in the natural environment of their homes.

The capture of vast quantities of data through the collection of physiological signals leaves researchers with an enormous problem. What should be done with the data to obtain the most information by the simplest method in the least possible time? There are a multitude of programs and algorithms developed for this type of signal analysis, however, the most useful results will only be obtained from algorithms and techniques which are tailored to the signals under investigation.

This chapter presents the physiological data collected from 9 infants in their homes and describes the development of signal processing techniques involved with the collection and analysis of the data. The data has been gathered in order to investigate normal infant body temperatures and respiratory behaviour in the home environment. In addition, the data has been used for comparison and validation of mathematical models of thermoregulation (Chapters 4 and 5) and respiration (Chapters 6 and 7). Section 3.1 gives a brief overview of the apparatus employed to collect the signals. Digital signal processing techniques used for investigating respiratory data are presented in section 3.2. Methods of extracting statistical information from the respiratory signals are included. Quantitative analysis techniques are discussed in section 3.3. Section 3.4 presents the results of the analysis of thermo-respiratory data from infants and section 3.5 is a brief discussion of the results.

3.1 Signal Collection

Many commercial polygraph systems are currently available which have been developed for medical applications. However, they are not designed for the collection of long term recordings of many signals with vastly different frequency bandwidths. Their analysis procedures are unsuitable for the detailed system analysis which is necessary to investigate infant thermoregulation and respiration. Commercial polygraph systems are not normally easily modified to accept new analysis procedures, nor is the stored signal data easily accessed to perform additional custom analysis. In summary, no commercial system has been found suitable for our detailed research into infant thermoregulation and respiration. To overcome this problem, the Paediatric and the Medical Physics and

Bioengineering Departments of Christchurch Hospital, in conjunction with the Electrical and Electronic Engineering Department of the University of Canterbury, have developed a computer-based polygraph system [Dove, 1988; Dove et al., 1990c; Dove et al., 1990a; Tuffnell et al., 1992]. A block diagram of the system is illustrated in figure 3.1. Five years of development have culminated in a system that comprises a signal collection unit known as *BabyLog*, which is connected to a host computer via the parallel port. Digital data storage devices are connected to the computer. The digitally stored signals are subsequently analysed with software procedures, discussed in section 3.2 and 3.3, which can be easily modified to reanalyse the signals so that many clinical hypotheses may be tested from the same data. *BabyLog* has been designed to simultaneously record a wide range of dynamic physiological signals while minimising noise pick up and amplification.

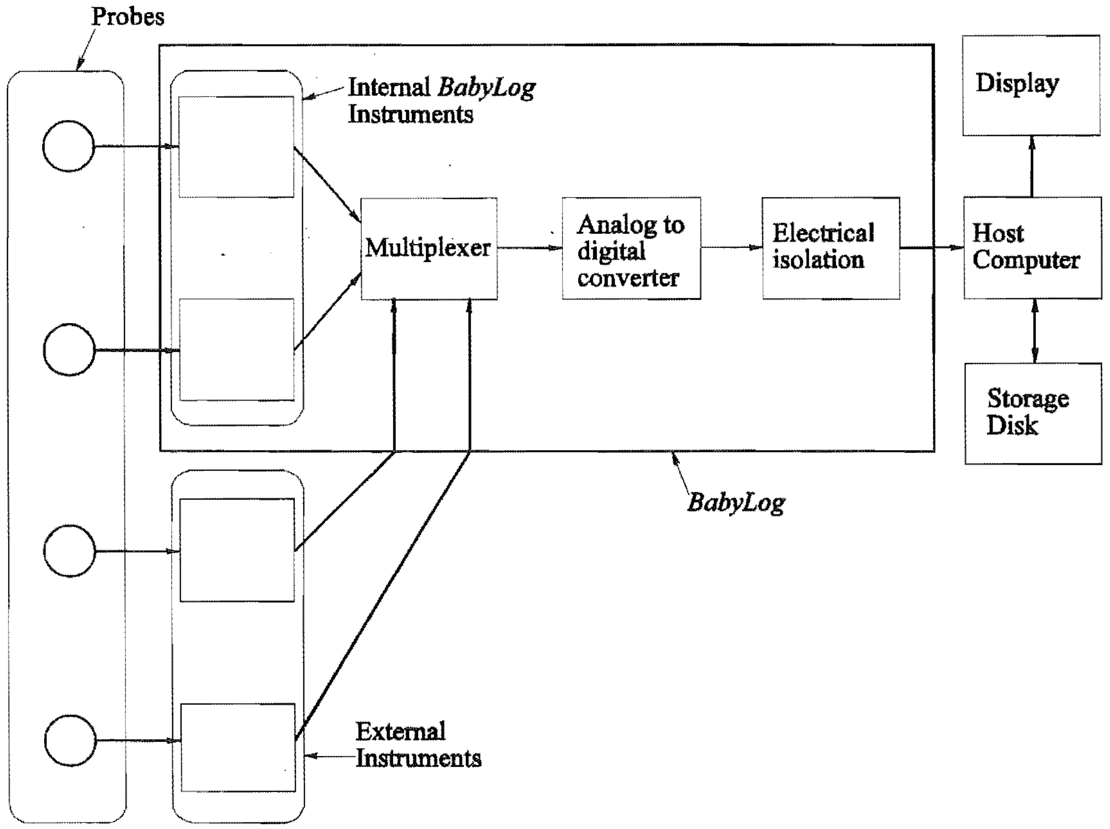

Figure 3.1 *BabyLog*: computer-based polygraph system incorporating both purpose built (internal) and commercial (external) clinical instrumentation.

BabyLog consists of dedicated internal physiological signal measurement instruments, connected through a multiplexer to a 12-bit analog to digital converter. These instruments are based on removable cards, designed for easy replacement or modification, and include electrical isolation for patient safety. The modular nature of the system allows any card to be replaced with another card which measures a different physiological signal. Instrument cards developed at present facilitate the measurement of multiple location body temperatures, respiration through nasal thermistors, body position, electroencephalogram (EEG) and oesophageal pH measurement. Additional external instrumentation with either digital or analog outputs may be connected to the system. Details of the instrumentation currently used with *BabyLog* are given in section 3.1.1.

BabyLog is completely software controllable from the host computer. This control includes the ability to set the sampling rate for each channel independently. The *BabyLog* software, executing from the host computer, performs signal collection, storage, analysis and allows fully interactive viewing of the data. An example of the viewing facilities is shown in figure 3.2. The *BabyLog* hardware is small, measuring only 280mm wide, 60mm high and 280mm deep. Therefore, if a notebook personal computer is connected to the system, it is sufficiently unobtrusive to allow the system to be used in the home.

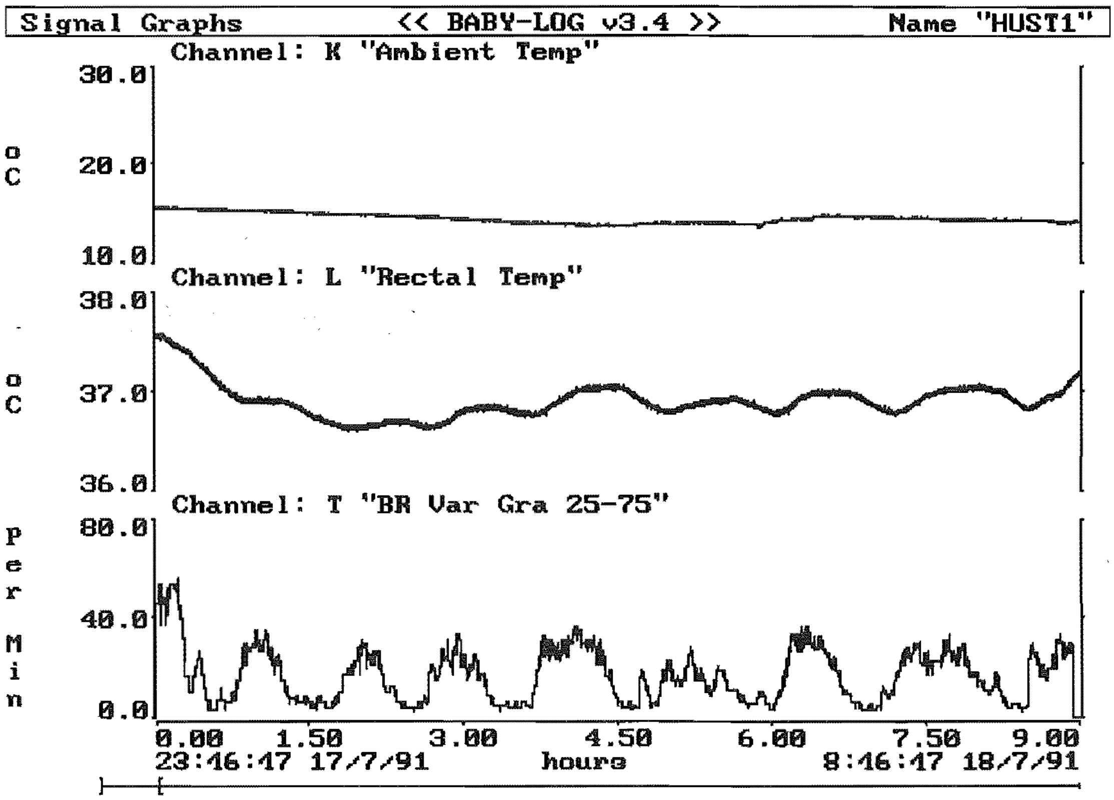

Figure 3.2 Typical computer display of *BabyLog* data. Any number of signals with similar or different sampling rates may be viewed together. Any epoch length from within the recording may also be chosen.

3.1.1 Clinical instrumentation

Table 3.1 lists the clinical instruments that have been used with *BabyLog*. All instruments have been chosen to be as non-invasive as practicable. Some instruments have probes which are easy to attach and therefore are suitable for parents to use in the home. Other instruments are unsuitable for home use because of their semi-invasive nature and the technical difficulties or safety procedures associated with probe attachment.

Physiological Signal	Detection Comments	Instrument Details	Sampling Rate (Hz)	Home use
Body Temperatures	Semiconductor diodes	*BabyLog* instrument	1	YES
Respiration	Pressure capsule on abdomen exterior	*Phillips* Graseby	10	YES
	Chest impedance	*Corometrics* Neo-Trak 502	10	YES
	Nasal air flow thermistors	*BabyLog* instrument	10	NO
Electrocardiogram	Electrical activity	*Corometrics* Neo-Trak 502	100	YES
Oesophageal pH	pH probe	*BabyLog* instrument	1	NO
Oxygen Saturation	Pulse Oximetry	*Ohmeda* Biox	1	NO
Body Position	Mercury Switch	*BabyLog* instrument	1	NO
EEG	Electrical activity	*BabyLog* instrument	100	NO

Table 3.1 Physiological signals and that have been recorded with the *BabyLog* system. The associated clinical instrumentation, sampling rate and applicability for use in the home environment is shown.

Body temperature and respiration are two physiological signals of primary importance to infant thermo-respiratory research and are, therefore, considered in detail in the following subsections with regard to noise reduction.

3.1.1.1 Respiration instrumentation

The simplest method of determining the quantity of air flowing into and out of the lungs is with an air flow meter attached to a face mask. However, this type of apparatus produces experimental procedure artifact by affecting the respiratory system through increasing both the respiratory dead space (exhaled respiratory gas volume which is re-breathed by the following inspiration) and lung back pressure. It is also invasive and many infants will attempt to pull the mask from their faces, therefore, it is not considered useful for this research. Non-invasive methods that have been investigated include abdomen movement, chest impedance and nasal thermistor air flow measurement. All of these systems are sensitive to artifact and they do not give consistent signal amplitude when the probes are re-positioned and as such cannot be calibrated to give reliable long term respiratory volume signals. However, the breath rate and apnoeic episodes can be satisfactorily measured from such signals. Relative changes in respiratory volume over short periods of time can be measured on the provision that no movement occurs during that time period. Figure 3.3 gives examples of external abdomen pressure, chest impedance and nasal thermistor waveforms.

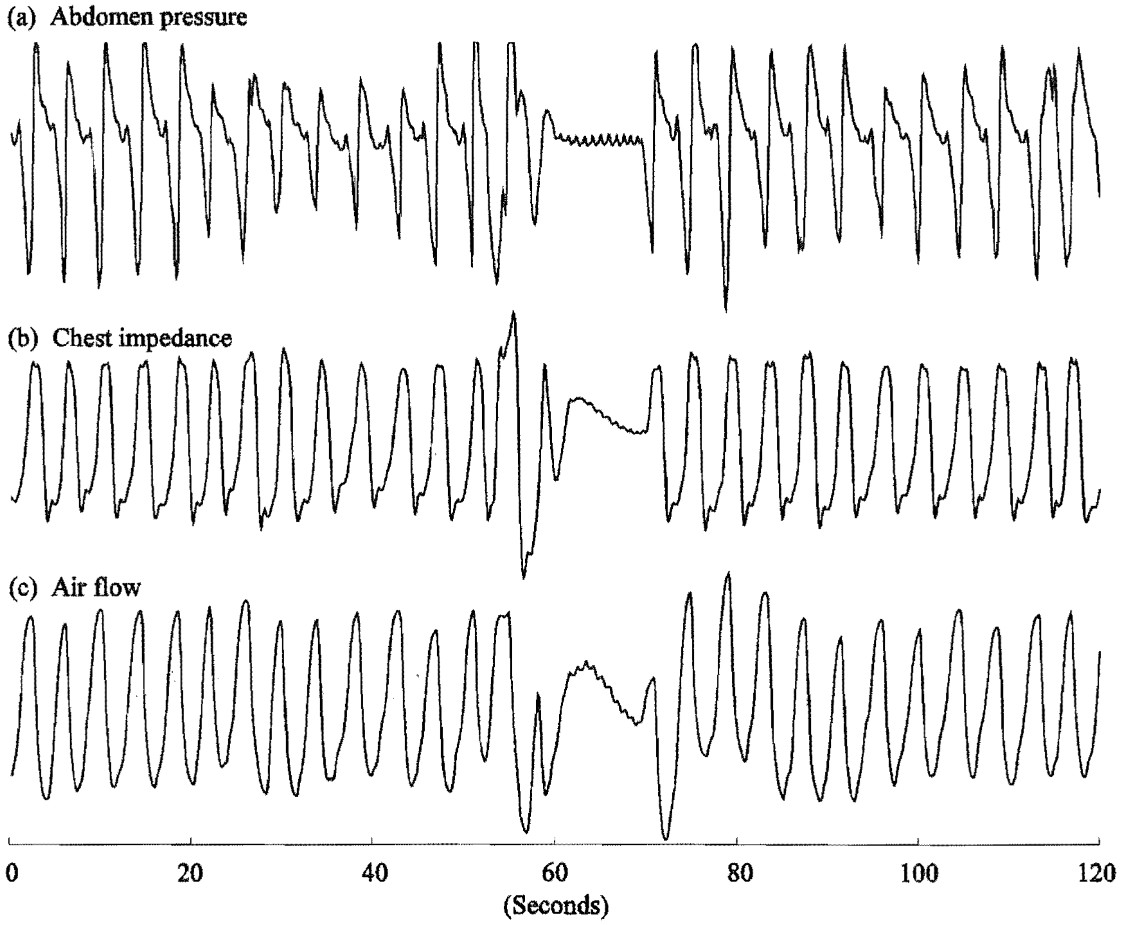

Figure 3.3 Two minute period of respiratory waveforms from a sleeping infant: (a) external abdomen pressure, (b) chest impedance and (c) nasal thermistor. An apnoea is evident in the middle of the period.

Normal infant breathing occurs at approximately 30-40 breaths per minute [Godfrey, 1981]. Much higher rates of breathing at up to approximately 60 breaths per minute commonly occur. Therefore, a sampling rate of 10Hz (600 samples per minute) is more than sufficient to recover the breathing waveform including harmonics of up to 5Hz. All respiratory instruments investigated here have output signals which are low pass filtered with a cut-off frequency which is less that 5Hz, thus no aliasing occurs. When measuring the breathing rate from the breathing waveform which is sampled at 10Hz, the breath lengths are quantised to lengths of 0.1 seconds by the sampling process. Thus, only changes in breath lengths which are greater than 0.1 seconds will be detected.

3.1.1.2 Temperature measurement

A system to continuously measure the environmental, rectal and multiple location skin surface temperatures has been developed to complement *BabyLog* [Dove et al., 1990b] and has now been incorporated into the *BabyLog* system. Rectal temperature has been shown to provide a significantly better representation of the body core temperature than the axilla temperature [Brown et al., 1992]. Therefore, although rectal temperature measurement is semi-invasive, it has been chosen as a measure of core temperature for this research. The probes are based on a semiconductor diode (Phillips KTY83-110) which gives an almost linear output with temperature and can be calibrated to give an absolute temperature accuracy of $< \pm 0.05$°C over the temperature range 30-40°C. Figure 3.4 illustrates the probe construction.

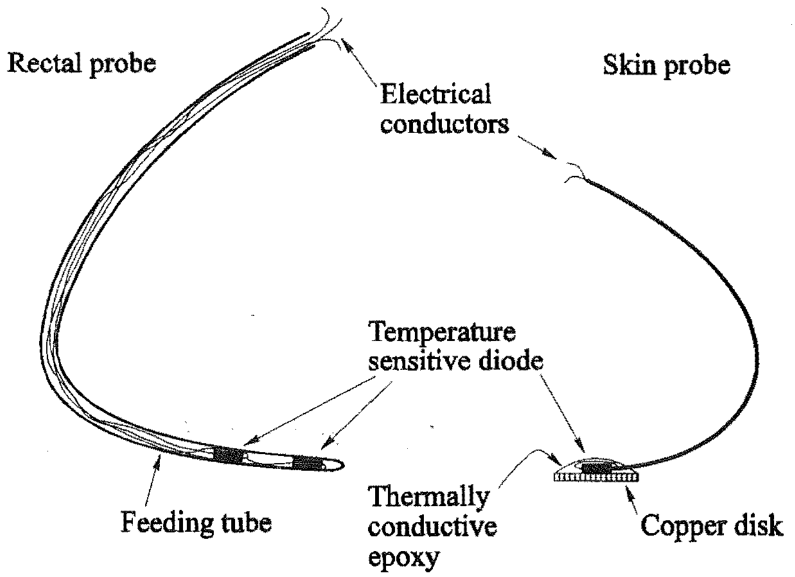

Figure 3.4 Rectal and skin temperature measurement probe construction (Actual Size).

The rectal probe is constructed by inserting two diodes into a sealed infant feeding tube to detect rectal and anal temperatures. The probe is inserted to a depth of 50mm into the infants' rectum. Nappies prevent the probe from falling out. Skin surface temperature measurement probes are constructed by attaching a diode to a copper disk with heat conductive epoxy resin. The flat circular disk gives reliable and consistent contact to the skin for a wide range of contact pressures. The probe is secured to the skin with tape.

Considering the size of body mass of the infants, it is anticipated that changes in temperature must occur over periods of minutes. For this reason, a sampling rate as low as 1/60 Hz (one sample per minute) would be more than sufficient to prevent aliasing. However, body temperatures have been sampled at a rate of 1 Hz so that detection of a probe fault or detachment may be made to the nearest second. The 1 Hz sampling rate also allows for unanticipated frequency components up to 0.5 Hz.

3.1.2 Experimental procedures

This subsection deals with the guidelines and limitations which clinical experiments outlined in this thesis are bounded by.

Experimental procedure artifact arises when the experimental procedures employed to measure a particular signal affect the system under investigation to such an extent that the signal being measured is significantly altered. Experimental procedure artifact effects are an important problem and must be considered during the design of experimental procedures. For example, when attempting to study sleep state patterns in infants, the hospital environment and the invasive nature of the measurement probes may prevent the infant from sleeping normally. Attempting the same experiment in the infant's home, with suitable equipment for home based experiments, will decrease the experimental procedure artifact. Many of the experiments described in this thesis have been performed in the infant's home, partly for this very reason.

Considering the aim of this research has been to investigate the relationship between respiration and thermoregulation in normal sleeping infants, it has been desirable to collect as much information as possible. To investigate the maturation of this relationship it has been necessary to collect physiological signals from each individual infant over a number of weeks. The data from nine infants are presented here in order to help account for differences between individuals. Obviously this type of long term experiment cannot be performed in the hospital because of the expense of hospitalisation, the disruption to normal routines of the infant and the aforementioned experimental procedure artifact problems. Also, home experimentation has the advantage of having natural environmental conditions. One disadvantage is that the probes must be attached by the parents. The parents were also required to note important events such as feeds, spills, or if the infant was picked up during the night. Bedding, heating and other environmental details were also recorded each night. Data was only collected during night time sleep, therefore, the instrument probes were only required to be attached each evening before the infant was put to bed. Instruction was given to the parents on how to safely attach the instrument probes to their infant. *BabyLog* was used to collect and store the physiological signals.

Experiments were performed on infants who were siblings of SIDS victims, or infants who had previously had one or more *apparent life threatening events* (ALTE). No other significant abnormalities had been diagnosed in any of the infants. Infants of both the ALTE and siblings of SIDS groups would normally have been issued with a *Graseby* respiration monitor (see table 3.1). Therefore, a Graseby monitor was used to measure respiratory data for *BabyLog*. Ethical approval has now been obtained to perform similar experiments on normal healthy infants.

3.1.3 Infant Database

During 1991 the first major polygraph recording study of infants in their home environment was carried out. For this study, 9 infants were enroled following the guidelines outlined in section 3.1.2. In most cases, only respiratory waveforms, collected via a Graseby respiration monitor, and body temperatures were recorded. Thus, the experiment was as non-invasive and non-disruptive as practical. The age, period of recording and time of year of the recording can be examined in figure 3.5 for each infant. The wide range of all these variables is clearly demonstrated. Each line and associated initials represents a single infant. The length of each line, projected onto the horizontal axis, gives the approximate total number of nights of data recorded from each infant. The initials for the infants shown in figure 3.5 are used throughout the remainder of this chapter. For most of the infants, a small number of nights were not recorded during the period of study. There were several reasons for these breaks in recording, usually associated with unsettled behaviour of the infant or if the parents were away for an evening.

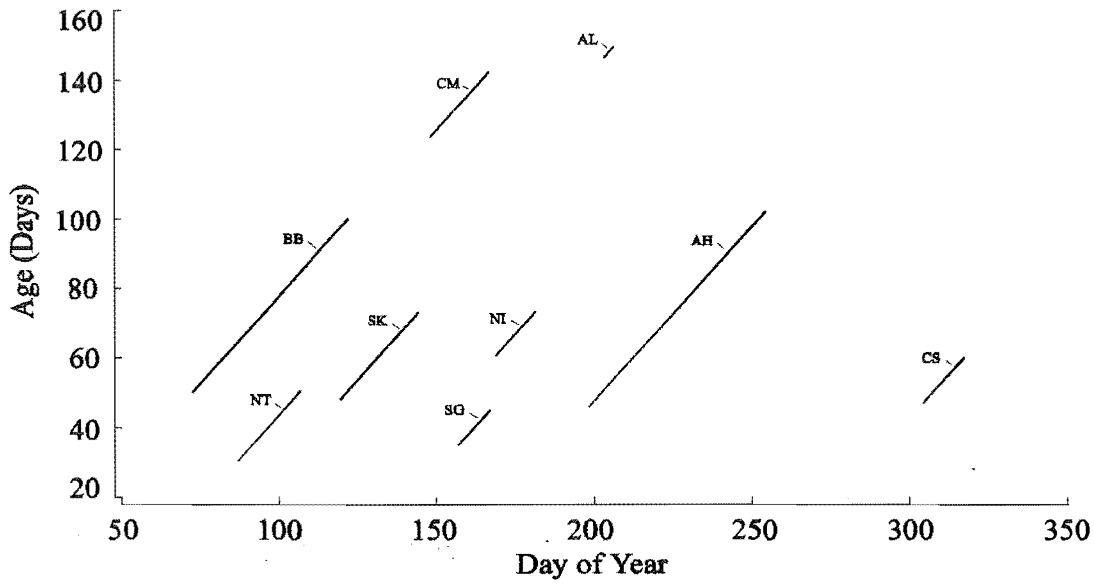

Figure 3.5 Age of each infant for each night of recording during 1991. Each line (and initials) represents an individual infant. The wide range of ages, recording period and dates of the recordings is evident.

Illness, in particular fever, alters human thermoregulation [Hensel, 1981, Section 14.4], therefore, only data collected while the infant was apparently free from illness is presented in this chapter. Consequently, the data is not confounded with complicated behaviour and can be considered as relatively normal.

The examples in the following sections use the data collected from the first night of infant "AH". However, all the respiratory data from all the infants has been processed in the same manner to enable subsequent quantitative analysis and to allow the results to be compared.

3.2 Preprocessing of Respiratory Signals

The nature of this research has required the comparison of signals with time constants in the order of minutes (body temperatures) to be made with signals which have much shorter time constants (respiration). A three hour recording of infant rectal temperature and respiration is presented in figure 3.6(a) and a 15 second section of this data in figure 3.6(b). Direct visual comparison of the signals presented in figure 3.6 is confusing. There is too much information within the 3 hour respiratory signal, most of which is redundant because the amplitude of the Graseby signal cannot be usefully calibrated (see section 3.1.1.1). The 3 hour graph of respiration is cluttered and un-interpretable, while the 15 second graph shows no long term temperature or respiratory trends. The mismatch between the signals is a result of the considerably different frequency components of the two signals, highlighted by the use of different sampling rates (see table 3.1). In addition, it is impossible to visualise the frequency components of the respiratory waveform when presented in this manner. Viewing and analysing long duration periodic signals which have high sampling rates, such as respiration or ECG signals, is time consuming and the waveforms are often difficult to interpret.

In order to make a mathematical correlation of respiratory and temperature signals, it is necessary to calculate the parameters of the respiratory signal which vary with the same frequency range as the temperature signal. Methods for calculating these parameters are presented in the following subsections.

For the purposes of this thesis, a signal *record* is an entire signal which is to be analysed, while an *epoch* is a small portion of that record.

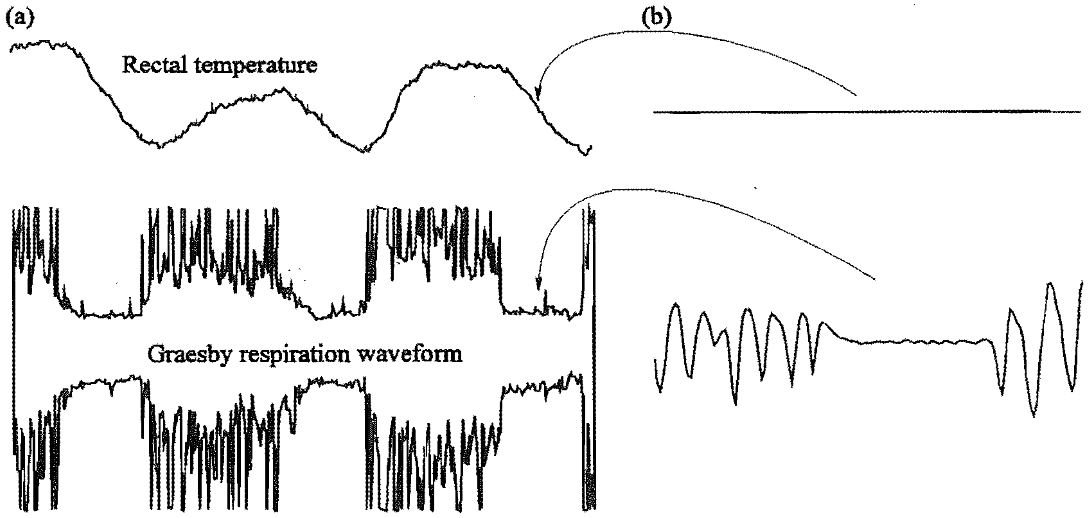

Figure 3.6 Typical rectal temperatures (top) and respiratory waveforms (bottom) from an infant: (a) 3 hour record, (b) 15 second epoch. Only the envelope of the respiratory signal is shown in (a).

3.2.1 Parameter evaluation of periodic signals

Parameter evaluation allows a complete overnight recording of periodic signals to be displayed as one clear image and provides for quick and easy analysis and interpretation of certain aspects of the data by the researcher or clinician.

Any stationary periodic signal may be reduced to a set of parameters which describe the amplitude, frequency and phase of the signal (see section 2.1.1.1). Consider a simple sinusoid, $g(t)$, which can be written as

$$g(t) = \alpha\cos(\omega t + \theta) . \tag{3.1}$$

The parameters of signals generated by this function are α, ω and θ, which are the amplitude, frequency and phase respectively. For a stationary signal these parameters are constant. For a non-stationary periodic signal, one or more of these parameters vary as a function of time. The frequency components of the parameter set are equal to those of the mechanism which produced the non-stationary behaviour. The time varying parameter set yields the same information as the original signal. Therefore, if the highest frequency component of the non-stationary mechanism is smaller than the highest frequency component of the signal, each parameter has a smaller bandwidth than the original signal. Parameter evaluation of periodic signals can therefore be used as a data reduction technique for signals with few frequency components of interest.

A breathing waveform, collected from a Graseby monitor (see figure 3.3(a)), is a typical example of a non-stationary signal which is suitable for this type of analysis. The signal is by no means a simple sinusoid, however, only the fundamental frequency is important because the harmonic content of the signal is dependent on probe placement and the transfer function of the measurement instrument and as such, the harmonics are of little value. Therefore, calculation of the breathing rate (the fundamental frequency) is sufficient to describe the frequency parameter of the signal. The amplitude of the respiratory waveform, collected from the Graseby monitor, is meaningless (see section 3.1.1.1) and therefore is not calculated from the breathing waveform. The phase of the signal is also of little use as there is no other signal to compare it with. If chest impedance was measured, then paradoxical breathing would be able to be identified from the phase difference between the chest impedance signal and the abdomen movement from the Graseby signal. Paradoxical breathing describes the situation when the abdomen moves in the opposite direction to the lungs and may occur if the airways are obstructed. In summary, only the breathing rate, calculated from the breath lengths is required.

Each peak of the Graseby waveform represents an inhalation. From this, the breath lengths have been measured using a simple peak detection algorithm. Peak detection was chosen over zero crossing detection (which may also be used to find the breath lengths) because the peaks of the Graseby signal are obvious and relatively free from noise (see figure 3.7). During apnoeic periods, the signal decays to zero where cardiogenic oscillations (heart movements picked up by the respiration monitor) become apparent. The range of frequencies for the breathing rate and heart rate overlap, thus frequency discrimination is inapplicable. Therefore, a zero crossing method would also require the amplitude of each peak in order to discriminate between the cardiogenic oscillations and breaths. Thus, peak detection has been chosen for this analysis.

Analysis of the respiratory waveform is divided into three consecutive steps, peak detection, breath length calculation and breathing rate calculation.

Peak detection: The peak detection algorithm operates as follows. All peaks and troughs are detected from the signal. A peak is considered to be a true representation of the start or end of a breath only if a valid trough has previously been detected and only if the peak is above a threshold which decays exponentially from the previous peak to a level which is above the maximum value of the cardiogenic oscillations (see figure 3.7(a)). Thus, two valid consecutive peaks cannot be detected unless a valid trough lies between them. It is assumed that the minimum breath amplitude is greater than the maximum amplitude of the cardiogenic oscillations. A similar criterion applies to the detection of troughs (the first sample of the signal record must be defined as both a valid peak and trough in order for the peak detection algorithm to succeed).

Breath lengths: The breath lengths are calculated from the time interval between each valid peak. Similarly, the breath lengths may also be calculated from the time interval between each trough, however, although this would provide

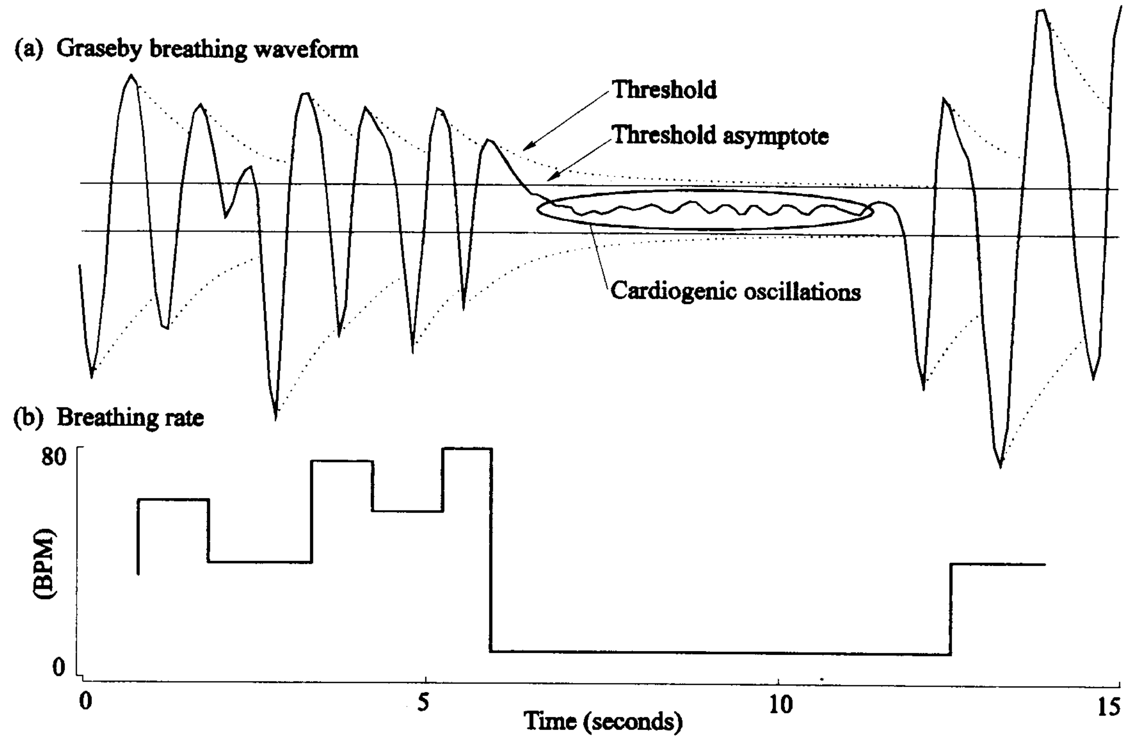

Figure 3.7 Breathing waveform to breathing rate conversion: (a) Graseby breathing waveform, (b) breathing rate calculated via peak detection of the breathing waveform and converted to breaths per minute (BPM).

additional information, it is not considered necessary.

Breathing rate: The breathing rate, calculated as the inverse of the breath lengths and converted to breaths per minute (BPM), is shown in figure 3.7(b). Because the breath lengths vary, the breathing rate is fixed over the entire period of each breath and then sampled at 1Hz. Therefore, the breathing rate waveform is comprised of a series of steps.

Figure 3.8 shows the breathing rate for a 9 hour respiratory signal. The signal is sufficiently long that the steps which occur at each breath are not obvious. Note the considerable variability of the signal.

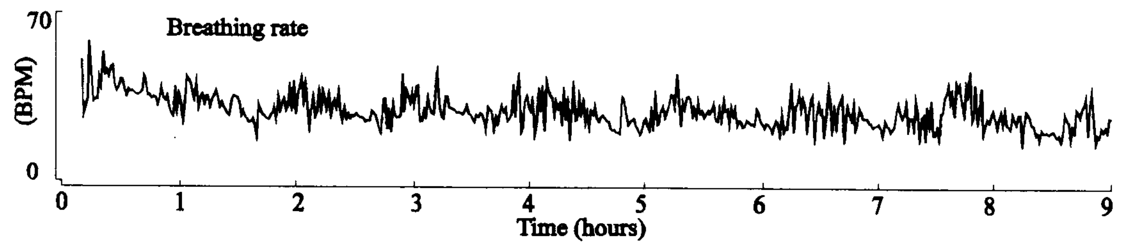

Figure 3.8 An example of a nine hour breathing rate signal, calculated from the breathing waveform of the first night recorded from infant "AH".

Any attempt to smooth the data assumes the underlying respiratory processes have a smooth behaviour and that any high frequency components are noise which has been introduced during measurement. The exact dynamics of respiration are unknown but are most likely to be non-linear. Therefore, any form of smoothing by linear filtering may remove vast amounts of information. However, when investigating the dynamics of the signal over short periods of time, linear filtering may clarify the signal behaviour. Over long periods, linear filtering may be of some benefit to ascertain overall trends, however, statistical estimates are often of more value. Statistical estimates are discussed in the following section.

3.2.2 Parameter estimates of random signals

Statistical evaluation of a stationary random process yields a parameter set which describes the behaviour of the data. This may include power spectral density, mean square, mean, standard deviation, median, range and probability density estimates. For a non-stationary random process, the parameter set varies with time.

In reality, statistical analysis can only be achieved if the signal is stationary. Therefore, a non-stationary signal must be divided into a series of epochs, each of which is assumed to be stationary. The accuracy and bandwidth of statistical estimates is determined by the amount of data available from each epoch. The amount of data is related to the length of the epoch.

Consider the result if the statistical estimate is made at every instant of time. Conceptually, this can be considered as performing the statistical evaluation on a rectangular window (or epoch) which is passed over the signal. If the estimate is the mean, $\mu(t)$, it is calculated as

$$\mu(t) = \frac{1}{T_e} \cdot \int_{t-\frac{T_e}{2}}^{t+\frac{T_e}{2}} g(\tau)d\tau , \tag{3.2}$$

where T_e is the epoch length. This is equivalent to multiplying $g(\tau)$ by a rectangular window function and evaluating the integral from $-\infty$ to ∞, therefore

$$\mu(t) = \frac{1}{T_e} \int_{-\infty}^{\infty} g(\tau)\,\mathrm{rect}(\tau - t)d\tau , \tag{3.3}$$

where

$$\mathrm{rect}(\tau) = \begin{Bmatrix} 1, & |\tau| \le T_e/2 \\ 0, & |\tau| > T_e/2 \end{Bmatrix} . \tag{3.4}$$

Since the rectangular windowing function is symmetrical about $\tau = 0$ then $\mathrm{rect}(\tau - t) = \mathrm{rect}(t - \tau)$. Thus (3.3) is a convolution resulting in

$$\mu(t) = \frac{1}{T_e} g(t) \odot \mathrm{rect}(t) . \tag{3.5}$$

Through a similar evaluation, it can be shown that the variance, $\sigma^2(t)$, over an epoch, T_e, which is passed over the data is also a convolution, viz

$$\sigma^2(t) = \frac{1}{T_e} [g(t) - \mu(t)]^2 \odot \mathrm{rect}(t) . \tag{3.6}$$

This is simply the power (or mean square) of the signal after subtraction of the mean, convolved with rect(t). As long as the statistical estimate is an integral function of the signal then a convolution with rect(t) will result. It is not possible to mathematically express equivalent convolution operations for median and interquartile range estimates. This is because the median and interquartile range are non-linear processes which do not incorporate an integration function. Since both mean and median are measures of central tendency and variance and interquartile range are measures of dispersion or spread, it is anticipated that median and interquartile range estimates would provide similar information to mean and variance estimates respectively. Assuming the data is symmetrical, the median is equal to the mean and if the distribution is normal, the interquartile range encompasses 50% of the data and the range between the first standard deviation either side of the mean encompasses 66.7%. Thus, equivalent information on the relative spread of the data is represented by the interquartile range or the standard deviation, σ, of a normal distribution.

The effect of calculating a continuous statistical estimate of the mean of a wide-band signal with a moving epoch is illustrated in figure 3.9. The signal depicted in 3.9(a) is convolved with the rectangular window of 3.9(c) to produce the estimate, shown in 3.9(e). The frequency responses of the signal, window and estimate, shown in 3.9(b), 3.9(d) and 3.9(f) respectively, illustrate the process in the frequency domain. Note that the narrow rect function in the time domain produces a wide sinc function in the frequency domain. High frequency components are attenuated and frequency components which are integer multiples of $1/T_e$ become zero. Thus, it is important that the highest frequency component of the signal, which is considered to be of value in the statistical estimate, is significantly less than $1/T_e$ (i.e. the estimate bandwidth is inversely related to the epoch length).

Replacing the rectangular windowing function (epoch) with any other windowing function will change the frequency components of both the mean and variance estimates (see section 2.1.2.1). Therefore, the appropriate window function must be chosen for the application. However, for median and interquartile range estimates, the window is restricted to a rect function because the rect function is inherent in the estimate calculation.

It is often more convenient to calculate the estimate at discrete intervals rather than continuously. This is particularly important for computation on digital computers, where a delay of L seconds between the start of each estimate epoch is required to sample the signal. The delay is equivalent to sampling the continuous statistical estimate at intervals of L seconds. Computation time, T_{COMP}, is inversely proportional to the delay, L, thus it is important to let L be as long as possible without degrading the signal estimate (see figure 3.9). The sampling

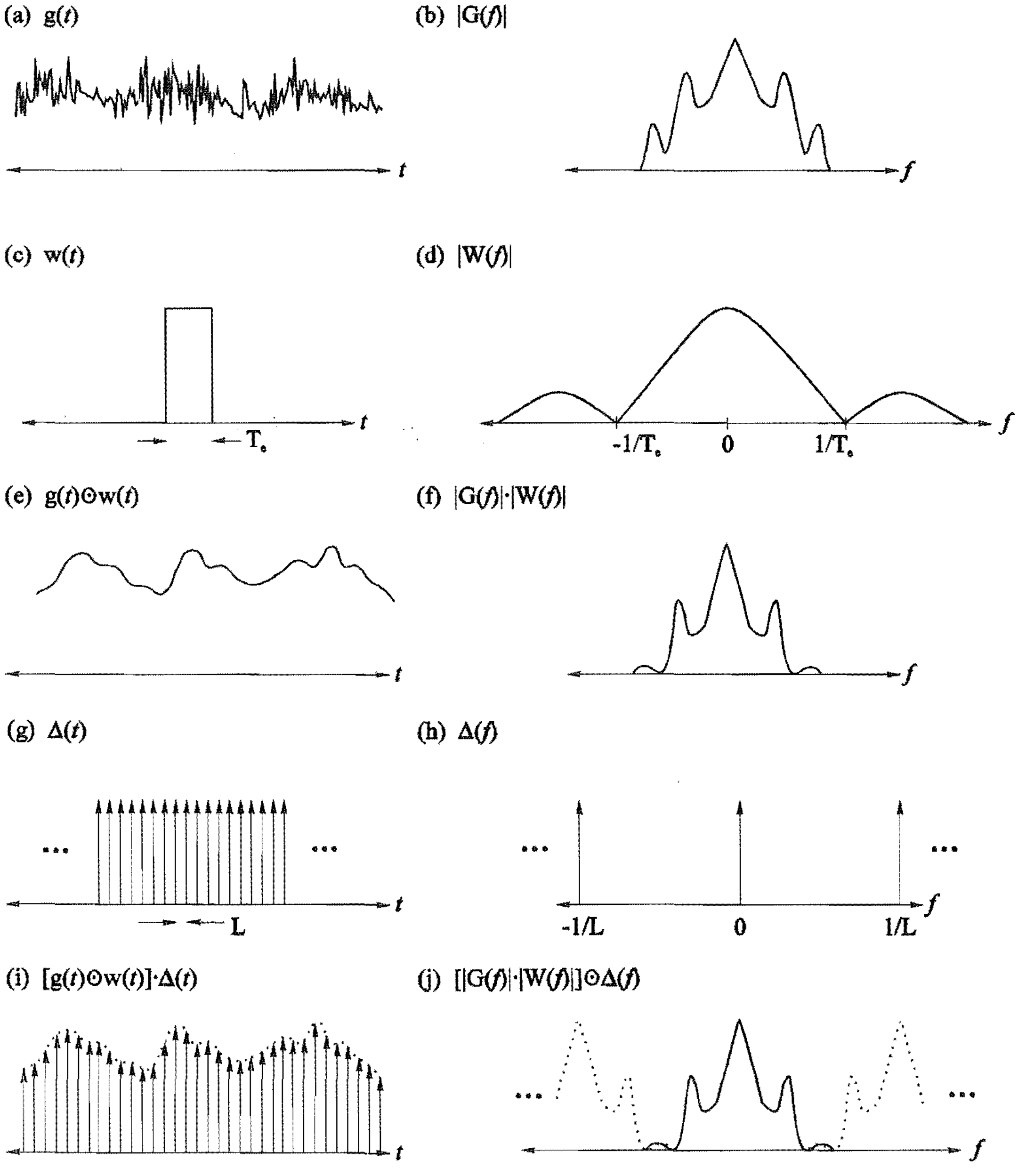

Figure 3.9 An illustration of parameter estimation of a signal: (a) A wide-band signal, (b) its spectrum, (c) the evaluation epoch rect function, (d) its spectrum, (e) the mean estimate obtained from the convolution of the signal with the rect function, (f) the estimate spectrum, (g) a sampling signal, (h) its spectrum, (i) the sampled estimate, (j) the sampled estimate spectrum.

function is shown in figure 3.9(g) and its spectrum in 3.9(h). Multiplication of the sampling function with the estimate yields the sampled estimate depicted in 3.9(i). This becomes a convolution in the frequency domain which results in the sampled estimate spectrum in 3.9(j). Obviously, if the estimate contains frequency components which are greater than half the new sampling rate then aliasing will occur (see section 2.1.2). However, this is unlikely for long epochs because the epoch window function behaves as a rough anti-aliasing filter. For the wide-band signal depicted in figure 3.9, the main lobes of the sampled estimate begin to overlap when the sampling period, L, is greater than half the epoch length, T_e. Ideally, the sampling period must be significantly smaller than half the epoch length to reduce the estimate error due to aliasing (overlapping side lobes of the rect function). Clearly, if the original signal, 3.9(a), was sampled by 3.9(g) the aliasing effects would be much larger.

In summary, both the bandwidth and the aliasing error of the estimate are inversely related to the epoch length. For discrete signals, the computation time is generally proportional to the sampling frequency, 1/L, and the epoch length, T_e, viz

$$T_{COMP} = \alpha \frac{T_e}{L}. \tag{3.7}$$

Thus, choice of the epoch length and sampling rate depends on the signal spectrum, bandwidth requirements of the estimate, accuracy requirements and available computer resources and is consequently highly subjective.

For estimates of the signal median and interquartile range (see section 3.2.2.2) it is likely that the required epoch lengths are less than those required for the mean and variance estimates respectively. This is because the median and interquartile range calculations are less sensitive to spurious or erroneous samples. Longer epochs are required for probability density estimates (see section 3.2.2.1) because events which seldom occur are of equal interest to those which occur frequently. Thus, a long epoch is required to collect sufficient samples of such events to produce a statistically viable estimate.

3.2.2.1 Probability density

The *probability density function* (PDF) describes the probability of every outcome of a continuous random variable. A variable such as the breath length or breathing rate can only be represented by an approximate PDF because the sampling process quantises the breath lengths to a resolution of 0.1Hz, forcing the variable to be discrete. The PDF must satisfy the following conditions on the probability, P, of each outcome, i,:

$$P_i \geq 0 \quad \text{for all } i,$$

$$\sum_{i=1}^{\infty} P_i = 1. \tag{3.8}$$

For the non-stationary respiratory signal, the discrete PDF is calculated by tabulating all breaths of the same length, for all possible breath lengths, to a resolution of 0.1 seconds. The discrete breathing rate PDF is calculated by multiplying each point in the breath length PDF by the corresponding breath length. Conversion of the dependent variable, breath length to breathing rate, is a simple inversion. However, because of the inversion, the new dependent variable (breathing rate) no longer has equally spaced resolution.

The distribution for each epoch of a record may be presented together to show the behaviour of the signal over time. This is shown in figure 3.10 where the breathing rate PDFs have been calculated from the respiratory signal which is divided into 20 minute epochs which overlap by 15 minutes. The rectal temperature is also shown for comparison. The non-stationary behaviour of the PDF and the correlation between the rectal temperature and respiration is clearly visible.

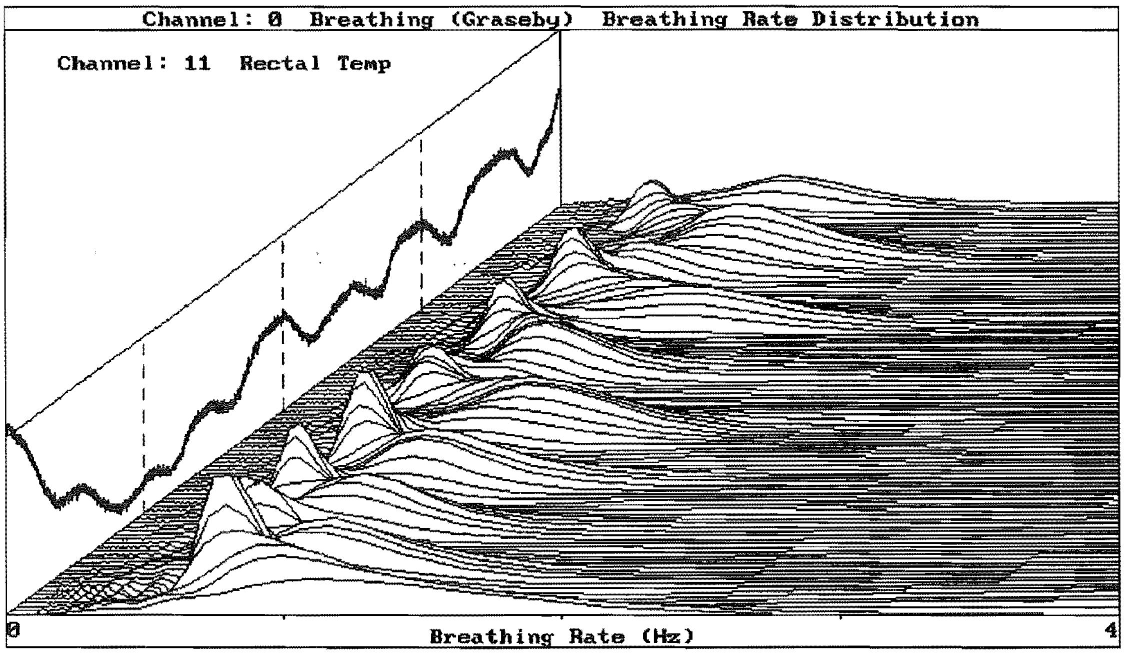

Figure 3.10 Three-dimensional computer screen plot of the breathing rate distribution for an entire night. The figure clearly shows variations in the breathing rate distribution over time.

Changes over time (non-stationary behaviour) of the central point of the breathing rate PDF are evident by the relative left to right position of the peak and changes in the spread of the data by the width of the distribution. Where the breathing rate is more variable (the low, wide regions), the central point of the breathing rate increases by a significant amount. The high peaks represent stable breathing. The PDF calculation technique forms the basis of a useful clinical evaluation tool but is of little use for detailed mathematical analysis.

The breathing rate PDFs depicted in figure 3.10 appear to be approximately normally distributed, therefore, calculating parameters which describe the distribution, such as the mean and variance, would also statistically describe the signal.

3.2.2.2 Median and interquartile range

The non-stationary PDF is a two-dimensional signal because it is dependent on the breathing rate in addition to time. As such, it cannot be directly correlated with one dimensional signals. However, one-dimensional parameters such as median and interquartile range, which describe the non-stationary PDF, can be calculated and correlated with other one-dimensional signals.

Median and interquartile range estimates have been chosen over mean and variance estimates because they are less sensitive to spurious errors in calculating the breath lengths. The median is perhaps a better measure of central tendency than the mean in many cases because the median is not significantly influenced by extreme values [Hines & Montgomery, 1980]. The apparent rapid breathing caused by movement artifact and the long apnoeic episodes caused by poor probe attachment are less likely to influence the median than the mean. The same argument holds for calculation of the interquartile range compared with the variance. The *breathing rate*, *median breathing rate* and *breathing rate interquartile range* signals are henceforth referred to as BR, MBR and IQBR respectively.

An epoch length of 300 seconds with a sampling period of 10 seconds has been chosen for calculation of the MBR and IQBR. Thus, any aliasing effects are minimised by the short sampling period in comparison to the epoch length and the bandwidth of the estimate will accurately resolve any frequency components having a period greater than approximately 10 minutes. The statistical estimates have been sampled at 1Hz so they may be displayed with other signals on the *BabyLog* system, although a sampling rate of 0.1Hz would be sufficient. At this stage, no attempt has been made to smooth the steps (see figure 3.7) between each epoch because the behaviour of the signal is clearly visible. The calculated MBR and IQBR are shown in figure 3.11.

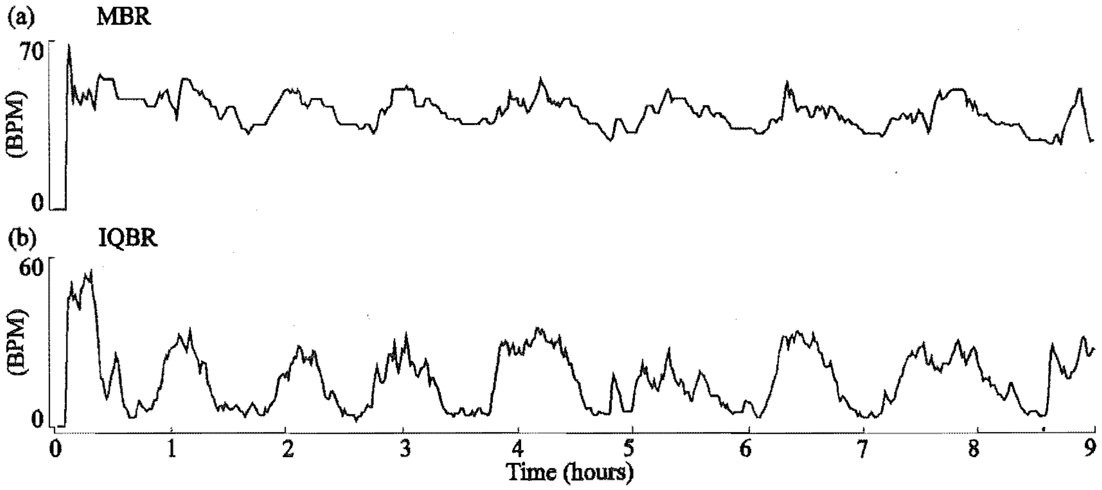

Figure 3.11 Calculated statistical estimates of a respiratory waveform: (a) Median breathing rate estimates, (b) breathing rate interquartile range estimates.

3.3 Quantitative Analysis Procedures

After retrieval of the data from the home of each infant, the BR, MBR and IQBR were calculated in the manner described in the previous section. Perusal of the collected and calculated data has yielded some interesting observations. Figure 3.12 depicts a typical recording of body temperatures and respiratory parameters from an infant.

In almost all recordings, a drop in rectal temperature occurred after the infant was put to bed. The magnitude of the drop varied between infants and across nights for an individual infant. The magnitude of the drop was normally less than 1°C. Oscillatory behaviour of the body temperatures, the MBR and the IQBR is evident in a large proportion of the recordings. The period of the oscillations was approximately 1 hour in all recordings. Note the large changes in IQBR for only relatively small changes in MBR in figure 3.12. The phase of the oscillations appears to differ between channels. For example, the peaks in MBR and IQBR appear to occur while the rectal temperature is rising. Both the drop in rectal temperature and the oscillatory behaviour are visible.

For the recording shown in figure 3.12, the forehead was subject to artifact, rendering the signal practically useless. This was found to be the case in many recordings, thus the use of the forehead probe was abandoned. The rising abdomen and shin temperatures can be explained by the addition of bedding when the infant is put to bed.

It must be reiterated that behaviour similar to that seen in figure 3.12 has been observed in the majority of infant recordings. Thus, a more detailed investigation of the data was deemed necessary so that the mechanisms of the observed behaviour may be studied. However, human expert analysis of such a large quantity of data is impractical. In order to present the collected data in a concise and compact form, it was necessary to computationally quantify the observed behaviour. For each night of the data collected from each infant the following parameters have been calculated as a measure of the behaviour of the signals:

- Median environmental temperature (T_{ENV})
- Median breathing rate (MBR)
- Change in rectal temperature after infant was put to bed (ΔT_{RECT})
- Median rectal temperature (T_{RECT})
- Period of the oscillations observed in temperature and respiratory signals
- Power of the rectal temperature, MBR and IQBR oscillations
- Correlation of respiratory and temperature signals

Each parameter is a single number describing a particular aspect of a signal over one entire night.

All the temperature and respiratory parameter signals to be analysed have a sampling rate of 1Hz. Prior to analysis of a complete overnight recording, all these signals have their sampling rates reduced to 1 sample per minute. This is achieved by averaging the 60 samples in each minute of data. The averaging process has two distinct purposes. Firstly, high frequency noise is eliminated from the data by the low-pass filtering effect of the averaging and, secondly, the reduced data set can be processed more efficiently. The averaging process behaves as a rough anti-aliasing filter prior to sampling at 1 sample per minute. Although the frequency spectrum of the filter is a sinc function (see section 2.1.1.3), which is far

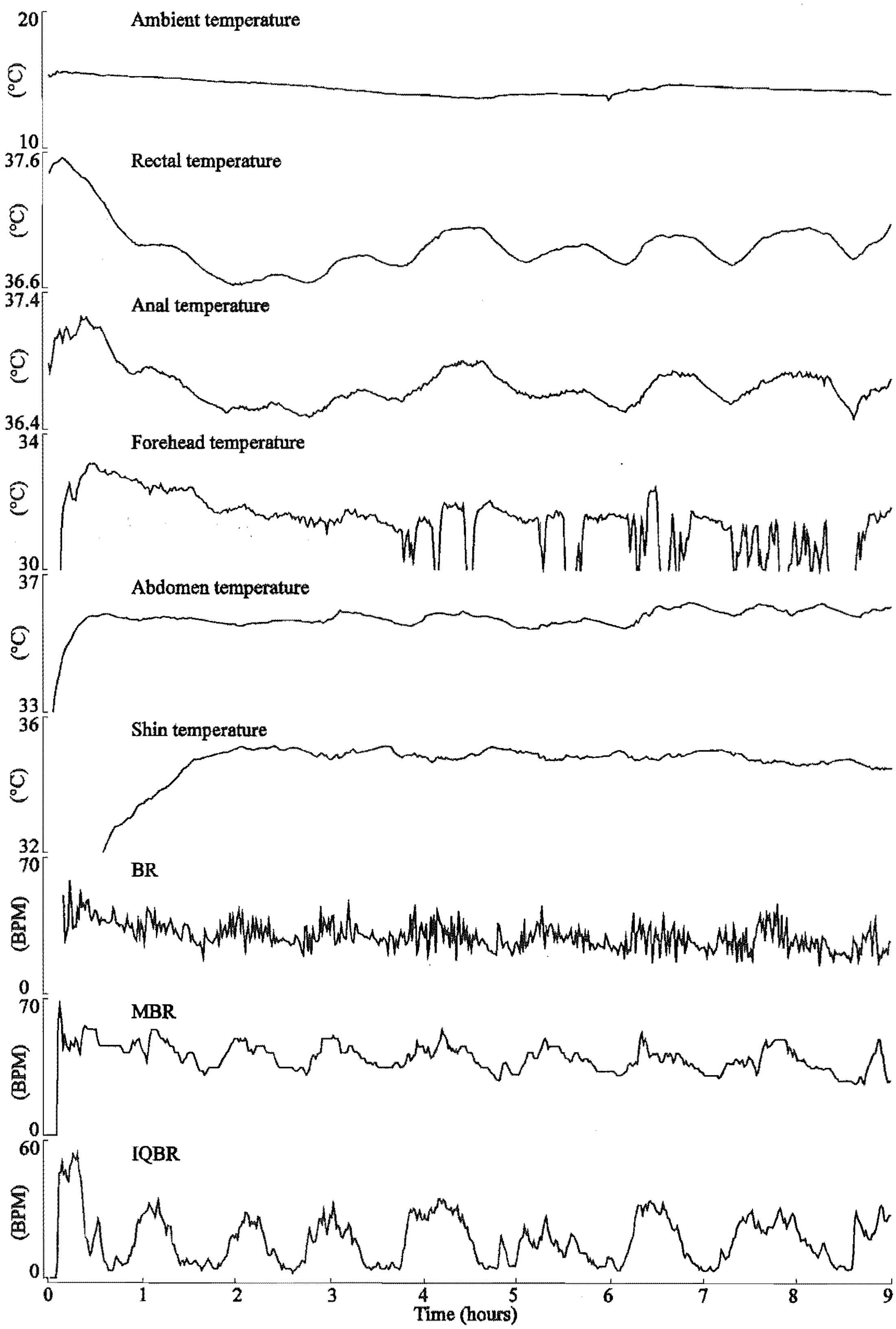

Figure 3.12 Temperature and respiratory data for the first night of recording from infant "AH".

from ideal for anti-aliasing, the dominant frequency components of the signals are much less than half the new sampling rate. The phase of the signal is not altered by the averaging process.

Analysis of the oscillatory behaviour of the body temperatures through spectral analysis or correlations requires the large low frequency components to be removed. Digital filtering has been employed to separate the frequency components by the application of ideal filter theory (see section 2.1.1.3). Considering the high frequency components have a maximum period of approximately 90 minutes, a filter with a cutoff frequency of $f_c = 1/(90*60)$ Hz has been used. For a discrete signal, the ideal filter impulse function, f[n], becomes

$$f[n] = \frac{2}{f_s}\mathrm{sinc}\left[2n\frac{f_c}{f_s}\right], \tag{3.9}$$

where f_s is the sampling frequency. Time domain convolution of the filter impulse function with the signal performs the low-pass filter operation (see section 2.1.1.1). Subtraction of the low-pass signal from the original yields the high frequency components. The filter does not alter the phase of the frequency components of the signal.

The finite record length of the filtered signals causes erroneous calculations to be made for the filter operations near the ends of the data. These errors have been significantly reduced by a modification to the convolution algorithm to account for the finite record length. This modification can be conceptually thought of as prepending the record with a time inverted copy of the first half of the record and appending the record with a time inverted copy of the last half of the record. The extended signal is then filtered by the convolution process, after which the prepended and appended portions are removed. The time inverted signal portions improve continuity at the signal ends. The result for the rectal temperature is demonstrated in figure 3.13. The oscillatory signal can then be analysed for period and magnitude and correlated with other signals. For the rectal temperature, the time varying offset (low frequency components) can be measured to obtain the change in temperature that occurs when the infant is put to bed.

The median environmental temperature and the change in rectal temperature can be directly calculated from the filtered data. The methods by which the remaining parameters are calculated are described in the following subsections. The numerical results are listed in the Appendix and graphical results are presented in section 3.4.

3.3.1 Power and period of the oscillations

The average power and frequency of a signal can be found directly from the power spectral density of the signal. The dominant frequency of the signal can be measured directly from the dominant peak of the power spectral density, while the average power is the integral of the function (i.e. the area under the curve on the graph) (see section 2.1.1.2). Figure 3.14 depicts the power spectral density of a typical breathing rate signal (after high pass filtering).

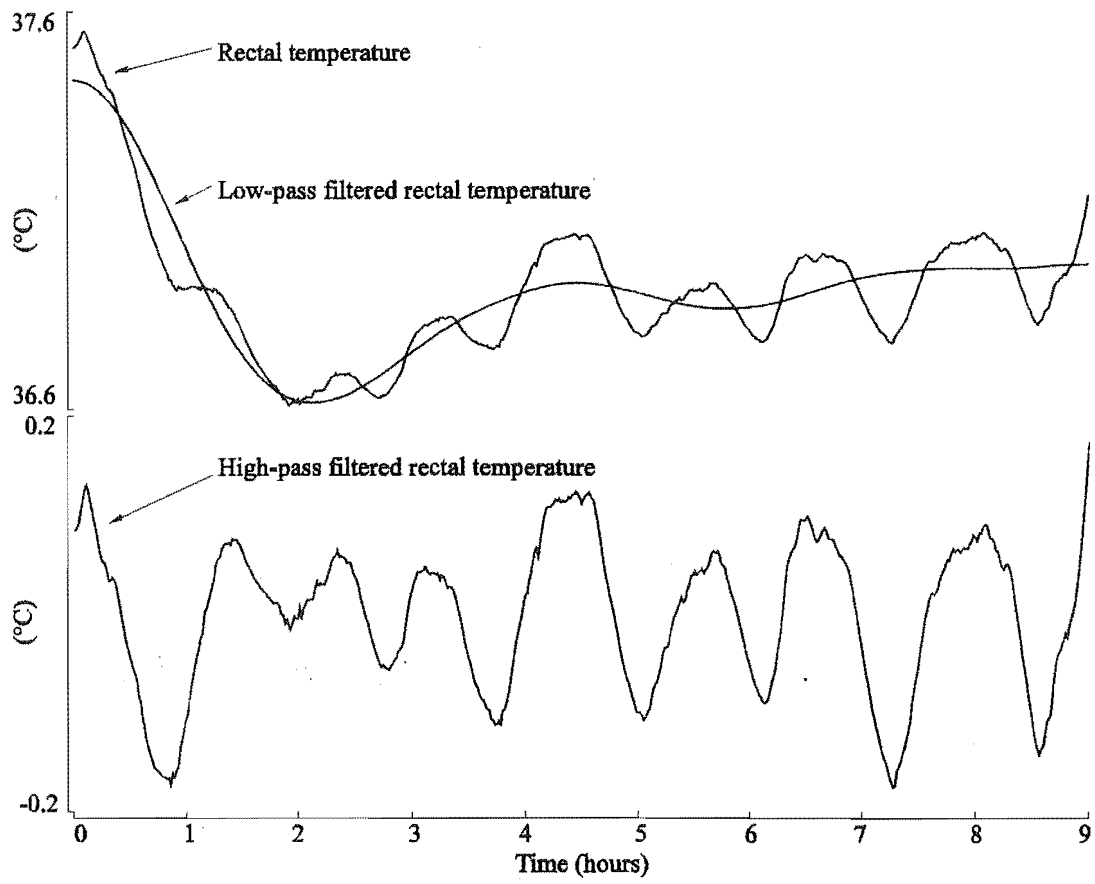

Figure 3.13 Filtering of the rectal temperature showing both the low-pass and high-pass components of the signal.

For this research, the period of the oscillations has been found from the peak of the power spectral density of the IQBR and, from observations of the signals, the period is the same for all the signals which show the oscillations. The power of the oscillations has been calculated directly from the mean square value of the high-pass filtered MBR, IQBR and rectal temperature. Although the average power incorporates the power of all harmonic frequency components of the signal, the power of any noise is also added, thus the power of the signal is unlikely to be zero, even when the oscillations are not present. The power of the signals can be used to help determine the nature of the oscillations by showing which conditions produce the greatest signal power.

3.3.2 Correlation analysis

The primary reason for correlating the respiratory and temperature signals has been to investigate whether the oscillations observed in each parameter are a result of a single mechanism and to provide evidence as to the causal nature of the oscillations. In particular, cross-correlation has been used here to identify the phase relationship between periodic signals. The shin and abdomen temperature

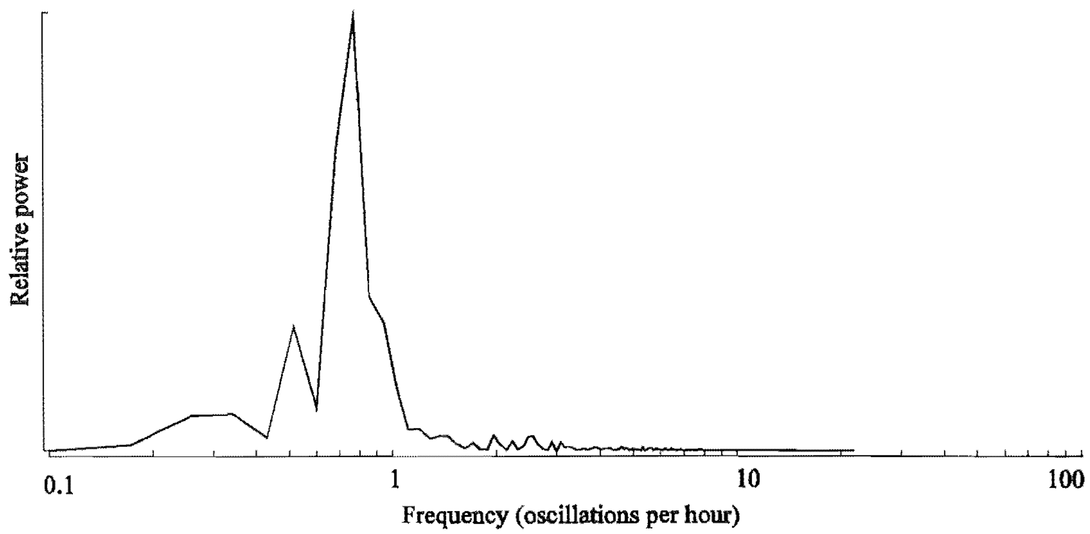

Figure 3.14 Power spectral density of the breathing rate. The horizontal axis is a logarithmic scale and the vertical axis shows the relative power (units not included).

signals have been correlated with the rectal temperature. The first derivative of the rectal temperature, calculated as the difference between each consecutive sample, has been correlated with the IQBR. The rectal temperature derivative has been used because, in all recordings where the oscillations were apparent, the rectal temperature increases while the IQBR and MBR are at a peak. A probable reason for this is that the IQBR represents heat input into the body and the rate of change of the temperature of a body of mass is proportional to the heat input. Thus, the first derivative of the rectal temperature is likely to be in phase with the IQBR. The cross-correlations have been normalised to be between -1 and +1, regardless of the magnitudes of the signals being correlated. This is achieved by dividing the cross-correlation function by the square root of the product of the mean square value of the two signals.

Figure 3.15 shows the cross-correlation of the rectal temperature with the shin temperature. From the cross-correlations of the recorded signals, the delay and correlation coefficient have been taken from the peak or trough which has the smallest delay (either positive or negative). A positive delay indicates the rectal temperature leads and a negative correlation coefficient indicates a decrease in a signal value for an increase in rectal temperature.

3.3.3 Insulation Properties

Quantitative measurement of the insulation effect of the mattress, bedding and bed clothes has been abandoned because of the lack of precise information on the calculation of the total effective insulation. Sleeping position, insulation of the mattress and the exact thermal properties of each type of bedding could not be collected to the accuracy which is necessary for calculation of the total effective insulation.

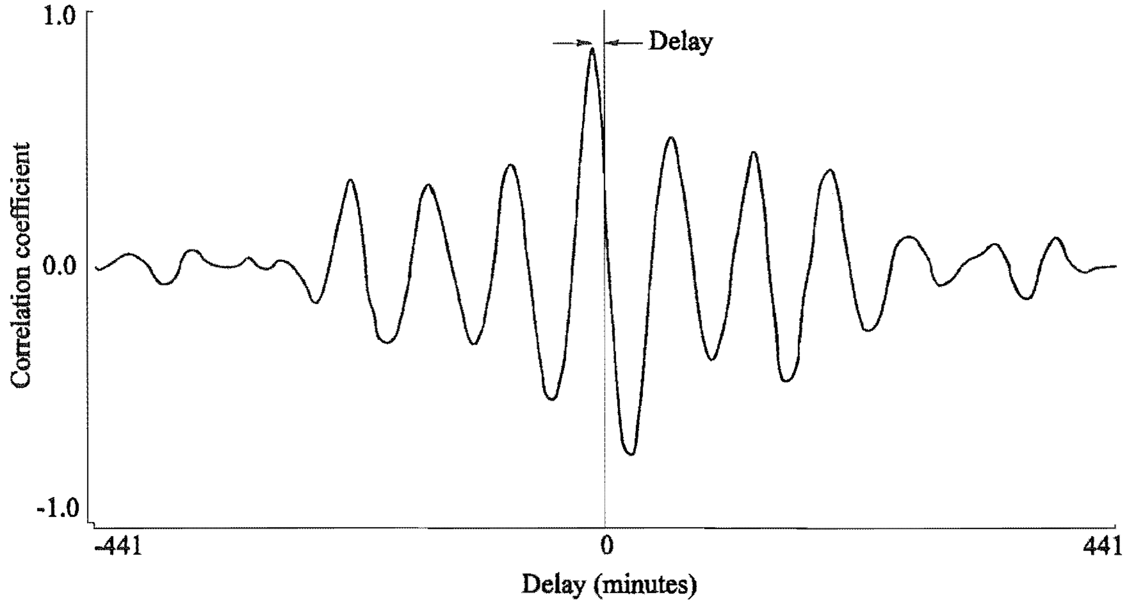

Figure 3.15 Cross-correlation of the rectal and shin temperatures.

To demonstrate the inaccurate nature of the total effective body insulation (tog value) evaluation, consider the effect of an infant in bed, who moves so that less of the body is insulated by the bed clothes. This may occur when an arm is moved from under the bed clothes or if the bed clothes shift.

The dry heat transfer, ϕ_{DHT}, from an area, A, of uninsulated skin is expressed as [Stolwijk & Hardy, 1966]

$$\phi_{DHT} = H_S \cdot A(T_S - T_{Env}) \quad W, \tag{3.10}$$

where T_S and T_{Env} are the skin and environmental temperatures respectively and H_S = 7.0 W/m^2/°C is the coefficient of heat loss from dry exposed skin. For insulated skin [Weatherall, 1983]

$$\phi_{DHT} = \frac{K_I \cdot A(T_S - T_{Env})}{I} \quad W, \tag{3.11}$$

where I is the insulation thickness, expressed in mm, and K_I = 36.0 W•mm/m^2/°C is the specific thermal conductivity of bedding insulation. Thus, the total dry heat transfer from an area of partially uninsulated skin, where μ is the fraction of exposed skin, is expressed as

$$\phi_{DHT} = A(T_S - T_{Env})\left[\frac{(1-\mu)36.0}{I} + \mu 7.0\right] \quad W, \tag{3.12}$$

Equating the dry heat transfer from completely insulated skin (3.11) to that of partially insulated skin (3.12), the effective insulation of the partially insulated skin, $\acute{I}$, can be investigated, viz

$$\frac{36.0A(T_S - T_{Env})}{I} = A(T_S - T_{Env})\left[\frac{(1-\mu)36.0}{\acute{I}} + \mu 7.0\right]. \tag{3.13}$$

Equation (3.13) can be rearranged to yield the ratio of the effective insulation to the completely insulated skin as

$$\frac{\acute{I}}{I} = \frac{(1-\mu)}{(1-\mu 7.0/36.0)}. \tag{3.14}$$

Thus, a commonly occurring event such as uncovering an arm of an infant or inconsistency of the position of the blankets on the infant's chest (μ = 0.05 to 0.10 [Lund & Browder, 1944]) is equivalent to a 4% to 8% decrease in insulation thickness. Thus, even if the tog values of each item of bedding are accurately known, the overall effective insulation cannot be accurately calculated for any period of time where the infant or bedding may move.

3.4 Analysis Results and Interpretation

The quantitative results, calculated for each individual night of recording from each infant are listed in the Appendix. The data is limited to the first significant sleep period of duration greater than 4 hours from each night where data was collected. Typically, the first sleep period of each night was the longest and the infant was more settled than at any other time, thus, the data from this period was least contaminated with artifact noise. Table 3.2 summarises the thermo-respiratory data for each infant individually and for the group as a whole.

The correlation results listed in table 3.2 indicate that the rate of change of rectal temperature is in phase with the IQBR because the correlation delays are very small. Thus, the rectal temperature oscillations probably reflect oscillations in the metabolic rate which are also reflected in the MBR and IQBR. Also, from table 3.2, the abdomen and shin temperature oscillations are in phase with the rectal temperature.

All the parameters listed in table 3.2 display large variations between consecutive nights (see the Appendix) resulting in a large variance in each parameter. Although, for a particular parameter, each individual infant has a different mean, the data values for each infant span a wide range and overlap significantly with the range of other infants. Furthermore, if each infant is considered in isolation, there is an insufficient number of samples to obtain useful results. Thus, the group data is an important indicator of trends which, due to the few samples, are not necessarily statistically significant in the data from individual infants. Some of the most interesting results are presented graphically in figures 3.16 through 3.19 for the combined group of infants.

Oscillatory behaviour of the rectal temperature, MBR and IQBR has been observed to varying degrees in all the infants studied. The age dependence of the oscillatory behaviour is presented in figure 3.16. The period of the oscillations, measured by way of power spectral analysis, is shown in figure 3.16(a). The median breathing rate, calculated over the entire recording, is shown in 3.16(b). The power of the high-pass filtered rectal temperature, MBR and IQBR signals

Parameter			Infant									
			BB	SG	AH	SK	CM	AL	CS	NT	NI	Group
Age (days)		S	50	35	46	48	124	133	47	30	60	30
		F	96	41	96	72	145	146	60	50	73	146
MEDIAN T_{ENV} (°C)		μ	17.58	14.55	14.97	14.57	13.77	20.73	16.53	20.05	11.06	16.32
		σ^2	2.21	0.70	1.17	1.31	1.42	2.21	1.50	1.47	1.01	3.00
MEDIAN BR (BPM)		μ	29.51	27.37	32.08	40.54	26.69	24.13	35.32	36.13	28.07	31.64
		σ^2	2.70	0.84	3.13	3.17	2.66	0.87	1.00	1.74	1.97	5.16
MEDIAN T_{RECT} (°C)		μ	36.73	37.13	36.95	36.67	36.36	36.91	37.52	36.85	36.77	36.83
		σ^2	0.24	0.09	0.21	0.08	0.28	0.07	0.13	0.13	0.08	0.31
DROP ΔT_{RECT} (°C)		μ	-0.29	-0.18	-0.58	-0.44	-0.71	-0.86	-0.40	-0.22	-0.52	-0.45
		σ^2	0.19	0.11	0.49	0.19	0.17	0.19	0.17	0.16	0.29	0.25
Oscillation	Period (minutes)	μ	70.59	60	70	68	60	57	57	91	60	68
		σ^2	37	9	11	11	19	8	6	15	6	18
	POWER $T_{RECT}\times10^3$ (°C²)	μ	4.13	2.40	5.89	9.46	6.49	6.94	4.21	3.35	6.49	5.46
		σ^2	2.21	1.53	2.65	3.92	2.97	1.85	1.94	1.30	5.02	3.21
	POWER BR (BPM²)	μ	7.42	5.48	17.27	41.28	6.66	5.17	14.76	16.84	13.44	14.81
		σ^2	4.56	2.48	7.24	11.05	2.21	10.18	3.77	5.27	9.23	12.17
	POWER IQBR (BPM²)	μ	30.45	13.25	31.88	71.34	15.25	9.03	18.32	70.43	18.69	35.33
		σ^2	16.53	5.79	14.43	24.01	3.65	2.06	6.57	21.07	4.62	25.86
Correlation	$dT_{RECT}/dt \otimes$ IQBR	R	0.56	0.66	0.49	0.67	0.52	0.75	0.66	0.49	0.70	0.58
		D	3	-2	0	0	10	-1	0	1	1	0
	$T_{RECT} \otimes T_{ABDO}$	R	0.60	0.69	0.64	0.79	0.67	0.63	0.75	0.65	0.67	0.67
		D	-1	0	-2	-5	-6	-10	-5	-1	-2	-3
	$T_{RECT} \otimes T_{SHIN}$	R	0.61	0.50	0.54	0.59	0.55	0.66	0.55	0.55	0.65	0.58
		D	-1	0	5	8	-11	1	-1	4	-8	1

Table 3.2 Summary of physiological signal behaviour recorded from nine infants. S = start, F = finish, μ = mean, σ^2 = variance, R = median correlation coefficient, D = median delay (mins).

is shown in 3.16(c), 3.16(d) and 3.16(e) respectively (this is a measure of the power of the oscillations). The mean, the 95% confidence interval of the mean and the standard deviation of the data are shown in the figure. The statistics in figure 3.16 have been calculated by dividing the data into a series of age groups, two weeks in duration. Each age group overlaps the preceding and following age groups by one week. For example, the 10 week age group includes data from infants ranging in age from 9 to 11 weeks. The number of samples in each group varies considerably, however, the grouping width has been selected to ensure that sufficient samples are in each group to reduce statistical errors. The overlapping of the groups helps to produce a smooth trend by interpolating between what would otherwise be widely spaced points.

The period, BR, MBR oscillations and IQBR oscillations all appear to decrease with age. The decrease in breathing rate with age agrees with results reported in the literature [Godfrey, 1981]. The age dependencies of the MBR oscillations and IQBR oscillations are hardly surprising since they are intimately related to the breathing rate. In contrast, the power of the rectal temperature oscillations appears to increase to a small extent with age. The age dependence of the period is relatively insignificant when the large standard deviation of the entire data set is taken into account.

When interpreting the data, one must consider the relative importance of each age group given the different confidence interval of each age group. In most cases, age group data which appear to deviate from a simple overall trend often have wide confidence intervals. The only parameters which show clear trends are the power of the MBR and IQBR oscillations. The means and standard deviation of these signals clearly decrease with age. Considering the different age range and small number of infants studied, it is hardly surprising that trends in the data are not strikingly obvious. If the infants matured at different rates then any maturational trends in the data would be hidden by the wide variance of the data.

The dependence of the average rectal temperature on age is shown in figure 3.17. The rectal temperature decreases only to a small extent with age. The reduction in average rectal temperature for the entire age range of 5 to 21 weeks is small compared with the variance of the rectal temperatures at any specific age. Thus, the rectal temperature is taken to be independent of age. Consequently, the rectal temperature may be a useful measure of the thermal state of the body for any age. Although the combination of environmental temperature and thermal insulation is probably a more direct measure of the thermal stresses placed on each infant, the thermal insulation cannot be measured with sufficient accuracy to provide a reliable indication of the thermal stress placed on the body (see section 3.3.3). The rectal temperature has been accurately measured but may be affected by other physiological conditions such as fever and digestion.

The dependence of the oscillatory thermo-respiratory behaviour on the median rectal temperature of the record is presented in figure 3.18 with the same parameters that are shown in figure 3.16. The statistics have been calculated for groups of data covering a range of 0.3°C, overlapping by 0.2°C with both the preceding and following group. For example, the 36.45°C group contains data from infants with a rectal temperature ranging from 36.3°C to 36.6°C. Figure 3.16 indicates that the period of the oscillations is not significantly related to the rectal temperature, however, the breathing rate appears to increase with rectal temperature. More significantly, the means and standard deviations of all the parameters, except the period, show a significant peak between approximately 36.5 and 36.8°C. The peaks occur at rectal temperatures which are fractionally lower than the mean rectal temperature of 36.83°C (see table 3.2). The peak in the power of the MBR oscillations is not as significant as in the power of the oscillations of other parameters. In the rectal temperature oscillations, the peak is possibly hidden by the first two data points, both of which have wide confidence intervals. Table 3.2 shows the relatively large variance of rectal temperatures for

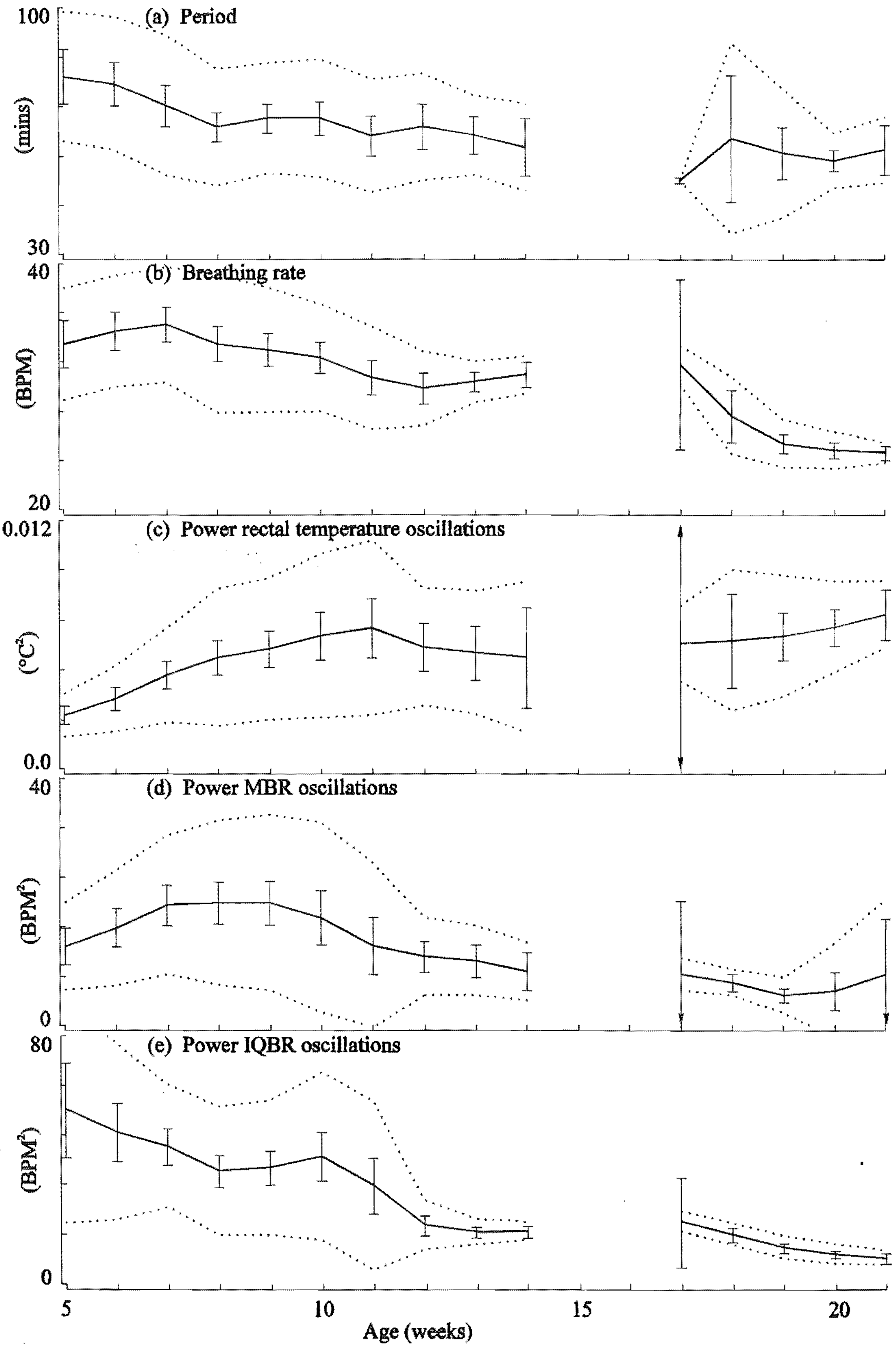

Figure 3.16 Age dependence of the infant physiological behaviour. Error bars show the 95% confidence intervals and the dotted lines show one standard deviation either side of the mean.

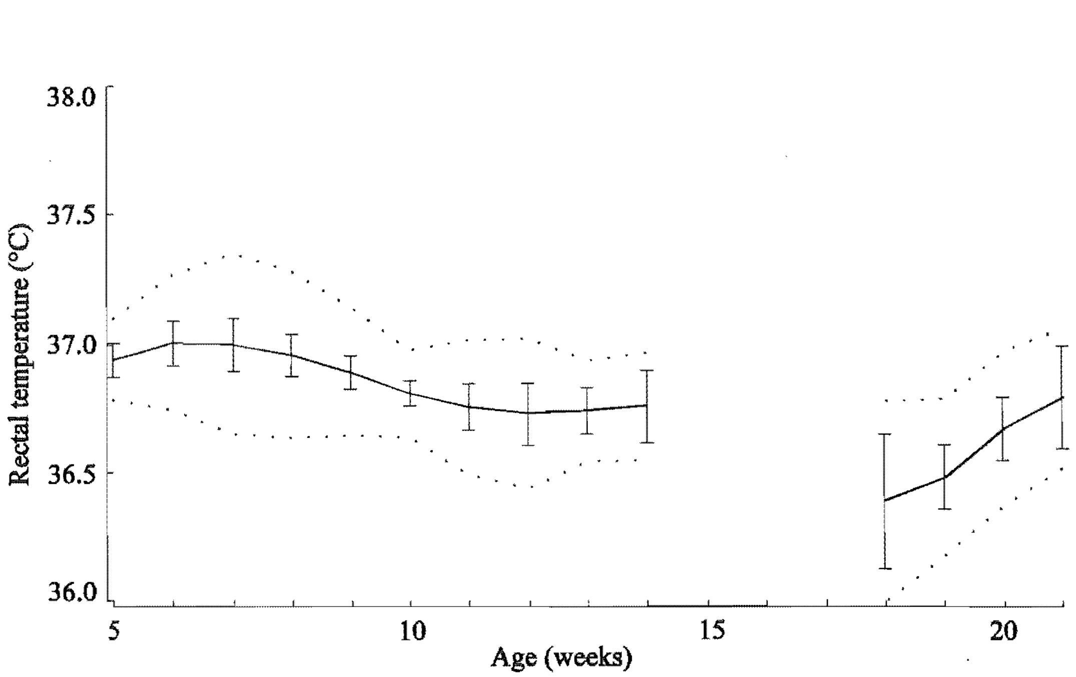

Figure 3.17 Relationship of rectal temperature with age. The error bars show the 95% confidence intervals and the dotted lines show one standard deviation either side of the mean.

each infant, thus, each data point represents information from many of the infants. Therefore, the peak in each parameter is not due to the extreme values of one individual infant. The width of the peak is probably wider than that expected in each individual infant because of inter-individual differences in mean core body temperatures.

The large standard deviation of each parameter in figure 3.18, Particularly around the peak, probably reflects the dependence of the oscillations on other variables such as age and inter-individual differences. Although the standard deviation is very large around the peak, the confidence interval remains relatively narrow. The power of the oscillations is greatest when the rectal temperature of the infants is close to the mean rectal temperature of the entire data set from all the infants (i.e. the oscillations may be normal behaviour for an infant in what could almost be considered as ideal thermal conditions).

To some extent, the rectal temperature probably reflects the temperature of a thermogenic region of the body since blood returning from muscles in the legs passes close to the rectum. This would account for the high breathing rate associated with high rectal temperatures during periods of high metabolic activity. If the infant was in a cool environment, then metabolic thermogenesis would produce additional heat which would be indicated by a rising rectal temperature. The increased breathing rate would be due to the increased oxygen required for thermogenesis. The fact that the rectal temperature rises during the peak of the MBR oscillations (see figure 3.12 and the correlation results in table 3.2) is further evidence to support the hypothesis that rectal temperature reflects thermogenesis in the body. Therefore, in many circumstances, a rectal temperature just below average probably reflects a warm thermal load and a rectal temperature just above average probably reflects a cool thermal load. If the environmental temperature

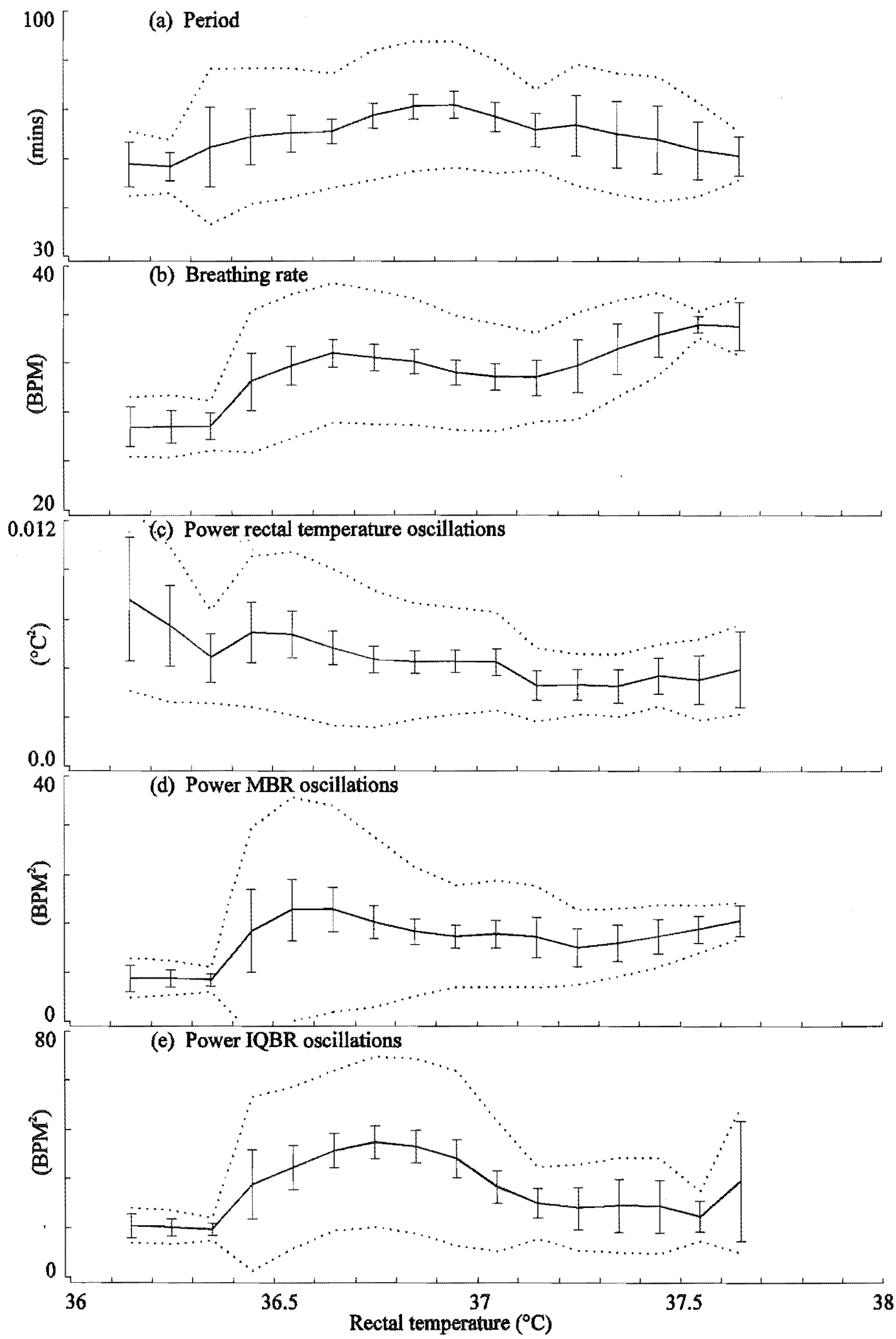

Figure 3.18 Dependence of physiological signals on rectal temperature. The error bars show the 95% confidence intervals and the dotted lines show one standard deviation either side of the mean.

is excessively cool or warm, such that the body is unable to thermoregulate satisfactorily, then the rectal temperature is most likely to follow trends in the environmental temperature.

The drop in rectal temperature which occurs when the infants are put to bed is presented in figure 3.19. As the infants mature, the magnitude of the drop in rectal temperature increases. This agrees with data collected from other researchers [Wailoo et al., 1989; Lodemore et al., 1991], although the significance of the drop is not clear. The most likely explanation is that the rectal temperature drop is due to a reduction in metabolic rate which occurs when the infant is put to bed. If this is indeed true, then this result provides more evidence that the rectal temperature reflects thermogenesis in the body. As such, the magnitude and velocity of the drop are likely to be influenced by the thermal mass of the infant, thermal insulation and level of activity of the infant prior to going to bed.

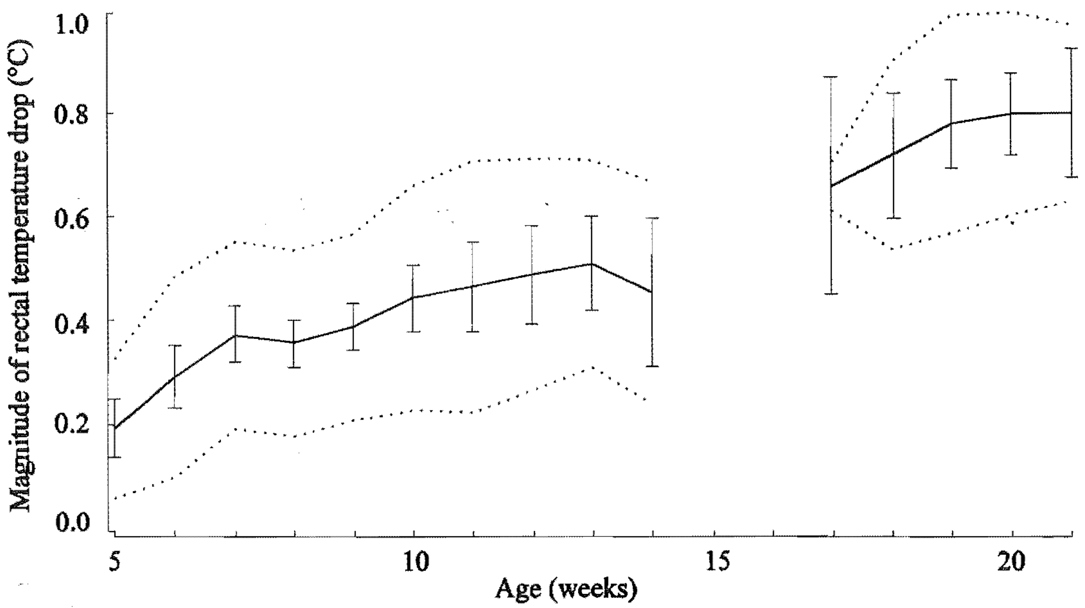

Figure 3.19 Drop in rectal temperature for each age. The error bars show the 95% confidence intervals and the dotted lines show one standard deviation either side of the mean.

For all the trends observed in the data, there is a relatively large standard deviation (see figures 3.16 through 3.19). This indicates that, although a trend may appear to be significant with respect to the confidence interval, there are normally other confounding variables which influence the trend, thus demonstrating the high degree of coupling between the systems within the body.

3.5 Discussion

The benefits of analysis tools, developed through engineering principles and applied to physiological experiments, has been demonstrated in this chapter. A number of useful results have been obtained that would have been difficult or impossible to achieve without the application of engineering techniques to the clinical research.

The data presented in this chapter has been produced via a number of innovative and computationally intensive algorithms. The heavy dependence on computer collection and analysis of the data reflects the difficult problem of processing physiological signals collected from subjects in their natural environment and where none of the physiological systems under investigation have been isolated or uncoupled from the rest of the body. Although computer analysis is generally less accurate than human expert analysis, processing the huge amount of data presented in this chapter by human experts would be impractical, if not impossible, particularly when preprocessing the respiratory data. Computer analysis is consistent but any analysis errors are likely to obscure trends in the data, particularly if the recorded signals are noisy.

The logistical difficulty of performing home based clinical experiments on infants and the difficulty of finding suitable infants with cooperative parents has limited the number of infants studied in the first year to nine, with a total of 162 nights of useful recordings. Within the data there is a gap in the age range around 15 weeks. Although a relatively large number of recordings have been used for the analysis, only nine infants were involved, therefore, inter-individual differences are likely to cloud the data. In order to reduce statistical errors in the data, a larger sample of infants is required, including infants around 15 weeks of age.

Every effort has been made in the design of analysis algorithms to reduce noise or analysis artifact. Data medians have been calculated where possible to avoid spurious data elements affecting the results. Rectal temperature measurements have been taken in addition to skin surface temperatures because of their greater accuracy in determining a measure of core body temperature [Brown et al., 1992]. The invasive nature of the experiments has been minimised to attempt to reduce experimental procedure artifact, thus, the data has been collected from infants in their normal environment. Therefore, the infants are only placed under extreme thermal loads on rare occasions and unintentionally. Considering this, the results obtained yield a surprising wealth of information for the small thermal loads placed on the infants.

From the observed body temperatures and respiratory variables of the infants, there are various patterns or trends in behaviour that are clearly defined and predictable. In particular, oscillatory thermo-respiratory behaviour and a drop in rectal temperature that consistently occurs after an infant is put to bed has been observed. The coincidence of IQBR and MBR oscillations has also been observed. This behaviour is as yet unexplained. Further clinical experimentation or modelling could be employed to investigate this behaviour in more detail.

An increase in the steady state ventilation rate of humans is normally associated with an increase in the metabolic rate since the purpose of ventilation is to supply O_2 and remove CO_2 from the metabolising tissue (see section 1.3). Even though the breathing rate is not a direct measure of the ventilation rate, under normal circumstances a change in ventilation rate is directly reflected by a similar change in the breathing rate [Mead & Agostioni, 1964]. Therefore, a change in breathing rate normally reflects a similar change in the metabolic rate. Ideally, tidal volume should be measured to help identify the ventilation and metabolic rates. In the experiments performed with the current technology, measurement of the tidal volume was considered to be too invasive. Thus, the lack of accurate assessment of the ventilation rate is a limiting factor to the conclusions which may be drawn from the data.

In this research, oscillations of the MBR, IQBR and the first derivative of the rectal temperature, which occur during sleep, have been found to be in phase. Thus, the peak of the MBR and IQBR oscillations occur where the rectal temperature is rising with maximum gradient. The rising rectal temperature is most likely to be a result of the increased metabolic rate, since an increase of heat input into a body of mass will cause its temperature to rise. However, for this to be the case, the rectal temperature must be a relatively direct measure of a region of the body which is being heated. This leads to the hypothesis that the rectal temperature measures the temperature of a region of the body which is directly heated by metabolic thermogenesis.

The regularity of the thermo-respiratory oscillations suggests that there is some form of controlling mechanism which is an oscillator. This mechanism would need to be intimately related to respiration and metabolic heat production in order to produce the observed trends. Considering that the response time of the thermoregulatory system of the body is in the order of minutes, it is conceivable that the observed thermo-respiratory oscillations may be due to unstable thermoregulation. This would explain both the oscillations in body temperatures and breathing rate signals. The occurrence of oscillations in the IQBR could possibly be explained by the sensitivity of the stability of the respiratory system to the state of thermal control. This seems possible because respiration is intimately related to thermoregulation through the metabolic rate.

Measurement of the head core temperature (approximated by either the tympanic or oesophageal temperature) would provide a wealth of additional information to the rectal temperature measurements. Head core temperature measurement would help to validate the hypotheses that the thermo-respiratory oscillations are due to marginally stable thermoregulation. Considering that the head core temperature is one of the variables upon which thermoregulation is dependent (see section 1.2.1), then if thermoregulation was unstable, one would expect to find oscillations of the head core temperature which are in phase with the respiratory variables (thus 90° out of phase with the rectal temperature). In which case, the oscillations would clearly be a result of the time required for the heat produced in the thermogenic regions on the body to travel to the head core.

In order to further investigate infant thermo-respiratory behaviour and to test the hypothesis developed in this discussion, mathematical models of infant thermoregulation and respiration have been developed. These models are presented in the following chapters and, once validated in this thesis, they enable the mechanisms which cause the behaviour presented in this chapter to be investigated.

Chapter 4

Mathematical Modelling of Human Thermoregulation

The history of mathematical modelling of human thermoregulation is discussed in this chapter. Following this, a model for thermoregulation of the human infant is developed in detail. This model is an adaption of a model which has previously been proposed and thoroughly investigated [Stolwijk & Hardy, 1966; Stolwijk, 1970]. Enhancements of the Stolwijk and Hardy model, included in this chapter, have been developed to further investigate the observed behaviour of infant body temperatures during sleep (see Chapter 3). In addition, an insulation layer has been incorporated into the model to simulate an infant in bed.

4.1 Adult Thermoregulation Models

The apparent capability of humans to survive in a relatively wide range of thermal extremes (see Section 1.2) has enticed many researchers to investigate, model and simulate thermoregulation physiology. Many scientific papers have been published regarding thermoregulation and the thermal properties of the body, including a variety of models which have been proposed.

4.1.1 Single element models

The first mathematical models of the human thermal system considered only a single element, representing an isolated section of the body such as a limb. During 1948, Harry Pennes published experimental results regarding the thermal distribution within the human biceps [Pennes, 1948]. In the same paper he presented a model of equilibrium heat flow in the human forearm and compared the behaviour of the model with his experimental results. The Pennes model considers a single cylindrical mass element and imposes the following conditions:

- Conduction of heat in the radial direction of the cylinder only.
- Uniformly distributed production of metabolic heat and blood flow distribution in the tissue.
- Convection of heat by the circulating blood.
- Heat loss from the uninsulated surface of the cylinder by convection, radiation and evaporation.

A mathematical statement of the first law of thermodynamics was employed by Pennes to model the radial flow of heat in the cylinder. Given the normal human forearm temperature, T, the metabolic heat production, ϕ_{MR}, and heat transfer due to local blood flow, ϕ_{Bl}, the mathematical expression which describes the model is as follows

$$-K\left[\frac{d^2T}{dr^2}+\frac{1}{r}\frac{dT}{dr}\right] = \phi_{MR} + \phi_{Bl}, \tag{4.1}$$

where K is the specific thermal conductivity of tissue and r is the radial distance from the centre of the cylinder. The terms on the left hand side of (4.1) represent the rate of heat conduction in the tissue. The boundary condition which must be applied to (4.1) is that the rate of heat transfer to the skin surface is equal to the rate of heat loss from the skin surface and is expressed mathematically as

$$-K\left[\frac{dT}{dr}\right]_{r=a} = H(T_S - T_{Env}), \tag{4.2}$$

where H is the coefficient of thermal heat loss from the skin surface, a is the radius of the skin surface, T_S is the skin temperature and T_{Env} is the environmental temperature. In addition, the heat transfer due to local blood flow in the tissue was defined to be a function of the difference between the tissue temperature and the temperature of the arterial blood, T_a,

$$\phi_{Bl} = \dot{Q}C_{Bl}(K-1)(T-T_a), \tag{4.3}$$

where $\dot{Q}$ is the volumetric blood flow and C_{Bl} is specific thermal capacity of blood.

Pennes solved the model analytically to provide a steady state solution for the radial temperature distribution in a single element. Although the model was designed for and tested on the human forearm, the model is essentially applicable to any cylindrical element of the body.

A model which considered only the core and average skin temperature was proposed in 1947 [Machle & Hatch, 1947]. In a similar manner to the Pennes model, Machle and Hatch formulated an equilibrium heat flow equation, however, they based their model on the rate of change of heat content of a single element, where the temperature was assumed to be homogeneous throughout the element. The rate of change of heat content of the element was equated to the metabolic heat production, ϕ_{MR}, minus the rate of heat loss to the environment through respiratory water vapour loss, ϕ_{Resp}, and convection, radiation and evaporation from the skin, ϕ_S. Thus

$$C_t m \frac{d(\bar{a}T_R + \bar{b}T_S)}{dt} = \phi_{MR} - \phi_S - \phi_{Resp}, \tag{4.4}$$

where C_t is the specific thermal capacity of tissue, T_R is the rectal temperature and T_S is the skin temperature. Heat loss through the skin was expressed as a function of skin and environmental temperatures and water vapour pressures. Note that $\bar{a}$ and $\bar{b}$ are weighting factors which sum to unity.

The single differential equation (4.4) of the Machle and Hatch model can be used to predict skin temperatures in the unsteady state for conditions of skin wetness, local metabolic rate and environmental temperature and water vapour pressure. Machle and Hatch analytically solved their model for constant values of metabolic rate, environmental temperature and respiratory heat loss, however, their model proved to be unable to predict skin temperatures in most circumstances because of difficulties in determining skin wetness [Kerslake & Waddell, 1958].

In 1958, Kerslake and Waddell extended the Machle and Hatch model to include the case of complete skin wetness [Kerslake & Waddell, 1958]. Results obtained by Kerslake and Waddell indicated that their model provided a satisfactory description of the changes in skin temperature with time.

4.1.2 Multi-compartment models

Wyndham and Atkins approximated a region of the human body by a cylinder consisting of a number of thin coaxial shells [Wyndham & Atkins, 1960]. Each coaxial shell compartment was described by an equilibrium heat flow equation representing the transient heat conduction in a shell

$$\rho_t C_t \frac{\delta T_i}{\delta t} = \frac{1}{r}\left[\frac{\delta}{\delta r}\left\{Kr\frac{\delta T_i}{\delta r}\right\}\right] + \phi_{MR,i}\,, \tag{4.5}$$

where i denotes the i^{th} compartment and ρ_t is the density of tissue. The left hand side of (4.5) represents the rate of accumulation of thermal energy and the right hand side represents the rate of heat conduction plus the rate of heat generation by metabolic reactions. The Wyndham and Atkins model consists of a set of first order differential equations (one for each coaxial shell compartment of the cylinder) and was solved on an analog computer by assuming that the rate of heat transfer between any two adjacent shells is proportional to the temperature difference between them. The following boundary conditions are assumed:

- At the centre of the cylinder, the temperature profile is symmetrical (i.e. the temperature gradient is zero).
- At the surface of the cylinder, the rate of heat loss to the surroundings is the sum of heat losses to the environment due to convection, radiation and evaporation.

The Wyndham and Atkins multi-shell model is capable of calculating a thermal distribution and transient response for a single region of the body.

Since 1961 Eugene Wissler has developed a series of mathematical models of the entire human body. In his earliest model, which is a direct extension of the Pennes model [Pennes, 1948], Wissler divided the body into six parallel compartments: the head, torso, two arms and two legs [Wissler, 1961]. For each compartment, Wissler made the following assumptions:

- Conduction of heat in the radial direction of the cylinder only.
- Uniformly distributed metabolic heat generation and blood supply.
- Isotropic thermal properties of the tissue within each cylinder.

The steady state equilibrium heat flow equation of the Pennes model, (4.1), was applied to each compartment such that

$$K\left[\frac{d^2T_i}{dr^2}+\frac{1}{r}\frac{dT_i}{dr}\right]+\phi_{MR,i}+\dot{Q}_i\rho C_{Bl}(T_{a,i}-T_i) = 0, \tag{4.6}$$

where ρ is the density of blood. Equation (4.6) states that the sum of the rate of conduction of heat into a unit volume, the rate of metabolic heat generation and the rate of transfer of heat from blood to the capillary bed in the compartment is equal to zero. The boundary condition of the Pennes model, (4.2), which states that the rate of heat transfer to the surface of the skin through the tissue is equal to the rate at which heat is transferred from the surface of the skin to the environment, is also applied to each compartment.

The compartments are coupled through the circulatory system (the third term in (4.6)). The six venous streams from each compartment are mixed to produce an arterial stream at an intermediate temperature, T_a. The counter current heat exchange which occurs between the large arteries and adjacent veins is also included into the blood flow heat transfer dynamics of the model. Thus, the temperature of the arterial blood entering the capillary bed of each compartment, $T_{a,i}$, can be found from T_a. Wissler solved this model analytically for the steady state for various environmental conditions.

As an extension of the Wyndham and Atkins model, Wissler developed an unsteady state model for the six compartments: the head, torso, two arms and two legs [Wissler, 1963]. Each of these parallel compartments are further divided into two thin coaxial shell compartments representing bone and tissue, covered with a layer of fat and skin.

In contrast to Wissler's earlier model, a differential heat flow equation was used to describe the heat flow in each shell compartment of each cylinder. For the i^{th} compartment of the model, the heat flow equation is

$$\rho_t C_t\frac{\delta T_i}{\delta t} = K\left[\frac{\delta^2 T_i}{\delta r^2}+\frac{1}{r}\frac{\delta T_i}{\delta r}\right]+\phi_{MR,i}+\dot{Q}_i\rho C_{Bl}(T_{a,i}-T_i). \tag{4.7}$$

This equation represents the transient counterpart of the steady state heat conduction described by equation (4.6). The difference between equation (4.7) and equation (4.5), the heat flow equation of the Wyndham and Atkins model, is that Wissler incorporated an additional term, $\dot{Q}_i\rho C_{Bl}(T_{a,i} - T_i)$, representing heat transfer by local blood circulation. Wissler solved his model with the boundary condition

$$-K\left[\frac{\delta T}{\delta r}\right]_{r=a_i} = H_i[T_i(a_i,t)-T_{Env,i}]. \tag{4.8}$$

Similar to Wissler's previous model, the circulatory system couples each element of each compartment.

Wissler produced an additional model which considered the body as 15 parallel cylinders [Wissler, 1964]. He solved the equations with a finite difference method where the radius of each element was divided into 15 points. Although Wissler's models consider many important thermal properties of the body, they do not incorporate any thermal regulation mechanisms.

4.1.3 Thermoregulation models

In contrast to the Wyndham and Atkins model, Crosbie and coworkers utilised the configuration of a slab of infinite length and width (finite thickness) [Crosbie et al., 1963]. The slab is divided into three layers, representing the skin, muscle and core of the body. A differential equation is employed to describe the equilibrium heat flow for each layer of the slab

$$\rho_t C_t \frac{\delta T}{\delta t} = K \frac{\delta^2 T}{\delta x^2} + \phi_{MR} - \phi_{Resp} - \phi_S \,, \tag{4.9}$$

where x is the distance from the side of the slab which represents the core of the body. Heat loss to the environment by radiation, convection and evaporation is from the skin layer and excess metabolic heat input (from exercise) only occurs in the muscle layer.

The most important feature of this model is that it includes properties of thermal control. The metabolic rate, ϕ_{MR}, peripheral heat loss, ϕ_S, and the coefficient of thermal conduction, K, of the model are defined to be functions of the mean body temperature, T_B, thus forming the first model of human thermoregulation. The controller equations are as follows:

If T_B is greater than basal

$$\begin{aligned} K &= K_0 \left[1 + \alpha_K + \Delta T_B + \gamma_K \frac{dT_B}{dt} \right] \le 1.7 K_0 \,, \\ \phi_{MR} &= \phi_{MR,0} + \phi_{EX} \,, \\ \phi_S &= \phi_{S,0} + \delta_{EX} (\alpha_S \Delta_B + \lambda_S \Delta T_B^4) \le 50 \phi_{S,0} \,. \end{aligned} \tag{4.10}$$

If T_B is less than basal

$$\begin{aligned} K &= K_0 \left[1 + \alpha_K - \Delta T_B + \gamma_K \frac{dT_B}{dt} \right] \ge 0.56 K_0 \,, \\ \phi_{MR} &= \phi_{MR,0} - \alpha_{MR} \Delta T_B + \phi_{EX} \,, \\ \phi_S &= \phi_{S,0} \,. \end{aligned} \tag{4.11}$$

The subscript 0 denotes a basal value, ϕ_{EX} is exercise heat and α_K, γ_K, α_S, λ_S and α_{MR} are constants. The model was simulated on an analog computer giving the transient response of an uninsulated, thermoregulating human.

In 1966, Stolwijk and Hardy proposed a model of human thermoregulation which considered the body as three cylinders: the head, trunk and extremities [Stolwijk & Hardy, 1966]. Each cylinder was further divided into coaxial shells. The head was divided into skin and core, the trunk into skin, muscle and core and the extremities cylinder into skin and muscle. A central blood compartment, representing the pool of blood in the core of the body was also included. It was assumed that heat flow between two adjacent shell compartments is by conduction and that all shell compartments exchange heat with the central blood compartment. Heat exchange between the skin and the environment is by conduction, convection, radiation and evaporation. For each shell compartment, i, the temperature was assumed to be constant within that compartment, thus, the equilibrium heat flow equation is described by

$$\begin{aligned} m_i C_t \frac{dT_i}{dt} &= \alpha \rho C_{Bl} \dot{Q}_i (T_{Bl} - T_i) + \phi_i - \phi_{Resp} \\ &+ \frac{(T_i - T_j)}{R_{ij}} - \frac{(T_k - T_i)}{R_{ki}} \\ &- H \cdot A_i (T_i - T_{Env}) - L \cdot A_i (E_{Ins,i} - E_{Sw,i}) , \end{aligned} \tag{4.12}$$

where j and k are adjacent shell compartments and L is the latent heat of sweat vaporisation. Respiratory heat loss was assumed to occur only from the head core and trunk core shell compartments. Thermoregulation was achieved by defining the evaporative heat loss, ϕ_{Sw}, change in skin blood flow, $\Delta\dot{Q}_S$, change in muscle blood flow, $\Delta\dot{Q}_M$, and the change in metabolic rate of the muscle, $\Delta\phi_{MR}$, to be functions of the head core, average muscle and average skin temperatures. The controller equations of the Stolwijk and Hardy model are as follows:

$$\begin{aligned} \phi_{Sw} &= \alpha_{Sw}(T_{HC} - 36.6)(T_{\bar{S}} - 34.1) + \beta_{Sw}(T_M - 35.88)(T_{HC} - 36.6) \geq 0 , \\ \Delta\dot{Q}_S &= \alpha_S (T_{HC} - 36.6)(T_{\bar{S}} - 34.1) + \beta_S (T_{\bar{S}} - 34.1) \geq 0 , \\ \Delta\dot{Q}_M &= \alpha_M \int_{t_1}^{t_2} (\Delta\phi_{MR} + EX - \beta_M MBF_W) dt + \gamma_M (T_{\bar{S}} - 34.1) \geq 0 , \\ \Delta\phi_{MR} &= \alpha_{MR}(T_{HC} - 36.6)(T_{\bar{S}} - 34.1) \geq 0 . \end{aligned} \tag{4.13}$$

The symbols α_{Sw}, β_{Sw}, α_S, β_S, α_M, β_M, γ_M and α_{MR} are constants. The control equations of (4.13) are limited by the following conditions: An increase in sweat rate and skin blood flow occurs only when both the skin and head core temperatures are greater than zero. Similarly an increase in muscle metabolism and blood flow occurs only when both the head core and average skin temperature are below zero.

The model was simulated on an analog computer and was validated with experimental data obtained from naked human adults. Stolwijk extended the model to 25 cylinders and removed the dependence of the thermal control equations on muscle temperature. He performed simulations of this new model on a digital computer [Stolwijk, 1970].

Wyndham and Atkins extended their model of temperature distribution in a multi-shelled cylinder to incorporate aspects of thermal control [Wyndham & Atkins, 1968]. Similar to the Stolwijk model, they defined the thermal control equations for muscle metabolic rate, blood flow and sweat rate to be functions of the core and skin temperatures.

A thermoregulation model proposed by Werner was developed to consider variables of human thermoregulation to be regarded as functions of time and of three-dimensional local coordinates within the human body [Werner, 1977]. Thus, the geometry and anatomy of the body have to be considered in great detail to obtain a useful prediction from the Werner model. The dynamic temperature profiles predicted by this model are difficult to validate because of ethical issues concerning the nature of the experiments required to obtain such data. Models consisting of lumped parameters [Crosbie et al., 1963; Stolwijk & Hardy, 1966] are generally simpler to simulate and validate compared to the Werner model.

Considering the vast quantities of data on thermoregulation and the large number of mathematical models that have been proposed over the past 50 years, there is a notable deficit of models which attempt to investigate infant thermoregulation.

4.2 A Mathematical Model of Infant Thermoregulation

The model described in this chapter is based on negative feedback control. It consists of the controlled system (*plant*) which describes heat flow within the body tissues and heat loss from the body surface. A *controller* is included which adjusts heat production (metabolism and muscle blood flow) and heat loss (skin blood flow and sweating) according to body temperature. The model is illustrated in figure 4.1. Parameters for the model including body dimensions, basal metabolism, blood flows and controller characteristics are adjusted according to age. This is discussed further in section 4.3.1. Time is the independent variable of the following equations which describe the infant thermoregulation model. In the interest of notational simplicity, explicit dependence of the variables on time is suppressed.

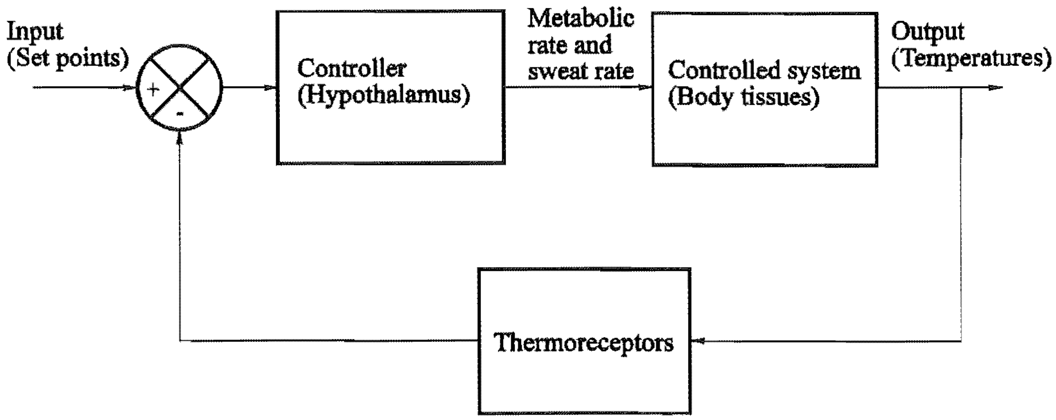

Figure 4.1 Schematic diagram of human thermoregulation showing the negative feedback control structure of the system.

4.2.1 Heat flow in the body

Figure 4.2 shows the form of the model of the controlled system. The model also includes the insulating effect of bedding which reduces heat loss from the trunk.

The human structure is modelled by two cylinders, representing the head and the rest of the body. No attempt has been made to consider the extremities (arms and legs) separately. This is because there is a considerable lack of precise information on the blood flow and metabolism of the extremities of infants when considered in isolation from the rest of the body. Consequently, for this model of infant thermoregulation, the extremities are combined with the trunk. This also simplifies the development of the model. For a first approximation of infant thermoregulation, the combination of the extremities and the trunk is not of major importance considering the small size of the extremities of infants in comparison to the trunk [Lund & Browder, 1944]. Note also, that while sleeping, the extremities are in close proximity to each other and the trunk, reducing the effective surface area and increasing the thermal coupling between the extremities and the trunk.

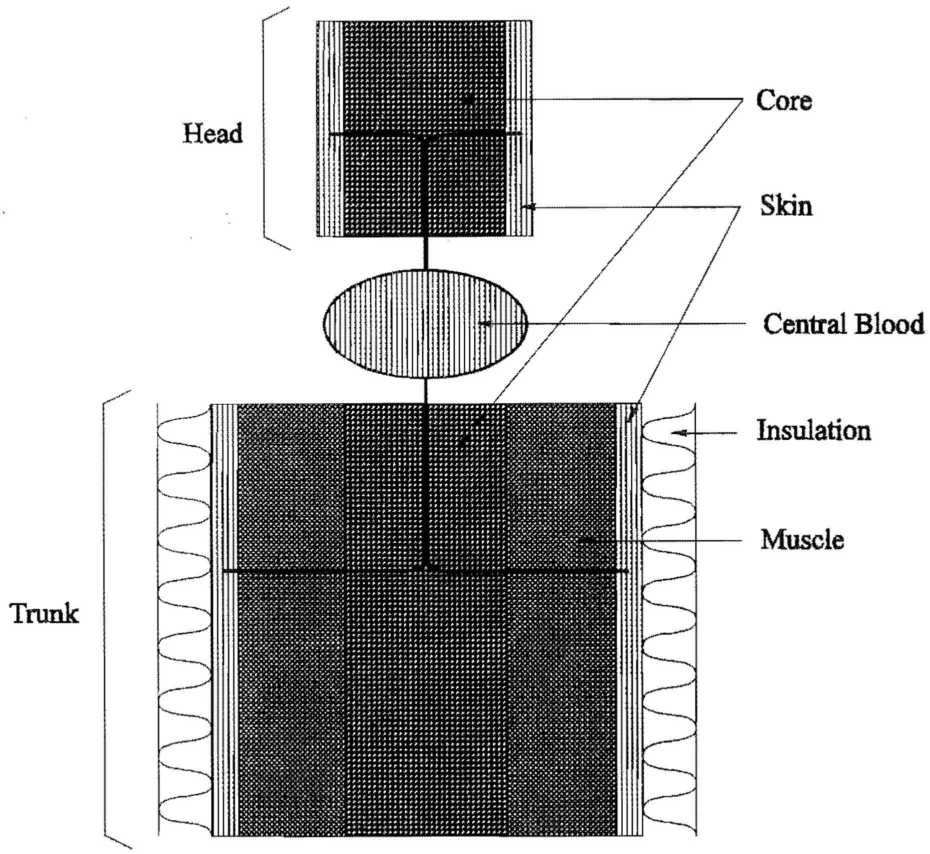

Figure 4.2 Illustration of the controlled system of the human thermoregulation model. The body is divided into the head and trunk which are further divided into concentric compartments where heat flows radially.

The head is divided into two coaxial shells (compartments) representing the skin and the core of the head. Similarly, the trunk is divided into three coaxial shells, the skin, muscle and core compartments. Each compartment of the model is a store of heat. The transfer of heat between compartments occurs through conduction to adjacent compartments and convection through the blood to other compartments. A central blood compartment that performs heat exchange with body tissues is also incorporated into the model and is connected to all other compartments through the circulatory system (see figure 4.2). The trunk muscle compartment incorporates the thermogenic effect of the muscles and brown adipose tissue and may therefore be considered as the thermogenic compartment of the model.

The following mathematical equations for the controlled system of the model describe the flow of heat in each region of the model. Conduction, convection, radiation and evaporation are all important mechanisms by which heat is transferred through the body and to the environment.

Conductive heat flow is considered to occur radially between each coaxial compartment in the model. For simplicity, heat flow through the ends of the cylinders is not directly considered, however, the length and radius of the head and trunk cylinders are calculated in order to preserve longitudinal surface area and volume to be the same as that of the human infant. The volume of a cylinder is $\pi r^2 l$ and the area is $2\pi rl$ where r is the radius and l is the length. Therefore, by substitution (ignoring the cylinder end surfaces) $r = 2V/A$ and $l = A^2/(4\pi V)$ where A is the surface area and V is the volume. Consequently, anatomical values for surface area and volume will yield the radius and length for the head and trunk. Each coaxial compartment radius can then be calculated such that the volume of the skin, muscle and core is preserved.

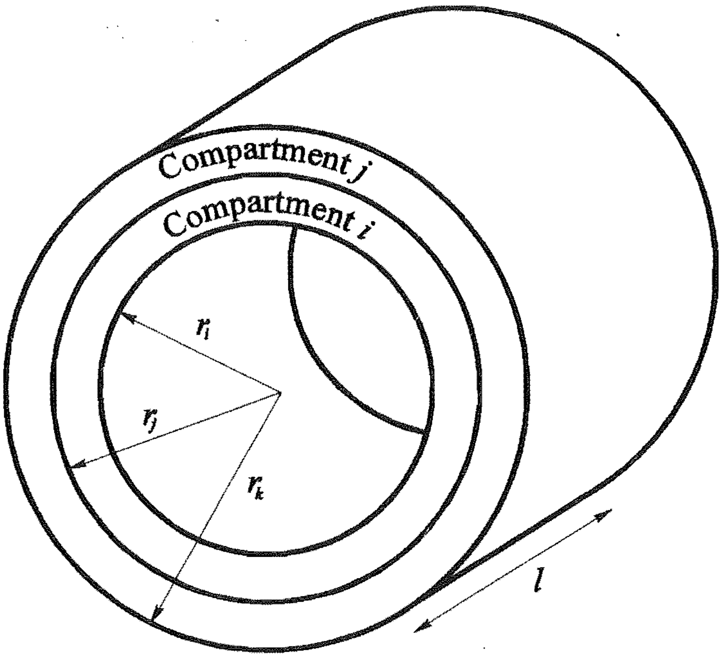

Figure 4.3 Coaxial compartment notation showing the inner radius of each compartment, r_i and r_j respectively and the overall outer radius, r_k. l is the length.

Resistance to conductive heat flow, R_{ij}, between any two coaxial compartments of either the head or trunk, the notation of which is illustrated in figure 4.3, is calculated by

$$R_{ij} = \frac{\Delta r_{ij}}{K_t A_{ij}} \quad {}^{\circ}\mathrm{CW}^{-1}, \tag{4.14}$$

where Δr_{ij} is the difference in the radii of the centres of mass of the two compartments, A_{ij} is the surface area at the midpoint between the centres of mass of the two compartments and K_t is the specific thermal conductivity of body tissue.

The variables Δr_{ij} and A_{ij} are calculated as follows:

$$\begin{aligned} \Delta r_{ij} &= \frac{\sqrt{r_i^2 + r_j^2} - \sqrt{r_i^2 + r_k^2}}{\sqrt{2}}, \\ A_{ij} &= \Pi l \frac{\sqrt{r_i^2 + r_j^2} + \sqrt{r_i^2 + r_k^2}}{\sqrt{2}}. \end{aligned} \tag{4.15}$$

The radial heat transfer between two coaxial compartments, $\phi_{Cond,ij}$, is thus

$$\phi_{Cond,ij} = \frac{(T_i - T_j)}{R_{ij}} \quad \mathrm{W}, \tag{4.16}$$

where T_i and T_j are the temperatures of compartments i and j respectively.

Blood flow throughout the body has the effect of redistributing internal body heat by convection. The change in heat content of compartment i as a result of blood flow can be described by

$$\phi_{Bl,i} = \alpha \rho C_{Bl} \dot{Q}_i (T_{CB} - T_i) \quad \mathrm{W}, \tag{4.17}$$

where ρ is the density of blood, C_{Bl} is the specific thermal capacity of blood and $\dot{Q}_i$ is the blood flow through compartment i. The constant α accounts for counter-current heat exchange that occurs when blood supplying the tissue transfers heat to blood returning from the same tissue. The counter current heat transfer occurs due to the close proximity of arterioles to the venules and arteries to the veins. In cases of high blood flow, counter-current heat exchange does not occur as efficiently. This effect is not included in (4.17), however, this inaccuracy in the model description is countered by a similar effect of incomplete transfer of heat occurring between the blood and tissue during periods of high blood flow. The convective heat which is transferred from the tissue compartment, $\phi_{Bl,i}$, must also be transferred to the central blood compartment. Blood rapidly perfuses the tissues of the body so that the respiratory gases, principly CO_2 and O_2, can be quickly exchanged between the blood and metabolising tissue. The tree like structure of the capillary bed allows the blood to rapidly transfer the respiratory gasses and also heat with all regions of metabolising tissue. Thus, it is assumed that during periods of normal blood flow, the blood enters the tissue at a temperature equal to the central blood temperature and it leaves the tissue at the tissue temperature.

Convection, conduction and radiation from the skin surface may be referred to collectively as *dry heat transfer*. Approximately 80% of the heat lost from the skin of a resting human in a thermally comfortable environment is through dry heat transfer and the remaining 20% is from evaporation [Weatherall, 1983]. When thermal insulation (bedding) is considered, convection and radiation play only a minor role and conductive heat flow dominates. This assumption is only valid when the insulation has sufficient thickness that the outside surface of the insulation is approximately the same temperature as the environment. For low values of insulation thickness, convection and radiation through the insulation layer begin to occur. Dry heat transfer from the skin, $\phi_{DHT,i}$, through an insulation layer [Weatherall, 1983] can be expressed as

$$\phi_{DHT,i} = \frac{K_I \cdot A_i (T_i - T_{Env})}{I_i} \quad \mathrm{W}, \tag{4.18}$$

where I_i is the insulation thickness, measured in mm, and A_i is the surface area of the skin of compartment i. The constant, K_I, is the specific thermal conductivity through an insulation layer. Most of the insulating effect of any common bedding material is due to the ability of the material to trap air which has a very low coefficient of thermal conductivity. Therefore, for most thermally insulating materials, regardless of construction, the value of insulation is proportional to the material thickness [Weatherall, 1983]. It is assumed in (4.18) that the insulation material does not store a significant amount of heat.

The remaining skin heat loss is through insensible evaporation (through the skin) and sweat evaporation [Weatherall, 1983]. If dry heat transfer processes are impeded or insufficient to maintain constant core body temperatures during periods of high heat production, the body will compensate by increasing evaporative heat loss through sweating. Evaporative heat loss from each skin compartment of the body, $\phi_{Evap,i}$, is described by

$$\phi_{Evap,i} = L \cdot A_i (E_{Ins,i} + E_{Sw,i}) \quad \mathrm{W}, \tag{4.19}$$

where $E_{Ins,i}$ is water vapour per unit area produced by insensible evaporation and $E_{Sw,i}$ is that produced by sweat. The constant L is the latent heat of vaporisation of sweat and has the units $\mathrm{W \cdot hr/g}$ [Weatherall, 1983]. The effect of bedding is to increase the resistance of vapour transport to the environment. Assuming the bedding does not have such an effect that moisture accumulates on the skin surface, then all water vapour is removed from the skin regardless of the resistance to vapour transport, thus (4.19) remains valid. In addition, if the bedding retains moisture, the thermal conductivity of the bedding increases dramatically. Therefore, to a certain extent, the effect of skin wetness is countered by the increased thermal conductivity of the bedding during periods of profuse sweating.

The large surface area of the gas exchange surface of the lungs ensures that rapid transfer of respiratory gasses occurs. Consequently, water on the surface of the alveoli is also rapidly transferred to the air in the lungs in the form of water vapour. Under normal breathing conditions, the expelled air is fully saturated with water vapour. Respiratory water vapour loss has the effect of transferring body heat to the environment. This is because the water which evaporates into the lungs, and is expelled on each expiration, consumes latent energy in the same manner as the evaporation of sweat. Because of the lack of precise information, for the purposes of this model, it is assumed that half of the respiratory heat lost is from the trunk core and half is from the head core. For resting adults, heat loss through respiratory water vapour, $\phi_{Resp,Ad}$, has been found to be approximately 10W [Stolwijk & Hardy, 1966]. The loss of heat, for both infants and adults, is assumed to be linearly related to the respiration rate. A typical value for the resting adult respiration rate, $\dot{V}_{Ad,0}$, is approximately 0.1 l/s [Guyton, 1971]. Therefore, total respiratory heat loss, $\dot{V}_{Resp}$, for any age is approximately

$$\phi_{Resp} = \phi_{Resp,Ad} \frac{\dot{V}_{Resp}}{\dot{V}_{Ad,0}} \text{ W.} \tag{4.20}$$

Although the respiratory rate changes with the metabolic rate, for the purposes of this model the respiratory rate is assumed to be constant and basal.

m	Mass
C_t	Specific thermal capacity of tissue
C_{Bl}	Specific thermal capacity of blood
T_i	Temperature of compartment i
T_{Env}	Environmental temperature
α	Counter current heat exchange
ρ	Density of blood
$\dot{Q}$	Blood flow rate
ϕ_{MR}	Metabolic heat production rate
A	Surface area
K_{DHT}	Specific thermal conductivity of insulation
L	Latent heat of sweat evaporation
R_{ij}	Resistance to radial heat flow between adjacent compartments i and j
E_{Ins}	Insensible evaporation rate
E_{Sw}	Evaporation rate due to sweat

Table 4.1 Mathematical symbols for the heat store equations of the model.

The change in heat content of each compartment of the model is expressed as a differential equation describing the change of heat in the compartment as equal to the amount of heat entering, ϕ_{IN}, minus the amount of heat leaving the compartment, ϕ_{OUT}. Also, the heat content of each compartment is equal to the product of the temperature, T, the mass, m, and the specific thermal capacity of the tissue C_t. Consequently, the rate of change in heat of each compartment, including the metabolic heat, ϕ_{MR}, can be expressed as

$$m_i C_t \frac{dT_i}{dt} = \phi_{MR,i} + \phi_{IN,i} - \phi_{OUT,i}\,, \tag{4.21}$$

where the subscript i denotes one of the compartments of the model. The compartments are the head skin, *HS*, head core, *HC*, trunk skin, *TS*, trunk muscle, *TM*, trunk core, *TC*, and the central blood, *CB*. Table 4.1 lists the mathematical symbols used for the heat store equations.

The set of equations which describe the heat flow through the six compartments of the controlled system, shown in figure 4.2, is as follows. Each equation has been formulated by substitution of the appropriate heat flow equations (4.14) through (4.20) into the heat store equation (4.21):

$$\begin{aligned}
m_{HS}C_t\frac{dT_{HS}}{dt} &= \alpha\rho C_{Bl}\dot{Q}_{HS}(T_{CB}-T_{HS}) + \phi_{MR,HS} + \frac{(T_{HC}-T_{HS})}{R_{HC\text{-}HS}} \\
&\quad -K_I\cdot A_{HS}\frac{(T_{HS}-T_{Env})}{I_{HS}} - L\cdot A_{HS}(E_{Ins,HS}+E_{Sw,HS})\,, \\
m_{HC}C_t\frac{dT_{HC}}{dt} &= \alpha\rho C_{Bl}\dot{Q}_{HC}(T_{CB}-T_{HC}) + \phi_{MR,HC} \\
&\quad -\frac{(T_{HC}-T_{HS})}{R_{HC\text{-}HS}} - \frac{\phi_{Resp}}{2}\,, \\
m_{TS}C_t\frac{dT_{TS}}{dt} &= \alpha\rho C_{BL}\dot{Q}_{TS}(T_{CB}-T_{TS}) + \phi_{MR,TS} + \frac{(T_{TM}-T_{TS})}{R_{TM\text{-}TS}} \\
&\quad -K_I\cdot A_{TS}\frac{(T_{TS}-T_{Env})}{I_{TS}} - L\cdot A_{TS}(E_{Ins,TS}+E_{Sw,TS})\,, \\
m_{TM}C_t\frac{dT_{TM}}{dt} &= \alpha\rho C_{Bl}\dot{Q}_{TM}(T_{CB}-T_{TM}) + \phi_{MR,TM} \\
&\quad +\frac{(T_{TC}-T_{TM})}{R_{TC\text{-}TM}} + \frac{(T_{TM}-T_{TS})}{R_{TM\text{-}TS}}\,, \\
m_{TC}C_t\frac{dT_{TC}}{dt} &= \alpha\rho C_{Bl}\dot{Q}_{TS}(T_{CB}-T_{TC}) + \phi_{MR,TC} \\
&\quad -\frac{(T_{TC}-T_{TM})}{R_{TC\text{-}TM}} - \frac{\phi_{Resp}}{2}\,, \\
m_{CB}C_{Bl}\frac{dT_{CB}}{dt} &= -\alpha\rho C_{Bl}[\dot{Q}_{HS}(T_{CB}-T_{HS}) + \dot{Q}_{HC}(T_{CB}-T_{HC}) \\
&\quad +\dot{Q}_{TS}(T_{CB}-T_{TS}) + \dot{Q}_{TM}(T_{CB}-T_{TM}) + \dot{Q}_{TC}(T_{CB}-T_{TC})]\,.
\end{aligned} \tag{4.22}$$

The equations of (4.22) are six highly coupled first order differential equations. If the metabolic heat production and blood flows for each compartment are constant, then the equations are linear, however, inclusion of the controller equations (see section 4.2.2) introduces significant non-linearities into the equations.

Equilibrium heat flow occurs in the body when the rate of change of each compartment temperature is equal to zero. At this point, the model is said to be in the steady state. This can be shown mathematically by equating the equations of (4.22) to zero. The equations of (4.22) can then be combined into a single equation describing the steady state equilibrium heat flow

$$\sum \phi_{MR,i} = \sum A_i(\phi_{DHT,i} + \phi_{Evap,i}) + \phi_{Resp}, \tag{4.23}$$

which shows that the total metabolic heat production of the model is equal to the total heat loss when the compartment temperatures are constant. Equation (4.23) describes the steady state behaviour which is typically observed in any internally heated mass, such as the human body.

4.2.2 Human thermal control mechanisms

Human thermoregulation occurs through both behavioural and autonomic control (see section 1.2.1). The infant thermoregulation model described in this chapter is designed to simulate the conditions of a sleeping human infant, during which time behavioural control does not occur. Autonomic control consists of increasing the skin blood flow and perspiration rate in response to overheating and increasing the muscle metabolism and muscle blood flow if the body is too cool.

The thermoregulation model control system described here is an approximation of human thermoregulation, derived from the available experimental data of other researchers. It is anticipated that future experimentation will produce refinements to this model. The controlled variables are the head core temperature, T_{HC}, and average skin temperatures, $T_{\bar{S}}$. The average skin temperature is calculated from area weighted averaging of the head skin and trunk skin temperatures.

Thermal control occurs in the hypothalamus of the brain. Both multiplicative and additive models have been proposed for the integration of the head core and average skin temperature thermoreceptor responses [Jessen, 1990, Chapter 7; Hensel, 1981, p128; Hwang & Konz, 1977]. Additive control is described by

$$\psi = \alpha(T_{HC} - T_{Set,HC}) + \beta(T_{\bar{S}} - T_{Set,\bar{S}}), \tag{4.24}$$

where ψ is the control response and α and β are constants. This is illustrated in figure 4.4(a). Multiplicative control, illustrated in figure 4.4(b), is expressed as

$$\psi = \gamma(T_{HC} - T_{Set,HC})(T_{\bar{S}} - T_{Set,\bar{S}}), \tag{4.25}$$

where γ is a constant. For both multiplicative and additive control, a cold response is elicited only when T_{HC} and $T_{\bar{S}}$ are simultaneously below their respective set points. Similarly, a heat response occurs only when both temperatures are above their set points. Therefore, if one temperature is above and one is below their respective set points then no control response is generated.

A control domain is where a control response is elicited within the plane of the head core and average skin temperatures (see figure 4.4). Similarly, a non-control domain is where no control response is elicited. The additive model produces a linear response within the two control domains. However, during transition from a control domain to a non-control domain a highly non-linear step in response occurs. This may have the effect of destabilising the model in the region where the control and non-control domains meet because of the infinite gain associated with the step in control. Multiplicative control is non-linear throughout the control domains, however, the step in response between the control and non-control domains is not present.

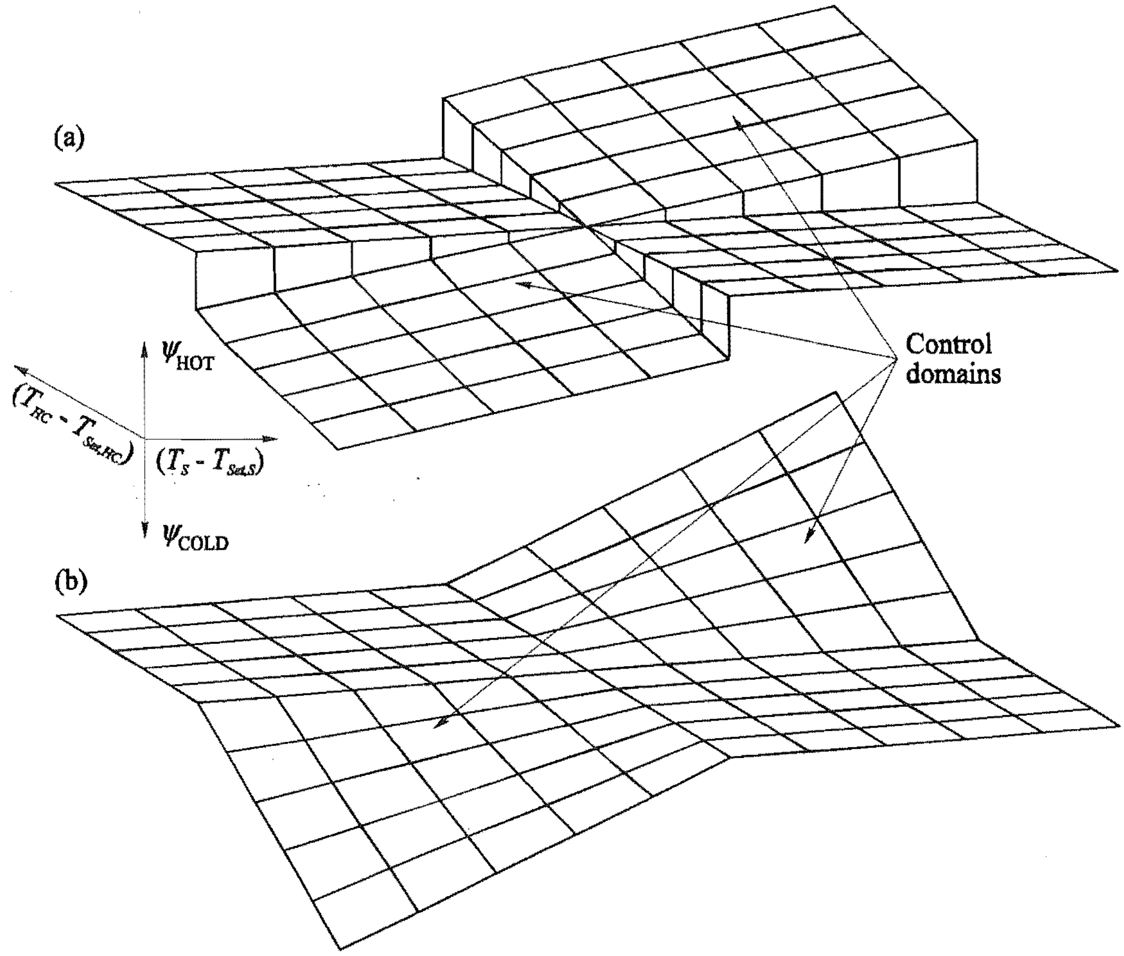

Figure 4.4 Thermal control schemes: (a) additive, (b) multiplicative control response planes.

The coexistence of both multiplicative and additive models reflects the diversity of experimental methods, results and concepts of human thermoregulation. A further complication is that in addition to the central integration of thermoreceptor responses, local skin temperature appears to affect thermal control through altering skin blood flow and sweat rate [Hensel, 1981, p166; Bullard ét al., 1970; Nadel et al., 1971].

Human thermal control has also been shown to be a function of the rate of change of the average skin temperature [Jessen, 1990, pp160-163; Hensel, 1981, pp51-55], however, the exact nature of the control mechanism is not well understood. The rate control effect is relatively small and only occurs for a negative change in skin temperature exceeding -0.1°C/min. Because of its small effect and for simplicity, the rate of change effect has not been incorporated into this model.

The control equations for the model of infant thermoregulation, described in this chapter, incorporate aspects of both multiplicative and additive control. The thermoregulation control equations are as follows.

<u>**Skin blood flow:**</u> An increase in skin blood flow occurs when the body is hot. This helps transfer heat from the core of the body to the skin surface where the heat is lost to the environment. The change in skin blood flow, ΔQ_S, can be expressed mathematically [Stolwijk & Hardy, 1966] as

$$\Delta Q_S = 20.0(T_{HC}-T_{Set,HC})(T_{\bar{S}}-T_{Set,\bar{S}}) + 0.51(T_{\bar{S}}-T_{Set,\bar{S}}) \ \ 1/\text{hr/m}^2. \quad (4.26)$$

The increase in skin blood flow for each 1°C increase in body temperature per unit surface area is assumed to be the same for both infants [Ryser & Jéquier, 1972] and adults [Hardy, 1970]. However, the average skin temperature set point is higher in the infant (see section 4.3). Equation (4.26) is dependent on surface area and as such can be incorporated in both the infant and adult models without any modification. It incorporates multiplicative control and an additive local skin temperature effect. Skin blood flow control is a form of positive feedback because an increase in skin temperature increases skin blood flow which in turn raises the skin temperature. The high skin temperature increases heat loss from the skin which serves to cool the body. When the head core temperature falls below the head core temperature set point, the skin blood flow decreases to reduce the cooling effect.

<u>**Muscle metabolic heat:**</u> The increase in muscle compartment metabolism, $\Delta\phi_{MR,TM}$, that occurs when the body is cool [Stolwijk & Hardy, 1966] is described by

$$\Delta\phi_{MR,TM} = m_{Total} \cdot \mathrm{G}(T_{HC}-T_{Set,HC})(T_{\bar{S}}-T_{Set,\bar{S}}) \ \ \mathrm{W}, \quad (4.27)$$

where G is an age dependent gain factor (see section 4.3.1). Brain and core compartment metabolism is assumed to remain constant for all thermal stresses since these organs perform the same vital survival functions regardless of the thermal stress placed on the body. This assumption is made in many models of adult thermoregulation [Stolwijk & Hardy, 1966; Wyndham & Atkins, 1968]. Additional production of heat through brown adipose tissue thermogenesis is included in (4.27).

<u>**Muscle blood flow:**</u> An increase in muscle blood flow of 0.43 l/hr occurs for each 1 W increase in metabolism [Stolwijk & Hardy, 1966]. This is assumed to be the same for both infants and adults since the mechanisms which liberate heat are principly the same for both infants and adults.

<u>**Evaporative heat loss:**</u> Sweating is the primary autonomic mechanism by which the body can reduce its temperature. A common result of most studies of evaporative heat loss from the skin indicates the importance of core temperature for sweat control. Below a core temperature range of 36.5 to 37°C, no sweating occurs, even with high skin temperatures [Jessen, 1990, p157]. Also, sweating is clearly inhibited by skin temperatures lower than approximately 34°C regardless of the core temperature [Jessen, 1990, p157]. Skin temperatures above 34°C have

been found to exert little drive to sweating but allow warm core temperatures to significantly increase the sweat rate. However, because skin temperature is directly controlled by sweating and the effect of sweating on the core temperatures is only a secondary or indirect effect, the effect of core temperature appears uncoupled and skin temperature remains an important variable for determining sweat rate. The sweat rate, E_{Sw}, can be described mathematically as [Hwang & Konz, 1977]

$$\begin{aligned} E &= 250(T_{HC}-T_{Set,HC})+100(T_{HC}-T_{Set,HC})(T_{\bar{S}}-T_{Set,\bar{S}}) \quad \mathrm{g/hr/m^2}, \\ E_{Sw} &= E \cdot 2^{(T_{\bar{S}}-T_{Set,\bar{S}})/3} \quad \mathrm{g/hr/m^2}. \end{aligned} \tag{4.28}$$

The two equations of (4.28) represent the central response to high body temperatures and a local skin temperature response which modifies vapour production.

The skin becomes 100% wetted at a vapour production rate of approximately 250g/hr/m^2 [Stolwijk & Hardy, 1966], even at a relatively low humidity. Maximum heat loss occurs at this point. In reality, 100% wetted skin probably occurs at a value which is lower than 250g/hr/m^2. For example, when the skin is covered with bedding, vapour transport is impeded.

The thermoregulatory control equations have been derived from data collected for small to mid range thermal stresses since experiments on humans involving large thermal extremes are unethical. Thus, it is anticipated that the control equations become less accurate for large thermal loads. Also, the nature of experiments which have been used to determine the maximum values of the thermoregulatory control mechanisms are such that they are unethical to perform on human infants. For this reason, there is little information available on these values and as such, they have not been included in this model. However, this is of little concern because we are only interested in the behaviour of the model around the thermoneutral point and only for relatively small perturbations. As such, the thermoregulation equations of this model are only used in the low to mid range of thermal stresses.

4.3 Model Parameters

This section details numerical values for the infant thermoregulation model. Values for adults are included for comparison. The parameter values have been obtained from a number of sources. Researchers over the past few decades have been investigating numerous quantitative aspects of human physiology including body proportions and nocturnal metabolism rates. It is from this work that the parameters listed in this section have been derived. Much of the data are averages calculated from measurements obtained from a number of individuals and little information is available regarding which parameters vary between individuals and by how much. Two perfectly healthy and normal individuals may have considerably different parameter sets. For example, one individual may have one parameter which is considerably different to the average (e.g. muscle mass), the effect of which may be countered by another parameter which is also considerably different to the average (e.g. controller sensitivity to temperature) yet this person appears perfectly healthy. Thus, the effect of the difference of one parameter from the average is compensated for by another parameter being different to the average. Furthermore, the parameters have been obtained from a number of experiments, each with a different set of subjects, experimental protocols and experimental conditions. It is difficult to estimate the significance this has on model simulations, but for the purposes of this model, which is to give qualitative results, average parameters from normal healthy humans are considered sufficient. In fact, the model may be used to test the sensitivity of humans to parameter variations and a comparison could be made of parameter sensitivity between infants and adults.

Table 4.2 lists the thermal properties of body tissue [Stolwijk & Hardy, 1966]. These values are required for calculation of the heat storage of the compartments of the model.

Description	Symbol	Value	Units
Specific thermal capacity of body tissue	C_t	0.96	W/°C/Kg
Specific thermal capacity of blood	C_b	1.07	W/°C/Kg
Specific thermal conductivity of tissue	K_t	418.7	$W \cdot mm/m^2/°C$
Specific thermal conductivity of bedding insulation	K_I	36.0	$W \cdot mm/m^2/°C$
Latent heat of vaporisation of sweat	L	0.65	$W \cdot hr/g$
Coefficient of heat loss from exposed dry skin	H_S	7.0	$W/m^2/°C$
Density of blood	ρ	1.0	Kg/l

Table 4.2 Thermoregulation model constants for the properties of the human body. These values are common to both infants and adults.

The model has been designed to investigate the effect of insulation on the trunk skin compartment, yet one must also consider the effect of insulation on the head skin compartment. A large fraction of the head is exposed to the environment with no insulation and heat loss through the heavily insulated area in contact with the mattress or pillow is negligible in comparison.

Total heat loss from the exposed skin, H_S, is approximately 7.0 $W/m^2/°C$ [Stolwijk & Hardy, 1966]. Therefore, if F is the fraction of the head which is assumed to be 100% thermally insulated, the average heat loss from the head is $(1\text{-}F) \cdot H_S$ $W/°C/m^2$. From (4.18) an average head insulation score, I_{HS}, can be approximated as

$$I_{HS} = \frac{K_I}{(1-F) \cdot H_S} \quad \text{mm.} \tag{4.29}$$

If $F = 0.5$, then $I_{HS} = 10\text{mm}$. This value of insulation thickness is used as the base value for head insulation in the model.

4.3.1 Maturation of the thermoregulation parameters

Many of the parameters of human thermoregulation change with age, this is termed maturation. It is because of the effects of maturation that infant thermoregulatory behaviour is considerably different to that of adults. Table 4.3 presents the parameters of the adult model which have been calculated from numerous sources [Farhi & Rahn, 1960; Stolwijk & Hardy, 1966; Widdiwson, 1974; Revow et al., 1989; Hill & Rahimtulla, 1965]. They have been included for comparison with the infant parameters which are presented in table 4.4 [Widdiwson, 1974; Wilmer, 1940; Cussen et al., 1990; ChMedSch, 1992; Dobbing & Sands, 1973; Revow et al., 1989; Hill & Rahimtulla, 1965; Settergren et al., 1976].

Body Tissue	Mass (Kg)	MR - O_2 Consumption (ml/min)	Blood Flow (ml/min)
Brain	$m_b = 1.4$	$MR_b = 41.0$	$\dot{Q}_b = 751$
Skin	$m_s = 4.2$	$MR_s = 4.6$	$\dot{Q}_s = 238$
Muscle	$m_m = 28.0$	$MR_m = 40.7$	$\dot{Q}_m = 610$
Combined organs	$m_o = 9.1$	$MR_o = 169.7$	$\dot{Q}_o = 3802$
Fat	$m_f = 17.5$	0	0
Skeleton	$m_k = 9.8$	0	0
Total	$m_t = 70$	$MR_t = 256$	$\dot{Q}_t = 5400$

Table 4.3 Parameters for adult thermoregulation model.

The metabolic rate is measured by the rate at which oxygen is consumed. Heat production is then calculated from oxygen consumption. Assuming no kinetic energy is lost to the environment, 4.8 W of heat is produced for every litre of oxygen consumed [Hill & Rahimtulla, 1965].

Body mass increases dramatically as the infant develops. From standard growth charts [ChMedSch, 1992], during the first year of life, the relationship of body mass with age can be described as

$$m_t = 4.74\ln(Age+17.4)-10.0 \quad \text{kg}, \quad Age<52\text{weeks}, \tag{4.30}$$

where *Age* is in weeks. Average adult body mass is assumed to be 70 kg. Over the first year of life the proportion of brain mass changes more significantly than any other region of the body. From the literature, the mass of the brain of infants less than one year of age is taken as [Dobbing & Sands, 1973]

$$m_b = \frac{(13.644 - 0.3673m_t)m_t}{100} \quad \text{kg}. \tag{4.31}$$

The values of the brain metabolism and brain blood flow have been obtained from the literature [Settergren et al., 1976] and are shown in table 4.4. Fat is assumed to be distributed through the tissue of the body and accounts for fat in the subcutaneous tissue, muscle and around the body organs. This assumption only alters the mass of each compartment, not the metabolic rate or blood flow.

The metabolic rate and blood flow to the skin, muscle and combined organs is not accurately known for each region for maturing infants. However, the total metabolic rate and blood flow to these regions combined is known. The total metabolic rate for these tissue regions is 1.3 times the total metabolic rate of the combination of these same regions in adults. The factor of 1.3 is multiplied by the adult metabolic rate per unit mass for each region to obtain an estimate of the metabolic rate for each region for infants. The blood flow to each of these regions is calculated by assuming the ratio of the blood flow to the metabolic rate of each region is the same for infants as for adults, thus accounting for the higher cardiac output per unit of total body mass for infants compared with adults. This method of metabolic rate and blood flow estimation appears suitable because the sum of the blood flow through each compartment closely matches the cardiac output.

Although the structure of the thermoregulation model is the same for both infants and adults, there is considerable difference in the parameters for the model. The most obvious difference is the mass and surface area of the infant in comparison to the adult. Proportions of fat, bone and muscle also change dramatically as the infant matures. The metabolism and blood flow per unit body mass for each compartment are also considerably different in the infant compared with the adult. These differences occur to maintain constant core temperatures at low environmental temperatures and are outlined in section 1.2.2. For similar reasons, the skin set point and gain of the controller equations change with age (see table 4.5).

Body Tissue	Mass (Kg)	MR - O_2 Consumption (ml/min)	Blood Flow (ml/min)
Brain	m_b see (4.31)	$MR_b = 23.3m_b$	$\dot{Q}_b = 690m_b$
Skin	$m_s = 0.4m_t$	$MR_s = 1.43m_s^*$	$\dot{Q}_s = 74.0m_s$
Muscle	$m_m = 0.37m_t - m_b$	$MR_m = 1.89m_m^*$	$\dot{Q}_m = 28.3m_m$
Combined organs	$m_o = 0.18m_t$	$MR_o = 24.2m_c^*$	$\dot{Q}_o = 541.7m_c$
Fat	$m_f = 0.23m_t$	0	0
Skeleton	$m_r = 0.18m_t$	0	0
Total	m_t see (4.30)	$MR_t = 7.2m_t$	$\dot{Q}_t = 200m_t$

Table 4.4 Parameters for the infant thermoregulation model (less than one year of age). * see text for details.

Total surface area of the infant body over the first year of life is given by [Hill & Rahimtulla, 1965]

$$A = 0.1m_t^{2/3} \quad \mathrm{m}^2, \tag{4.32}$$

and the head surface area is approximately 20% of the total [Lund & Browder, 1944]. The surface area of a 70 kg adult is approximately 1.8 m^2 [Stolwijk &

Hardy, 1966] and 9% of this is the head [Lund & Browder, 1944]. The total mass of the head is estimated at 7.3% of the total body mass for adults and approximately 20% for infants less than one year of age.

The total volume of blood in the human body has been calculated by researchers and is approximately proportional to the total body mass. For humans up to 13 years of age, the total blood volume, V_{Bl}, is $85.27m_t$ l [Sheenah & Russell, 1949]. This relationship gives a typical blood volume of 6 l for adults. The volume of the central blood compartment for the model is approximated to be 23% of the total blood volume [Stolwijk & Hardy, 1966]. This percentage is assumed to be the same for infants and adults. Thus, the volume of the central blood compartment is

$$V_{CB} = 19.6m_t \ \mathrm{l}. \tag{4.33}$$

Age dependent controller parameters are shown in table 4.5. Note that the infant metabolic rate control loop gain has been calculated from experimental data to be six times that of the adult [Brück, 1961]. If this were not the case, then infant core temperatures could not be held constant in cool environments (see section 1.2.2). No information is available regarding how the gain varies as the infant matures and by today's ethical standards it would certainly not be possible to attempt investigative experiments regarding infant thermoregulation gain factors. Over the first year of life the gain may start to decline towards adult values as the infant matures, however, the gain needs to remain relatively high for the infant to adequately thermoregulate with such a large surface area to volume ratio (see section 1.2.2). Consequently, for the purposes of this model, the gain is assumed to be constant over the first year of life.

Parameter	Infant (< 1 year)	Adult
$T_{Set,HC}$	36.6	36.6
$T_{Set,S}$	36.0	34.5
G	63.7	12.7

Table 4.5 Age dependent thermal control parameters.

The gain of the infant sweat rate control loop is assumed to be the same as that of adults. This is appropriate because the total sweat produced is proportional to the surface area of the body and the high surface area to volume ratio of infants is the cause of high heat loss.

The behaviour of the thermoregulation model is presented in the following chapter. Both the steady state values and dynamic response of the model are investigated for a range of environmental conditions, using the parameters presented in this section.

Chapter 5

Behaviour of the Infant Thermoregulation Model

The mathematical model of human thermoregulation, described in Chapter 4, is based on six non-linear ordinary differential equations, (4.22). Solving this system analytically is not feasible because the approximations required to linearise the system would result in highly inaccurate solutions. Therefore, the method of analysis chosen was via simulation of the system on a digital computer. Simulation of the six differential equations has been achieved using a fourth order Runge-Kutta numerical integration algorithm (see section 2.2.4.1).

For a set of initial conditions (body temperatures) the integration algorithm gives the responses of the six compartment temperatures of the model (the compartments are shown in figure 4.2). The temperature of each compartment is known as a *state variable* since knowledge of the value of all of the state variables completely defines the state of the model. The compartment temperatures change as a function of time until equilibrium heat flow is achieved. At this point, the compartment temperatures (state variables) are constant and the model is said to be in the *steady state*. Figure 5.1 depicts a typical example of a simulation of the model. The time required to perform a simulation such as that of figure 5.1 is in the order of a few seconds but may represent many hours of temperature data. Metabolism, sweat rate and blood flows are also known, but are not shown in figure 5.1 for simplicity. Under certain circumstances, the simulation may not attain equilibrium heat flow but results in sustained oscillations.

This chapter describes the behaviour of the thermoregulation model for a sleeping infant. Section 5.1 presents the steady state and dynamic behaviour of the model for varying environmental temperatures and insulation thicknesses. The mechanism of the oscillations of the thermoregulation model is investigated in section 5.2. A comparison of the model and infant behaviour is presented in section 5.3, followed by a summary of the behaviour of the model in section 5.4.

5.1 Model Characteristics

Heat loss from the human body to the environment is primarily dependent on the difference between the skin and ambient temperatures and the amount of thermal insulation on the skin. Since the state of the model is dependent on the environmental heat loss, the insulation thickness and environmental temperature have a major bearing on the behaviour of the model. This section discusses the behaviour of the model for conditions of varying environmental temperature and trunk insulation thickness. The effective insulation thickness on the head is independent of the trunk skin insulation and is fixed at 10mm (see section 4.3). The effect of increasing the insulation thickness on the trunk skin is not identical to that of increasing the environmental temperature. This is because heat flow from the head is directly altered by the environmental temperature but is not

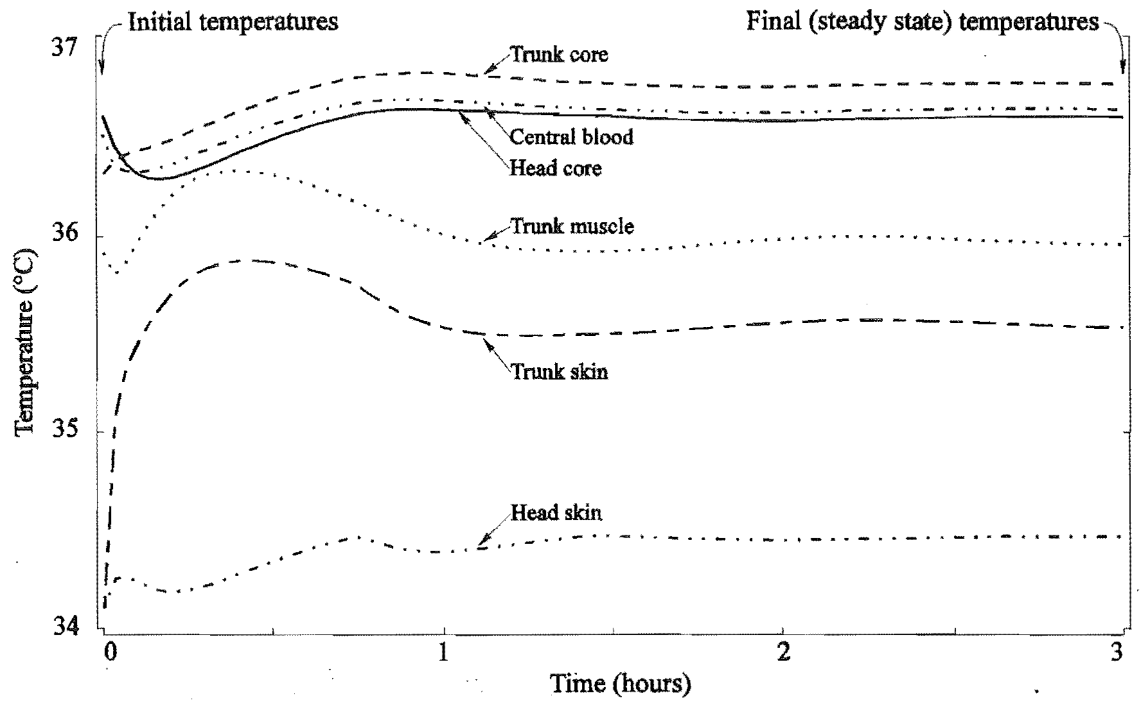

Figure 5.1 Time response of the model after a set of initial temperatures. The simulation represents a 3 hour period (I_{TS} = 30mm, T_{ENV} = 15°C).

affected by the trunk insulation. Altering the insulation covering the entire body (including the head) is equivalent to altering the environmental temperature and is therefore not discussed in this section.

For the purposes of this research, it is necessary to compare the simulation results of the model with the data collected from infants (presented in Chapter 3). From the infant data, the average base value for the environmental temperature is approximately 16°C and, consequently, this value has been used in the model simulations. Although this is an average environmental temperature value taken from many infants bedrooms over many months, the model has been studied for a wide range of temperatures around this value. Therefore, most normal thermal stresses that are likely to occur for infants have been investigated with the model for a range of environmental temperatures centred at 16°C.

The results presented in the following subsection are for a normal infant at an age of 12 weeks. The model is also assigned the basal metabolic rate and basal blood flows of sleeping infants (see section 4.3.1).

5.1.1 Steady state behaviour

The steady state behaviour of the model is presented in figure 5.2 for variations in both insulation thickness, 5.2(a), and environmental temperature, 5.2(b). The temperatures for each compartment are shown in the top graphs of the figure. The metabolic rate ratio (middle) gives the ratio of the metabolic rate to the basal muscle metabolic rate. Sweat rate is presented at the bottom of the figure. The *thermoneutral point* is where steady state equilibrium heat flow occurs while active thermal control is unnecessary for maintaining body temperatures close to the set points. This requires all blood flows, the muscle metabolic rate, and the evaporative heat loss to be at a minimum while the model is in the steady state. At the thermoneutral point, it is probable that minimum energy consumption occurs [Jessen, 1990, p5].

Figure 5.2(a) depicts the steady state behaviour of the model for insulation thicknesses ranging from 20mm to 40mm. The environmental temperature was fixed at 16°C. From the figure, the thermoneutral point for the infant model at an environmental temperature of 16°C is at approximately 29mm of insulation. Typical values for sleeping infants in New Plymouth, New Zealand suggest that for an average environmental temperature of 16.7°C (standard deviation = 13°C), the level of insulation placed on infants is approximately 33mm [Tuohy & Tuohy, 1990]. At this insulation thickness the thermoneutral point of the model occurs at an environmental temperature of 14.5°C. Thus, assuming the infants are close to their thermoneutral point, which is unlikely considering the subjective nature by which clothing is selected by the parents, the model and the infant data agree to within 2.2°C. This is well within one standard deviation (±13°C) of the mean room temperature reported by Touhy who also suggested that the infants they studied may be over-wrapped [Tuohy & Tuohy, 1990]. Thus, the values for the infants and the model are surprisingly similar.

Parents select the clothing for their infants prior to the infant going to sleep, therefore, as the room temperature varies during the night, it is unlikely that the infants are at their thermoneutral point throughout the entire night, even if they were at their thermoneutral point when put to bed. For this reason, it is expected that the model thermoneutral point may differ from the thermoneutral point estimated from measurements from infants. Also, the calculation of the effective insulation thickness of the infants is relatively inaccurate (see section 3.3.3).

It is clear that the thermoregulation model of the human infant is capable of maintaining relatively constant core body temperatures (head core, trunk core and central blood) over a wide range of thermal stresses. At the thermoneutral point, the trunk skin temperature of the model is close to the expected value of 35.5°C [Ryser & Jéquier, 1972; Brück, 1961], however, the head skin temperature is significantly lower than the trunk skin temperature. This reflects the higher level of insulation on the trunk skin compared with the head skin. For high values of insulation, the trunk skin temperature increases as expected, however, the head skin temperature falls because of the increased evaporation of sweat from the head which is necessary to cool the body.

For environmental temperatures ranging from 10 to 20°C and an insulation thickness of 29mm, the steady state behaviour of the model is shown in figure 5.2(b). Once again, relatively constant core body temperatures are maintained over the entire range of temperatures shown. Head skin temperature of the model decreases with low environmental temperatures because the head has little insulation and is therefore exposed to the environment. However, the trunk skin temperature drops when the environmental temperature increases. This is because the trunk skin is in close proximity to the trunk muscle, therefore a high degree of thermal coupling occurs between the muscle and skin. At high environmental temperatures, the trunk muscle has a reduced heat production and thus a corresponding temperature reduction.

The significance of heat loss from the exposed surface of the head at high thermal stresses is evident from the high head skin temperature at elevated

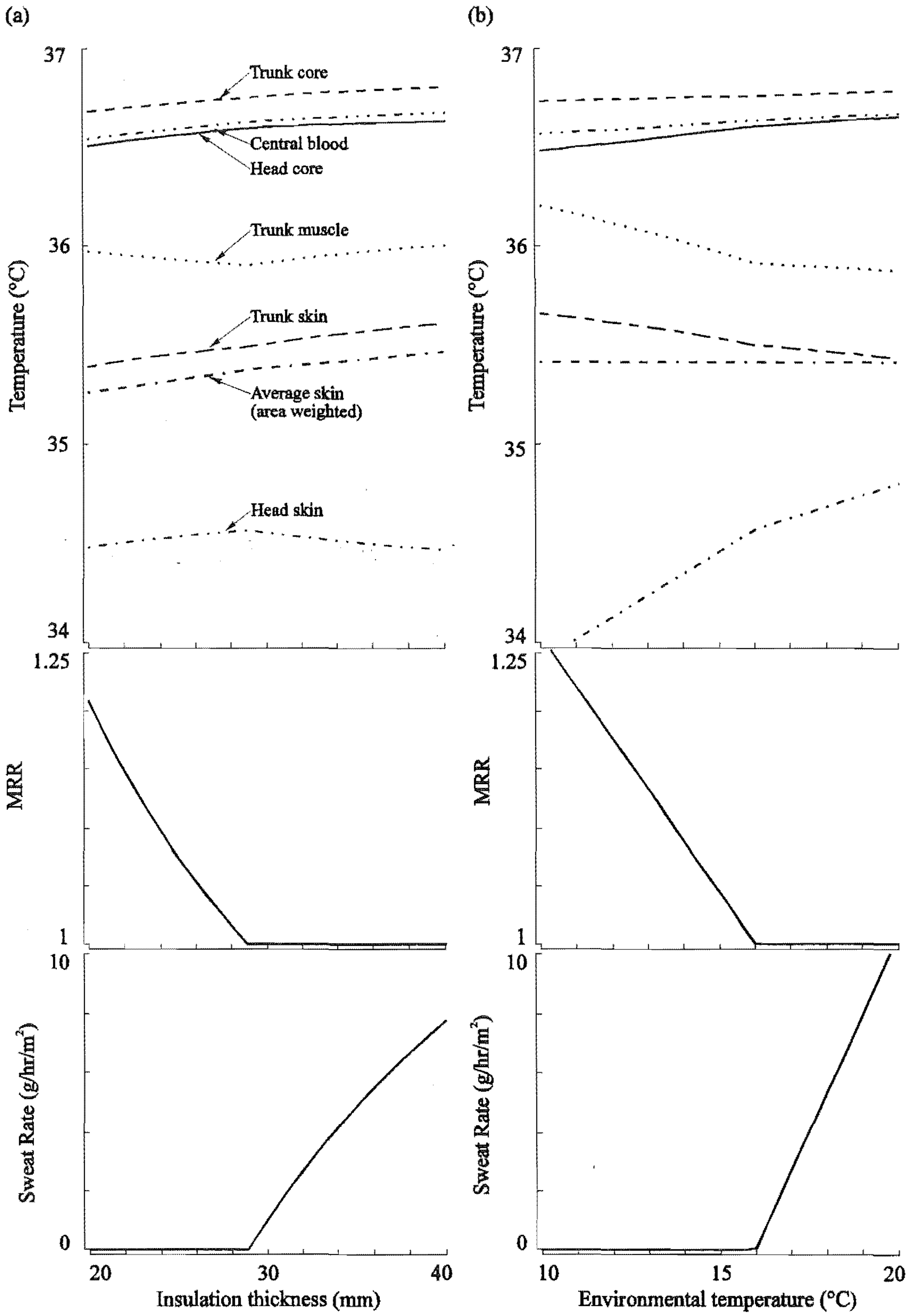

Figure 5.2 Steady state behaviour of the model: (a) Varying insulation thickness (T_{ENV} = 16°C), (b) Varying environmental temperature (I_{TS} = 29mm).

environmental temperatures. High environmental temperatures reduce heat loss from the entire body while thick insulation reduces heat loss from the entire body excluding the head. The exposed surface of the head allows the body to successfully thermoregulate under a wide range of thermal stresses.

Possible non-structurally related inaccuracies in the steady state response of the model are a result of two factors. Firstly, the human thermoregulatory system has maximum values of the metabolic rate and sweat rate. For large thermal extremes, these limiting values prevent the thermoregulatory system from adequately controlling the core body temperatures. These thresholds have not been incorporated into the model because of a lack of precise information on their characteristics. However, this effect is not likely to occur for the small thermal stresses shown in figure 5.2. Secondly, the evaporative heat loss calculations of the model assume total water vapour evaporation from the skin, thus maximising heat loss. In humans, this is not normally the case, particularly in a high humidity environment or with a thick insulation layer which impedes the flow of water vapour. Thus, under high thermal extremes, the core temperatures are likely to deviate from normal by a greater extent than that which is shown in figure 5.2.

5.1.2 Dynamic response

Attempting to show the dynamic behaviour or relative stability of the thermoregulation model is not a simple task because of the non-linear nature of the model. There are many techniques which may be employed to present the dynamic behaviour of the model, however, all of these techniques have certain limitations. Short of presenting the time response of the model for all possible inputs and system parameters, there is no practical technique available that gives ideal results.

The response of the model to a step input may be investigated in order to ascertain the relative stability of the model. Figure 5.3 depicts the response of the model to a step in insulation thickness, for both cool and hot environmental conditions. In a cool environment, oscillatory behaviour which decays to zero after a few hours is evident in 5.3(b). In a hot environment, the steady state response is more rapidly attained, as shown in 5.3(c). It is also evident that the step response of the model behaves in a manner which is similar to a second order system with adjustable damping (see section 2.2.3.2). Adjusting the value of the thermal stress appears to alter the damping of the system.

The stability of the model has been investigated by examining the response of the model to a step change in the head core temperature set point. The head core set point was chosen for step response analysis because it is a control input of the model, although a step input to any system parameter would produce a suitable disturbance. Figure 5.4 shows the peak overshoot for a step change in head core set point where the step sizes range from 0.01 to 0.2°C. Each line on the graph displays the peak overshoot at different thermal stresses. For a linear system the lines would radiate from the origin of each axis (i.e. step size = 0°C, overshoot = 0°C). Undoubtedly, the behaviour of the model appears to be less linear as the step size increases. This is because the large perturbations produced by large step sizes will increase the probability of the state of the model passing through the thermoneutral point where highly non-linear, discontinuous control occurs. This is evident in figure 5.4(a) for step inputs greater than 0.07°C. For

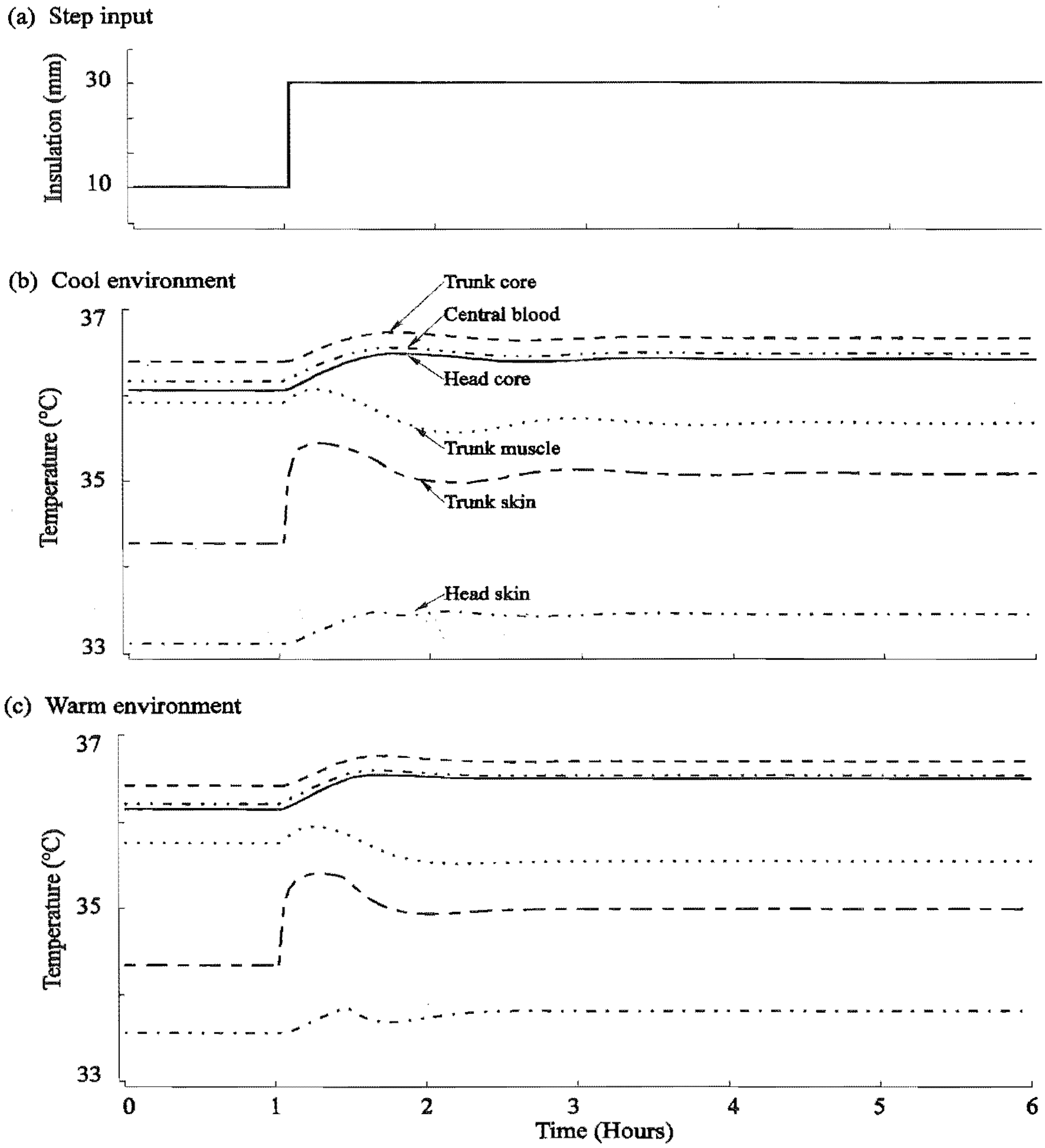

Figure 5.3 Response of the model to a step in trunk insulation from 10 to 30mm: (a) Insulation input, (b) cool environment (T_{ENV} = 14°C), (c) warm environment (T_{ENV} = 17°C).

small step sizes, the responses at different thermal loads appear to radiate from the origin of each axis. Therefore, the ratio of the step responses at different thermal stresses, for a constant small step size, is independent of the absolute value of the step size. This is presented in figure 5.4(b) for the same range of step sizes presented in 5.4(a). Where the ratios remain constant, the characteristics of the step response are independent of the step size. If the step size is too small, then the overshoot cannot be accurately measured. If it is too large, then it is affected by the state of the model passing through the thermoneutral point. Provided the step size is fixed, then for step sizes within the range of 0.025 to 0.07°C, the relative stability of the model can be found for the thermal loads shown in the figure. This method of stability analysis becomes inaccurate when the level of thermal stress places the state of the model near the thermoneutral point, but the effect can be minimised by choosing the smallest practical step size (i.e. 0.025°C). The relative stability can be established from the inverse of the magnitude of the overshoot (i.e. where the overshoot is highest, the stability is lowest).

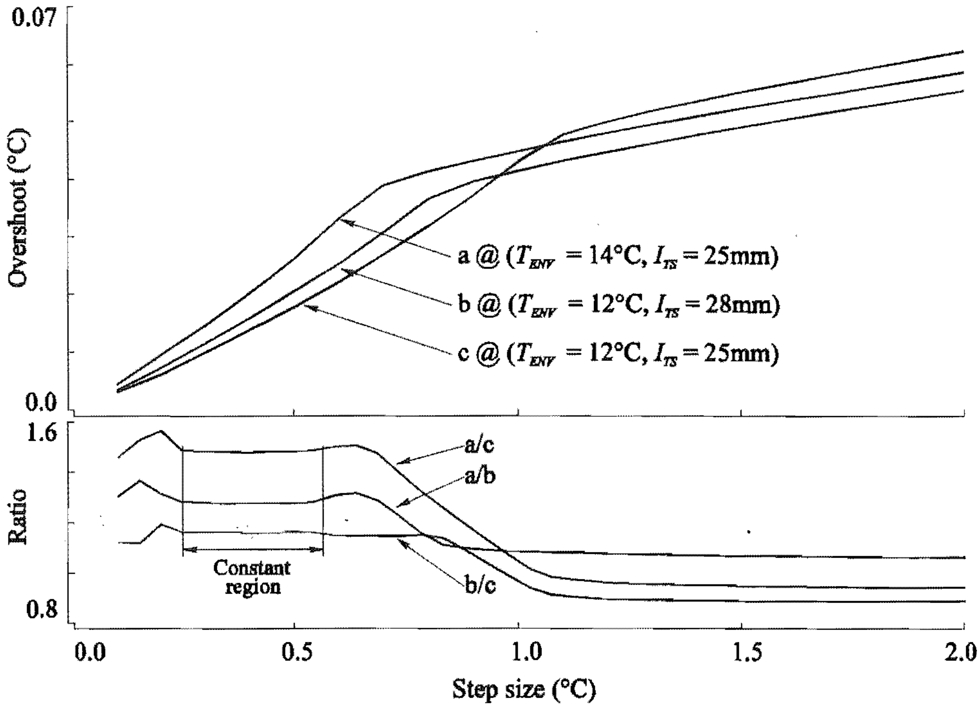

Figure 5.4 (a) Peak overshoot of the head core temperature of the model for a range of step sizes at three different environmental heat loss conditions, (b) Ratio of the overshoot response curves of part (a).

The peak overshoot analysis is a suitable method of stability analysis because it closely reflects typical environmental conditions such as a change in insulation or other forms of environmental noise. An alternative method would be to investigate the level of system gain required to produce sustained oscillations in the model. However, altering the system gain means that the model no longer operates under normal physiological conditions. Furthermore, altering the gain also affects the relative magnitude of any oscillations, thus, even when sustained oscillations occur, their magnitude may be so small that they are physiologically insignificant. The peak overshoot method is not subject to these limitations because the model is operating under normal physiological conditions.

The peak overshoot and period of the head core temperature oscillations, for a range of insulation thicknesses, is presented in figure 5.5(a). The environmental temperature was fixed at 16°C and the responses for four different step sizes are shown. Similarly, figure 5.5(b) shows the peak overshoot and period for a range of environmental temperatures with the insulation thickness fixed at 29mm. The figure shows that in a cool environment, the model of infant thermoregulation demonstrates oscillatory behaviour and in a warm environment it is considerably more stable. The region in which the overshoot response curves have negative slopes (to the left of the thermoneutral point), indicates where the responses are influenced by the overshoot crossing the thermoneutral point. As expected, the overshoot response for different step sizes has the same shape, except near the thermoneutral point. Clearly, the smaller the step size, the less influence the thermoneutral point has on the response curve. However, the effect of the thermoneutral point reflects what happens when any real disturbance affects the model. A step size of 0.025°C has been chosen for the simulations presented in the following sections. This allows effects which are both dependent and independent of the thermoneutral point to be investigated for the range of temperatures between 10 and 20°C and insulation thicknesses between 20 and 40mm.

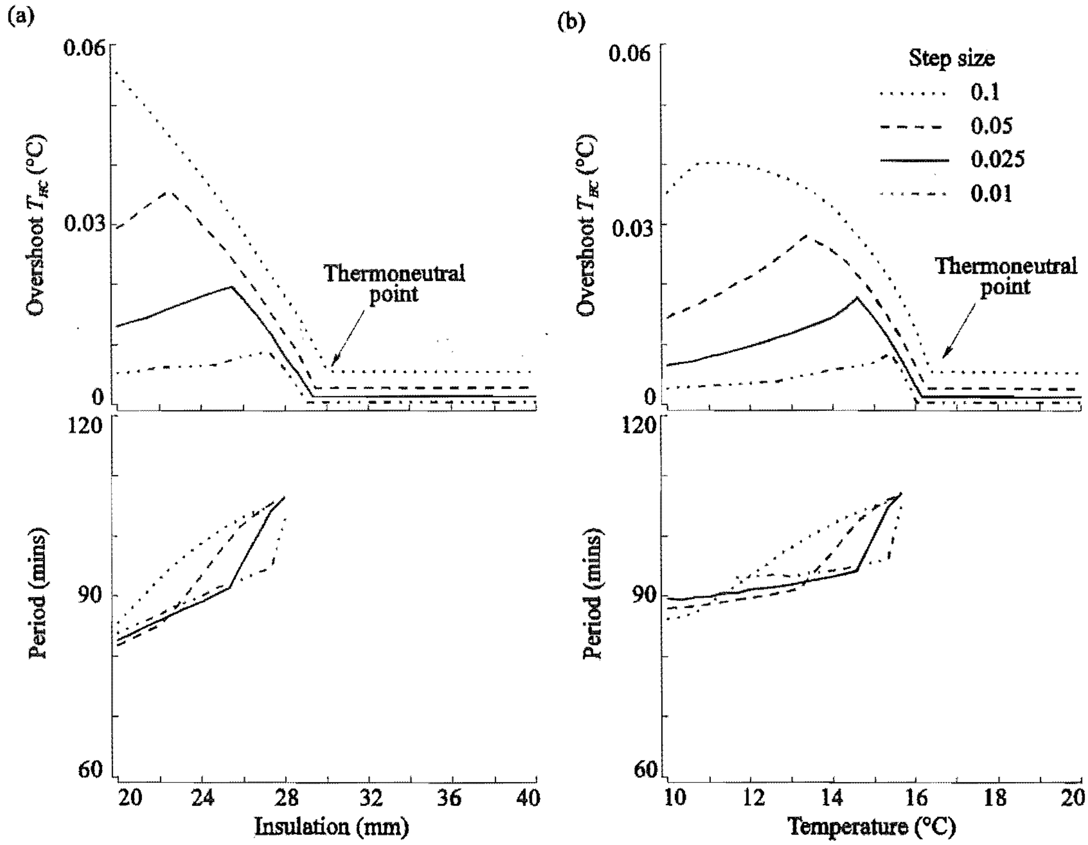

Figure 5.5 Peak overshoot and period for a step in head core set point: (a) Varying insulation thickness (T_{ENV} = 16°C), (b) Varying environmental temperature (I_{TS} = 29mm).

In figure 5.5 the period is only shown where the oscillations are significant. In a warm environment and for small step sizes in a cold environment, the period was not measurable. The period is not altered significantly with varying thermal extremes, however, as the state of the model nears the thermoneutral point, the period is affected by the oscillations passing through the thermoneutral point. This effect is decreased for smaller step inputs.

5.1.3 Summary of the behaviour of the model

The aim of this section is to pictorially present the characteristics of the model for different combinations of insulation thickness and environmental temperature. Both the steady state and dynamic responses of the model are presented in the figures.

The normal behaviour of the infant thermoregulation model for a range of both insulation thicknesses and environmental temperatures is presented in figure 5.6. The left and right sides of the figure represent cold and hot environments respectively. For simplicity, only the temperatures of the head core, 5.6(a), and trunk muscle, 5.6(b), are shown. The muscle metabolic rate ratio, sweat rate and normalised peak overshoot of the head core temperature are shown in parts (c), (d), and (e) respectively. The period of the oscillations is not shown because it does not change significantly with insulation thickness and environmental temperature and because it cannot be measured for all the thermal stresses presented. Figure 5.6 clearly demonstrates the ability of the model to maintain relatively constant head core temperatures by adjusting the muscle metabolic rate (heat production), sweat rate and blood flows for a given thermal load. A thermoneutral line is evident by the discontinuity present in the graph of each variable presented in figure 5.6, although it is difficult to see in the head core temperature graph. The thermoneutral line occurs where the head core temperature is at the temperature set point of the head core (36.6°C).

The stability of the model is particularly interesting. A ridge of low stability occurs on the cool side of the thermoneutral line. On the warm side of the thermoneutral line, the model is considerably more stable. Therefore, the instability of the model is elicited through the metabolic rate control loop since this is the dominant form of control in a cool environment. Sweat rate control does not significantly destabilise the model.

The loss of heat from the exposed, uninsulated, surface of the head to the environment comprises a large proportion of the total heat loss from the body and is an important consideration when investigating the effect of insulation. Figure 5.7 shows the behaviour of the model under the same conditions as figure 5.6 except that the head insulation thickness has been increased from 10mm to 13mm. This represents the addition of a hat which covers the top of the head and the ears. As expected, the thermoneutral line is moved to the left because of the increased insulation. Moreover, when the model is cooler than thermoneutral, the step response overshoot indicates lower stability than the normal case (figure 5.6).

The behaviour of the infant model when the metabolic rate control loop gain is $1/6^{th}$ that of normal for infants is presented in figure 5.8. This is the behaviour of the model if adult thermoregulation control equations are used for thermoregulation of an infant body. The stability is not shown since the low gain value makes the model highly stable and any overshoot in head core temperature is insignificant. Although the model is now more stable, it fails to maintain the head core temperature at close to the set point when in a cool environment. This confirms the need for high gain in the metabolic rate control loop of infants. Thermoregulation in a hot environment continues to perform adequately because sweat rate control is dependent on surface area and is, therefore, inherently adjusted to the size of the infant body (i.e. normal infant sweat rate control is assumed to be the same as the adult - see section 4.2.2).

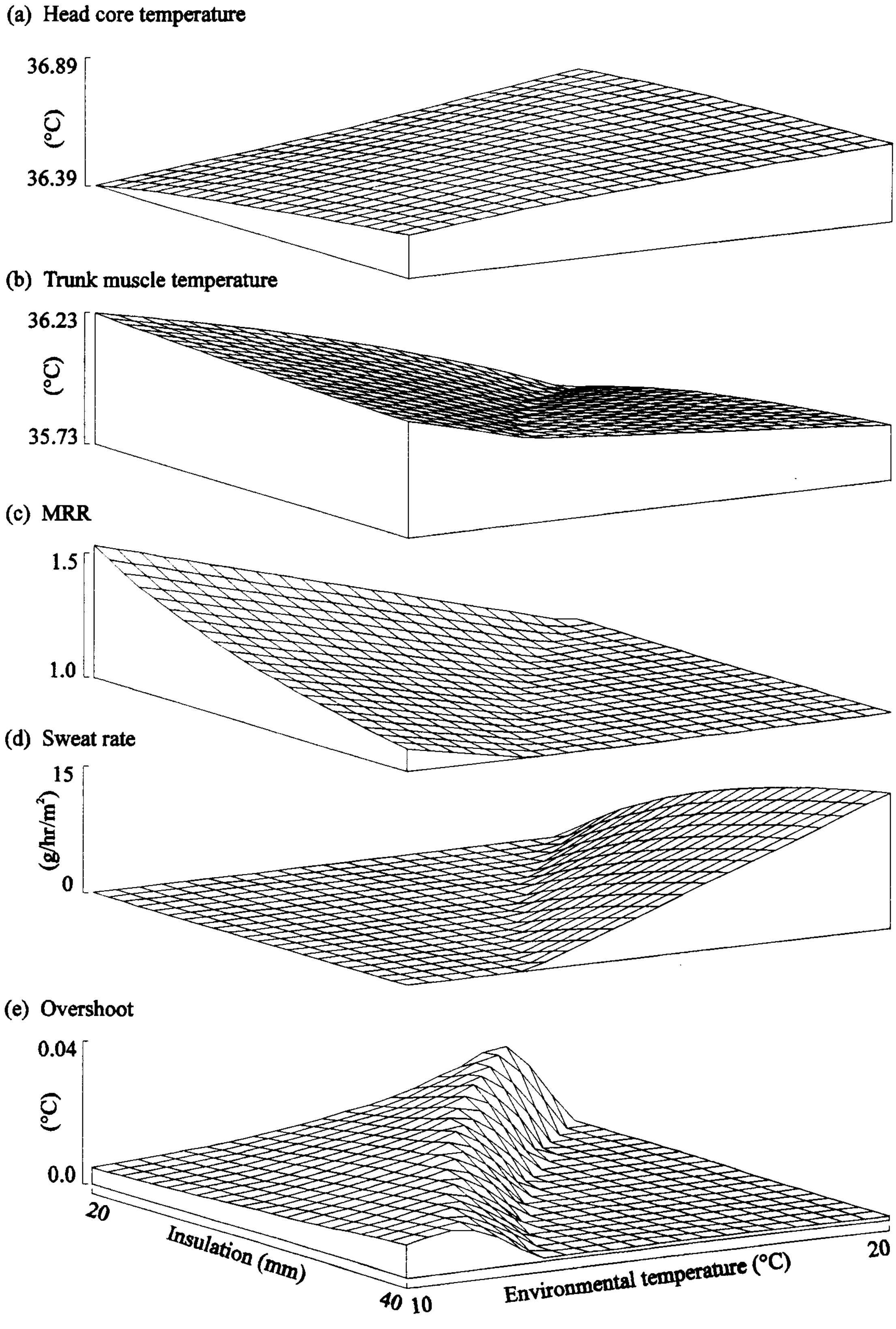

Figure 5.6 Behaviour of the model for a range of environmental temperatures and insulation thicknesses: (a) Head core temp., (b) Trunk muscle temp., (c) MRR, (d) Sweat rate, (e) Head core peak overshoot.

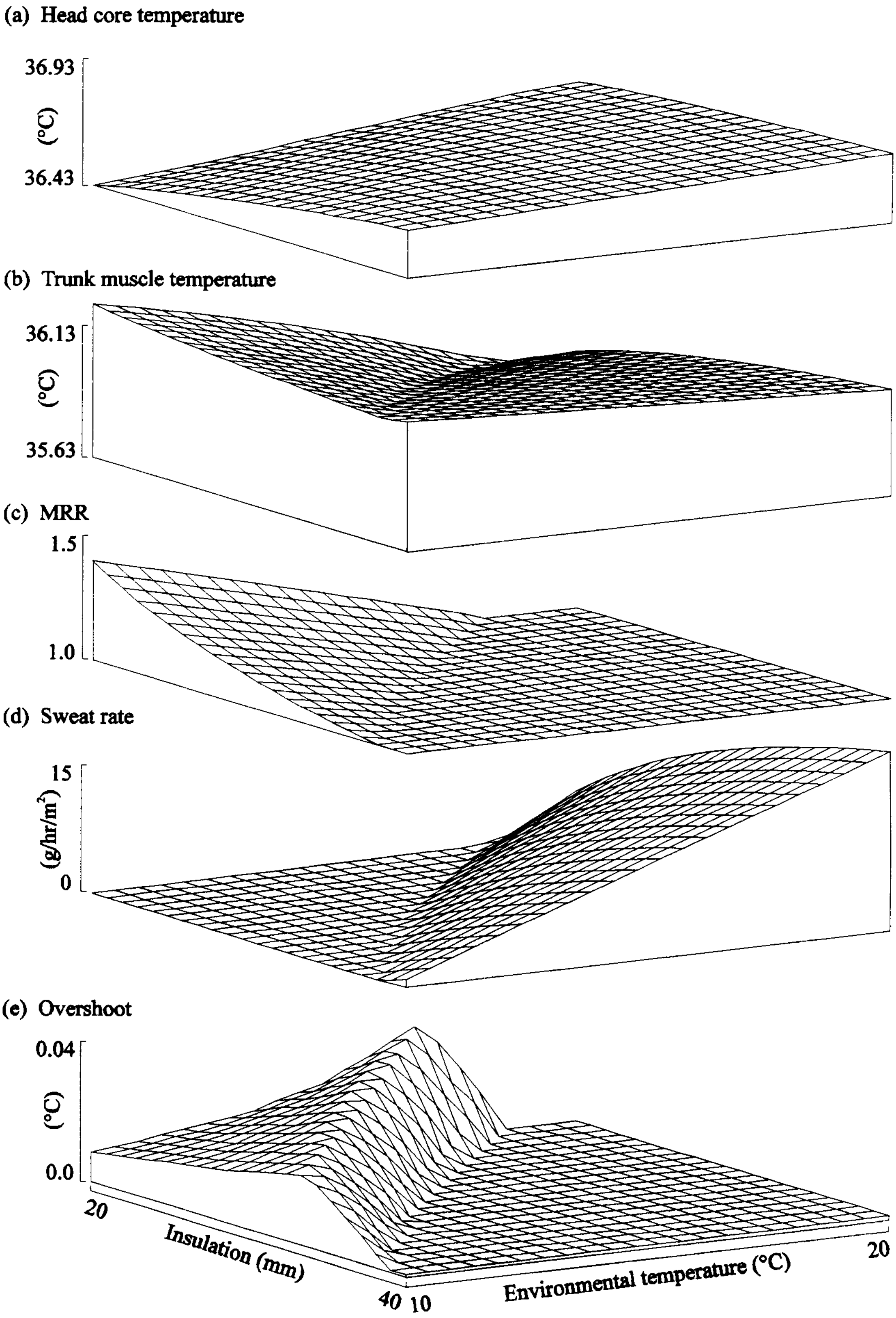

Figure 5.7 Behaviour of the infant thermoregulation model with head insulation thickness increased from 10mm to 13mm, representing the addition of a hat.

THE LIBRARY
UNIVERSITY OF CANTERBURY
CHRISTCHURCH, N.Z.

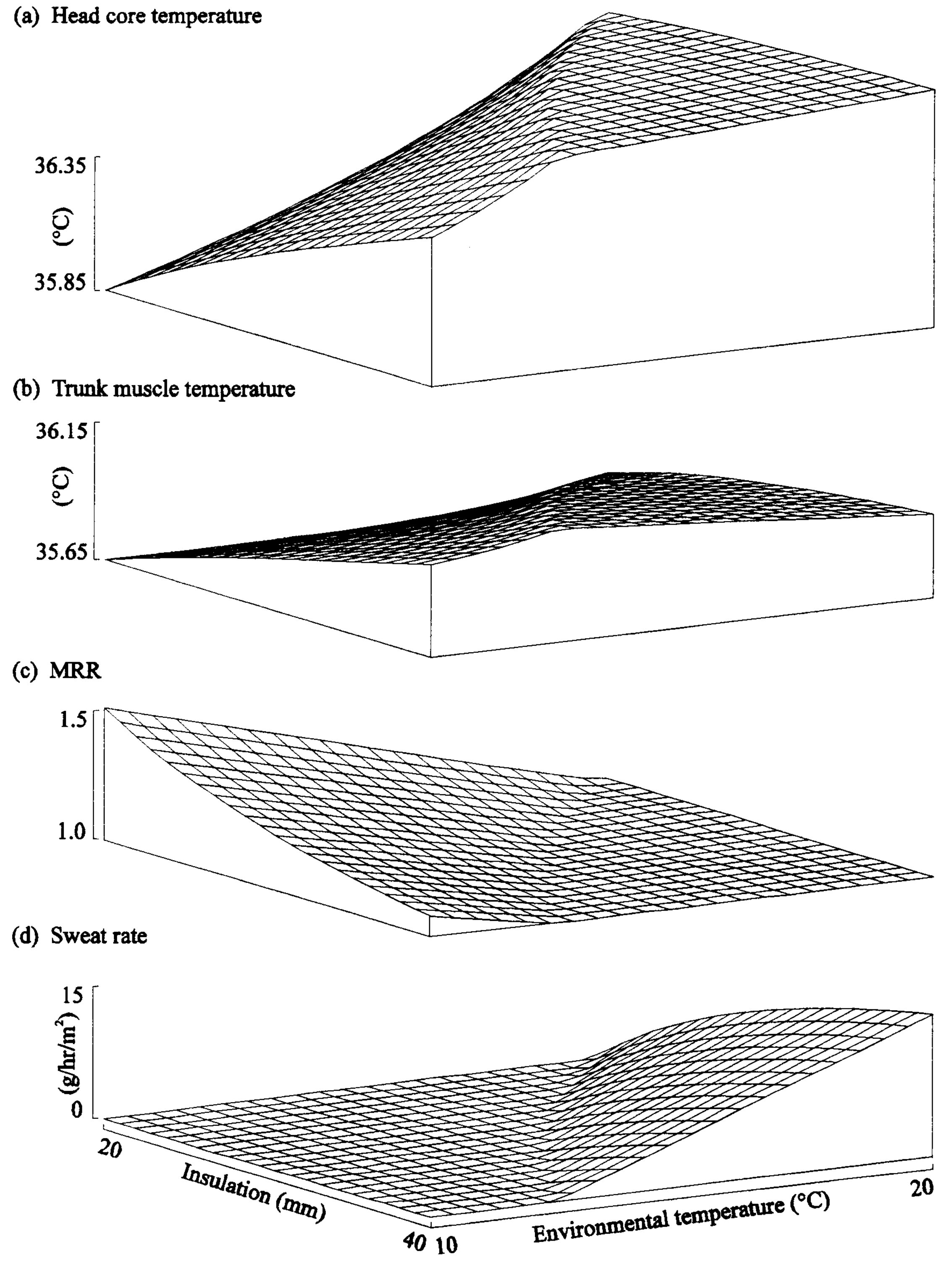

Figure 5.8 Infant thermoregulation model behaviour when the metabolic rate control loop gain is $1/6^{th}$ that of normal infants (i.e. the same thermal control as adults).

5.2 Characteristics of Infant Thermoregulation Model Oscillations

Although the model of infant thermoregulation is not unstable under normal physiological and environmental conditions, the oscillatory behaviour that occurs after a step input is of great interest. This is because oscillatory behaviour of a similar nature to that of the model has been observed in sleeping infants (see section 3.3). Considering the oscillatory behaviour is predominant when the model is slightly cooler than at thermoneutral, an insulation thickness of 27mm and an environmental temperature of 15°C have been chosen to further investigate the characteristics of the oscillatory behaviour. These values place the model in a state which is just cooler than thermoneutral so that the stability is relatively low, yet the body temperature changes produced by the small oscillations are not likely to force the state of the model to repeatedly cross the thermoneutral point (i.e. to repeatedly switch from shivering to sweating and back to shivering).

5.2.1 Controller characteristics

The stability of any feedback control system is dependent on the gain of the system (see section 2.2.5). Therefore, the characteristics of the human thermal controller, which vary between individuals, will have a major bearing on the thermoregulation system stability. Figure 5.9 shows the stability of the model for small changes in the gain and skin temperature set point. The range of gain and set point values have been chosen to represent the normal interindividual differences and inaccuracies in the clinical measurement of these parameters. Changes to the head core temperature set point are not investigated because if both set points are altered, only the steady state operating point of the model is altered, not the stability (i.e. the stability is altered by changing the difference between the two set points).

Figure 5.9 demonstrates the sensitivity of both the stability and the period of the oscillations to the characteristics of the controller. The thermoregulation model has previously been shown to be marginally stable under certain circumstances (see figure 5.6). However, figure 5.9 demonstrates that at an environmental temperature of 15°C and insulation thickness of 27mm, small physiologically possible changes in gain and skin temperature set point cause the model to becomes unstable and produces limit cycle oscillations. This result suggests that infant thermoregulation may indeed be unstable or marginally stable under certain conditions.

5.2.2 Mechanism

Adjustment of the gain of the system to produce sustained oscillations (a limit cycle) enables the mechanism through which the oscillations are elicited to be examined. Figure 5.10 shows the behaviour of the model with the gain increased by a factor of 1.6. The area weighted average skin temperature is shown because it is involved with thermal control within the model (see section 4.2.2).

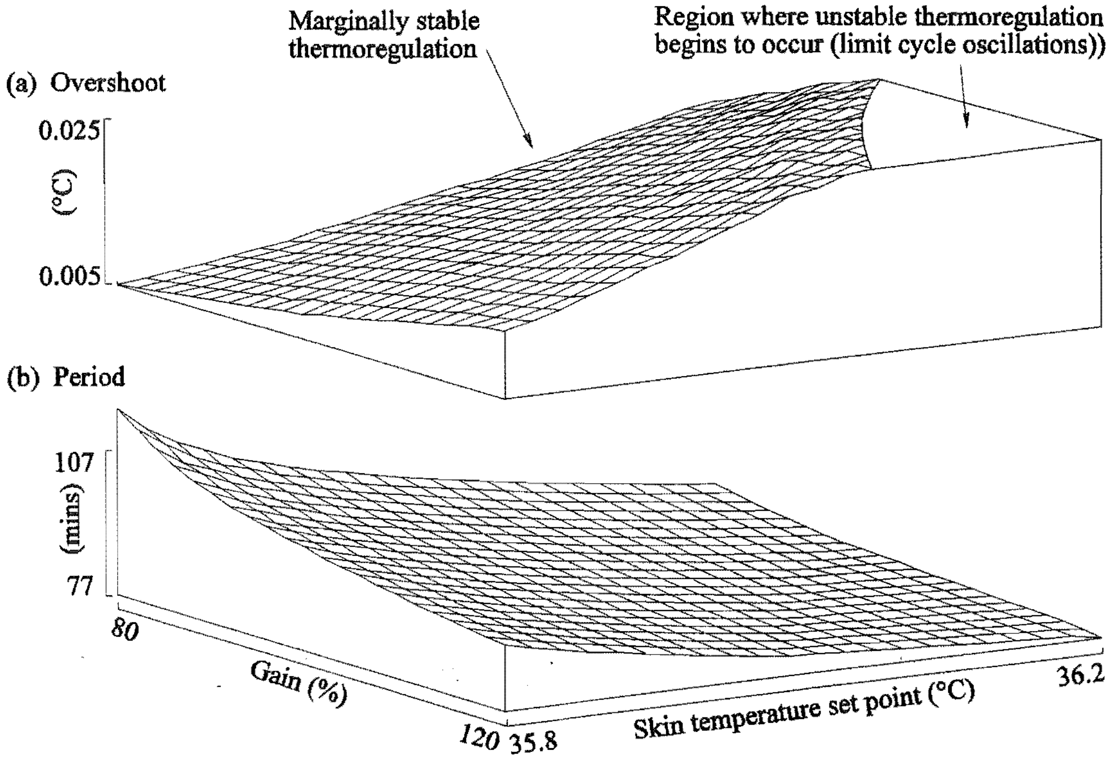

Figure 5.9 Effect of small changes in the controller gain and skin temperature set point on the period and stability of the model (T_{ENV} = 15°C, I_{TS} = 27mm).

The head core temperature is closer to the head core set point of 36.6°C than the average skin temperature is to the skin set point of 36.0°C. For this reason, any variations in head core temperature will initiate a greater fractional change in the control response than similar magnitude changes of the average skin temperature (see section 4.2.2). The muscle metabolic rate control response is an instantaneous function of the error signal and is therefore in phase with the error signal. Because the metabolic rate ratio in figure 5.10 is in phase with the error signal ($T_{HC,SET}$ - T_{HC}) rather than ($T_{S,SET}$ - T_S), the oscillations are elicited through the head core, not the average skin temperature.

There is a high degree of thermal coupling between the head core, trunk core and central blood compartments of the model. Therefore, the flow of blood between the head core and trunk core transfers sufficient heat to maintain the temperatures of these compartments to within a small fraction of a degree of each other. Thus, the core temperatures all have oscillatory behaviour of approximately the same phase. However, the trunk muscle temperature is significantly out of phase with the temperatures of the core compartments of the model, indicating that the response of thermal control is limited by the slow transfer of heat from the muscle to the trunk core. The slow transfer of heat is further emphasised by the peak of the metabolic rate ratio occurring during the maximum rise of the muscle temperature and at the trough of the core temperature. Low head core temperatures will increase the metabolic rate which will in turn produce an increase in the muscle temperature. Note that the oscillations of the core temperatures have a much smaller magnitude than the oscillations of the trunk

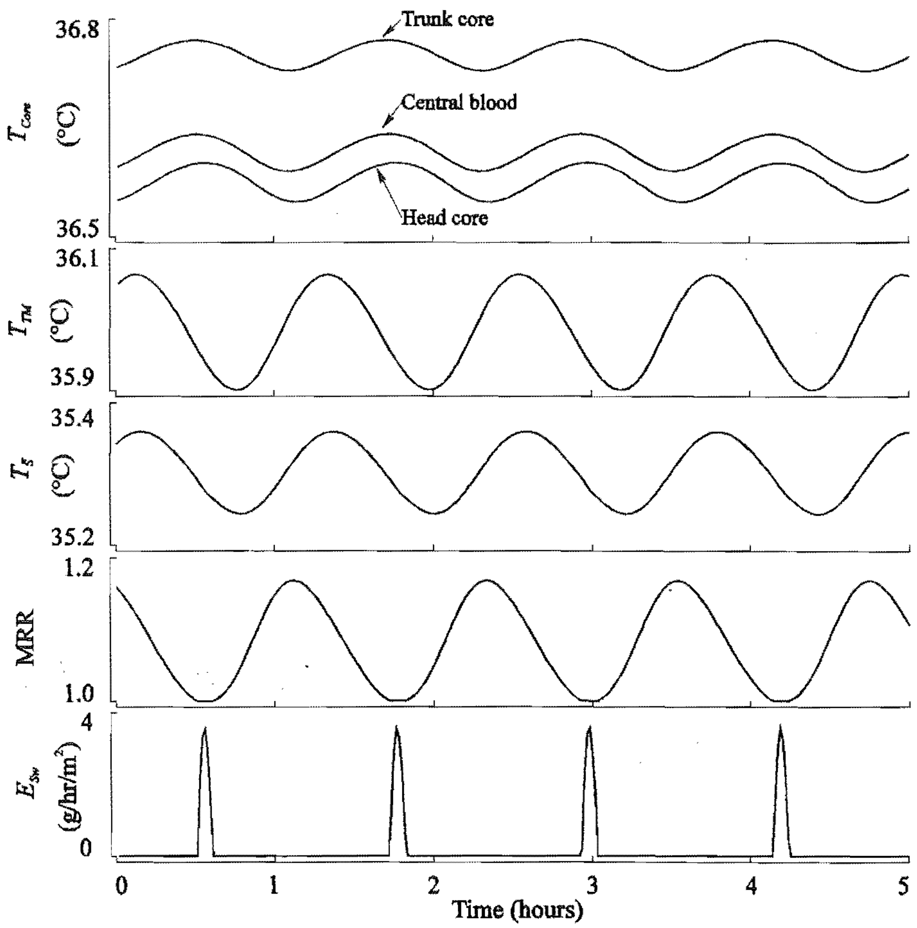

Figure 5.10 Sustained oscillations present in the model when the gain is multiplied by a factor of 1.6 (T_{ENV} = 15°C, I_{TS} = 27mm).

muscle temperature.

5.2.3 Compartment size

The period of the oscillatory behaviour of the model is governed by the phase delay through the feedback network (see section 2.2.5). In this model, the rate at which heat is transferred from the thermogenic compartment (muscle) to the core of the head has a significant affect on the phase delay. The rate of flow of heat between each compartment is dependent on the blood flow, conducting surface area and relative thermal capacities of each compartment. The thermal capacity of each compartment is dependent on the compartment size, thus, the model response is dependent on the relative sizes of each compartment. Figure 5.11 illustrates the effect that changes in head core and trunk core compartment size have on the head core temperature, 5.11(a), period, 5.11(b), and relative stability, 5.11(c), of the model. As the head core compartment size increases, the period increases, however, the stability of the model is not significantly altered. The opposite occurs as the trunk core compartment size increases. Therefore, the stability and period of the model are dependent, to a small extent, on the head core and trunk core compartment sizes. In contrast, the head core temperature is not significantly altered by variations of the compartment sizes. Thus, the model is capable of accurately regulating the head core temperature for a range of body proportions.

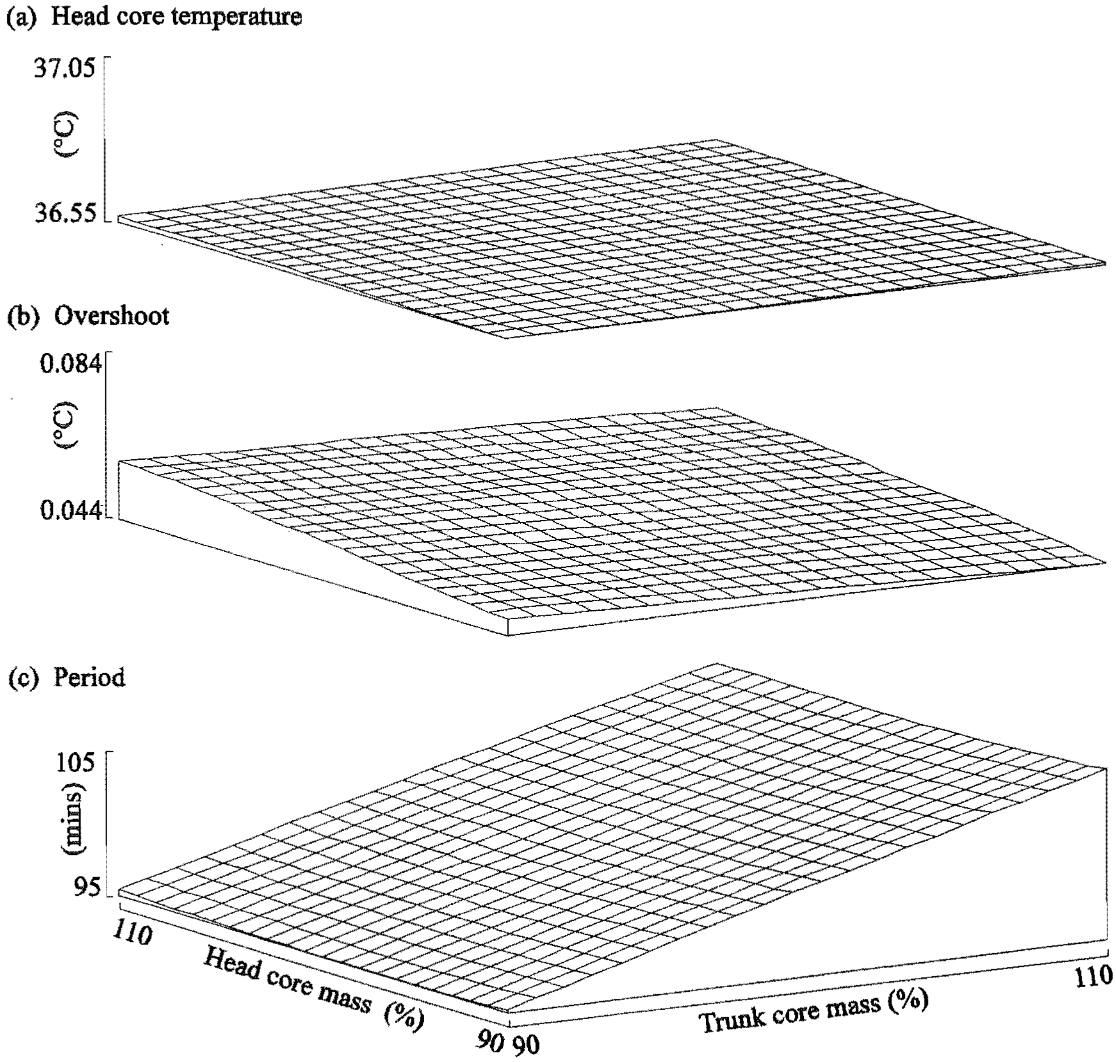

Figure 5.11 Effect of changes in head core and trunk core compartment size (T_{ENV} = 15°C, I_{TS} = 27mm): (a) Head core temperature, (b) Relative stability, (c) Period.

5.3 Comparison of Infant and Model Results

The infant thermoregulation model satisfactorily regulates the temperatures of the core compartments of the model for a wide range of environmental stresses and physiological conditions. In doing so, the sweat rate, metabolic rate, blood flows, temperature distribution and stability change according to the thermal stresses placed on the model. A number of these variables have been measured in infants (see section 3.4) and are compared with the model in this section.

5.3.1 Maturation

During the first six months of life, the infant undergoes a great deal of physiological change [Godfrey, 1981]. The effect of maturation on thermoregulation occurs through changes in the sizes, blood flows and metabolic rate of each compartment and also the controller sensitivity [Hensel, 1981, Chapter 16]. Little information is available on how the thermoregulation controller changes during the first six months of life. However, the changes in compartment sizes, blood flows and basal metabolic rates are well documented and have been presented in section 4.3. Figure 5.12 illustrates the effect of maturation on infant thermoregulation for the age range of 4 to 32 weeks. The results for four different thermal loads close to the thermoneutral point are shown. For the purposes of this investigation, it is assumed the controller sensitivity remains constant over the first year.

From figure 5.12, the stability of the model decreases with age over the first 32 weeks of life. A similar trend has also been shown for the mean square value of the rectal temperature oscillations of infants (see figure 3.16). For both the infants and the model, the period of the oscillations are relatively independent of age. However, both the infants and the model show a slight increase in the period for ages less than 8 weeks.

5.3.2 Trunk muscle temperature dependence

According to the behaviour of the model (discussed in sections 5.1 and 5.2), an infant who is cool is likely to display oscillatory behaviour, while an infant who is very cold or hot is not. This observation has been compared with data obtained from clinical experiments on infant thermoregulation.

Recordings of rectal, skin and ambient temperature and breathing rate from infants in their home environment have been presented in Chapter 3. The data illustrates that oscillations in these variables are more likely to occur when the rectal temperature of the infant is near the mean value. If the mean rectal temperature of the infants is near the thermoneutral point, then the model and infant data agree (see figure 5.6). However, the infant data has been presented with respect to rectal temperature, while the model has been presented with respect to thermal load. Assuming that the trunk muscle temperature of the model is a close representation of infant rectal temperature, then a direct comparison of the model with the infant data can be made. Figure 5.13 presents the characteristics of the model with respect to trunk muscle temperature. The data has been found for combinations of insulation and environmental temperature. The thermal stresses (combinations of environmental temperature and insulation thickness) required to produce the data are shown in figure 5.13(a). The resulting behaviour is shown in 5.13(b). Repeated values of rectal temperature may occur since the same rectal temperature may result from different combinations of environmental temperature and insulation thickness.

Assuming that the metabolic rate ratio is directly related to the ventilation rate and therefore breathing rate (a valid assumption since the purpose of respiratory control is to cater for the metabolic demands of the body (see Chapter 6)) [Mead & Agostioni, 1964], then the behaviour of the model (figure 5.13) is very similar to the infant data (figure 3.18). There is a peak in the power of the rectal

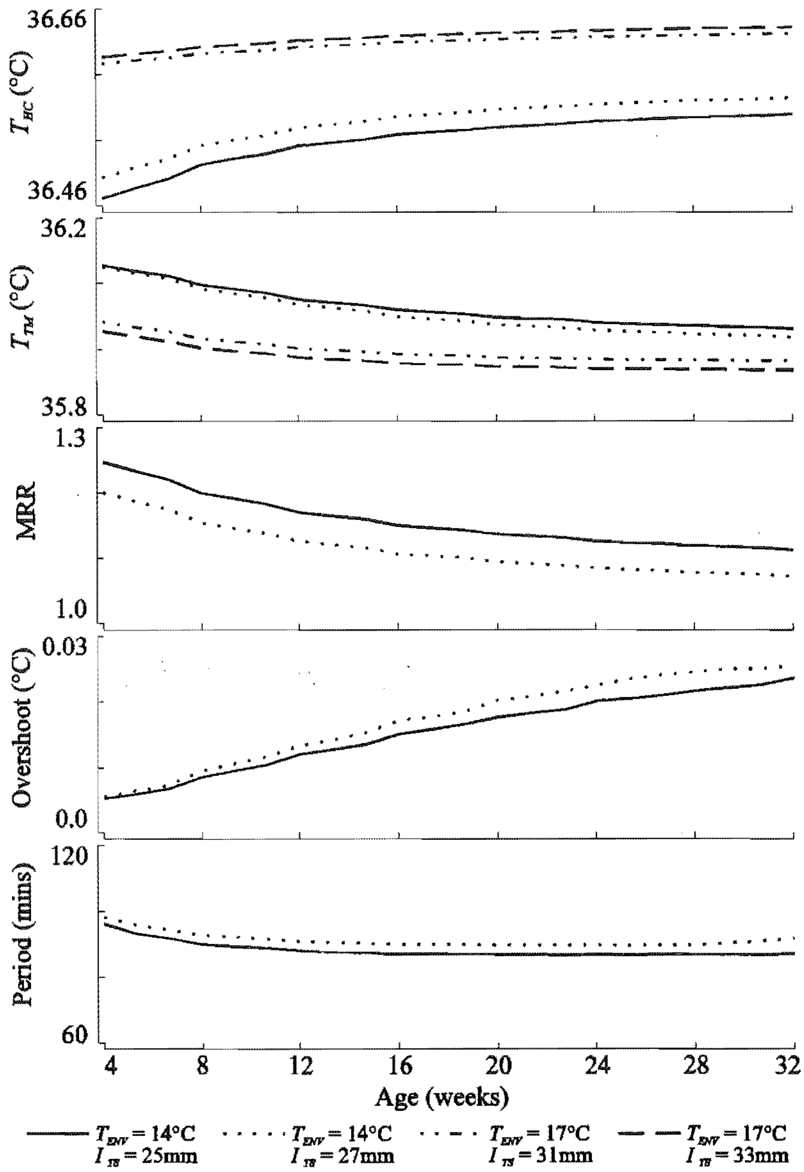

Figure 5.12 Dependence of the behaviour of the model on age during the first to eighth month of life for two cool and two warm thermal loads.

temperature, BR and IQBR oscillations of the infant data which matches a similar peak in the head core temperature overshoot of the model. This data supports the hypothesis that the oscillations in infant body temperatures and respiration are a result of unstable thermoregulation and that the trunk muscle temperature of the model is equivalent to infant rectal temperature.

5.3.3 Wakefulness to sleep transition

When an infant falls asleep, a significant drop in rectal temperature occurs (see section 3.4). Possible mechanisms for this include a reduction in metabolism or a reduction in thermal set points. The aim of this section is to investigate the

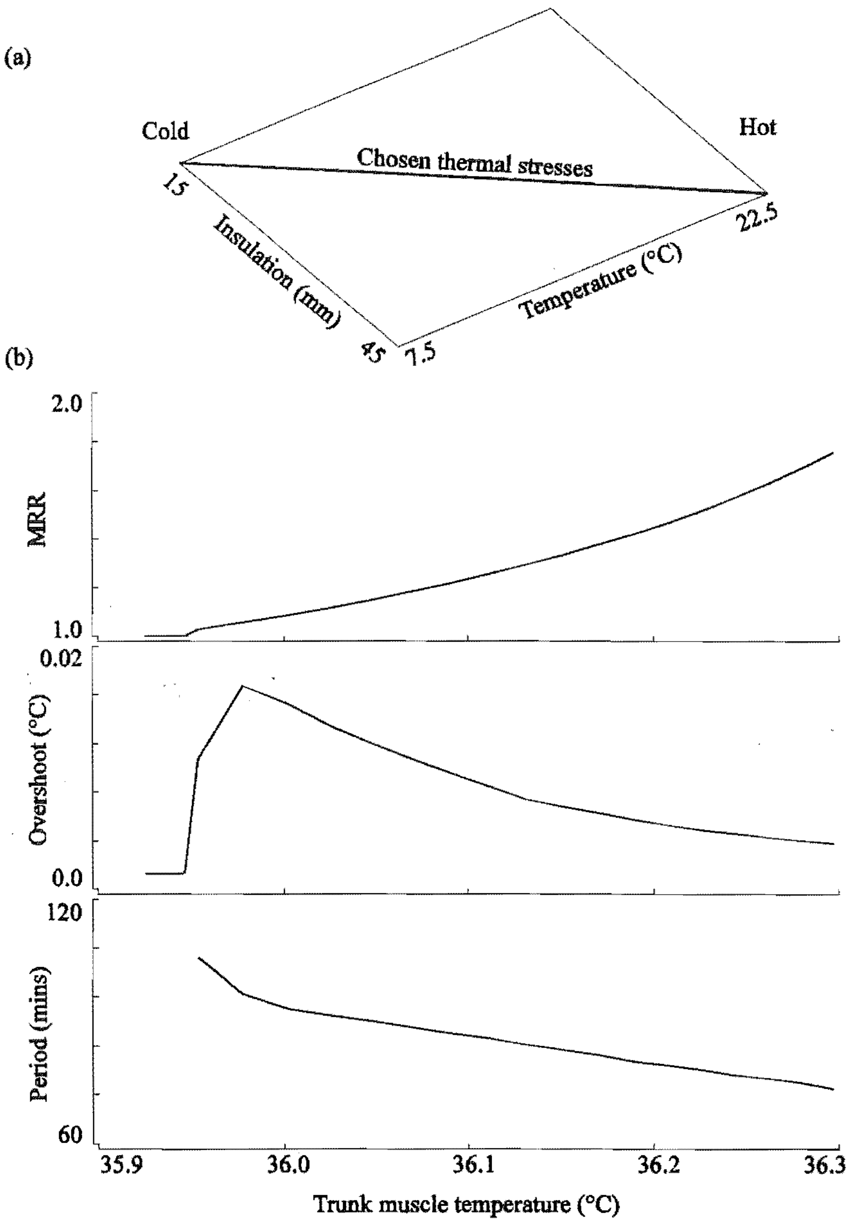

Figure 5.13 Behaviour of the model with respect to trunk muscle temperature.

observed temperature behaviour of an infant in bed with simulations from the mathematical model of infant thermoregulation.

Two major changes occur at bed time which are relevant to thermoregulation. Firstly, the insulation layer is normally increased with the addition of bedding. The increase in insulation counters the second effect, which is a significant reduction in the metabolic rate and associated blood flows. These two mechanisms, along with the effect of a reduction in head core temperature set point, are investigated as possible mechanisms which may produce the temperature behaviour that is observed when infants are put to bed. In both examples which follow, values for bed insulation and environmental temperature are 29mm and 16°C respectively. This places the model in a thermoneutral environment.

Figure 5.14 illustrates the effect of a 0.5°C decrease in the head core temperature set point. All the temperatures of the model decrease with the drop in the set point and a peak in the metabolic rate ratio occurs approximately one hour after the disturbance. This peak has not been observed in infant studies. The sweat rate also increases after the disturbance. Therefore, a reduction in set point at the onset of sleep does not appear to be a possible mechanism for the bed time drop in rectal temperature observed in human infants.

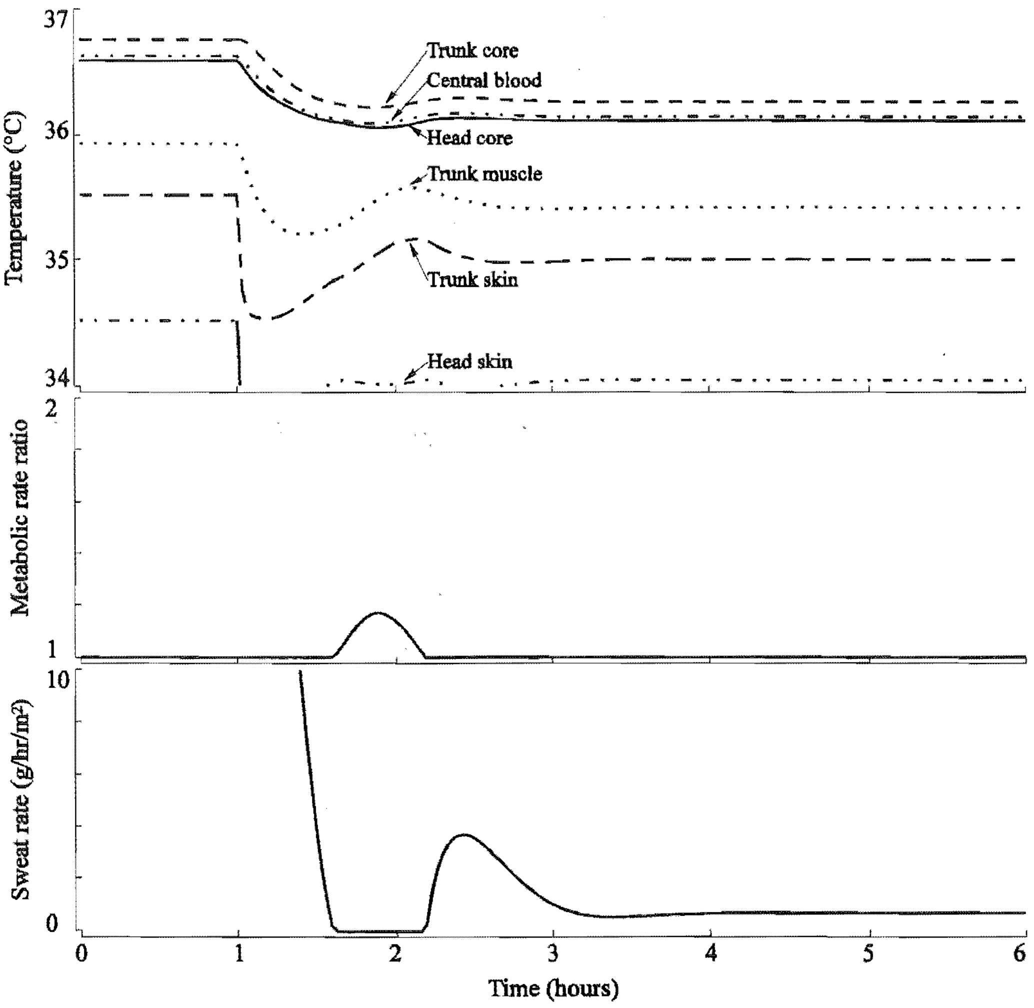

Figure 5.14 Effect of a 0.5°C drop in head core set point temperature.

Figure 5.15 illustrates the effect of the increase in trunk insulation which occurs when an infant is put to bed. As expected, the model core temperatures increase by a small amount with the increased insulation thickness. If the muscle compartment temperature is considered to be the best representation of rectal temperature, then the model and infant data agree. In figure 5.15 the muscle temperature behaviour closely reflects the observed rectal temperature behaviour of infants at bed time. A small rise in muscle temperature occurs at bed time which then falls to approximately 0.3°C below the initial temperature. The trunk skin temperature of the model rises rapidly in a manner similar to the abdomen temperature observed in infants. Also, the peaks in the metabolic rate ratio of the model are in phase with those observed in the breathing rate of infants. In particular, the metabolic rate is high at sleep onset and peaks occur during rising muscle temperature.

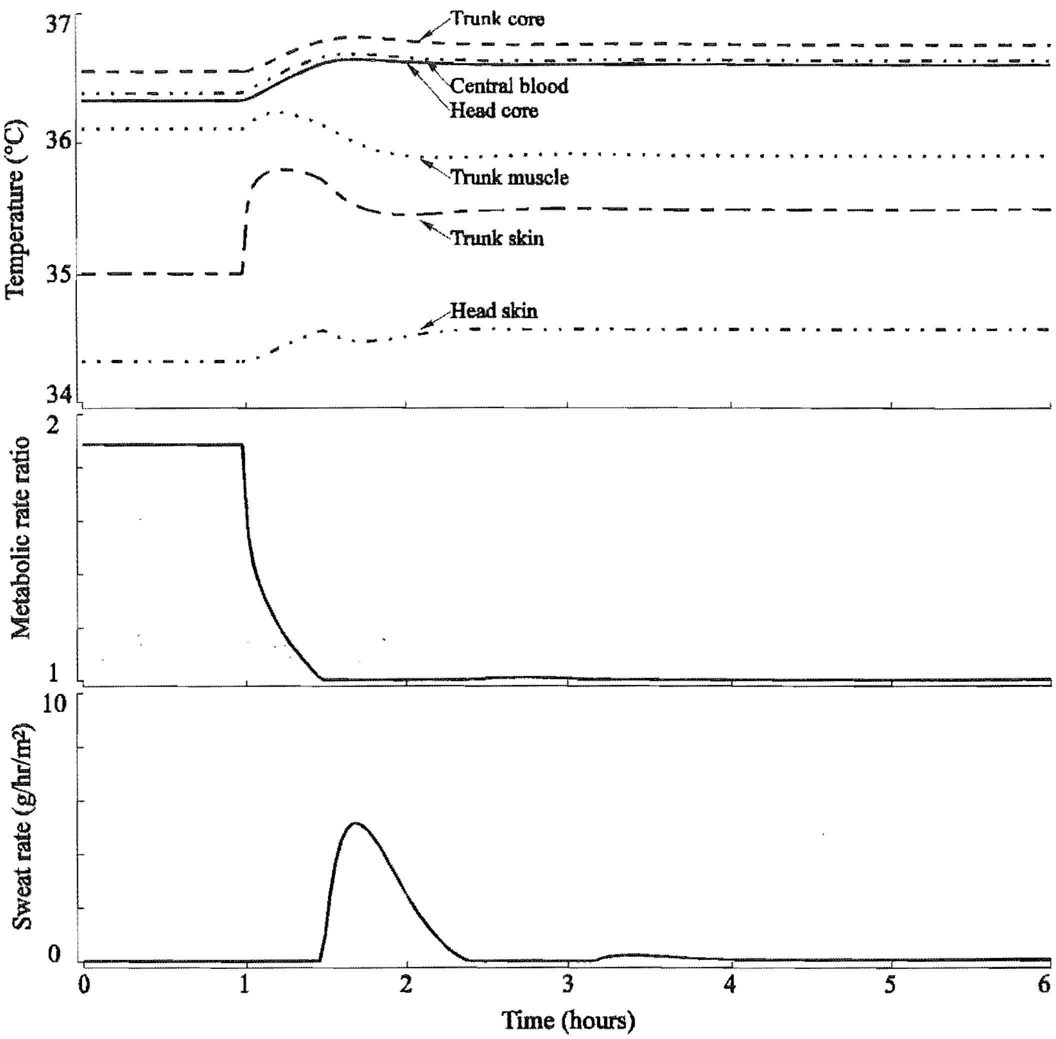

Figure 5.15 Effect of a step increase in insulation from 10 to 30mm.

The metabolic rate ratio of the model prior to and at the point where the insulation layer is added is higher than that which would occur in resting infants, although limited data is available on this aspect. However, when a resting adult falls asleep, the basal metabolic rate and cardiac output fall by up to 15% [Khoo et al., 1991; Brebbia & Altshuler, 1965] and 12% [Khatri & Freis, 1967] respectively. This is probably due to a reduction in gross muscle activity at sleep onset. For an active infant these drops may be considerably larger [Stabell et al., 1977; Childs, 1993]. This could be accounted for in the model by the elevated metabolic rate of the muscle compartment prior to and at the point where the insulation is added.

The simulation presented in figure 5.15 not only includes the effect of the addition of insulation, but also the reduction in metabolic rate caused by reduced muscle activity. It is not known if a reduction in gross muscle activity of an infant is due to reduced demand for metabolic heat production (i.e. thermoregulation), or a direct result of sleep, or if the two events are coincidental. Regardless of this, the model behaves in almost the same manner as that observed in infants. In a normally thermoregulating system, the addition of insulation and reduction of heat production cannot be considered to be mutually exclusive. This is clearly demonstrated in figure 5.15.

Under different environmental conditions, the bed time temperature behaviour observed in figure 5.15 may alter. Table 5.1 presents the bed time thermoregulation behaviour in terms of the difference in the steady state temperatures and metabolic rate of the model prior to and after a step increase in insulation or a decrease in muscle metabolic rate. The data has been collected at environmental temperatures of 16, 20 and 24°C. For the circumstances presented in table 5.1, the head core temperatures remain relatively constant, while the muscle and trunk skin temperatures change by a larger extent. This is because the head core temperature is a controlled variable while the muscle temperature is not. In all but one case, there is a drop in trunk muscle temperature, however, the trunk skin temperature is less predictable. This illustrates that measuring skin surface temperatures as an estimate of core temperature is unreliable and changes in body temperatures (excluding the core compartments) are highly dependent on environmental conditions. For the one case presented in table 5.1 in which the trunk muscle temperature increased, there was only a small reduction in metabolism, coincident with an increase in insulation. In summary, any reduction of the muscle compartment temperature of the model occurs because of reduced muscle activity. This could explain the reduction in rectal temperature observed in infants when they are put to bed.

T_{ENV} (°C)	Prior activity	Insulation added	ΔT_{HC} (°C)	ΔT_{TM} (°C)	ΔT_{TS} (°C)	ΔMRR (total)
16	Yes	Yes	0.07	-0.42	0.32	-0.92
16	No	Yes	0.28	-0.20	0.52	-0.92
16	Yes	No	-0.21	-0.23	-0.21	0.0
20	Yes	Yes	-0.01	-0.49	0.12	-0.75
20	No	Yes	0.23	-0.04	0.41	-0.5
20	Yes	No	-0.24	-0.39	-0.29	-0.25
24	Yes	Yes	-0.06	-0.63	-0.05	-0.75
24	No	Yes	0.16	0.19	0.37	-0.15
24	Yes	No	-0.22	-0.82	-0.42	-0.5

Table 5.1 Effect of environmental temperature, metabolic rate and insulation on compartment temperatures of the model. This represents the behaviour of infant body temperatures at bed time.

The mechanisms described here, which occur when the infant is put to bed, independently have a significant effect on thermoregulation. However, the coexistence of a drop in metabolic activity and an increase in thermal insulation is most likely to occur when an infant is put to bed. This combined effect yields some of the largest drops in trunk muscle temperature of the model (see table 5.1). It seems unlikely that any other mechanism could exist which would cause an effect similar to that observed in infants without affecting the body through other physiological variables. For example, a drop in set point does not explain the behaviour of the skin temperature or metabolic rate. Hence, a decrease in muscle metabolic activity provides the most plausible explanation of the observed behaviour of infant thermoregulation (drop in rectal temperature) that occurs at bed time. However, this assumes the rectal temperature is a reflection of the temperature in or near a thermogenesis region of the body. Further clinical experiments are necessary to ascertain if this is in fact the case, although other aspects of the behaviour of the model indicate that the trunk muscle compartment of the model reflects infant rectal temperature (see section 5.2).

In order to determine whether the bed time drop in rectal temperature is caused by sleep or coexists with sleep, clinical experiments on awake subjects going to bed but not falling asleep must be carried out. If the drop in rectal temperature occurs when bed clothes are placed on an awake subject then the mechanism is independent of sleep. This type of experiment is impractical to perform on infants but the results would be equally valid from experiments performed on adults, provided the rectal temperature drop does occur.

A preliminary experiment has been carried out on an adult to investigate whether the rectal temperature drop is independent of sleep. Figure 5.16 shows the environmental, abdomen and rectal temperatures for one adult after going to bed and remaining awake. A normal bed time routine with no significant exercise was carried out prior to the study. Once in bed, the subject was at rest but remained alert.

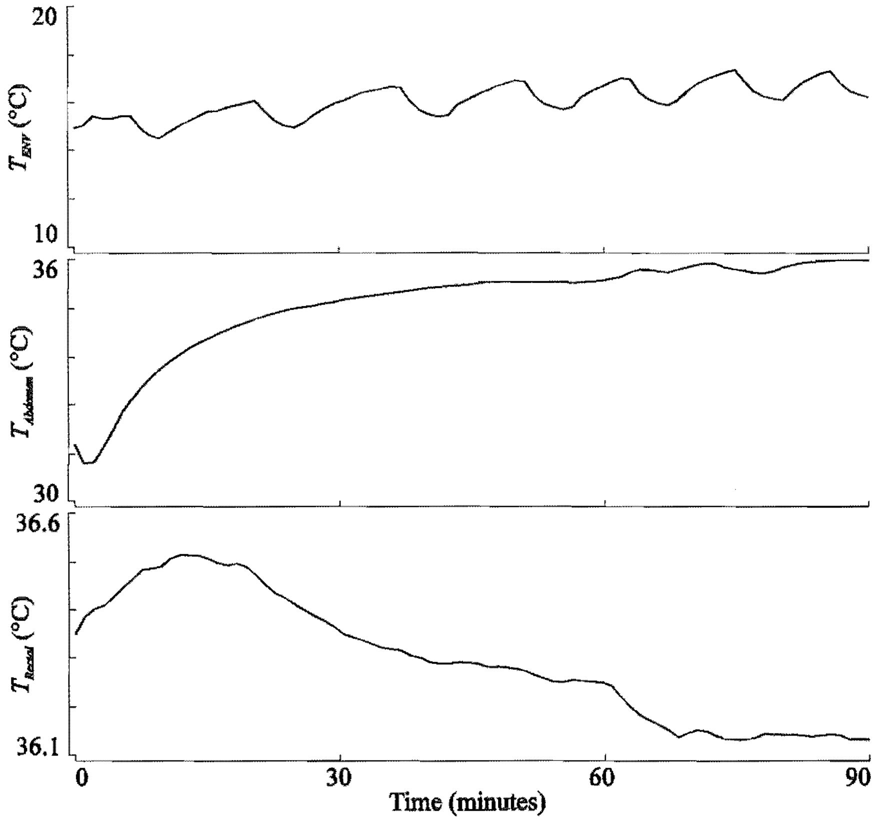

Figure 5.16 Effect of going to bed (without sleeping) on an adult.

The addition of bed clothes is reflected in the rising abdomen temperature. Stabilisation of the temperatures occurred after approximately 70 minutes. A small peak, followed by a 0.4°C drop in rectal temperature occurred. Clearly, the drop in rectal temperature in this example is independent of sleep. However, the above experiment must be repeated for a number of adults in a variety of different environmental conditions in order to generalise this conclusion.

An interesting observation in figure 5.16 is the oscillatory behaviour of the environmental temperature. This behaviour is a result of a thermostatically controlled heater repeatedly switching on and off. The environmental temperature oscillations are not present in the rectal or abdomen temperatures, therefore, the oscillations had an insignificant effect on the thermoregulation of the subject during the experiment.

5.4 Summary

The similarity of the behaviour of the infant thermoregulation model to that observed in infants is clearly evident. The comparison of the thermo-respiratory behaviour of a 3 month old infant and the model are shown in figure 5.17. Considering 5.17(a) is a single recording from one infant and 5.17(b) is the model of an average infant, the infant and model data appear to be surprisingly similar.

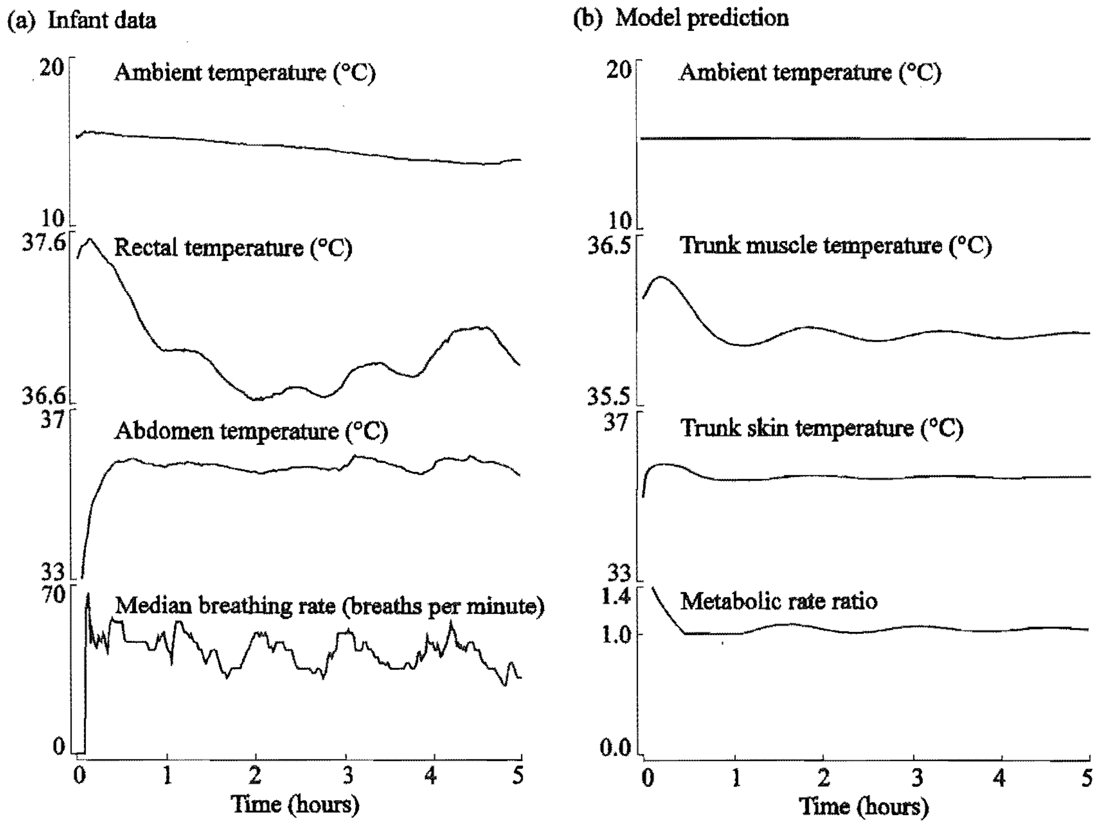

Figure 5.17 (a) Physiological signals from a sleeping infant (3 months), (b) the model prediction. Initially the trunk insulation of the model is increased from 10mm to 27mm to simulate the infant being put to bed.

The following is a list of the key characteristics of the model which are similar to the behaviour measured in infants (see Chapter 3):

- The thermal model successfully regulates core body temperatures under a wide range of thermal stresses. The thermoneutral point of the model is similar to that of infants under similar thermal conditions.
- Oscillations of infant body temperatures occur. Oscillations with a similar period occur in the model.
- The magnitude of the rectal temperature oscillations of the infants is similar to the temperature oscillations of the trunk muscle compartment of the model.
- The infant rectal temperature oscillations are reflected in the breathing rate (indicating a similar change in metabolic rate). In a similar manner, the trunk muscle temperature oscillations of the model are reflected in the metabolic rate of the model. The phase difference between the infant rectal temperature and breathing rate is the same as the phase difference between the trunk muscle temperature and metabolic rate of the model.
- A drop in infant rectal temperature occurs when infants are put to bed. In the model, a drop in trunk muscle temperature occurs under similar conditions (i.e. significantly increasing the insulation thickness). The temperature drops are of similar magnitude in the infant and the model.
- Age dependent parameters of the model are similar to those of infants.

The similarities summarised above rely on the model trunk muscle temperature being equivalent to infant rectal temperature. Physiologically this is plausible because blood returning from the muscles of the legs passes through the rectal region of the body. The rectal temperature probably reflects a combination of both the core and muscle temperatures. However, since the core temperature is held relatively constant by the thermoregulation controller, the dynamic behaviour observed in the infant rectal temperature is most likely to be a result of changes in muscle temperature.

The thermoregulation oscillations of the model are a result of the slow transfer of heat from the muscle compartment to the core of the body combined with the high gain of the negative feedback metabolic control loop. The similarity of the model to the infant behaviour indicates that the model is probably a qualitatively accurate representation of the mechanisms observed in sleeping infants.

During wakefulness, oscillatory behaviour of infant thermoregulation is less likely to occur. This is due to the higher basal metabolic rate and factors such as movements and exercise which produce effects that overshadow the oscillations. The model is not capable of explaining oscillations of the interquartile range of the breathing rate which has been observed in infants (see Chapter 3). To examine this, a model of infant respiration is required. Such a model is developed and discussed in Chapters 6 and 7.

Chapter 6

Mathematical Modelling of Human Respiration

This chapter describes the history of mathematical modelling of the human respiratory system and develops a model of respiration for the human infant. The model has been designed to investigate the effect of temperature on the behaviour of the respiratory system of infants. To achieve this, the temperature sensitivity of parameters of the respiratory system have been researched and incorporated into the model.

6.1 Respiration Models

One of the earliest mathematical models of the human respiratory system was published in 1949 [Gray, 1949]. This model described the steady state, chemical control of ventilation and was followed in 1954 by the first dynamic model of ventilation [Grodins et al., 1954].

Mathematical models of respiratory control usually consider only the CO_2 and O_2 stores in the body and relate the ventilation rate to the amount of these gases in the body, producing a negative feedback control system model (see figure 1.3). Respiratory models consider the body tissues to be divided into regions or compartments. Within each compartment, the CO_2 is assumed to be stored in the body tissues while O_2 is assumed to be stored in the venous blood which perfuses that tissue. In addition, gaseous CO_2 and O_2 is stored in the lungs and O_2 is stored in the arterial blood. Within each tissue compartment, CO_2 is produced and O_2 is consumed by metabolic processes. The CO_2 and O_2 stored in the lungs is exchanged with the environment outside the body at a rate which is proportional to the ventilation rate.

Dynamic models of the gas stores of the human respiratory system are typically based on the law of conservation of mass. Thus, for each gas species considered in a respiratory model, the rate of change of the partial pressure of the gas, P, in each region of the body, is proportional to the content of gas entering that region (volume of gas per volume of blood), C_{IN}, minus the content of gas leaving, C_{OUT}, thus

$$\frac{dP_i}{dt} = \alpha(C_{IN,i} - C_{OUT,i}), \tag{6.1}$$

where i is the compartment of the body under consideration and α is a constant. Therefore, a typical respiratory model consists of a set of differential equations where each equation describes the rate of change of gas partial pressure in each region of the body. Controller equations, which describe the lung compartment ventilation rate, are included to complete the negative feedback control of ventilation (see sections 1.3.1 and 2.2.5). Equation (6.1) is highly non-linear since the partial pressure of gas is a non-linear function of the gas content (see section 6.3).

The major differences between many of the proposed mathematical models of human respiration are found in the model structures (number and nature of the compartments), controller equations and methods of solving the set of differential equations. Some models have also specifically considered the infant respiratory system [Revow et al., 1989; Nugent & Finley, 1987; Kelly et al., 1988; Tehrani, 1990; Cleave et al., 1985; Tehrani, 1993].

The structure of gas storage in some of the early models of respiration is characterised by a division of the gas stores into the muscle compartment and a compartment consisting of the remaining metabolising tissue [Longobardo et al., 1966]. Other models have been developed which consider either a single tissue compartment [Carley & Shannon, 1988; Revow et al., 1989] or the brain compartment and a compartment consisting of all other metabolising tissue (including muscle) [Grodins et al., 1967; Fincham & Tehrani, 1983; Khoo et al., 1982; Longobardo et al., 1989].

Respiratory control has traditionally been incorporated into respiratory models by defining the ventilation rate as a function of the partial pressures of CO_2 and O_2 in the blood of the carotid artery [Longobardo et al., 1966; Grodins et al., 1967; Rebuck et al., 1977]. However, subsequent research has shown that the ventilation rate is also a function of brain CO_2 and this effect has been incorporated into recent models [Fincham & Tehrani, 1983; Khoo et al., 1982; Longobardo et al., 1989; Revow et al., 1989; Nugent & Finley, 1987]. Some models assume that the lungs are ventilated by a continuous flow of gases [Longobardo et al., 1966; Grodins et al., 1967; Carley & Shannon, 1988; Nugent & Finley, 1987] while others have attempted to model the inspiratory and expiratory phases of breathing [Fincham & Tehrani, 1983; Longobardo et al., 1989; Khoo et al., 1991; Revow et al., 1989].

Early models of respiration were typically simulated on analog computers [Gray, 1949; Grodins et al., 1954]. More recently, the advent of digital computers has allowed such models to be simulated by invoking numerical integration techniques (see section 2.2.4) to solve the set of differential equations [Longobardo et al., 1966; Fincham & Tehrani, 1983; Longobardo et al., 1989; Khoo et al., 1991; Revow et al., 1989; Tehrani, 1990]. In contrast, some researchers have attempted to linearise their models of respiration and produce an approximate analytical solution [Khoo et al., 1982; Carley & Shannon, 1988; Nugent & Finley, 1987].

There is no single mathematical model which accounts for all observations of the respiratory system. Each model tends to concentrate on a few aspects of respiration. Typical examples of mathematical models of respiration for various areas of research are presented in table 6.1.

The mathematical models of infant and adult respiration, which have been developed over the past decade, include significant mathematical detail. However, little emphasis has been placed on the effects of temperature and thermoregulation on the steady state and dynamic response of the respiratory system.

Respiratory Behaviour	Reference
CO_2 inhalation	Grodins et al., 1967; Fincham & Tehrani, 1983
O_2 inhalation	Grodins et al., 1967
Hyperventilation	Longobardo et al., 1966; Fincham & Tehrani, 1983; Khoo et al., 1982
Apnoea, Asphyxia	Grodins et al, 1967
Exercise, CO_2 infusion	Fincham & Tehrani, 1983
Periodic breathing, Stability	Longobardo et al., 1966; Kelly et al., 1988; Khoo et al., 1982; Nugent & Finley, 1987; Bruce & Modarreszadeh, 1990; Longobardo et al., 1989; Cleave & Levine, 1984; Cleave et al., 1986; Carley & Shannon, 1988; Khoo et al., 1991
Infant respiration	Nugent & Finley, 1987; Revow et al., 1989; Tehrani, 1990; Cleave et al., 1985; Tehrani, 1993

Table 6.1 Examples of respiratory models presented in the literature for various areas of research.

6.2 A Mathematical Model of Infant Respiration

The mathematical model of infant respiration described in this section is based on negative feedback control and is comprised of a *controlled system* and a *controller* (see figure 6.1). The model structure is simpler than those proposed by other researchers because mechanical aspects of air flow are not included. However, the effects of inspiration and expiration are largely removed by the mixing or averaging that occurs in the blood pool formed by the heart and large arteries [Lange et al., 1966]. Any small perturbations of arterial gas partial pressures resulting from the respiratory cycle are of sufficiently high frequency that they are not important for this study. Of particular interest to this research is the relative temperature dependence of the respiratory system, therefore the small improvement in accuracy achieved by including lung mechanics is not warranted. Furthermore, only respiratory elements with time responses of a few minutes are included because long term effects are not important in this investigation. However, much emphasis has been placed on the accuracy of the mathematical representation of the gas dissociation curves (see section 6.2.2) in an attempt to improve on inaccuracies of other respiratory models. Also, temperature forms the crux of the research presented in this thesis and the dissociation curves are dependent on temperature.

The controlled system consists of the circulation, the CO_2 (carbon dioxide) and O_2 (oxygen) stores in the body, and describes the exchange and transport of CO_2 and O_2 at the lungs and metabolising tissue sites. A block diagram of the model illustrating the gas storage compartments is shown in figure 6.2. The CO_2 and O_2 stores are divided into three parallel compartments connected by the circulation. Each compartment is assigned its own blood flow, metabolic rate, tissue dissociation curve for CO_2 and blood O_2 dissociation curve. A pathway for the circulation through the skin is also included because, although there are no significant gas stores in the skin, vasomotor action may change the blood flow

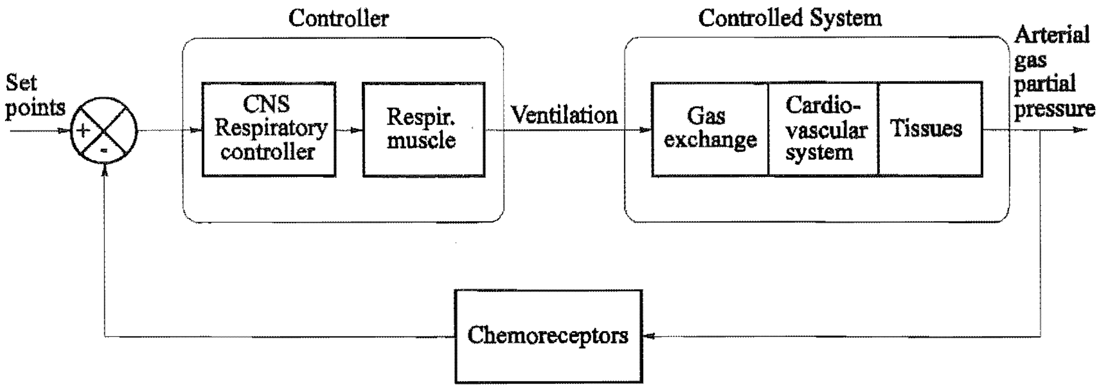

Figure 6.1 Schematic diagram of human respiration illustrating the negative feedback structure of respiratory control.

through this path, thus modifying the behaviour of the model.

Perfect matching of the partial pressures of the arterial and alveoli (the smallest gaseous compartments of the lung) gases does not occur. For this model, a significant O_2 partial pressure gradient across the lung membrane is included, however, the alveoli CO_2 partial pressure is taken to be equal to arterial CO_2 partial pressure [Koch, 1968]. An anatomical shunt is included in the model to account for the physiological anatomical shunt which is present in young infants and ventilation perfusion mismatching [West, 1979]. Although these two mechanisms are independent, their effects on the model are the same and they may be lumped together.

The compartments where gas is stored are the *lung* functional residual capacity (FRC), the *brain* and a compartment comprising all *other* metabolising body tissues (including muscles and organs, but excluding fat and bone). The blood associated with each compartment also acts as a gas store. Although significant stores of CO_2 occur in the bone, accumulation and release only occurs over long periods of time [Farhi & Rahn, 1960], therefore bone is not included in this model. The skin is where most of the heat exchange of the body occurs and the rate of heat exchange is controlled to some extent by vasomotor action. Thus, thermoregulation influences peripheral blood flow and, consequently, thermoregulation influences the respiratory system behaviour as well. Therefore, peripheral blood flow has been included in this model.

The controller relates the ventilation rate to the CO_2 and O_2 gas partial pressures at the central and peripheral chemoreceptor sites and attempts to maintain the CO_2 and O_2 stored in the body at normal partial pressure values. This completes a dual feedback loop by altering the rate at which gas is inhaled and exhaled by the lungs. The central chemoreceptor is sensitive to CO_2 in the brain [Bruce, 1987] and the peripheral chemoreceptor is sensitive to both CO_2 and O_2 in the carotid artery [Comroe, 1964].

Time is the independent variable in the following equations which describe the respiratory system model. In the interest of notational simplicity, explicit dependence of the variables on time is suppressed except where it is necessary for clarity.

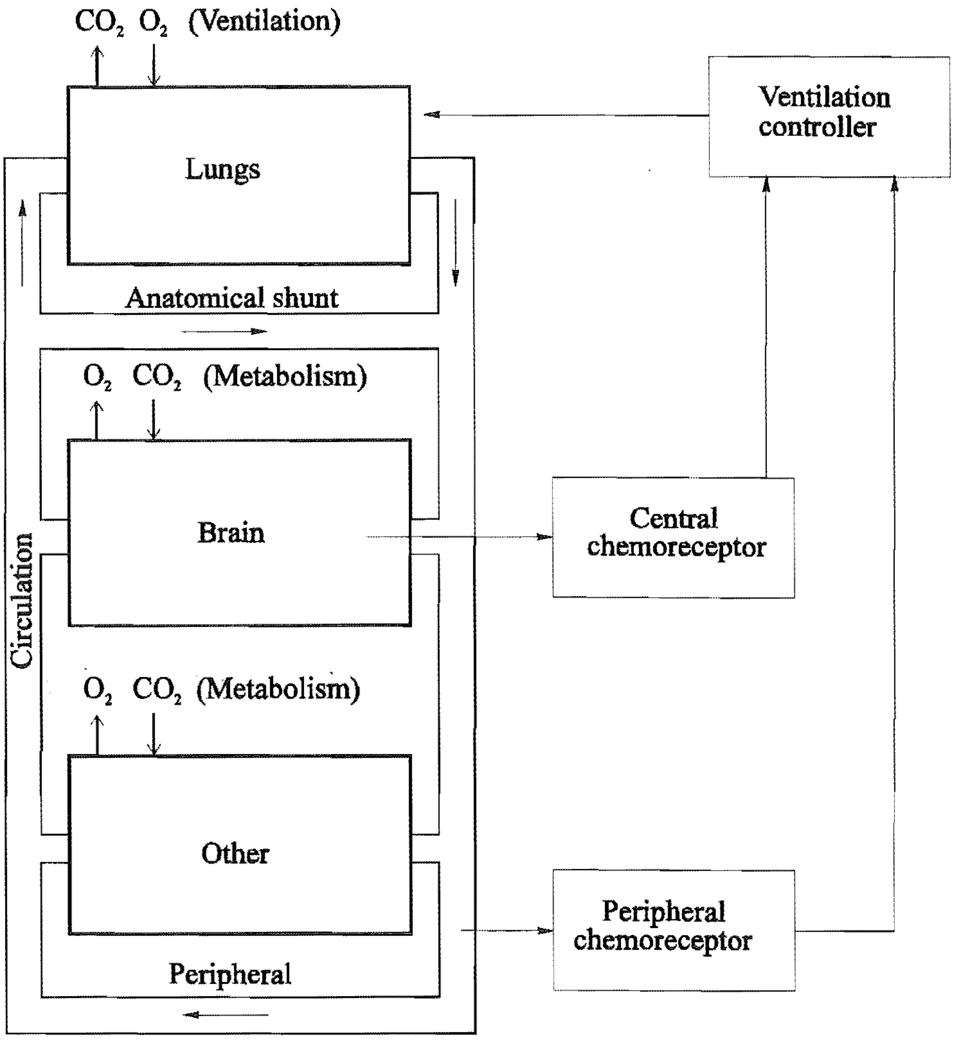

Figure 6.2 Block diagram of the model of the human respiratory system showing the gas storage compartments (left) and the receptors and controller components (right).

6.2.1 Gas stores in the body: The controlled system

For the purposes of this model, gas is stored within the body in three separate compartments for each gas type. For the CO_2 store in each compartment, there is a corresponding O_2 store. The CO_2 and O_2 stores are similar in form, but the mechanism by which CO_2 is stored is completely different to the mechanism by which O_2 is stored. Using the law of conservation of mass, dynamic equations for the store of gas in each compartment of the body can be formulated (see equation (6.1)). Therefore, there are six differential equations that describe the controlled system. The following subsections present the CO_2 and O_2 gas store equations using the symbols listed in table 6.2. Each of the following gas store equations is based on equation (6.1).

Vr	Functional residual capacity of the lung (FRC)
Va	Arterial blood volume
Vv_i	Venous blood volume for compartment i
Pa	Arterial gas partial pressure
PI	Inspired gas partial pressure
PA	Alveolar gas partial pressure
Ca	Arterial gas content
Cv_i	Compartment i venous blood gas content
$C\bar{v}$	Total mixed venous blood gas content
$\dot{Q}i$	Blood flow through compartment i
$\dot{Q}c$	Total blood flow (cardiac output)
MR_i	Metabolic rate of compartment i
$\dot{V}A$	Alveolar minute ventilation
P_B	Barometric pressure
$P(A\text{-}a)_{O2}$	Lung diffusion gradient for O_2
η	Fraction of blood flow through anatomical shunt
τ_i	Circulation delay to compartment i

Table 6.2 Mathematical symbols for the gas store equations. The subscript i denotes either the *brain* or *other* compartment.

6.2.1.1 Oxygen stores

Arterial/Lung O_2 Stores: The arteries and lung FRC form significant stores of O_2. These two stores can be combined to form a single gas store described by the differential equation

$$\frac{d}{dt}\left[\frac{Vr}{P_B-47}\cdot Pa_{O_2}+Va\cdot Ca_{O_2}\right] = \dot{Q}_c(C\bar{v}_{O_2}-Ca_{O_2}) + (1-\eta)\dot{V}A\frac{PI_{O_2}-PA_{O_2}}{P_B-47}. \tag{6.2}$$

where 47 mmHg is the vapour pressure of water in saturated alveolar air. Diffusion of O_2 across the lung membrane is assumed to be instantaneous. The anatomical shunt is roughly modelled by the term $(1 - \eta)$ which alters the quantity of gas transferred across the lung membrane into the arterial blood. Also, the alveoli O_2 partial pressure is considered to be equal to the arterial O_2 partial pressure plus a constant, $P(A\text{-}a)o_2$, which accounts for the O_2 diffusion gradient across the lung membrane, that is

$$P_{A_{O_2}} = Pa_{O_2} + P_{(A\text{-}a)_{O_2}}. \tag{6.3}$$

Venous O_2 stores: There are no significant stores of O_2 in the body tissues, therefore, the dominant stores of O_2 are in the blood (excluding the lung FRC). The two remaining compartments consist of O_2 stored in the venous blood associated with the *brain* and the *other* compartments, thus

$$\frac{d}{dt}(Vv_i \cdot Cv_{i,O_2}) = \dot{Q}_i(Ca_{O_2}(t-\tau_i) - Cv_{i,O_2}) - MR_{i,O_2}. \tag{6.4}$$

6.2.1.2 Carbon dioxide stores

Arterial/Lung CO_2 stores: The arteries and, more significantly, lung FRC form stores of CO_2. These two stores can be combined to form a single gas store described by the differential equation

$$\frac{d}{dt}\left[\frac{Vr}{P_B-47} \cdot Pa_{CO_2} + Va \cdot Ca_{CO_2}\right] = \dot{Q}_c(C\bar{v}_{CO_2} - Ca_{CO_2}) + (1-\eta)\dot{V}_A \frac{P_{I_{CO_2}} - Pa_{CO_2}}{P_B - 47}. \tag{6.5}$$

Diffusion across the lung membrane is assumed to be instantaneous. Also, It is assumed that the alveolar CO_2 partial pressure is the same as the arterial CO_2 partial pressure.

Tissue CO_2 stores: The two remaining tissue compartments are the *brain* and an *other* compartment, both of which consist of CO_2 stored in the tissue, which is assumed to be at equilibrium with the CO_2 partial pressure of the venous blood associated with each compartment, thus

$$\frac{d}{dt}(V_i \cdot C_{i,CO_2}) = \dot{Q}_i(Ca_{CO_2}(t-\tau_i) - Cv_{i,CO_2}) + MR_{i,CO_2}. \tag{6.6}$$

In order to investigate the system described by equations (6.2) through (6.6) it is necessary to be able to convert oxygen and carbon dioxide partial pressures to oxygen and carbon dioxide contents respectively. This is described fully in section 6.2.3.

6.2.2 Circulation

The transportation of the respiratory gases through the circulatory system to the metabolising tissues of the body forms an integral part of the respiratory system. However, the circulatory system comprises a group of feedback regulators which operate to the demands of the respiratory system, but in doing so, the circulatory system increases the complicated behaviour of respiration. Regions of the body independently adjust their flow of blood according to their CO_2 and O_2 partial pressures and temperature [Kelman, 1971, Chapter 5; Talbot & Gessner, 1973, Chapter 16]. In order to provide sufficient blood flow to each region of the body, the action of the heart is adjusted according to the blood pressure [Kelman, 1971, Chapter 4; Talbot & Gessner, 1973, Chapter 16].

The circulatory system mixes blood returning from each compartment of the body. Venous mixing of the content of each gas species returning from each compartment, i, is modelled by weighting the gas content from each compartment in proportion to the blood flow from each compartment. Thus,

$$C_{\bar{V}} = \frac{\sum \dot{Q}_i C_i}{\dot{Q}_c}, \tag{6.7}$$

where $C_{\bar{V}}$ is the mixed venous gas content.

For the purposes of this model, the cardiac output and blood flow to each compartment are assumed to be constant. The values used are dependent on the metabolic rate of each compartment which, in the short term, is held constant. However, the metabolic rate of the model is adjusted according to the thermal state of the body (see section 6.3) but is fixed for each simulation. The fixing of the metabolic rate for a single simulation is valid since the thermal state of the body changes over a period of many minutes (long term) and the properties of the respiratory system which are of interest change over a period of seconds (short term).

Associated with the circulatory system are significant delays in transporting the respiratory gases around the body. However, reliable values for the circulation delay are difficult to calculate. This is because of large inter-individual variations, different circulation delays through each region of the body and the dependence on the cardiac output. For this model, the values for the circulation delays are constant. Section 6.4 gives details of the parameter values used in the model.

6.2.3 Gas dissociation

The dissociation curve of a gas relates the content of that gas, in ml/100ml of storage material (such as blood), to its partial pressure. This relationship is required in both the controlled system and controller equations of the model. The processes by which CO_2 and O_2 are stored are completely different, thus their dissociation curves are also different. Much attention has been paid to the accuracy of the dissociation curves used in this model. Highly accurate dissociation curves are required for this model of infant respiration because CO_2 and O_2 dissociation in the blood are dependent on parameters such as haemoglobin, haematocrit and 2,3-diphosphoglycerate, all of which are dependent on age. The dissociation curves are also dependent on temperature. Details of the CO_2 and O_2 dissociation curves are given in the following two subsections.

Both the CO_2 and O_2 dissociation curves are dependent on the pH which is in turn dependent on the partial pressure of CO_2 and the oxygen saturation, thus the dissociation curves are coupled. The pH is calculated as [West & Wagner, 1977, Chapter 5]

$$pH = 7.590 + [0.003Hb(1 - S_{O_2})] - 0.274\log(P_{CO_2}/20), \tag{6.8}$$

where Hb is the haemoglobin concentration in ml/100ml of blood and So_2 is the oxygen saturation expressed as a fraction. Equation (6.8) can only be used if the oxygen saturation of the blood is known. However, section 6.2.3.1 shows how the oxygen saturation is dependent on the pH. Therefore, an iterative technique has been used to calculate the oxygen saturation. The first iteration assumes fully oxygenated blood. In practice, only two iterations for calculating the pH are required to give results of suitable accuracy for calculating the dissociation curves [Kelman, 1968].

Calculation of the dissociation curves through piece-wise approximations, which have been incorporated in many other models [Longobardo et al., 1966; Khoo et al., 1982], introduces discontinuities in the model which form regions of unnatural, unstable behaviour. The methods described in the following subsections do not include piece-wise approximations.

6.2.3.1 Oxygen dissociation curve

Calculation of the blood oxygen dissociation curve is well documented in the literature [West & Wagner, 1977, Chapter 5] and is divided into the following three steps.

Step 1. A shift in the O_2 dissociation curve occurs when the Pco_2, P_{50} (the oxygen partial pressure at which haemoglobin is half saturated. The P_{50} is related to the 2,3-diphosphoglycerate concentration) and blood temperature, T_{Bl}, deviate from normal. This is accounted for by calculating the *virtual* O_2 partial pressure, $Po_{2,Virt}$ as follows

$$P_{O_2,Virt} = \frac{26.8}{P_{50}} P_{O_2} 10^{[0.024(37 - T_{Bl}) + \ln 40 - \ln P_{CO_2})]} \quad \text{mmHg}. \tag{6.9}$$

Step 2. The fractional oxygen saturation, So_2, is calculated from $Po_{2,Virt}$ via an empirical or functional relationship which by no means represents the structural mechanisms of any biochemical processes (see section 2.2.2). The equation is of the form

$$S_{O_2} = \frac{U}{U+1},$$
$$U = 0.925 \cdot 10^{-2} P_{O_2} + 2.8 \cdot 10^{-4} P_{O_2}^2 + 3.06 \cdot 10^{-5} P_{O_2}^3. \tag{6.10}$$

Note that the oxygen saturation is independent of the haemoglobin concentration of the blood, as the haemoglobin only has an effect on the oxygen content of the blood.

Step 3. The oxygen content in the blood, Co_2, is calculated using the equation

$$C_{O_2} = 1.39Hb \cdot S_{O_2} + 0.003P_{O_2} \quad \text{ml/100ml}, \qquad (6.11)$$

where Hb is the haemoglobin concentration in ml/100ml of blood. The oxygen saturation is expressed as a fraction of fully saturated blood, 0.003 is the solubility of O_2 in ml/mmHg/100ml of blood, and 1.39 is the volume of oxygen in ml, at standard temperature and pressure, which combines with 1g of haemoglobin at full saturation. The blood oxygen dissociation scale is illustrated in figure 6.3 for a range of blood temperatures. A scale giving an approximation of the oxygen saturation is also shown since it is almost linearly related to the O_2 content for a constant haemoglobin concentration. Around the normal operating point, which is close to 100% saturation, the blood oxygen dissociation curve is relatively linear. It is not until the blood becomes significantly desaturated that the response becomes significantly non-linear and temperature dependent.

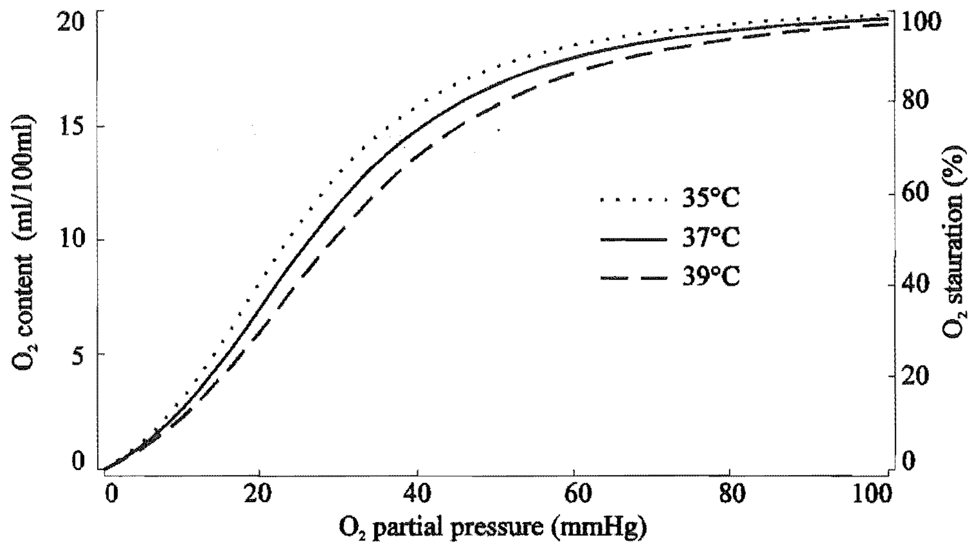

Figure 6.3 Normal adult blood oxygen dissociation curves for different blood temperatures (Hb = 14.3 ml/100ml, Pco_2 = 40mmHg, P_{50} = 27.0mmHg).

6.2.3.2 Carbon dioxide dissociation curve

Short term tissue CO_2 buffering is described by the same dissociation curve as for blood [Revow, 1987]. The blood CO_2 dissociation curve is well documented in the literature [West & Wagner, 1977, Chapter 5] and is dependent on temperature, oxygen saturation and haematocrit. Calculation of the blood carbon dioxide content, Cco_2, consists of the following five steps.

Step 1. Calculate the pK value and solubility, Sol, of carbon dioxide in plasma

$$pK = 6.086 + 0.0047(37.0 - T_{Bl}),$$
$$Sol = 0.037 + 0.00057(37.0 - T_{Bl}) + 0.00002(37.0 - T_{Bl})^2 \quad \text{mmol/l/mmHg}. \tag{6.12}$$

Step 2. Calculate the total carbon dioxide content of plasma, $Cco_{2,Plas}$, that is

$$C_{CO_2,Plas} = Sol \cdot P_{CO_2}(1 + 10^{[7.4 - pK]}). \tag{6.13}$$

Step 3. Calculate the ratio, R_{CC}, of CO_2 cells to CO_2 plasma

$$R_{CC} = 0.590 + 0.074(1 - S_{O_2}), \tag{6.14}$$

where the oxygen saturation is expressed as a fraction of fully saturated blood.

Step 4. Calculate the CO_2 content of the cells, $Cco_{2,Cells}$, from $Cco_{2,Plas}$ and R_{CC}, that is

$$C_{CO_2,Cells} = R_{CC} \cdot C_{CO_2,Plas}. \tag{6.15}$$

Step 5. Calculate the CO_2 content, Cco_2, of the whole blood

$$C_{CO_2} = 2.22[Hct \cdot C_{CO_2,Cells} + C_{CO_2,Plas}(1 - Hct)] \quad \text{ml/100ml}, \tag{6.16}$$

where Hct is the haematocrit expressed as a fraction. The constant 2.22 converts the units from mmole/l to ml/100ml. The carbon dioxide dissociation curve is illustrated in figure 6.4 for a range of temperatures. The dissociation of CO_2 is almost linear near the normal operating point of Pco_2 = 40mmHg and is not significantly affected by small deviations of temperature around the normal operating value of approximately 37°C.

6.2.4 Respiratory controller

The respiratory control centre, located in the cantral medulla of the brain, responds to information from blood gas chemoreceptors, pain receptors, and lung stretch receptors. To a certain extent, conscious respiratory control is also possible [Widdicombe, 1964]. During periods of quiet sleep, automatic (or metabolic) respiratory control is dominant since respiratory intervention, such as talking, coughing and sneezing do not occur. The neural signal generated from a chemoreceptor in response to the concentration of a particular chemical is known as a *chemoflex*. Although many mathematical expressions which describe ventilation in terms of CO_2 and O_2 chemoflex responses have been proposed, an expression developed by Rebuck and coworkers [Rebuck et al., 1977] has become popular because of its simplicity. This expression relates the minute ventilation rate, $\dot{V}_E$, to a single arterial chemoflex response and has been modified to

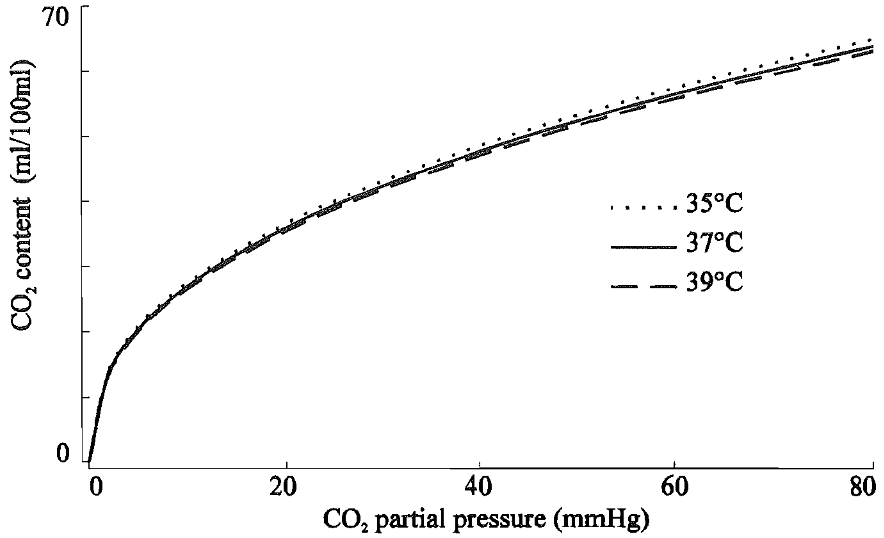

Figure 6.4 Normal adult carbon dioxide dissociation curves for different temperatures (Hct = 0.45, Po_2 = 80mmHg).

incorporate both central and peripheral chemoflex responses [Khoo et al., 1982; Revow et al., 1989]. For inclusion into the model it is written as

$$\dot{V}_E = G_P(1 - S_{P,O_2}/100)(P_{P,CO_2} - I_P) + G_C(P_{C,CO_2} - I_C), \tag{6.17}$$

where the effect of respiratory dead space, $\dot{V}_D$, [Bouhuys, 1964] is taken into account by

$$\dot{V}_A = \dot{V}_E - \dot{V}_D. \tag{6.18}$$

The right hand side of (6.17) is comprised of two terms, with gain factors G_P and G_C, respectively. The first term is dependent on both CO_2 and O_2 and is therefore associated with the peripheral chemoflex of the arterial blood [Delivoria-Papadopoulos et al., 1971]. The peripheral chemoflex senses arterial CO_2 and O_2 but is delayed by a blood circulation delay, τ_p [Zierler, 1962]. The response of the ventilation controller is highly sensitive to the exact value of the oxygen saturation. This highlights the need to accurately calculate the oxygen saturation. The second term in (6.17) is only dependent on CO_2 and is therefore associated with the steady state central chemoflex in the cantral medulla (i.e. that of the brain compartment CO_2 partial pressure) [Bruce, 1987]. I_P and I_C are CO_2 thresholds below which the respective chemoflex contribution to ventilation ceases.

6.3 Temperature

The human body has a highly sensitive thermoregulatory control system (see section 1.2). As a consequence of a thermal stress placed on the body, the thermoregulation system adjusts the metabolic rate and blood flow distribution of the body to maintain constant core temperatures (see section 4.2.2). Environmental temperature changes alter the behaviour of the respiratory system because of the dependence of respiration on the aforementioned variables. This is an *indirect* influence of temperature on respiration. Should the thermoregulatory system fail to maintain the body at close to its normal temperature, then the temperature dependence of certain aspects of the respiratory system, such as the nervous system and CO_2 and O_2 dissociation, will alter the behaviour of the respiratory system. This is a *direct* effect of temperature. Note that the direct influence of temperature occurs when body temperatures are different to normal values, while the indirect thermoregulation effects occur when the body is under a thermal stress which initiates a thermal control response but the core body temperatures may be very close to normal.

The indirect influence of thermoregulation on the respiratory model can be accounted for by incorporating the thermoregulation control equations described in Chapter 4 (excluding that of sweat rate control) (4.26) and (4.27) directly into the respiratory model. The metabolic heat produced due to (4.27) can be expressed as oxygen consumption since 1W of heat requires approximately 0.207 l of O_2 [Hill & Rahimtulla, 1965].

The indirect effect of body temperature changes affect respiration through the nervous system. A significant amount of research on the effect of temperature on the respiratory controller has been achieved through the study of cats. Kiley and coworkers have shown that cooling the whole body produces a significant drop in controller output [Kiley et al., 1984] and that most of this is due to cooling of the intermediate areas of the ventral medulla of the brain [Milhorn et al., 1982; Kiley et al., 1985]. The results indicate that the intermediate areas process both the peripheral and central chemoreceptor activity. It has also been shown that the relationship between respiratory output and input from the combination of the peripheral and central chemoreceptors of the cat is curvilinear [Milhorn et al., 1982] and has been interpreted as saturation of a common neuronal pathway. From this experimental data, a relationship for the modulation effect of head core temperature, T_C, and saturation at the intermediate areas of the ventral medulla on the respiratory controller output has been derived

$$\dot{V} = \dot{V}_{Thn}\,(0.055T_C - 1.05)\,. \tag{6.19}$$

where $\dot{V}_{Thn}$ is the ventilation rate at 37°C (thermoneutral).

The effect of temperature on the chemoreceptors is another major consideration. Research in this area indicates that the relationship between temperature and carotid chemoreceptor activity is logarithmic [McQueen & Eyzaguirre, 1974]. Therefore, the effect of peripheral chemoreceptor temperature, T_P, on ventilation, due to arterial chemoflex modulation, can be defined as

$$\dot{V} = 140\, \dot{V}_{Thn} \exp(-180/T_P)\,. \tag{6.20}$$

The effect of temperature on the O_2 and CO_2 dissociation curves has been shown in section 6.2.3. The temperature effects of the dissociation curves used for solving the gas store equations (6.2) through (6.6) are insignificant because each equation calculates the difference between arterial and venous gas contents and any temperature effect is largely cancelled. However, the respiratory controller (equation (6.17)) is dependent on oxygen saturation and in this case no cancellation occurs.

6.4 Model Parameters

This section presents numerical values for the parameters of the respiratory system model. Many of the parameters have been derived from the same sources as those parameters used in the thermoregulation model, hence, their values have the same accuracy limitations. Where data values are the same as those presented for the thermoregulation model, appropriate reference is made to section 4.3. In addition, some of the parameters have been measured from experiments on non-human subjects. Although, in these few cases, similar behaviour has also been observed in human subjects, it has not been accurately measured.

Table 6.3 lists the properties of air which are required for simulations using the respiratory model [Lide, 1990].

Description	Symbol	Value	Units
Barometric pressure at sea level	P_B	760	mmHg
CO_2 partial pressure of saturated inspired air	PI_{CO2}	0	mmHg
O_2 partial pressure of saturated inspired air	PI_{O2}	149	mmHg

Table 6.3 Properties of air which are relevant to the respiration model.

6.4.1 Maturation of the respiratory system

Most of the respiratory model parameters change considerably with age. Thus, it is not surprising that infant and adult respiratory system behaviour is considerably different. Parameters for adult respiration are presented in table 6.4 and have been taken from numerous sources [Longobardo et al., 1966; Farhi & Rahn, 1960; Revow et al., 1989; Hill & Rahimtulla, 1965]. They have been included for comparison with the infant parameters presented in table 6.5. The volumes, metabolic rates and blood flows presented in tables 6.4 and 6.5 have been compiled from the thermoregulation model data (tables 4.3 and 4.4, section 4.3). The *other* compartment includes the total body tissue volumes minus the brain, fat and skeleton. The tissue volumes have been calculated by assuming that the density of the tissue of interest (brain, muscle and combined organs) is 1 kg/l [Bell et al., 1980].

Compartment	Volume (l)	Blood Vol (l)	MR - O_2 consumption (ml/min)	Blood Flow (ml/min)
Lung/arteries	$V_r = 2.5$	$V_a = 2.4$	0	$\dot{Q}_t = 5400$
Brain/venous	$V_b = 1.38$	$V_{v,b} = 0.63$	$MR_b = 41.0$	$\dot{Q}_b = 751$
Other/venous	$V_o = 34.3$	$V_{v,o} = 3.2$	$MR_o = 215.0$	$\dot{Q}_o = 4649$
Total	$V_t = 35.68$	$V_{bl,t} = 6.23$	$MR_t = 256$	$\dot{Q}_t = 5400$

Table 6.4 Compartment parameters for the adult respiratory model.

As an infant matures, the respiratory system undergoes considerable changes. The most obvious of these changes are as a result of the small body size of infants in comparison to adults. The tissue compartment mass, blood flow and blood volume and metabolic rate of each region of the body change dramatically as the infant matures (see table 6.5).

Compartment	Volume (l)	Blood Vol (l)	MR - O_2 consumption (ml/min)	Blood Flow (ml/min)
Lung/arteries	V_r see (6.20)	$V_a = 0.38V_t$	0	$\dot{Q}_t = 200V_t$
Brain/venous	V_b see (4.31)	$V_{v,b}=0.61V_{Bl,t}\cdot\dot{Q}_b/\dot{Q}_t$	$MR_b = 23.3V_b$	$\dot{Q}_b = 690V_b$
Other/venous	$V_o = V_t\text{-}V_b$	$V_{v,o}=0.61V_{Bl,t}\cdot\dot{Q}_o/\dot{Q}_t$	$MR_o = MR_t\text{-}MR_b$	$\dot{Q}_o = \dot{Q}_t\text{-}\dot{Q}_b$
Total	V_t see (4.30)	$V_{Bl,t} = 60V_t$	$MR_t = 7.2V_t$	$\dot{Q}_t = 200V_t$

Table 6.5 Compartment parameters for the infant respiratory model (see text for details).

The total blood volume for infants under one year of age is assumed to be proportional to the body mass [Sheenah & Russell, 1949]. Arterial blood volume is assumed to have the same proportion of the total blood volume as adults. The *brain* and *other* blood volumes are assumed to be proportional to the blood flow to each region.

For infants up to one year of age, the lung FRC has been found to change according to [Godfrey, 1981]

$$Vr = 12.43 + 30.38m_t \;\; 1, \tag{6.21}$$

where m_t is the total body mass of the infant. A mathematical expression for the total body mass of the maturing infant is presented in Chapter 4, equation (4.30). The respiratory dead space for infants, children and adults is [Godfrey, 1981]

$$V_D = 2.2m_t \quad 1. \tag{6.22}$$

Significant postnatal changes in haemoglobin, haematocrit and 2,3-diphosphoglycerate content of blood occur which have a major bearing on the CO_2 and O_2 dissociation curves. Studies have shown that, as a result of these changes, the full term infant begins life with blood that has an increased affinity for oxygen [Delivoria-Papadopoulos et al., 1971]. Figure 6.5, which has been compiled from the research of Delivoria-Papadopoulos and coworkers, shows the haemoglobin, haematocrit and P_{50} values for the first 40 weeks of a normal full term infant. The P_{50} changes primarily as a result of variations in the 2,3-diphosphoglycerate concentration of the blood [Delivoria-Papadopoulos et al., 1971]. For comparison, values for adults are shown in figure 6.5.

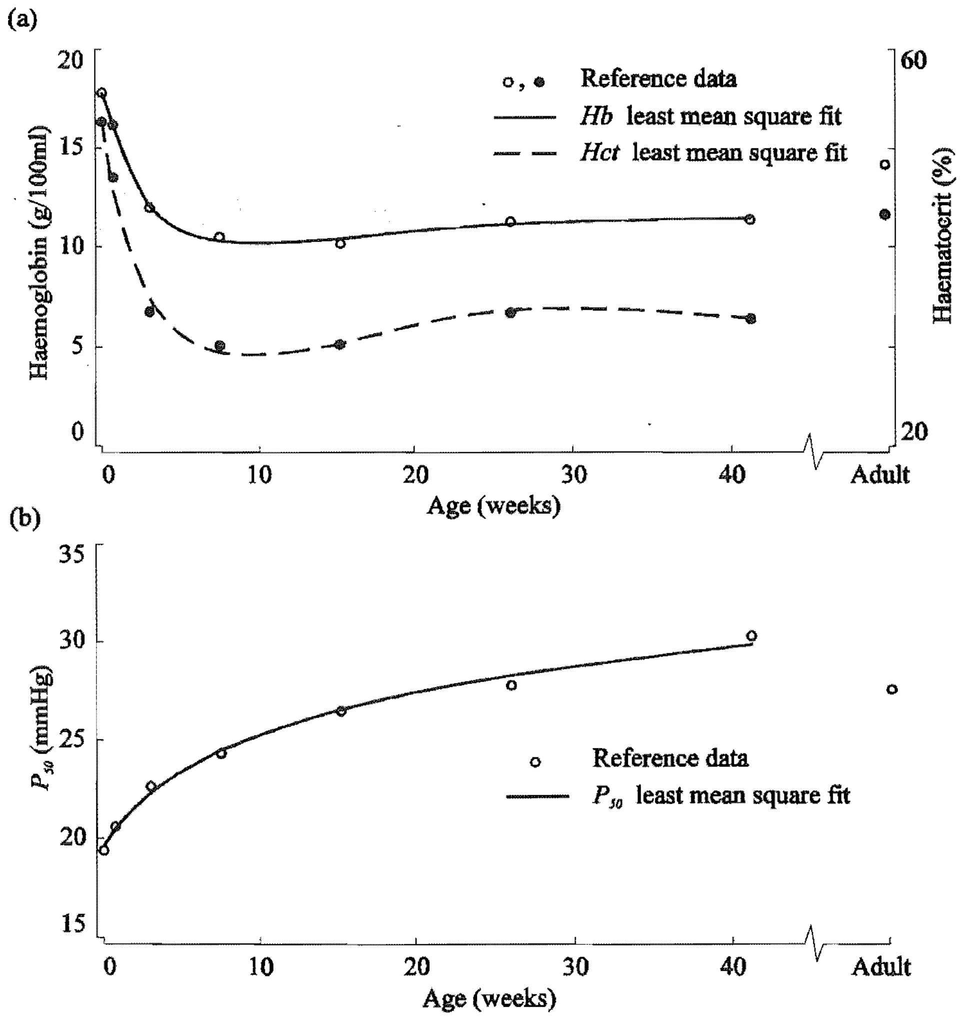

Figure 6.5 Parameters of blood for the maturing infant: (a) *Hb* and *Hct*, (b) P_{50}.

The curves fitted to the data in figure 6.5 have been calculated in a least mean squares sense to yield age dependent equations for the haemoglobin, *Hb*, haematocrit, *Hct*, and 2,3-diphosphoglycerate effects, P_{50}, The equations are as follows:

$$
\begin{aligned}
Hb &= 16.12 - 0.989Age + 8.632Age^{0.618} \\
&\quad - 13.35\mathrm{Ln}(Age + 0.882) \qquad \mathrm{g/100ml\ blood}, \\
Hct &= 64.39 + 3.759Age - 0.209Age^{1.626} - 26.19\ln(Age + 1.535)\ \%, \\
P_{50} &= 16.10 + 3.64\ln(Age + 2.609) \qquad \mathrm{mmHg}.
\end{aligned}
\tag{6.23}
$$

The effect of age on the O_2 and CO_2 dissociation curves is illustrated in figure 6.6. From the figure it is evident that age has a significant effect on O_2 dissociation but not on CO_2 dissociation.

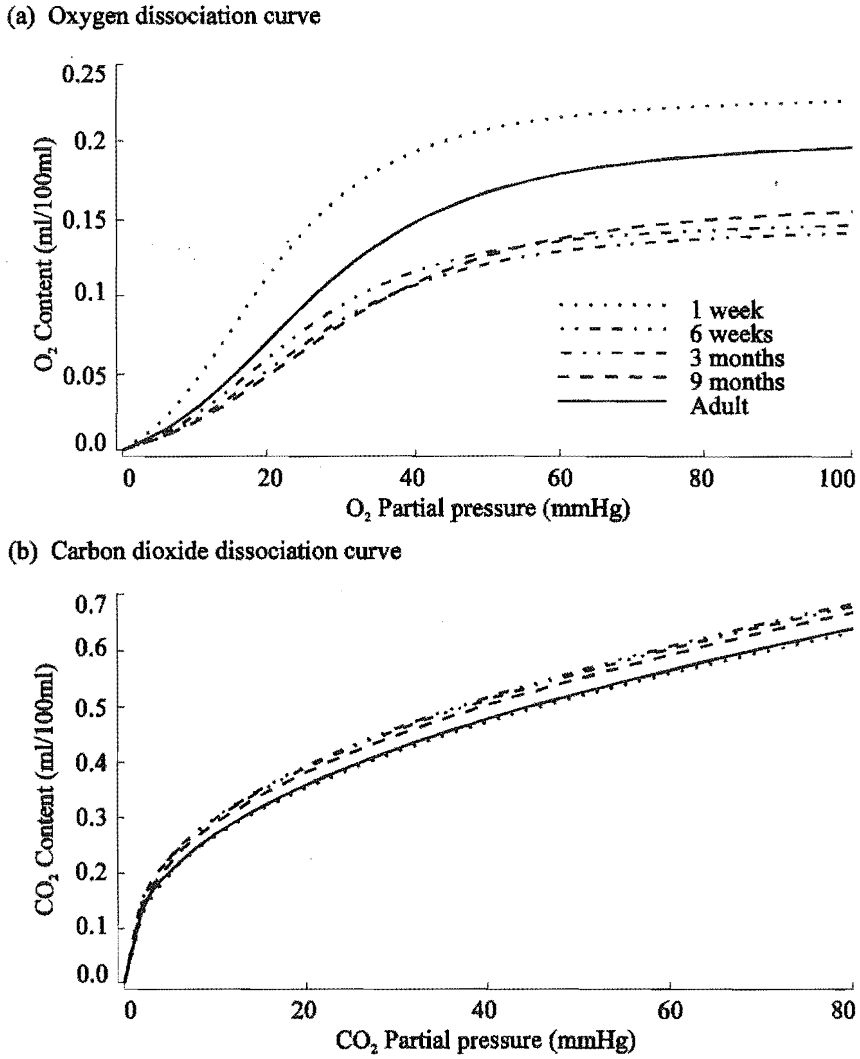

Figure 6.6 Effect of age on the dissociation curves: (a) O_2, (b) CO_2.

Additional age dependent parameters of the respiratory model are presented in table 6.6 [Lahiri et al., 1983; Longobardo et al., 1966; Koch, 1968; Revow, 1987]. These parameters have only been evaluated for a limited set of ages.

Parameter	1 Week	6 Weeks	12 Weeks	Adult
$P(A\text{-}a)$ (mmHg)	30	20	10	4
η	0.29	0.1	0.05	0.05
RQ	0.94	0.94	0.94	0.81

Table 6.6 Age dependent parameters specific to respiration and respiratory control.

The parameters which describe respiratory control (equation (6.17)) vary considerably between individuals [Rebuck et al., 1977]. Nominal values for G_P and G_C for adults are 16 l/min/mmHg and 2 l/min/mmHg respectively [Rebuck et al., 1977]. These values are of a similar magnitude to those included in models of adult respiration [Khoo et al., 1982; Longobardo et al., 1989]. From equation (6.17), G_P and G_C give a CO_2 sensitivity of approximately 3 l/min/mmHg under normal oxygen saturation conditions which is consistent with the literature [Avery et al., 1963].

There is little information available about the control of breathing throughout childhood, principally because children make poor subjects for experiments. The data that is available suggests that the sensitivity of ventilation to CO_2 per unit of total body mass is approximately the same for infants through to adults [Godfrey, 1981]. Thus, by dividing the adult gain values by the approximate adult body mass of 70kg, age independent gain values have been calculated as G_P = 0.23 l/min/mmHg/kg and G_C = 0.03 l/min/mmHg/kg. However, it has also been shown that the peripheral chemoflex is minimally functional at birth and matures in 1 to 6 weeks [Wilkie et al., 1987; Godfrey, 1981].

The respiratory set points I_P and I_C have nominally been assigned adult values of 38mmHg and 45mmHg respectively. The 7mmHg difference between I_P and I_C reflects the difference between the arterial and brain CO_2 partial pressures. Similar to CO_2 sensitivity, these values mature from I_P = 30mmHg and I_C = 37mmHg over the first few weeks of life [Revow, 1987].

The behaviour of the respiratory model is presented in the following chapter. Both the steady state and dynamic response of the model for a range of ages and temperatures is shown, using the parameters presented in this section. The sensitivity of the model to small variations in the parameters (presented in this section) is also demonstrated.

Chapter 7

Behaviour of the Respiratory Model

The aim of this chapter is to present the steady state and dynamic behaviour of the model of infant respiration developed in Chapter 6. Emphasis is placed on determining the sensitivity of the model to variations in temperature in order to investigate how temperature affects infant respiration.

The analysis of mathematical models of human respiration has involved two approaches. Most researchers have obtained solutions through numerical integration while others have produced analytical solutions by linearising their models around an equilibrium point (steady state). With the exception of investigating the steady state behaviour of the respiratory system, the pure time delays of the model introduce mathematical complications which are difficult to overcome and hinder an analytical solution. In addition, linearisation techniques cannot accurately describe the respiratory system behaviour after typical respiratory disturbances such as a sigh or apnoea. These disturbances cause the respiratory system to move considerably from the equilibrium point, thus preventing accurate solutions from a linearised model. The method of analysis chosen for this study was numerical integration performed with a digital computer. Numerical integration is capable of simulating the behaviour of the model near and away from the equilibrium point, thus it is capable of simulating respiratory disturbances. Although the numerical integration method is computationally intensive, it allows for accurate simulation and the comparison of the results from the model with data obtained from humans.

Simulation of the set of differential equations has been achieved with a fourth order Runge-Kutta numerical integration algorithm (see section 2.2.4.1). In a similar manner to the thermoregulation model of Chapter 5, numerical integration of the respiratory system model gives the time response of the state variables of the system. In this model, the state variables are the partial pressures of each gas species in each compartment.

In order to present the behaviour of the infant respiratory model in a manner which is consistent with recorded physiological signals collected from human infants (Chapter 3), it has been necessary to collectively present the minute ventilation rate, arterial oxygen saturation and arterial CO_2 partial pressure together in many of the figures in this chapter. Figure 7.1 depicts a typical 5 minute simulation of the model. From a set of initial conditions (the partial pressure of each gas species in each compartment), the integration algorithm proceeds until the equilibrium point (steady state) is achieved.

This chapter describes the behaviour of the model of human respiration for a sleeping infant. The analysis presented in this chapter is based on investigating the variability of normal breathing, thus allowing the behaviour of the model to be compared with breathing rate interquartile range (variability) data collected from infants (Chapter 3). Section 7.1 presents the steady state and dynamic behaviour of the model in order to validate the suitability of the model for this research. The sensitivity of the model to variations in parameters is shown in

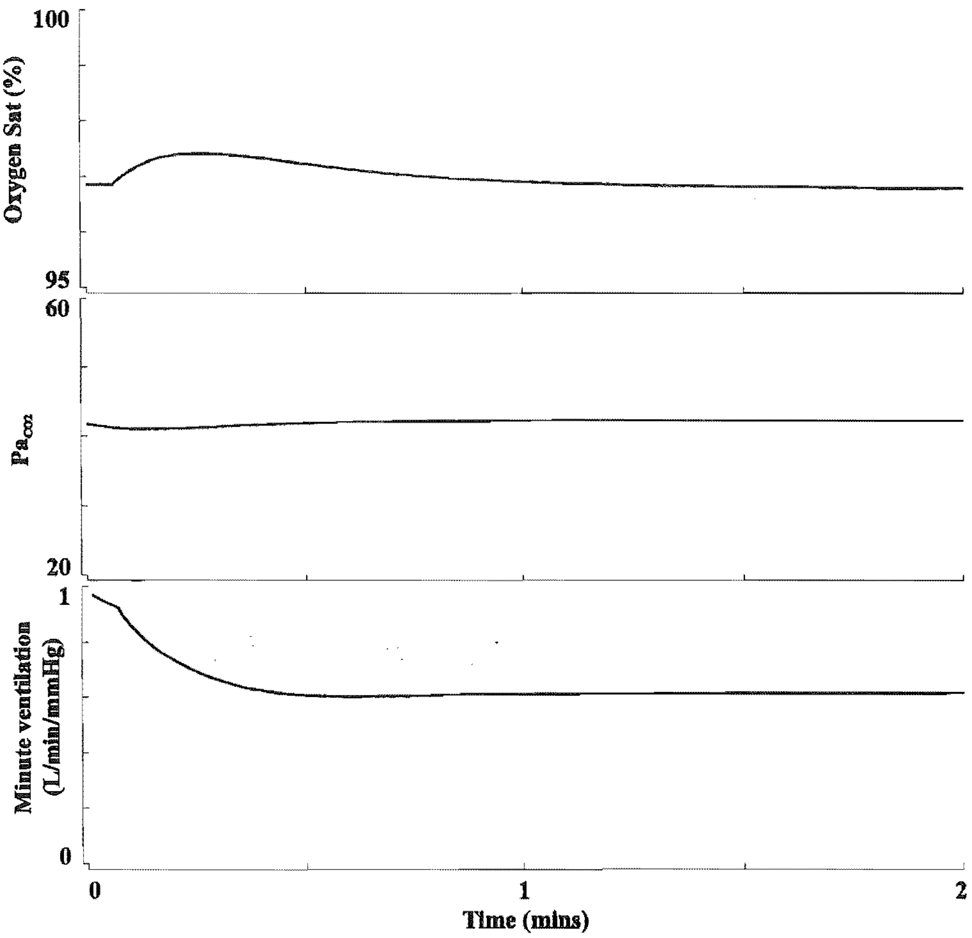

Figure 7.1 Time response of the respiratory model for a 12 week old infant.

section 7.2, followed in section 7.3 by the temperature sensitivity of the model. The behaviour of the model is compared with that of infants, which has been presented in Chapter 3. Section 7.4 briefly discusses the implications of the results presented in this chapter.

7.1 Model Characteristics

The human respiratory system is not significantly affected by normal, small variations in environmental gas partial pressures at sea level. However, the large changes in environmental conditions which occur with altitude alter the behaviour of respiration [Lahiri et al., 1983]. Altitude is not considered in this study because it is not relevant to the studies of infant respiration which are presented in Chapter 3. As the human infant grows and develops into a child and then an adult, considerable changes in the body occur which are important to respiratory behaviour (see section 1.3.2). In order to adapt to the changing metabolic demands of the body, the respiratory controller also undergoes considerable change. The following subsections present the steady state and dynamic behaviour of the respiratory model for the maturing infant and adult under normal physiological conditions at sea level.

7.1.1 Steady state behaviour

The normal resting steady state behaviour of the model is shown in table 7.1. The model successfully maintains a steady state CO_2 partial pressure, Pa_{CO2}, and oxygen saturation, S_{O2}, at normal values (approximately 40 mmHg and 97% respectively) for each age shown in the table. The O_2 saturation is comparable with similar behaviour observed in humans [Godfrey, 1981]. For both the model and humans, the S_{O2} is held close to 97% for each age group even in the face of the lower O_2 partial pressure, Pa_{O2}, at young ages. The Pa_{O2} drops to approximately 70 mmHg at one week of age. This is similar to the behaviour that has been observed in infants [Godfrey, 1981]. The S_{O2} remains nearly fully saturated at young ages because of changes to the O_2 dissociation curve (see section 6.4.1).

The results in table 7.1 show how the control response (ventilation rate) is adjusted to the demands of the metabolising tissue. The steady state ventilation rate of the model, $\dot{V}$, is lower than the value of 6 l/min for adults [Guyton, 1971, p330] and the value of 300 ml/min/kg for infants [Godfrey, 1981; Schulze et al., 1981]. The differences probably reflect the higher metabolic rate in awake human subjects compared with the model which is simulating ventilation during quiet sleep.

Age	1 Week	6 Weeks	12 Weeks	Adult
Mass (Kg)	3.5	4.5	5.5	70
$\dot{V}$ (l/min)	0.468	0.542	0.615	3.934
Pa_{CO2} (mmHg)	42.4	42.3	42.3	40.3
Pa_{O2} (mmHg)	71.7	82.3	91.7	101.6
S_{O2} (%)	96.5	96.5	96.8	97.3

Table 7.1 Steady state behaviour of the respiratory model.

7.1.2 Dynamic response

Historically, one of the most common reasons for investigating human respiration has been to study the stability of respiration. Under certain environmental and physiological conditions, the human ventilation rate has been shown to oscillate with a period in the range of approximately a few seconds to one minute, thus producing periodic breathing [Kelman, 1971, p358; Lahiri et al., 1983]. A mathematical model of respiration can be used to investigate the mechanism which produces the respiratory oscillations [Khoo et al., 1982; Longobardo et al., 1966; Carley & Shannon, 1988; Nugent & Finley, 1987; Khoo et al., 1991; Longobardo et al., 1989].

Linearised models of respiration are obtained by calculating an approximate linear transfer function in order to determine the frequency domain response of the model near an equilibrium point. However, these models are unable to demonstrate the effect of a natural disturbance to respiration. Non-linear models (such as the model described in Chapter 6) must be disturbed in order to measure the dynamic response to the disturbance, thus gaining an insight into the stability of the model. The disturbance may take the form of hyperventilation, asphyxia (or apnoea) or step changes in the inspired fraction of CO_2 or O_2.

The effect of a 20 second apnoea on the behaviour of the respiratory model is illustrated in figure 7.2 for a 12 week old infant and an adult. Clearly, there is a significant age dependence of both the steady state and dynamic response of the model. However, quantitative measurement of the stability of the model is not a simple task. A short apnoea is a common event in the respiration of sleeping infants and adults [Southall, 1988], therefore, measuring the magnitude of the overshoot of the first trough of the minute ventilation rate from the steady state minute ventilation rate is one possible measure of relative stability of the model. This measure is useful because the stability is inversely related to the magnitude of the overshoot.

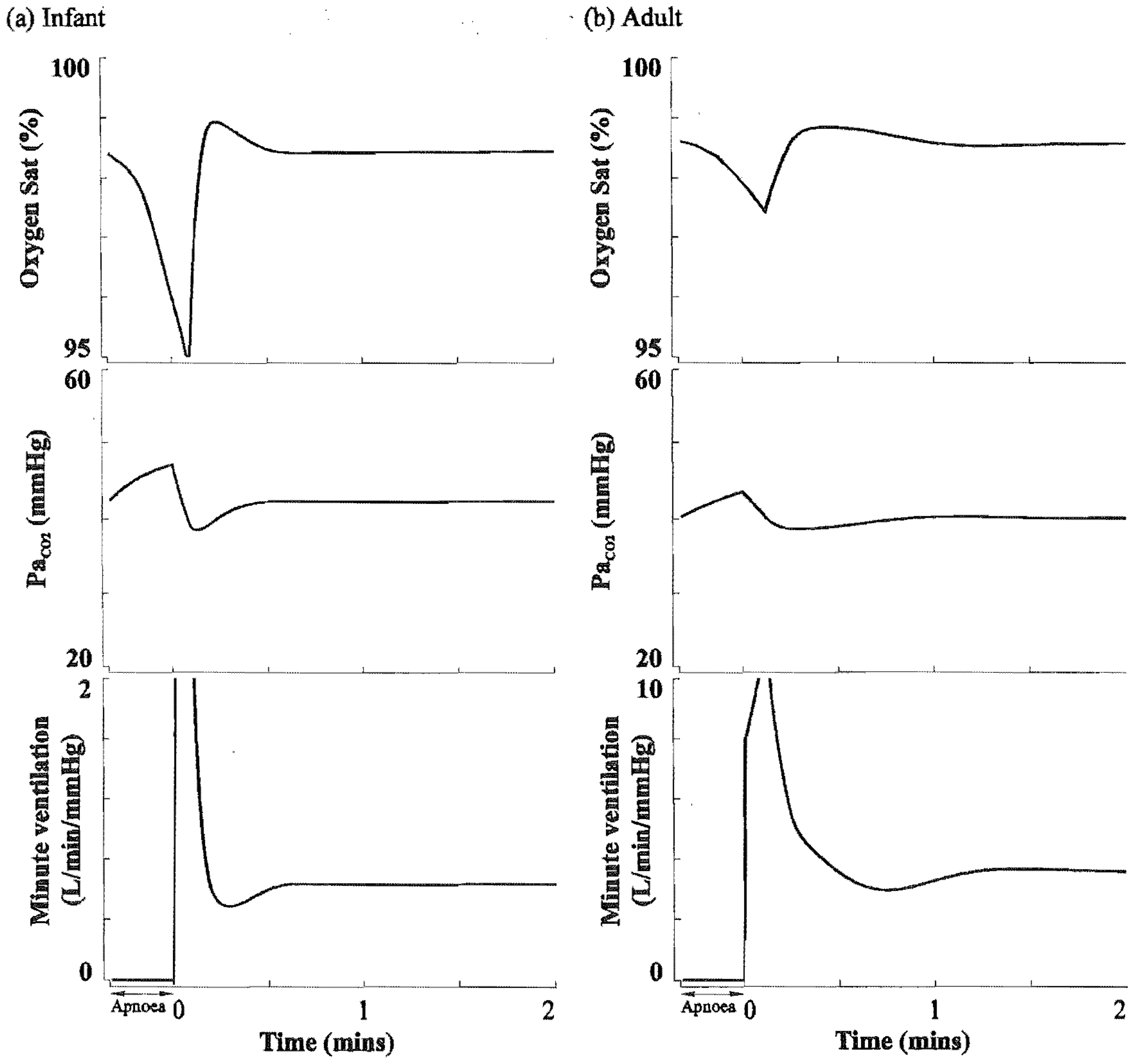

Figure 7.2 The effect of a 20 second apnoea on human respiration: (a) 12 week old infant, (b) adult.

An alternative to apnoea analysis is to simulate normal breathing patterns of infants. Typical respiratory patterns exhibit considerable breath to breath variability in both the awake state and during active sleep [Harper et al., 1987] (see Chapter 3 for examples). It has been shown that this breathing variability could be a result of random noise disturbances in chemoflex loops [Bruce & Modarreszadeh, 1990]. The results of the study by Bruce and Modarreszadeh indicate that physiological levels of random uncorrelated noise, added to arterial blood gases or to pulmonary or brain blood flow of their model of respiration, produces variations in minute ventilation similar to that seen in normal humans. Periodic breathing (recurrent central apnoeas) was also observed since the noise excited resonant frequencies within their model.

The technique of noise addition forms the basis of a practical method of determining the relative stability of the respiratory system model under physiologically normal conditions. If noise is added to the model, then the relative stability of the model can be obtained from the inverse of either the variance or interquartile range of the minute ventilation rate. The more noise that appears in the ventilation rate, the more unstable the system is and the more likely it is to oscillate and produce periodic breathing. The noise addition technique has a considerable advantage over apnoea analysis because the measure of respiratory variability is similar to that used in the study of infant breathing rate (described in Chapter 3) since the variance of the breathing rate is simply the power of the signal with the mean removed. Therefore, the infant data and the behaviour of the model can be directly compared.

The effect of adding uncorrelated noise to the respiratory model is demonstrated in figure 7.3 for a 12 week old infant and an adult. Noise with a square probability distribution has been added to the arterial CO_2 and O_2 partial pressures with a maximum value of $\pm 3\%$ of the normal steady state values. The larger the variability of the ventilation rate, the less stable the model is.

A measure of the variability of the respiration rate is the interquartile range of the respiration rate, $\dot{V}_{IQR}$. Figure 7.4 shows the interquartile range of a 2.5 minute epoch of the minute ventilation rate of the model for a range of noise levels. The effect of both blood flow noise and arterial gas partial pressure noise is shown. The respiratory variability of the model is more sensitive to blood flow noise than arterial gas partial pressure noise. The linear responses to noise show that any value of noise within the range presented in figure 7.4 will give a relative measure of the variability of the minute ventilation rate which is not dependent on the absolute value of the noise. The arterial gas partial pressures are relatively constant for all ages (see table 7.1), therefore, they form a more suitable noise input than the blood flow because, for the arterial gas noise, the noise level does not need to be adjusted for age. Thus, for the remainder of this chapter, $\pm 3\%$ arterial gas partial pressure noise over a 2.5 minute epoch has been used for the analysis of the variability of the ventilation rate.

The dependence of the respiratory variability of the model on age is indicated by the respiratory parameter values listed in table 7.2. The minute ventilation rate, $\dot{V}$, interquartile range of the ventilation rate, $\dot{V}_{IQR}$, and the ventilation rate overshoot response to an apnoea, $\dot{V}_{OVER}$, are shown. The ratios of the interquartile range and overshoot values to the minute ventilation rate are also presented in order to express the relative stability in a form which can be compared for different ages. The lower the value of any of the measures of respiratory variability, the more stable the model is.

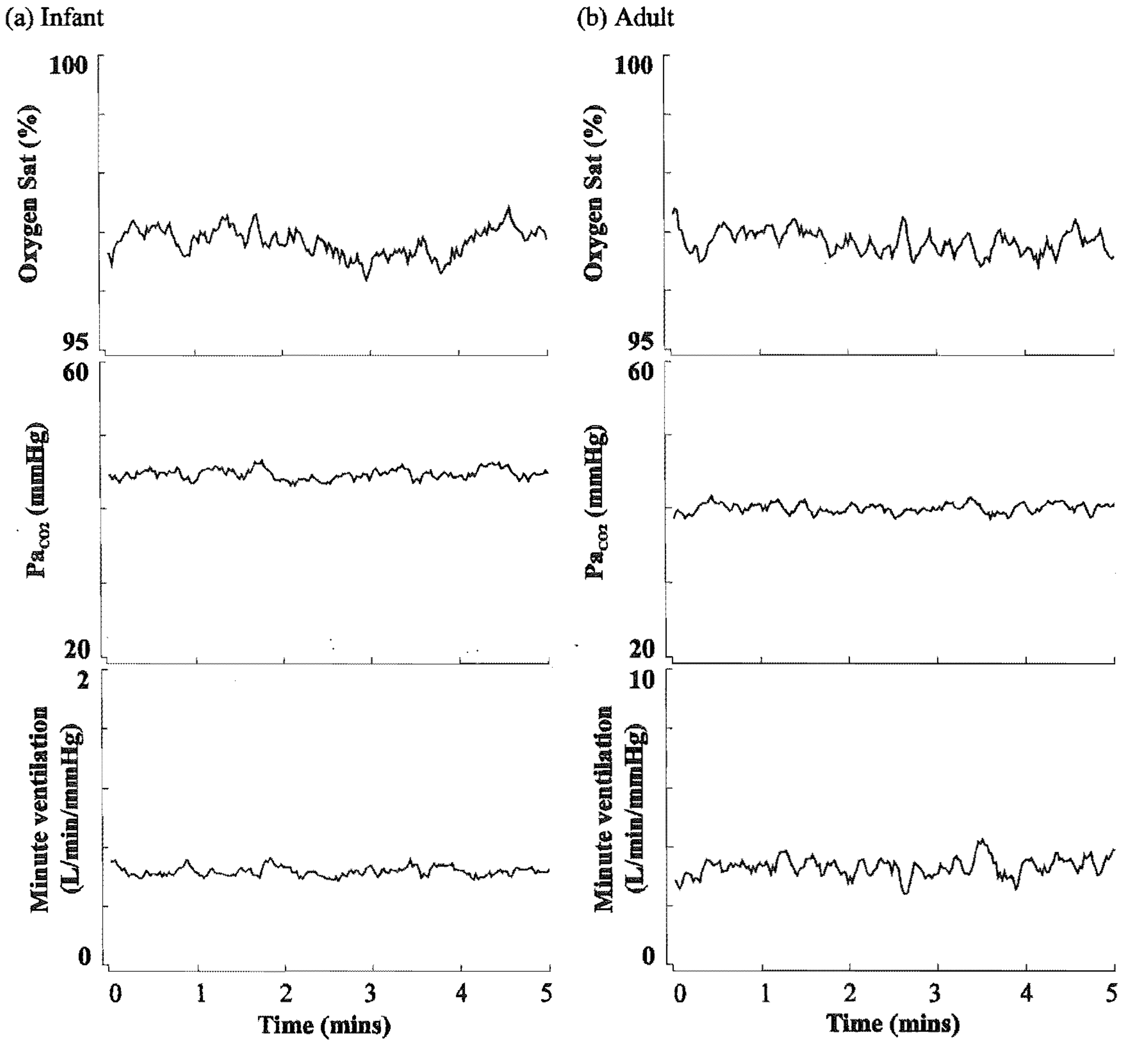

Figure 7.3 Effect of adding 3% noise to arterial gas tensions: (a) 12 week old infant, (b) adult.

Age	1 Week	6 Weeks	12 Weeks	Adult
$\dot{V}$ (l/min)	0.468	0.542	0.615	3.934
$\dot{V}_{IQR}$ (l/min)	0.045	0.060	0.069	0.845
$\dot{V}_{IQR}/\dot{V}$	0.096	0.111	0.111	0.215
$\dot{V}_{over}$ (l/min)	0.053	0.135	0.115	1.293
$\dot{V}_{over}/\dot{V}$	0.113	0.248	0.186	0.390

Table 7.2 Dynamic behaviour of the respiratory model.

The data presented in figure 7.4 and table 7.2 show how small levels of arterial gas partial pressure noise produce large amounts of noise in the minute ventilation rate of the model. Thus, the noise induced variability of the minute ventilation

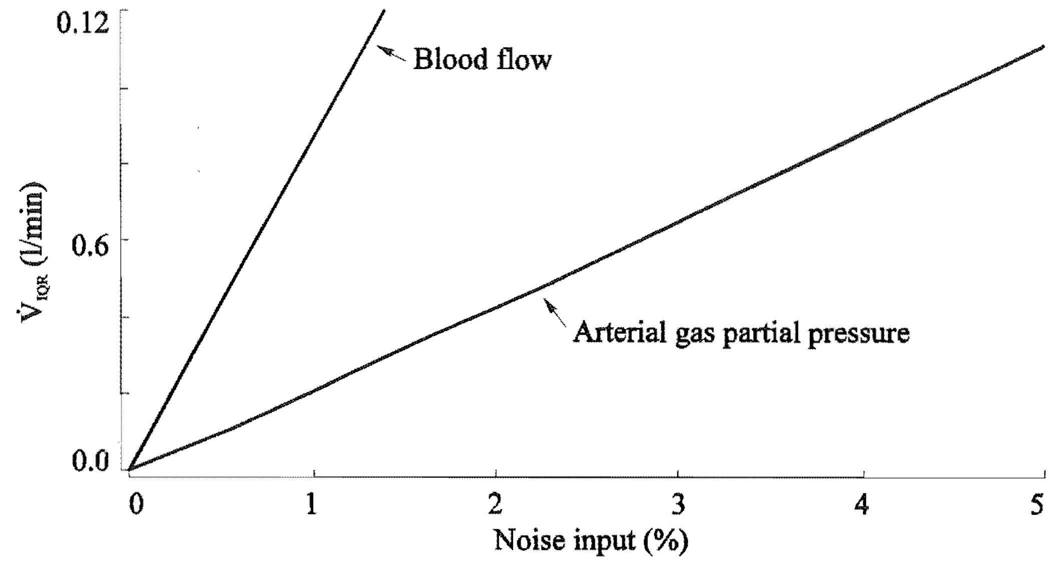

Figure 7.4 Variability of the minute ventilation rate for a range of input noise levels for both the addition of noise to the arterial blood flow and the partial pressure of CO_2 and O_2 gas.

rate is a suitable parameter for obtaining an estimation of the relative stability of the model.

7.2 Sensitivity to Parameter Variations

The aim of this section is to provide insight into how the behaviour of the respiratory system alters with small changes in a number of the respiratory parameters. The parameters investigated include compartment sizes, isolated blood flows and isolated metabolic rates for regions of the body and respiratory controller parameters. It is not ethically possible to perform experiments on humans which alter the parameters considered in this section, thus the model provides information which would otherwise be difficult to obtain. However, a detailed validation of the model is limited by the lack of human experimental data regarding the same parameters.

For each investigation presented in the following subsections, the range of deviation of each parameter from the normal value has been estimated to reflect the normal physiological variation and measurement accuracy of each parameter. Consultation of growth charts show the wide range of body proportions at any age [ChMedSch, 1992; Widdiwson, 1974; Wilmer, 1940]. The investigations also indicate which parameters of the model are the most sensitive to inaccuracies in parameter measurement. Thus, future development of the model could incorporate more accurate measurements from humans of the parameters which the behaviour of the model is particularly sensitive to.

For simplicity, only the interquartile range of the minute ventilation rate (which is an estimate of the respiratory stability or variability) and in some cases the actual minute ventilation rate are shown in the figures in this section.

7.2.1 Compartment size

The body proportions of humans have been measured and presented in the literature with considerable accuracy, but are subject to large inter-individual differences [ChMedSch, 1992; Widdiwson, 1974]. Figure 7.5 illustrates the effect of a ±20% variation in the *brain* and *other* compartment volume. This includes both the variations in the tissue volume and volume of blood perfused with the tissue. The figure shows that small changes in compartment volumes have little effect on the respiratory variability of the model. The ventilation rate is not shown in figure 7.5 because it is unaffected by compartment size.

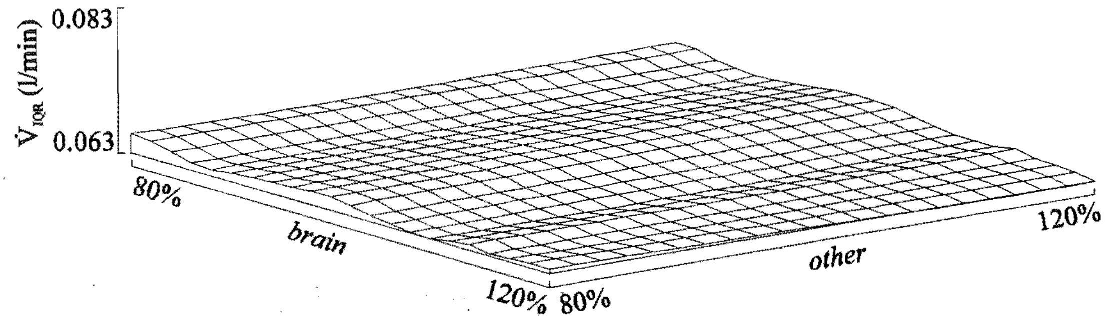

Figure 7.5 Effect of the *brain* and *other* compartment size on the stability of the model.

7.2.2 Metabolism and blood flow

The metabolic demands of the body tissues form the basis of the need for the respiratory system, thus, the respiratory behaviour is highly dependent on the metabolic rate. Similarly, the blood flows in the body are related to the metabolic rate [Kelman, 1971, Chapter 4]. The effects that ±20% variations in the metabolic rate and blood flow have on the behaviour of the model are shown in figure 7.6 for both the *brain* and *other* compartment.

As expected, an increase in metabolism in any tissue compartment of the model produces an increase in the ventilation rate. However, the respiratory variability is affected in a different manner. An increase in the *other* compartment metabolism or a decrease in the *brain* compartment metabolism produces an increase in the respiratory variability of the model. In contrast to the effects of metabolism, changes in the *brain* and *other* tissue compartment blood flows do not significantly alter the ventilation rate. Also, the effect of changes in blood flows on the respiratory variability are opposite to the metabolism effects. Considering the blood flows to regions of the body are proportionally coupled to the metabolic rate, the opposing effects of metabolism and blood flow may help to maintain the stability of the model at relatively constant levels under conditions where the metabolic demands of the tissue increase.

Changes in the circulatory system also affect the circulation delays. However, the circulation delays do not have any affect on the steady state behaviour of the model. Figure 7.7 depicts the effect of changes in the circulation delays on the

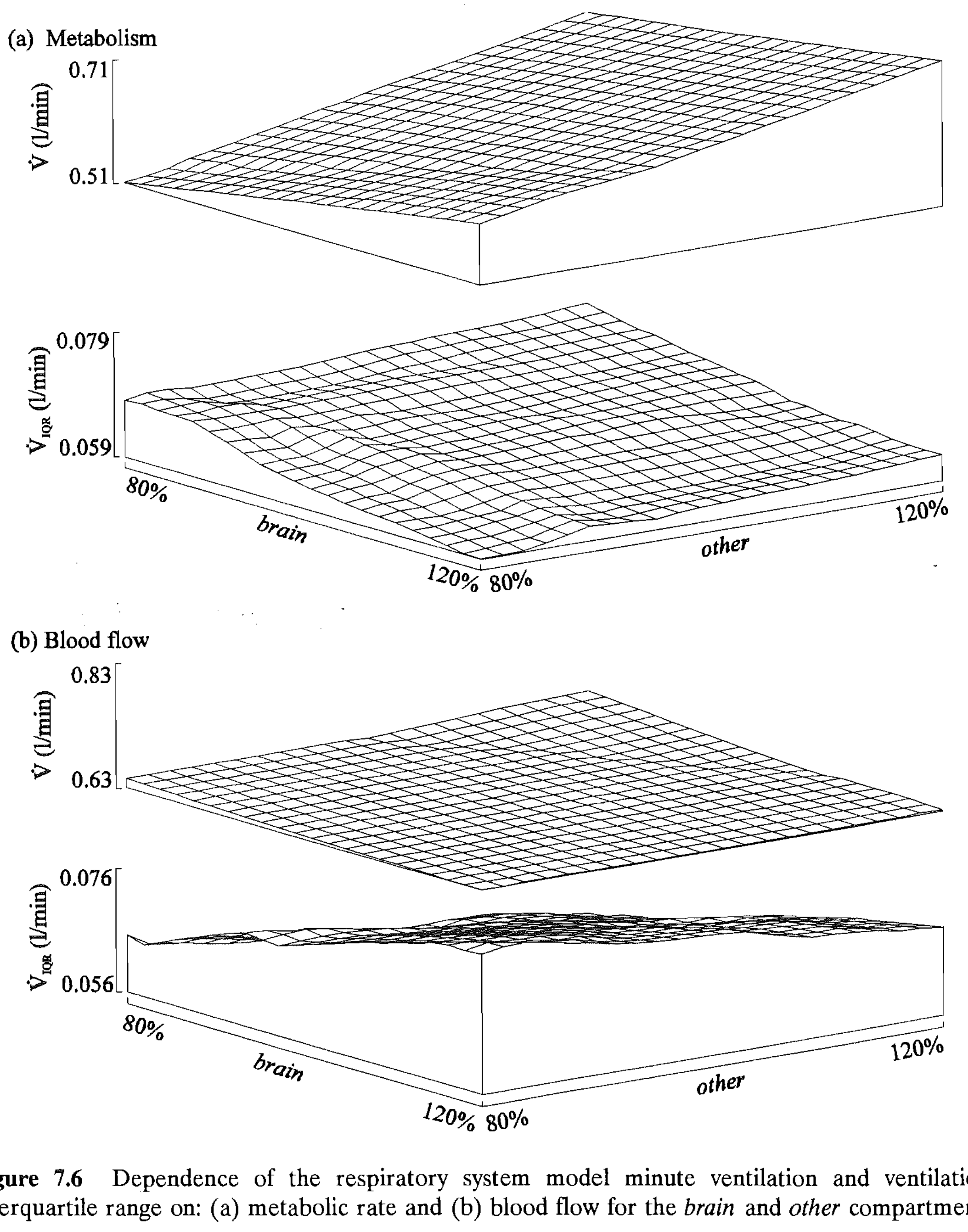

Figure 7.6 Dependence of the respiratory system model minute ventilation and ventilation interquartile range on: (a) metabolic rate and (b) blood flow for the *brain* and *other* compartment.

respiratory variability of the model. Only the brain and peripheral receptor delays are shown since they directly affect the delay through the feedback loops of the system. For any typical feedback control system, the stability is affected by the delay through the closed feedback loop (see section 2.2.5). The figure indicates that this model behaves as a typical negative feedback system since an increase in the peripheral chemoreceptor circulation delay produces a decrease in stability. However, the brain circulation delay has little effect, indicating that the instability is propagated through the peripheral chemoflex.

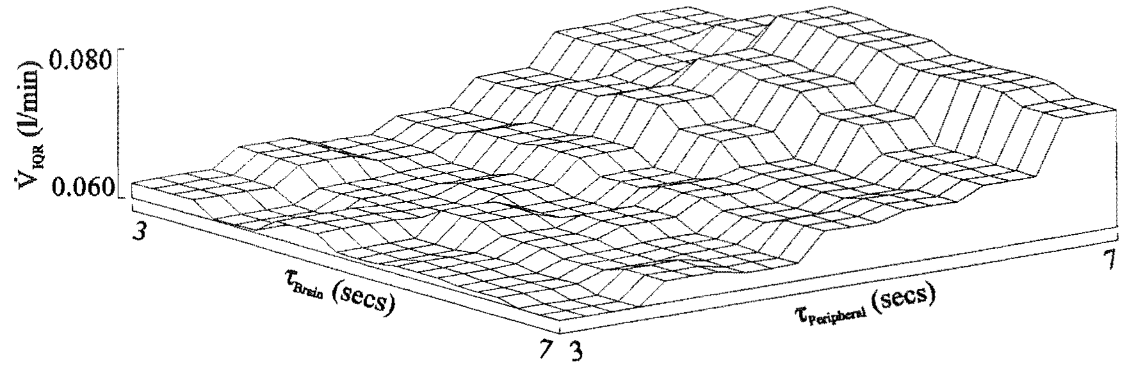

Figure 7.7 Effect on the stability of the respiratory model for changes in the brain and peripheral circulation delays.

7.2.3 Controller gain

Considering that the exact mechanisms of respiratory control are not well understood, the parameters which define the gain of the respiratory controller are likely to be the least accurate parameters of the model. The inter-individual differences of the respiratory parameters also introduce significant variability into their values. Figure 7.8 illustrates the effects of ±50% changes in the controller gains.

As anticipated by feedback control theory (section 2.2.5), the ventilation rate shown in figure 7.8 is not altered significantly by variations in either the central or peripheral gain parameter of the system. However, as either gain parameter is increased, the interquartile range of the ventilation rate increases, indicating a decrease in stability of the model. These results are what would be expected for a linear feedback control system (see section 2.2.5), since gain values vary considerably between individuals [Rebuck et al., 1977] and the model stability is highly sensitive to variations in gain. The wide variations in the respiratory behaviour of individuals may be partially accounted for by the inter-individual variations in controller gain.

7.3 Temperature Effects

The main aim of developing this model of human infant respiration has been to investigate the effects of temperature and thermoregulation on infant respiration. This section outlines these effects and relates them to the model of thermoregulation.

Assuming the distribution of temperatures throughout the core of the body is homogeneous, then the O_2 dissociation curve, equation (6.9), ventilation controller sensitivity to temperature, equation (6.19), and peripheral chemoreceptor temperature sensitivity, equation (6.20), can be assumed to be dependent on the same temperature variable, the *core temperature*, T_c. This assumption has been validated with the thermoregulation model for infants (see section 5.1.1) where the core temperatures of the model differ by only a small amount. Figure 7.9

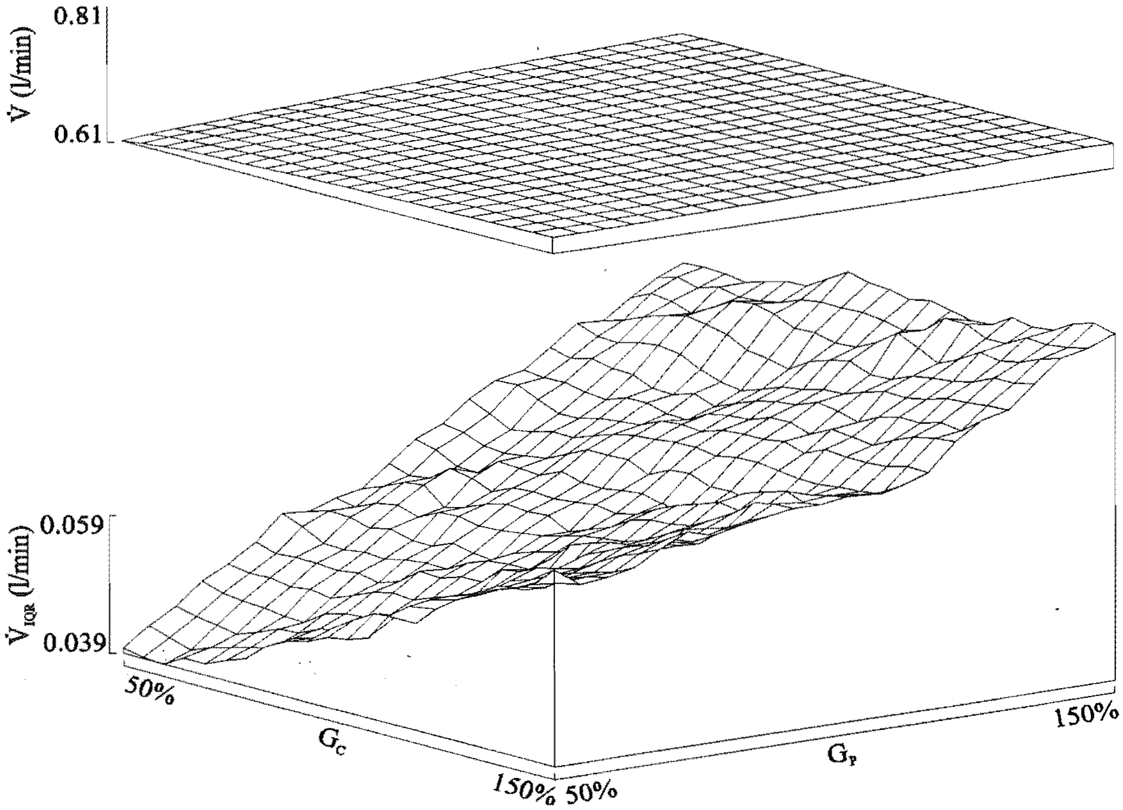

Figure 7.8 Effect of controller gain variations on the behaviour of the model (G_C and G_P are the central and peripheral chemoflex gains respectively).

illustrates the dependence of the behaviour of the model for a ±0.2°C range of core body temperatures, centred at 36.6°C (the head core thermoregulation set point). This range reflects the small range of core temperatures for wide environmental extremes observed in the thermoregulation model results (Chapter 6).

The indirect influence of thermoregulation on respiratory behaviour is shown in figure 7.10 with respect to the head *core* and average *skin* temperatures. The combined effect of the changes in muscle metabolism, the associated muscle blood flow and the skin blood flow is shown. The muscle metabolic rate and associated blood flow affect the *other* compartment when in a cool environment. The skin blood flow effects occur in a warm environment. The figure shows a large increase in the ventilation rate when the core and skin temperatures are below normal. Associated with the increase in ventilation rate is a small increase in the respiratory variability for the same cool temperatures. Since both the metabolic rate and the blood flow increase in response to cool body temperatures, their effects on stability, which are opposing, largely cancel (see section 7.2.2).

The combined effect of temperature, figure 7.9, and thermoregulation, figure 7.10, are shown in figure 7.11. Clearly, the figure indicates that cool body temperatures dramatically increase the ventilation rate of the respiratory model. However, the stability is not significantly altered by temperature. There is little difference between figures 7.10, the indirect, thermoregulation effect of temperature, and 7.11, the combined direct and indirect effects of temperature.

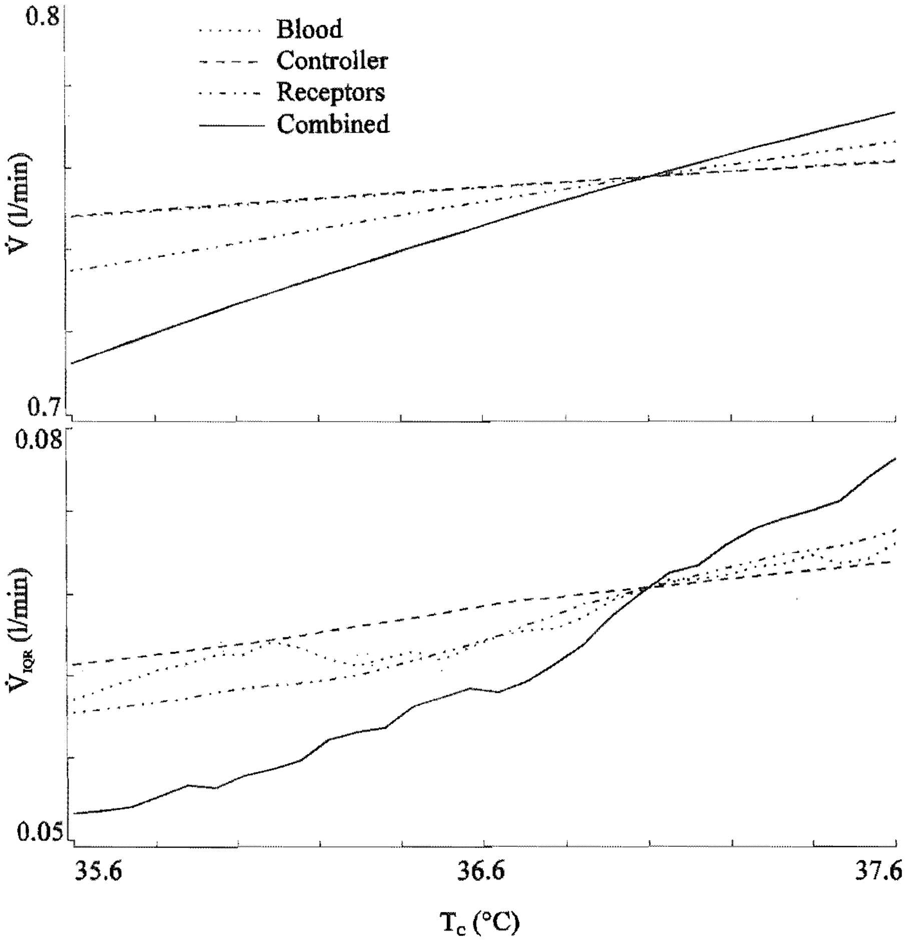

Figure 7.9 Direct effect of core temperature, T_C, on the respiratory behaviour of the model.

Thus, the effect of temperature on the respiratory model is principly through thermoregulation mechanisms.

Undoubtedly, any changes in body temperatures will produce dramatic changes in the ventilation rate of the respiratory model if the average body temperatures are cooler than normal. Thus, oscillating body temperatures, which may also occur when the body is just cooler than thermoneutral (see Chapter 6), will produce similar oscillations in the ventilation rate of the respiratory model. Therefore, a combination of thermoregulation instability and the dependence of the ventilation rate on temperature may account for the oscillating thermo-respiratory behaviour which has been observed in infants.

The respiratory model stability does not significantly change for a wide range of body temperatures and as such does not explain why oscillations in the variability of the breathing rate of infants occur in phase with the breathing rate oscillations (see section 3.4). One possible hypothesis to explain this is that the magnitude of the noise input into the respiratory system is related to the metabolic rate and blood flow. This seems plausible because the infant heart rate variability increases with the heart rate during active sleep [Harper et al., 1987]. However, it is not clear whether heart rate variability affects breathing rate variability or vice versa. An increase in gross body movements during active sleep may also

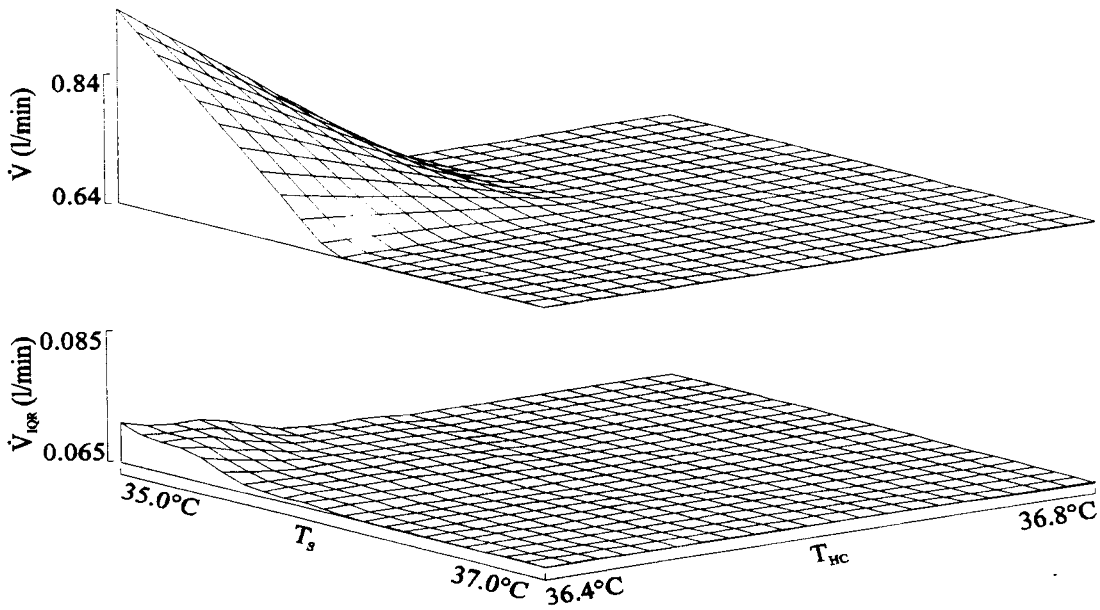

Figure 7.10 Indirect effect of thermoregulation on the respiratory behaviour of the model (T_S and T_{HC} are the skin and head core temperatures respectively).

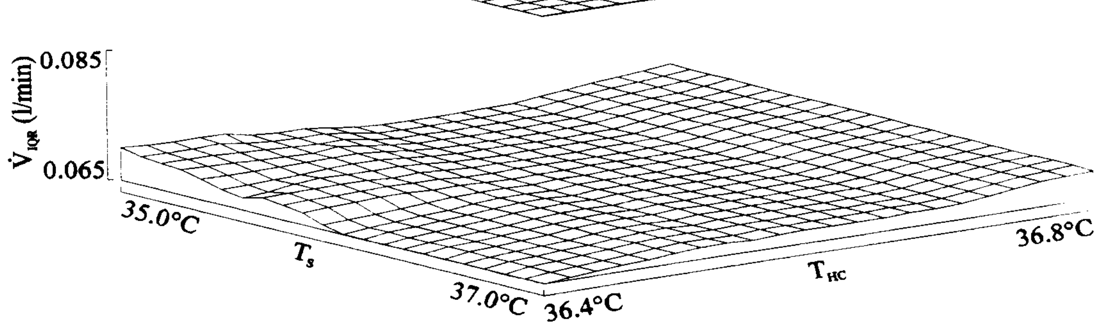

Figure 7.11 Combined effect of temperature and thermoregulation on the respiratory system model (T_S and T_{HC} are the skin and head core temperatures respectively).

contribute to noise within the respiratory system.

7.4 Summary

Many mathematical models of human respiration have been developed over the past few decades which successfully demonstrate both infant and adult respiration for a practical range of circumstances. The infant respiratory model presented in Chapter 6 is no exception, however, it also incorporates the sensitivity of respiration to temperature. The following is a list of key characteristics of the model which are similar to the respiratory behaviour observed in humans:

- The respiratory system model successfully regulates the levels of CO_2 and O_2 in the body for the metabolic demands of the tissue and the minute ventilation is similar to that observed in human subjects of a similar age.
- The ventilation rate of the respiratory system model increases for higher metabolic rates. This agrees with observations of infants who show a higher breathing rate for cooler body temperatures during oscillations of the body temperatures.

Noise from control systems within the body is amplified by the respiratory system model, producing significant variability of the ventilation rate. The magnitude of the noise amplification is highly dependent on the gain of the respiratory controller, which has been reported to have considerable inter-individual variability [Rebuck et al., 1977]. Therefore, the model shows how respiratory variability is dependent on the characteristics of respiratory control of each individual infant.

Compartment size has little effect on the behaviour of the respiratory model. However, small changes in the metabolic rate affect both the ventilation rate and the respiratory variability. The blood flow rate also affects the respiratory stability, but, its effect opposes the effects of metabolism since an increase in blood flow occurs as a result of increased metabolism. Thus, the respiratory variability of the model does not alter significantly during periods of high metabolic demand associated with exercise or cool thermal environments.

Chapter 8

Conclusions and Suggestions for Further Research

This thesis presents an investigation of certain aspects of infant thermo-respiratory behaviour. This chapter compiles, summarises and discusses the conclusions which have been presented in previous chapters of this thesis. Some suggestions for further research are also included.

8.1 Cohesion of Engineering and Medical Research

Biological control systems are structurally similar to the systems with which an engineer deals. Thus, the understanding of engineering control systems theory provides a basis to attempt to explain what is observed in human control systems. The application of engineering principles allows human physiological behaviour to be analysed and modelled in order to understand the processes that are occurring.

This thesis presents an example of the practical application of engineering techniques to medical research. The demands of medical research have required the development of engineering techniques which are capable of providing solutions to the less than ideal engineering problems which are found in the medical field. Signal processing and mathematical modelling techniques have been employed to investigate infant thermo-respiratory behaviour and explanations for the behaviour observed in clinical experiments are provided.

8.2 Thermo-respiratory Behaviour

The temperature and respiratory signals obtained during clinical experiments of infant thermo-respiratory behaviour, outlined in Chapter 3, presented a rich source of information. Processing these signals has revealed a wealth of previously unreported characteristics. The most significant of these are as follows:

- Oscillations of the body temperatures of infants, including the skin and rectal temperatures.
- Oscillations of the breathing rate which are 90° out of phase (advanced) compared with the rectal temperature oscillations.
- Oscillations of the interquartile range of the breathing rate which are in phase with the breathing rate oscillations. There was no evidence that periodic breathing was related to the interquartile range.

In addition to these results, a drop in rectal temperature that occurs at sleep onset has been observed. This observation agrees with the behaviour reported by other researchers [Wailoo et al., 1989; Lodemore et al., 1991].

The development and simulation of mathematical models of the respiratory and thermoregulatory systems of infants has provided a valid explanation for most of the characteristics listed above. The models not only reflect the observed behaviour but also provide a tool for detailed investigation of the mechanisms which cause and the conditions which influence the behaviour of infant thermoregulation and respiration.

The thermoregulation model demonstrates that thermoregulation in infants may be marginally stable, with a resonant period of approximately one hour. Thus, transient disturbances may be sufficient to produce oscillatory behaviour in infant body temperatures. It is difficult to estimate the overall accuracy of the infant thermoregulation model. However, the stability of the model is sensitive to the model parameters and environmental conditions, thus, under certain conditions, the model may indeed be unstable. The isolated respiratory system model also shows oscillatory behaviour under certain conditions, but, in contrast to the thermoregulatory system model, the period of the respiratory oscillations is in the order of only a few seconds to one minute.

The hourly oscillations observed in infant breathing rate can be explained by the coupling between the thermoregulatory and respiratory systems. When the body temperatures of the thermoregulation model are cooler than normal, the metabolic rate increases in order to heat the body and raise the body temperatures. As a result, the increased metabolic rate leads to an increase in the ventilation rate of the respiratory model. Thus, any oscillations in thermoregulation involving the metabolic rate would produce oscillations in the ventilation rate, the phase of which are 90° advanced when compared to the rectal temperature oscillations.

The respiratory model also demonstrates how the respiratory system may be highly sensitive to small amounts of noise introduced into the system. Noise levels of $\pm 3\%$, added to the arterial gas partial pressures, produce over 10% variations in the minute ventilation rate.

The increase in breathing rate interquartile range which occurs with an increase in the breathing rate (during thermo-respiratory oscillations) cannot be completely explained by the models presented in this thesis. It seems unlikely that a decrease in respiratory stability produces the observed behaviour because a decrease in stability would increase the likelihood of periodic breathing occurring in infant respiration, yet periodic breathing has not been observed during periods of high breathing rate interquartile range. The respiratory system model agrees with this hypothesis since its stability is not significantly sensitive to temperature. The insensitivity of the respiratory system model to temperature results because during cool body temperatures both the metabolic rate and blood flow increase and the effects of these parameters on the stability of the model are opposite and largely cancel. Therefore, temperature and thermoregulation probably do not contribute significantly or directly to the increase in breathing rate interquartile range which occurs with an increase in infant breathing rate. One possible hypothesis to explain the behaviour is that increases in metabolic rate noise and blood flow noise occur during periods of increased metabolic activity. This would increase the noise in the ventilation rate without decreasing the stability of the model.

Oscillatory behaviour in the infant thermoregulation model only occurs when the compartment temperatures of the model are below the thermoneutral point. The oscillations are elicited through the metabolic heat production feedback loop of the model. The metabolic heat required during heating phases of the oscillations may come from shivering or non-shivering thermogenesis. Active sleep may also play an important role for heat production. Researchers have shown that active sleep occurs during periods of high respiratory rate, respiratory rate variability, heart rate and heart rate variability [Harper et al., 1987]. The experimental data studied in this thesis show high breathing rate and breathing rate variability during periods when the rectal temperature is rising. Therefore, it is probable that gross muscle activity during active sleep contributes to the increased breathing rate and rising rectal temperatures. The gross muscle activity may also contribute to noise in the respiratory system which manifests itself in high breathing rate variability during active sleep. In young infants, non-shivering thermogenesis of the brown adipose tissue may also be involved in heat production [Jessen, 1990, Chapter 14].

The research presented in this thesis shows that respiratory changes (which are correlated to sleep state [Harper et al., 1987]) are also correlated with body temperatures (see Chapter 3) by way of an oscillatory mechanism. Furthermore, the oscillatory behaviour of the infant thermoregulation model is apparent in the brain compartment temperatures and thermoregulation also modulates respiratory processes (see Chapter 5). Similar temperature oscillations occurring in human infants may modulate the neural processes which occur in the brain. Thus, sleep state in infants may be contributed to by the brain temperature or thermoregulatory processes. This is in contrast to the traditional view that sleep state affects the thermo-respiratory behaviour. A review of how temperature may affect sleep state has recently been presented by other researchers [McGinty & Szymusiak, 1990]. The research presented in this thesis suggests that active sleep is a means of producing the heat required to maintain core body temperatures at constant levels in a cool environment.

Evidence from both the thermoregulation model and the observed infant thermo-respiratory behaviour suggests that infant rectal temperature probably reflects the temperature of a thermogenic region of the body which is important for producing heat in cool thermal extremes. Both the rectal temperature in infants and the trunk muscle compartment temperature of the thermoregulation model show a rising temperature during periods of increased metabolic activity. Core temperatures of the model do not consistently rise during periods of high metabolic activity, nor do they significantly vary for a wide range of thermal extremes. The behaviour of the rectal and core temperatures of infants suggests that infant rectal temperature may be significantly influenced by the temperature of blood returning from the leg muscles which are regions of increased metabolic activity.

The thermoregulation model also provides a possible explanation for the drop in rectal temperature that occurs when an infant is put to bed. The small drop in muscle metabolism which occurs when the model simulates an infant going to bed is sufficient to produce a drop in muscle compartment temperature which is comparable to the rectal temperature drop observed in infants. The exact magnitude of the temperature drop of the model is dependent on the thermal extremes placed on the model. The dependence of the magnitude of the drop on the thermal stresses placed on the model could explain the considerable variability of the magnitude of the drop observed for consecutive nights of each individual infant.

Table 8.1 shows the characteristics of infant thermo-respiratory behaviour that have been observed from the experimental data following analysis with signal processing techniques. Possible explanations of the observed behaviour, obtained through mathematical modelling, are also provided in the table.

Observed Behaviour	Model Explanation
Body temperature oscillations	Marginal stability of thermoregulation
Breathing rate oscillations (coupled to, but delayed with, body temperature oscillations)	Thermoregulation influencing the metabolic rate which leads to changed ventilation rate
Breathing rate interquartile range oscillations	Unexplained
Drop in rectal temperature at bed time	Drop in metabolic rate (independent of sleep)
Overall rectal temperature behaviour	Thermogenic compartment (as opposed to core compartment)

Table 8.1 Summary of the observed thermo-respiratory behaviour with possible explanations provided by the mathematical models.

8.3 Suggestions for Further Research

There are numerous clinical and engineering aspects of infant thermo-respiratory behaviour which could be investigated as an extension of the research presented in this thesis. Of these, there are a few important areas which, if thoroughly investigated, could further validate the results presented in this thesis.

The first suggestion is to repeat the study of infant respiratory and temperature signals with the addition of the measurement of an approximation to the head core temperature. If the head core temperature oscillations are 180° out of phase with the breathing rate oscillations then this would provide almost conclusive evidence that the oscillatory behaviour of the model is representative of the oscillatory behaviour that occurs in infants. This is because the breathing rate (and therefore the metabolic rate) would be high when the controlled variable (the head core temperature) is below its set point, thus agreeing with the behaviour of the thermoregulation model. Although a non-invasive direct measurement of the head core temperature is not possible, a less invasive estimate may be obtained from measurement of either the tympanic (inner ear) or oesophageal (within the throat) temperatures. Historically (and unwittingly), this viewpoint has been expressed by a famous 19^{th} century physiologist:

Failure to examine the throat is a glaring omission, especially in children.
One finger in the throat and one in the rectum makes a good diagnostician.

Sir William Osler

Another important clinical experiment would be a detailed investigation of the thermo-respiratory behaviour of humans which occurs at bed time. Investigations of both infant and adult body temperatures while going to bed, with and without the occurrence of sleep, and with different thermal loads would provide valuable information on the effect of sleep and the mechanisms that cause the drop in rectal temperature. Both a preliminary experiment and the thermoregulation model suggest that the rectal temperature drop is independent of sleep and a detailed experiment would help to confirm this. The inclusion of EEG analysis may also assist this type of study.

The infant thermoregulation model is based on two cylinders with coaxial compartments. The body extremities have been incorporated into the trunk cylinder. In future investigations, separating the extremities from the trunk may improve the accuracy of the model. This separation may decrease the stability of the model by reducing the heat flow rate from the thermogenesis regions to the core of the body. In addition, the insulation layer may be modelled as a dynamic compartment. An insulation layer compartment may improve the accuracy of the model because heat is stored within the insulation and, therefore, the insulation is similar in function to the tissue compartments of the model (except that blood does not flow through the insulation layer).

Although linearisation of the thermoregulation model would provide a concise solution to the system of differential equations, it is unlikely to be as accurate as the simulation of the set of non-linear differential equations. This is because there are many non-linear terms which are related to thermal control. Linearisation of these terms may considerably degrade the accuracy of the dynamic response of the model.

Many approximations have been made in the development of both the thermoregulation and respiration models. The accuracy of the models may be improved by attempting to more tightly constrain these approximations. However, both models have been developed for the average normal human subject, assuming that each model parameter is independent of every other (e.g. thermoregulation gain is independent basal metabolic rate). Therefore, it may be more appropriate to develop each model for individual subjects by substituting the average parameters with parameters measured from an individual subject. This may help to account for parameters of the models which are not independent of each other.

The respiratory system model presented in this thesis may be improved by incorporating mechanical aspects of air flow into and out of the lungs. However, it is not anticipated that this would significantly influence the behaviour of the model because of the averaging effect of the blood pool which filters out much of the respiratory cycle perturbations.

The development of a model of the cardiovascular system of infants and adults would also be of interest. A cardiovascular model could be adapted so that it is sensitive to temperature and, therefore, it could be investigated to see if temperature is likely to influence the stability of the cardiovascular system. Such an investigation may help to show why the breathing rate is more variable during periods of high metabolic activity and high blood flow. The combined analysis of thermoregulation, respiration and cardiovascular control may help to gain further understanding of the complicated coupling between these three systems.

References

Avery M. E., Chernick V., Dutton R. E., and Permutt S., (1963), Ventilatory response to inspired carbon dioxide in infants and adults. *Journal of Applied Physiology* **18:**895-903.

Bell G. H., Emslie-Smith D., and Paterson C. R., (1980), Textbook of Physiology 16th Ed. Churchill Livingstone, Edinburgh.

Borman B., Fraser J., and de Boer G., (1988), A national study of sudden infant death syndrome. *New Zealand Medical Journal* **101:**413-415.

Bouhuys A., (1964), Chapter 28, Respiratory dead space. In: Handbook of physiology, Section 3, Respiration Fenn, W. O., and Rahn, H., (Eds.), American Physiological Society, Washington D.C., pp. 699-714.

Bracewell R. N., (1978), The Fourier transform and its applications, 2nd Ed.. Mcgraw-Hill Kogahusha, Tohyo.

Brebbia D. R., and Altshuler K. Z., (1965), Oxygen consumption rate and electroencephalographic stage of sleep. *Science* **150:**1621-1623.

Brown P. J., Christmas B. F., and Ford R. P. K., (1992), Taking an infant's temperature: axillary or rectal thermometer?. *New Zealand Medical Journal* **105:**309-311.

Bruce E. N., (1987), Central chemoreceptors. *Journal of Applied Physiology* **62(2):**389-402.

Bruce E. N., and Modarreszadeh M., (1990), The ventilatory consequences of noise in respiratory chemical feedback loops. *IEEE Engineering in Medicine and Biology Society Conference* **12(4):**1865-1866.

Brück K., (1961), Temperature regulation in the newborn infant. *Biologia Neonatorum* **3:**65-119.

Bullard R. W., Banerjee M. R., Chen F., Elizondo R., and MacIntyre B. A., (1970), Skin temperature and thermoregulatory sweating: a control systems approach. In: Physiological and behavioural temperature regulation Hardy, J. D., Gagge, A. P., and Stolwijk, J. A. J., (Eds.), Thomas, Springfield, pp. 597-610.

Carley D. W., and Shannon D. C., (1988), A minimal mathematical model of human periodic breathing. *Journal of Applied Physiology* **65(3):**1400-1409.

Childs C., (1993), Metabolic rate at rest and during sleep in a thermoneutral environment. *Archives of Disease in Childhood* **68:**658-661.

ChMedSch, (1992), "Growth Charts". Paediatric Handbook Christchurch School of Medicine.

Cleave J. P., Flemming P. J., Levine M. R., and Long A. M., (1985), "Stability of the control of breathing in newborn infants: a non-linear mathematical analysis". In: "The Physiological Development of the Fetus and Newborn", Academic Press; London pp. 267-272.

Cleave J. P., Levine M. R., Flemming P. J., and Long A. M., (1986), "Hopf bifurcations and the stability of the respiratory control system". *Journal of Theoretical Biology* **119:**299-318.

Cleave J. P., and Levine M. R., (1984), "The control of ventilation: a theoretical analysis of the response to transient disturbances". *Journal of Theoretical Biology* **108:**261-283.

Comroe J. H., Jr., (1964), "Chapter 23, The peripheral chemoreceptors". In: "Handbook of physiology, Section 3, Respiration" Fenn, W. O., and Rahn, H., (Eds.), American Physiological Society, Washington D.C., pp. 557-583.

Crosbie R. J., Hardy J. D., and Fessenden E., (1963), "Electrical analog simulation of temperature regulation in man". In: "Temperature - its measurement and control in science and industry, Volume 3, Part 3" Hardy, J. D., (Ed.), Reinhold, New York, pp. 627-635.

Cussen L., Scurry J., Mitropoulos G., McTigue C., and Gross J., (1990), "Mean organ weights of an Australian population of fetuses and infants". *Journal of Paediatrics and Child Health* **26:**101-103.

Delivoria-Papadopoulos M., Poncevic N. P., and Oski F. A., (1971), "Postnatal changes in oxygen transport of term, premature, and sick infants: the role of red cell 2,3-diphosphoglycerate and adult haemoglobin". *Pediatric Research* **5:**235-245.

Dobbing J., and Sands J., (1973), "Quantitative growth and development of human brain". *Archives of Disease in Childhood* **48:**757-767.

Dove R., Brown J., Fright R., Ford R. P. K., and Tuffnell C., (1990a), "Computer polygraphic system for infants at risk for sudden infant death syndrome". *Australasian Physical & Engineering Sciences in Medicine* **13:**188-191.

Dove R., Brown J., Price B., Fong S., and Ford R. P. K., (1990b), "Multiple location body temperature measurement of infants". *Proc. IEEE Engineering in Medicine and Biology Annual Conference* **12:**1052-1053.

Dove R., Fright R., Ford R. P. K., Tuffnell C., and Brown J., (1990c), "Polygraphic assessment system for infants at risk for SIDS". *Proc. IEEE Engineering in Medicine and Biology Annual Conference* **12:**2031-2032.

Dove R. A., (1988), "Instrumentation for paediatric cardio-respiratory assessment". Masters thesis, University of Canterbury, New Zealand.

Engleberts A., (1991), Cot Ceath in the Netherlands: an epidemiological study. VU University Press, Amsterdam.

Farhi L. E., and Rahn H., (1960), Dynamic changes in carbon dioxide stores. *Anesthesiology* **21(6)**:604-614.

Fincham W. F., and Tehrani F. T., (1983), A mathematical model of the human respiratory system. *Journal of Biomedical Engineering* **5**:125-133.

Flemming P. J., Azaz Y., and Wigfield R., (1992), Development of thermoregulation in infancy: possible implications for SIDS. *Journal of Clinical Pathology* **45 (Suppliment)**:17-19.

Ford R. P. K., McCormick H. E., Schluter P. J., and Harnett P. M., (1991), Two decades of change: cot deaths and birth scores in Canterbury, New Zealand. *Journal of Paediatrics and Child Health* **27**:158-163.

Godfrey S., (1981), Growth and development of the respiratory system: functional development. In: Scientific Foundations of Paediatrics Davis, J. A., and Dobbing, J., (Eds.), Heinemann, London, pp. 432-450.

Gray J. S., (1949), In: Pulmonary ventilation and its physiological regulation, Thomas; Illinois.

Grodins F. S., Buell J., and Bart A. J., (1967), Mathematical analysis and digital simulation of the respiratory control system. *Journal of Applied Physiology* **22(2)**:260-276.

Grodins F. S., Gray J. S., Schroeder K. R., Noris A. L., and Jones R. W., (1954), Respiratory responses to CO_2 inhalation. A theoretical study of a non-linear biological regulator. *Journal of Applied Physiology* **7**:283-308.

Guyton A. C., (1971), Basic human physiology: Normal function and mechanisms of disease. W. B. Saunders, Philadelphia.

Hardy J. D., (1970), Thermal comfort: skin temperature and physiological thermoregulation. In: Physiological and Behavioural Temperature Regulation Hardy, J. D., Gagge, A. P., and Stolwijk, J. A. J., (Eds.), Thomas, Springfield, pp. 856-873.

Harper R. M., Schechtman V. L., and Kluge K. A., (1987), Machine classification of infant sleep state using cardiorespiratory measures. *Electroencephalography and Clinical Neurophysiology* **67**:379-387.

Harris F. J., (1978), On the use of windows for harmomic analysis with the discrete Fourier transform. *Proceedings of the IEEE* **66(1)**:51-83.

Haykin S., (1983), Communication systems, 2nd Ed. John Wiley and Sons, New York.

Hensel H., (1981), "Thermoreception and Temperature Regulation". Academic Press, London.

Hill J. R., and Rahimtulla K. A., (1965), "Heat balance and the metabolic rate of new-born babies in relation to environmental temperature; and the effect of age and weight on basal metabolic rate". *Journal of Physiology* **180:**239-265.

Hines W. W., and Montgomery D. C., (1980), "Probability and statistics in engineering and management science, 2nd Ed". John Wiley and Sons, New York.

Hunt C. E., and Brouillette R. T., (1987), "Sudden infant death syndrome: 1987 perspective". *The Journal of Pediatrics* **110(5):**669-677.

Hwang C.-L., and Konz S. A., (1977), "Engineering models of the human thermoregulatory system - a review". *IEEE Transactions on Biomedical Engineering* **24(4):**309-325.

Jessen C., (1990), "Thermal afferents in the control of body temperature". In: "Thermoregulation: Physiology and Biochemistry" Schonbaum, E., and Lomax, P., (Eds.), Pergamon Press, New York, pp. 153-183.

Kelly D. H., Carley D. W., and Shannon D. C., (1988), "Periodic breathing". *Annals New York Academy of Sciences* pp. 301-304.

Kelman G. R., (1968), "Computer program for the production of O_2 - CO_2 diagrams". *Respiration Physiology* **4:**260-269.

Kelman G. R., (1971), "Applied cardiovascular physiology". Butterworth, London.

Kerslake D. M., and Waddell J. L., (1958), "The heat exchanges of wet skin". *Journal of Physiology* **141:**156-163.

Khatri I. M., and Freis E. D., (1967), "Hemodynamic changes during sleep". *Journal of Applied Physiology* **22(5):**867-873.

Khoo M. C. K., Gottschalk A., and Pack A. I., (1991), "Sleep-induced periodic breathing and apnea: a theoretical study". *Journal of Applied Physiology* **70(5):**2014-2024.

Khoo M. C. K., Kronauer R. E., Strohl K. P., and Slutsky A. S., (1982), "Factors inducing periodic breathing in humans: a general model". *Journal of Applied Physiology* **53(3):**644-659.

Kiley J. P., Eldridge F. L., and Milhorn D. E., (1984), "The effect of hypothermia on central neural control of respiration". *Respiration Physiology* **58:**295-312.

Kiley J. P., Eldridge F. L., and Millhorn D. E., (1985), "Respiration during hypothermia: effect of rewarming intermediate areas of ventral medulla". *Journal of Applied Physiology* **59(5):**1423-1427.

Koch G., (1968), Alveolar ventilation, diffusing capacity and the A-a Po_2 difference in the newborn infant. *Respiration Physiology* **4**:168-192.

Lahiri S., Maret K., and Sherpa M. G., (1983), Dependence of high altitude sleep apnea on ventilatory sensitivity to hypoxia. *Respiration Physiology* **52**:281-301.

Lange R. L., Hogan J. D., Botticelli J. T., Sagaris T. T., Carlile R. R., and Kuida H., (1966), Pulmonary to arterial circulatory transfer function: importance in respiratory control. *Journal of Applied Physiology* **21**:1281-1291.

Lide D. R., (1990), CRC handbook of chemistry and physics. CRC Press, Boca Raton.

Lodemore M., Petersen S. A., and Wailoo M. P., (1991), Development of night time temperature rhythms over the first six months of life. *Archives of Disease in Childhood* **66**:521-524.

Longobardo G. S., Cherniack N. S., and Fishman A. P., (1966), Cheyne-Stokes breathing produced by a model of the human respiratory system. *Journal of Applied Physiology* **21(6)**:1839-1846.

Longobardo G. S., Cherniack N. S., and Gothe B., (1989), Factors affecting respiratory system stability. *Annals of Biomedical Engineering* **17**:377-386.

Ludeman L. C., (1987), Fundamentals of digital signal processing. John Wiley and Sons, New York.

Lund C. C., and Browder N. C., (1944), The estimation of areas of burns. *Surgery, Gynecology and Obstetrics* **79**:352-358.

Machle W., and Hatch T. F., (1947), Heat: mans exchanges and physiological responses. *Physiological Reviews* **27**:200-227.

McGinty D., and Szymusiak R., (1990), Keeping cool: a hypothesis about the mechanisms and functions of slow-wave sleep. *Trends in Neurosciences* **13(12)**:480-487.

McQueen D. S., and Eyzaguirre C., (1974), Effects of temperature on carotid chemoreceptor and baroreceptor activity. *Journal of Neurophysiology* **37**:1287-1296.

Mead J., and Agostioni E., (1964), Chapter 14, Dynamics of breathing. In: Handbook of physiology, Section 3, Respiration Fenn, W. O., and Rahn, H., (Eds.), American Physiological Society, Washington D.C., pp. 422-427.

Milhorn D. E., Eldridge F. L., and Waldrop T. G., (1982), Effects of medullary area $I_{(S)}$ cooling on respiratory response to chemoreceptor inputs. *Respiration Physiology* **49**:23-39.

Mitchell E. A., Ford R. P. K., Taylor B. J., Stewart A. W., Becroft D. M. O., Scragg R., Barry D. M. J., Allen E. M., Roberts A. P., and Hassall I. B., (1992a), "Further evidence supporting a causal relationship between prone sleeping position and SIDS". *Journal of Paediatrics and Child Health* **28 Supplement 1:**S9-9S12.

Mitchell E. A., Taylor B. J., Ford R. P. K., Stewart A. W., Becroft D. M. O., Thompson J. M. D., Scragg R., Barry D. M. J., Allen E. M., and Roberts A. P., (1992b), "Four modifiable and other major risk factors for cot death: The New Zealand study". *Journal of Paediatrics and Child Health* **28 Supplement 1:**S3-3S8.

Nadel E. R., Bullard R. W., and Stolwijk J. A. J., (1971), "Importance of skin temperature in the regulation of sweating". *Journal of Applied Physiology* **31:**80-87.

Nagrath I. J., and Gopal M., (1986), "Control systems engineering, 2nd Ed.". Wiley, Singapore.

Nugent S. T., and Finley J. P., (1987), "Periodic breathing in infants: a model study". *IEEE Transactions on Biomedical Engineering* **34(6):**482-485.

Paintal A. S., (1971), "The responses of chemoreceptors at reduced temperatures". *Journal of Physiology* **217:**1-18.

Pennes H. H., (1948), "Analysis of tissue and arterial blood temperatures in the resting human forearm". *Journal of Applied Physiology* **1(2):**93-122.

Ponsonby A.-L., Dwyer T., Gibbons L. E., Cochrane J. A., Jones M. E., and McCall M. J., (1992), "Thermal environment and sudden infant death syndrome: case-control study". *British Medical Journal* **304:**277-282.

Press W. H., Flanning B. P., Teukolsky S. A., and Vetterling W. T., (1986), "Numerical recipes: the art of scientific computing". Cambridge University Press, Cambridge.

Rebuck A. S., Slutsky A. S., and Mahutte C. K., (1977), "A mathematical expression to describe the ventilatory response to hypoxia and hypocapnia". *Respiration Physiology* **31:**107-116.

Revow M., England S. J., O'Beirne H., and Bryan C., (1989), "A model of the maturation of respiratory control in the newborn infant". *IEEE Transactions on Biomedical Engineering* **36(4):**414-423.

Revow M., (1987), "A modelling approach to the maturation of respiratory control in human infants". PhD Thesis, University of Toronto.

Ryser G., and Jéquier E., (1972), "Study by direct calorimetry of thermal balance on the first day of life". *European Journal of Clinical Investigation* **2:**176-187.

Schulze K., Kairam R., Stefanski M., and Sciacca R., (1981), "Continuous measurement of minute ventilation and gaseous metabolism of newborn infants". *Journal of Applied Physiology* **50:**1098-1103.

Sedra A. S., and Smith K. C., (1982), Microelectronic Circuits . Holt-Saunders, Japan, 563-565.

Settergren G., Lindblad B. S., and Persson B., (1976), Cerebral blood flow and exchange of oxygen, glucose, keytone bodies, lactate, pyruvate and amino acids in infants . *Acta Paediatrica Scandinavica* **65:**343-353.

Sheenah J. M., and Russell M. D., (1949), Blood volume studies in healthy children . *Archives of Disease in Childhood* **24:**88-98.

Siebert W. M., (1986), Circuits, signals, and systems . MIT Press, Cambridge.

Southall D. P., (1988), Role of apnoea in the sudden infant death syndrome: A personal view . *Pediatrics* **80(1):**73-84.

Stabell U., Junge M., and Fenner A., (1977), Metabolic rate and O_2 consumption in newborns during different states of vigilance . *Biologia Neonatorum* **31:**27-31.

Stolwijk J. A. J., (1970), Mathematical model of thermoregulation . In: Physiological and behavioural thermoregulation Hardy, J. D., Gagge, A. P., and Stolwijk, J. A. J., (Eds.), Thomas, Springfield, pp. 703-721.

Stolwijk J. A. J., and Hardy J. D., (1966), Temperature regulation in man - a theoretical study . *Pflügers Archives* **291:**129-162.

Talbot S. A., and Gessner U., (1973), Systems physiology . Wiley, New York.

Tehrani F. T., (1990), Computer simulation of the respiratory control system in the newborn infant . *IEEE Engineering in Medicine and Biology Society Conference* **12(4):**1848-1850.

Tehrani F. T., (1993), Mathematical analysis and computer simulation of the respiratory system . *IEEE Transactions on Biomedical Engineering* **40(5):**475-481.

Tuffnell C., Dove R., Brown J., and Ford R., (1992), Collection and analysis of physiological signals from infants in the home . *Proc. IEEE Engineering in Medicine and Biology Annual Conference* **14:**2736-2737.

Tuohy P. G., and Tuohy R. J., (1990), The overnight thermal environment of infants . *New Zealand Medical Journal* **103:**36-38.

Wailoo M. P., Petersen S. A., Whittaker H., and Goodenough P., (1989), Sleeping body temperatures in 3-4 month old infants . *Archives of Disease in Childhood* **64:**596-599.

Weatherall I. L., (1983), Thermal properties of bedding . In: Proceedings of the Eleventh Annual Conference of the Textile Institute of New Zealand Story, L. F., (Ed.), , Christchurch, 107-116.

Werner J., (1977), "Mathematical treatment of structure and function of the human thermoregulatory system". *Biological Cybernetics* **25:**93-101.

West J. B., (1979), "Respiratory physiology - the essentials, 2nd Ed.". Williams and Wilkins, Baltimore.

West J. B., and Wagner P. D., (1977), "Pulmonary gas exchange". In: "Bioengineering Aspects of the Lung" West, J. B., (Ed.), Marcell Dekker, New York.

Widdicombe J. G., (1964), "Chapter 24, Respiratory reflexes". In: "Handbook of physiology, Section 3, Respiration" Fenn, W. O., and Rahn, H., (Eds.), American Physiological Society, Washington D.C., pp. 585-630.

Widdiwson E. M., (1974), "Changes in body proportions and composition during growth". In: "Scientific Foundations of Paediatrics" Davis, J. A., and Dobbing, J., (Eds.), William Heineman, pp. 153-163.

Wilkie R. A., Bryan M. H., Gaston S., and Bryan A. C., (1987), "Maturation of peripheral chemoreceptors in normal newborn infants". *Federation Proceedings* p. 823.

Wilmer H. A., (1940), "Changes in structural components of human body from six lunar months to maturity". *Experimantal Biology and Medicine* **43:**545-547.

Wissler E. H., (1963), "An analysis of factors affecting temperature levels in the nude human". In: "Temperature - its measurement and control in science and industry, Volume 3, Part 3" Hardy, J. D., (Ed.), Reinhold, New York, pp. 603-612.

Wissler E. H., (1964), "A mathematical model of the human thermal system". *Bulletin of Mathematical Biophysics* **26:**147-166.

Wissler E. H., (1961), "Steady-state temperature distribution in man". *Journal of Applied Physiology* **16:**734-740.

Wyndham C. H., and Atkins A. R., (1960), "An approach to the solution of the human biothermal problem with the aid of an analog computer". *Proceedings 3rd International Conference on Medical Electronics* London.

Wyndham C. H., and Atkins A. R., (1968), "A physiological scheme and mathematical model of temperature regulation in man". *Pflugers Archive* **303:**14-30.

Zierler K. L., (1962), "Chapter 18, Circulation times and the theory of indicator dilution methods for determining blood flow and volume". In: "Handbook of Physiology" Hamilton, W. F., and Dow, P., (Eds.), American Physiological Society, Washington D.C., pp.585-615.

Zylke J. W., (1989), "Sudden infant death syndrome: resurgent research offers hope". *Journal of the American Medical Association* **262(12):**1565-1566.

Appendix

Infant Temperature and Respiratory Data

The data presented in this appendix are the result of the analysis of temperature and respiratory signals collected from nine infants, all of whom were less than six months of age. The analysis has been performed on the signals from each individual night during which the signals were recorded.

Patient: **BB** DOB: **22 Jan 1991**

Age (days)	Median environment temperature (°C)	Median breathing rate (BPM)	Median rectal temperature (°C)	Rectal temperature drop (°C)	Oscillation period (mins)	Power rectal temp oscillations (°C^2)	Power MBR oscillations (BPM^2)	Power IQBR oscillations (BPM^2)	d/dt rectal temp ⊗ IQBR R	d/dt rectal temp ⊗ IQBR Delay (mins)	Rectal temp ⊗ abdo temp R	Rectal temp ⊗ abdo temp Delay (mins)	Rectal temp ⊗ shin temp R	Rectal temp ⊗ shin temp Delay (mins)
5.0000E+1	1.9036E+1	3.0416E+1	3.7790E+1	-2.7033E-1	6.4000E+1	4.1923E-3	1.5409E+1	7.8417E+1	-3.4519E-1	-3.2000E+1	8.9810E-1	4.0000E+0	-6.7583E-1	4.1000E+1
5.1000E+1	1.9072E+1	2.5636E+1	3.6513E+1	-4.4853E-1		7.8276E-3	5.7011E+0	5.1193E+1	3.8265E-1	-2.9000E+1	4.0163E-1	1.2000E+1	7.6424E-1	0.0000E+0
5.3000E+1	1.8296E+1	2.7442E+1	3.6647E+1	-2.5335E-1	4.2666E+1	3.9852E-3	7.3764E+0	3.1069E+1	5.8504E-1	-2.8000E+1	8.4780E-1	1.0000E+0	-4.4092E-1	4.5000E+1
5.4000E+1	2.0173E+1	2.6966E+1	3.6766E+1	-4.3075E-2	3.4133E+1	3.0305E-3	1.2907E+1	3.9152E+1	7.1391E-1	1.1700E+2	7.1397E-1	-4.0000E+0	-7.5792E-1	0.0000E+0
5.5000E+1	1.9462E+1	2.5632E+1	3.6759E+1	-1.3975E-1	6.4000E+1	3.4751E-3	6.0400E+0	2.1298E+1	6.5865E-1	5.0000E+0	5.4715E-1	0.0000E+0	8.7540E-1	-1.4000E+1
5.6000E+1	1.9649E+1	2.5908E+1	3.7303E+1	-4.1709E-1	6.4000E+1	4.7907E-3	1.1080E+1	2.0668E+1	6.8961E-1	1.4000E+1	-4.1753E-1	-1.1000E+1	-6.6635E-1	2.5000E+1
5.7000E+1	2.0162E+1	2.7014E+1	3.6945E+1	-1.0876E-1	4.2666E+1	1.8640E-3	8.0232E+0	2.4662E+1	7.7906E-1	-7.9000E+1	6.1821E-1	0.0000E+0	-3.8167E-1	2.6000E+1
5.8000E+1	1.9474E+1	2.7134E+1	3.6666E+1	-3.9361E-1	8.5333E+1	4.2358E-3	4.3797E+0	3.7337E+1	-6.2808E-1	9.0000E+1	8.7626E-1	-3.0000E+0	3.7029E-1	-1.9000E+1
5.9000E+1	2.0609E+1	2.7974E+1	3.6822E+1	0.0000E+0	8.5333E+1	5.2862E-4	7.9305E+0	6.6463E+1	3.9427E-1	-2.7000E+1	4.8088E-1	0.0000E+0	6.0738E-1	3.7000E+1
6.0000E+1	1.9505E+1	2.8513E+1	3.6795E+1	-1.6666E-1	5.6888E+1	1.8151E-3	4.0597E+0	5.2533E+1	4.6680E-1	-2.9000E+1	-4.9473E-1	-5.7000E+1	-5.3085E-1	-3.4000E+1
6.1000E+1	1.8317E+1	2.7605E+1	3.6717E+1	-3.0088E-1	8.5333E+1	6.4656E-3	4.5242E+0	5.4618E+1	6.6870E-1	-3.4000E+1	6.3178E-1	-1.0000E+1	8.1859E-1	-2.9000E+1
6.3000E+1	1.9397E+1	3.4255E+1	3.7025E+1	-2.9619E-1	7.3142E+1	3.1035E-3	1.6379E+1	3.7389E+1	6.2888E-1	3.0000E+0	6.9120E-1	-1.0000E+0	5.0790E-1	-1.9000E+1
6.4000E+1	1.8891E+1	2.9692E+1	3.6743E+1	-1.7904E-1	1.0239E+2	6.2859E-3	4.0992E+0	3.7151E+1	5.6245E-1	2.2000E+1	7.8872E-1	0.0000E+0	-5.7497E-1	4.0000E+0
6.5000E+1	1.7960E+1	3.2045E+1	3.6792E+1	-4.3700E-2	1.0239E+2	5.7873E-3	1.1439E+1	4.8261E+1	5.7552E-1	1.0000E+0	2.9912E-1	-1.7000E+1	-7.8611E-1	1.5000E+1
6.7000E+1	1.6733E+1	3.0460E+1	3.6680E+1	-3.9610E-1	1.0239E+2	3.7559E-3	4.9139E+0	3.9118E+1	-3.3817E-1	-1.3000E+1	3.7810E-1	6.1000E+1	-5.2478E-1	0.0000E+0
6.8000E+1	1.7826E+1	3.2215E+1	3.6779E+1	-1.8805E-1	8.5333E+1	6.4121E-4	3.7070E+0	2.3348E+1	4.3560E-1	8.0000E+0	6.0267E-1	-3.0000E+0	-6.8208E-1	-1.0000E+0
6.9000E+1	1.9847E+1	3.2963E+1	3.6820E+1	-2.5543E-1	1.0239E+2	1.4151E-3	8.3024E+0	3.8104E+1	-4.6510E-1	-2.3000E+1	6.6290E-1	5.0000E+0	4.9401E-1	-2.4000E+1
7.0000E+1	2.1729E+1	2.9605E+1	3.6763E+1	-3.1869E-1	5.1199E+1	3.9229E-3	3.2795E+0	3.6415E+1	-5.3831E-1	1.1000E+1	4.2279E-1	-3.0000E+0	-6.7239E-1	6.0000E+0
7.1000E+1	1.9510E+1	2.9659E+1	3.6799E+1	-2.3188E-1	5.1199E+1	2.7703E-3	2.4837E+0	3.0672E+1	-6.6082E-1	-1.0000E+1	8.2214E-1	-2.0000E+0	4.5617E-1	-8.0000E+0
7.3000E+1	1.7380E+1	3.1832E+1	3.6633E+1	-5.5773E-1	3.4133E+1	5.8918E-3	6.4395E+0	3.8539E+1	4.5221E-1	-5.0000E+0	-3.8217E-1	-8.0000E+0	-5.9516E-1	1.0000E+0
7.4000E+1	1.7031E+1	2.8544E+1	3.6619E+1	-2.0431E-1	5.1199E+1	1.4452E-3	1.9667E+0	4.5566E+1	-5.7382E-1	-3.0000E+0	5.5617E-1	0.0000E+0	5.6863E-1	-7.0000E+0
7.5000E+1	1.7513E+1	2.8003E+1	3.6609E+1	-4.0108E-1	6.4000E+1	3.5122E-3	3.4718E+0	7.3591E+0	5.6005E-1	2.1000E+1	4.9321E-1	0.0000E+0	4.8522E-1	-6.0000E+0
7.7000E+1	1.5213E+1	2.4789E+1	3.6643E+1	-4.4551E-1	8.5333E+1	4.9008E-3	5.3039E+0	1.6634E+1	5.9763E-1	7.0000E+0	7.5918E-1	2.0000E+0	8.9371E-1	-1.5000E+1
7.8000E+1	1.5734E+1	2.6938E+1	3.6623E+1	-7.2349E-1	5.1199E+1	4.2602E-3	3.5040E+0	1.4794E+1	4.3015E-1	-3.0000E+1	8.2711E-1	-1.0000E+0	-6.8257E-1	3.3000E+1
8.0000E+1	1.5816E+1	3.4477E+1	3.6524E+1	-1.3906E-1	4.2666E+1	6.6783E-3	3.0876E+0	4.7756E+0	-7.4649E-1	1.0000E+0	4.7842E-1	-1.1000E+1	8.0143E-1	-3.0000E+0
8.1000E+1	1.6776E+1	3.6040E+1	3.6711E+1	-4.2592E-1	4.6545E+1	3.7514E-3	2.2548E+1	2.9876E+1	3.3773E-1	-4.0000E+0	6.5900E-1	-3.6000E+1	7.2061E-1	-4.0000E+1
8.2000E+1	1.6692E+1	2.7497E+1	3.6662E+1	-8.3300E-2	3.9384E+1	4.1168E-3	3.3822E+0	1.6829E+1	5.4607E-1	2.0000E+1	5.7524E-1	-7.0000E+0	-6.9915E-1	1.0000E+0
8.3000E+1	1.6660E+1	2.9570E+1	3.6610E+1	-4.1461E-1	8.5333E+1	8.9262E-3	1.4140E+1	2.5053E+1	6.9222E-1	1.4000E+1	-7.0345E-1	2.8000E+1	4.1908E-1	-1.4000E+1
8.4000E+1	1.7713E+1	3.2192E+1	3.6630E+1	-3.5705E-1	8.5333E+1	6.3927E-3	1.1627E+1	1.4293E+1	-6.8961E-1	4.6000E+1	5.6690E-1	-1.5000E+1	6.3224E-1	2.5000E+1
8.7000E+1	1.2156E+1	3.1554E+1	3.6524E+1	-5.7238E-1	7.3142E+1	5.2416E-3	1.0050E+1	1.8835E+1	5.5047E-1	6.0000E+0	8.2842E-1	1.1900E+2	8.2868E-1	-1.0000E+0
8.8000E+1	1.4210E+1	2.7318E+1	3.6515E+1	-4.0590E-1	6.4000E+1	1.4966E-3	7.6447E+0	8.6285E+0	4.5122E-1	8.0000E+0	-5.7951E-1	-5.6000E+1	5.3961E-1	-1.8000E+1
9.0000E+1	1.2803E+1	2.8895E+1	3.6593E+1	-4.9078E-1	5.6888E+1	8.9586E-3	8.8327E+0	2.3779E+1	6.4132E-1	7.0000E+0	8.1437E-1	4.0000E+0	-3.5274E-1	3.9000E+1
9.1000E+1	1.5857E+1	3.2285E+1	3.6702E+1	-5.0556E-1	6.4000E+1	5.1846E-3	7.6698E+0	1.5425E+1	5.1777E-1	8.0000E+0	-5.5948E-1	0.0000E+0	4.4891E-1	-3.0000E+0
9.2000E+1	1.4828E+1	3.1535E+1	3.6657E+1	-3.8443E-1	5.6888E+1	5.2657E-3	9.8954E+0	2.2990E+1	6.2908E-1	6.0000E+0	8.9404E-1	-7.4000E+1	4.7619E-1	-8.0000E+1
9.4000E+1	1.7925E+1	2.8657E+1	3.6604E+1	-3.4866E-2	5.1199E+1	8.4502E-4	4.5413E+0	1.7730E+1	5.6175E-1	0.0000E+0	8.0632E-1	0.0000E+0	3.8313E-1	-1.9000E+1
9.5000E+1	1.5312E+1	3.0309E+1	3.6574E+1	-3.7544E-1	7.3142E+1	1.0596E-3	4.1175E+0	1.8962E+1	-4.1621E-1	3.4000E+1	4.9062E-1	5.0000E+0	-1.2921E+0	2.0000E+2
9.6000E+1	1.5134E+1	3.0290E+1	3.6552E+1	-4.1213E-1	3.6571E+1	4.9594E-3	4.2441E+0	1.8778E+1	6.4540E-1	-1.6000E+2	5.4795E-1	-3.0000E+0	7.9381E-1	1.4700E+2

Patient: AH DOB: **1 Jun 1991**

Age (days)	Median environment temperature (°C)	Median breathing rate (BPM)	Median rectal temperature (°C)	Rectal temperature drop (°C)	Oscillation period (mins)	Power rectal temp oscillations (°C²)	Power MBR oscillations (BPM²)	Power IQBR oscillations (BPM²)	d/dt rectal temp ⊗ IQBR R	Delay (mins)	Rectal temp ⊗ abdo temp R	Delay (mins)	Rectal temp ⊗ shin temp R	Delay (mins)
4.6000E+1	1.4363E+1	3.6512E+1	3.6907E+1	-7.1735E-1	6.4000E+1	5.7919E-3	3.0061E+1	8.0713E+1	6.9705E-1	0.0000E+0	8.2254E-1	-1.0000E+0	-7.6125E-1	1.1000E+1
4.7000E+1	1.5989E+1	3.4224E+1	3.7038E+1	-5.8313E-1	6.4000E+1	5.0015E-3	1.5098E+1	3.9531E+1	3.8392E-1	0.0000E+0	5.7000E-1	-5.0000E+0	-4.2123E-1	1.3000E+1
4.8000E+1	1.4816E+1	3.5069E+1	3.6932E+1	-4.4854E-1	1.0239E+2	6.2627E-3	1.6697E+1	5.5248E+1	4.0600E-1	-1.0000E+0	5.4644E-1	-8.0000E+0	5.7724E-1	-1.2000E+1
4.9000E+1	1.5271E+1	2.7481E+1	3.6882E+1	-2.7141E-1	5.6888E+1	1.8994E-3	4.9312E+0	1.5470E+1	2.1436E-1	1.0000E+0	-2.7606E-1	-3.5000E+1	4.0795E-1	-1.7000E+1
5.0000E+1	1.5058E+1	3.6321E+1	3.6661E+1	-5.9919E-1	7.3142E+1	5.7838E-3	4.0975E+1	5.5320E+1	4.8839E-1	-5.0000E+0	8.3766E-1	-1.5000E+1	7.7597E-1	-3.2000E+1
5.1000E+1	1.4666E+1	3.5681E+1	3.7051E+1	-4.8966E-1	6.4000E+1	3.6552E-3	1.9190E+1	4.5770E+1	5.1460E-1	0.0000E+0	4.5628E-1	1.1200E+2	5.4437E-1	-2.0000E+1
5.2000E+1	1.5344E+1	3.6601E+1	3.6966E+1	-3.5104E-1	6.4000E+1	2.3899E-3	2.4272E+1	4.1124E+1	-2.9755E-1	3.0000E+1	6.0627E-1	4.8000E+1	-5.0867E-1	3.0000E+0
5.3000E+1	1.4619E+1	3.6392E+1	3.6923E+1	-4.4784E-1	8.5333E+1	3.6625E-3	1.7884E+1	2.1702E+1	4.8544E-1	0.0000E+0	-3.6065E-1	6.6000E+1	4.7951E-1	9.5000E+1
5.4000E+1	1.4293E+1	3.7654E+1	3.6972E+1	-2.6214E-1	7.3142E+1	3.1089E-3	1.4417E+1	5.4712E+1	4.8041E-1	1.0000E+0	5.4751E-1	0.0000E+0	-6.0311E-1	1.7000E+1
5.6000E+1	1.3649E+1	3.2211E+1	3.6939E+1	-4.9280E-1	6.8266E+1	6.0447E-3	2.6306E+1	4.2526E+1	5.7694E-1	0.0000E+0	8.6119E-1	-2.0000E+0	-5.2941E-1	5.0000E+0
5.7000E+1	1.3259E+1	3.0945E+1	3.6909E+1	-4.7429E-1	6.4000E+1	8.1259E-3	2.0286E+1	4.0279E+1	5.3380E-1	0.0000E+0	6.2827E-1	-3.0000E+0	3.1424E-1	9.7000E+1
5.8000E+1	1.5132E+1	3.1764E+1	3.6773E+1	-5.7946E-1	6.0235E+1	5.3986E-3	2.7320E+1	2.2606E+1	6.1668E-1	-1.0000E+0	7.4386E-1	-9.0000E+0	-5.3414E-1	1.5000E+1
5.9000E+1	1.5102E+1	3.9140E+1	3.7157E+1	-3.9428E-1	1.0239E+2	3.4180E-3	2.0444E+1	2.6449E+1	3.3288E-1	-1.0000E+0	7.5514E-1	-4.0000E+0	7.2355E-1	-1.3000E+1
6.0000E+1	1.5566E+1	3.1388E+1	3.6962E+1	-5.9809E-1	6.4000E+1	6.5318E-3	1.8824E+1	3.8014E+1	6.6830E-1	1.0000E+0	8.0797E-1	0.0000E+0	-8.5426E-1	1.4000E+1
6.2000E+1	1.2235E+1	3.0623E+1	3.7105E+1	-4.0422E-1	6.4000E+1	4.8538E-3	1.8119E+1	2.5114E+1	6.0316E-1	2.0000E+0	7.2176E-1	-4.0000E+0	-4.9884E-1	1.7000E+1
6.3000E+1	1.3159E+1	3.0909E+1	3.7068E+1	-5.0506E-1	6.4000E+1	4.7811E-3	2.4422E+1	3.1436E+1	6.6017E-1	1.0000E+0	4.4996E-1	-6.0000E+0	-5.2128E-1	1.0000E+1
6.4000E+1	1.3795E+1	3.1041E+1	3.7173E+1	-1.1077E-1	7.3142E+1	3.1182E-3	1.6465E+1	2.8928E+1	6.7233E-1	0.0000E+0	8.5891E-1	-6.0000E+0	-5.9194E-1	-7.2000E+1
6.6000E+1	1.6149E+1	3.2761E+1	3.7010E+1	-5.4410E-1	6.4000E+1	6.1938E-3	1.9195E+1	3.9161E+1	5.8873E-1	0.0000E+0	8.3537E-1	-3.0000E+0	-6.2317E-1	1.0000E+1
6.8000E+1	1.6447E+1	3.1025E+1	3.6968E+1	-5.3041E-1	7.3142E+1	9.0603E-3	1.3400E+1	3.6187E+1	5.6630E-1	1.0000E+0	7.9019E-1	1.0000E+0	8.1214E-1	-1.6000E+1
6.9000E+1	1.3782E+1	3.1938E+1	3.7014E+1	-4.1224E-1	7.3142E+1	5.8927E-3	1.5674E+1	3.5637E+1	4.7734E-1	0.0000E+0	4.8756E-1	5.0000E+0	3.6553E-1	-5.0000E+0
7.1000E+1	1.4873E+1	3.0044E+1	3.6916E+1	-5.9707E-1	7.8769E+1	8.8171E-3	1.8663E+1	3.2761E+1	6.5071E-1	-1.0000E+0	6.9634E-1	-1.0000E+0	-5.6697E-1	6.1000E+1
7.2000E+1	1.5621E+1	2.8480E+1	3.6883E+1	-7.3283E-1	6.8266E+1	9.9937E-3	1.2652E+1	2.6050E+1	4.8805E-1	1.0000E+0	5.8381E-1	-5.0000E+0	4.6922E-1	-1.1000E+1
7.3000E+1	1.6066E+1	2.8996E+1	3.6966E+1	-3.4709E-1	7.3142E+1	6.1425E-3	1.0019E+1	1.9157E+1	6.3157E-1	1.0000E+0	7.8068E-1	0.0000E+0	-6.3864E-1	-5.4000E+1
7.6000E+1	1.7460E+1	3.3381E+1	3.7195E+1	-2.6360E-1	5.3894E+1	3.5975E-3	9.0968E+0	1.9812E+1	4.4973E-1	-4.0000E+0	6.7986E-1	-5.0000E+0	5.7848E-1	-2.4000E+1
7.7000E+1	1.4775E+1	3.1775E+1	3.7208E+1	-5.0171E-1	6.8266E+1	4.6496E-3	8.3281E+0	2.1828E+1	4.8714E-1	-1.0000E+0	7.4595E-1	-7.0000E+0	-3.7017E-1	2.0000E+0
7.8000E+1	1.3685E+1	3.3829E+1	3.7499E+1	-7.8141E-1	9.3090E+1	4.6595E-3	1.8557E+1	3.8561E+1	4.3360E-1	0.0000E+0	6.3751E-1	-1.0000E+1	-4.1210E-1	1.5000E+1
8.0000E+1	1.4487E+1	2.9766E+1	3.6174E+1		7.3142E+1	1.4152E-2	1.2554E+1	2.8914E+1	2.2111E-1	-6.0000E+0	6.2663E-1	0.0000E+0	3.3839E-1	-2.9000E+1
8.2000E+1	1.5028E+1	2.6479E+1	3.6600E+1	-1.5081E-1	6.4000E+1	2.3111E-3	1.1658E+1	1.8708E+1	3.5828E-1	0.0000E+0	5.3328E-1	0.0000E+0	-7.1375E-1	1.4000E+1
8.3000E+1	1.3943E+1	2.7538E+1	3.6805E+1	-5.9511E-1	6.8266E+1	6.2344E-3	1.0237E+1	2.3713E+1	6.7336E-1	0.0000E+0	4.8690E-1	-1.0000E+0	2.6532E-1	-1.2000E+1
8.6000E+1	1.5410E+1	2.9124E+1	3.6992E+1	-5.9237E-1	6.4000E+1	6.2106E-3	2.5133E+1	2.2245E+1	6.8098E-1	3.0000E+0	8.1693E-1	-1.0000E+0	8.8520E-1	-7.0000E+0
8.7000E+1	1.6882E+1	2.9025E+1	3.6928E+1	-8.6549E-1	6.8266E+1	6.3186E-3	8.3888E+0	1.4988E+1	5.2812E-1	-1.0000E+0	5.4116E-1	-5.0000E+0	-5.0907E-1	1.2000E+1
8.8000E+1	1.6666E+1	3.0048E+1	3.6840E+1	-6.9952E-1	6.4000E+1	6.4823E-3	1.6095E+1	2.1588E+1	3.2708E-1	0.0000E+0	5.9392E-1	0.0000E+0	-5.7860E-1	1.2000E+1
9.3000E+1	1.3894E+1	3.3628E+1	3.6925E+1	-5.3739E-1	6.8266E+1	1.1987E-2	1.8091E+1	1.9555E+1	4.7358E-1	-6.0000E+0	6.2114E-1	-8.0000E+0	7.1319E-1	-1.5000E+1
9.4000E+1	1.6215E+1	3.0234E+1	3.6900E+1	-7.8270E-1	6.0235E+1	8.4522E-3	1.0610E+1	1.3858E+1	5.2020E-1	2.0000E+0	6.3822E-1	0.0000E+0	-6.6489E-1	1.6000E+1
9.6000E+1	1.6157E+1	3.0605E+1	3.7144E+1	-5.5390E-1	7.3142E+1	5.3189E-3	1.0550E+1	1.8066E+1	4.2620E-1	3.0000E+0	8.8835E-1	-1.0000E+0	3.6879E-1	3.8000E+1

Age (days)	Median environment temperature (°C)	Median breathing rate (BPM)	Median rectal temperature (°C)	Rectal temperature drop (°C)	Oscillation period (mins)	Power rectal temp oscillations ($°C^2$)	Power MBR oscillations (BPM^2)	Power IQBR oscillations (BPM^2)	d/dt rectal temp ⊗ IQBR R	d/dt rectal temp ⊗ IQBR Delay (mins)	Rectal temp ⊗ abdo temp R	Rectal temp ⊗ abdo temp Delay (mins)	Rectal temp ⊗ shin temp R	Rectal temp ⊗ shin temp Delay (mins)
Patient: SK	DOB: **12 Mar 1991**													
4.8000E+1	1.5758E+1	4.3832E+1	3.6749E+1	-3.6763E-1	7.3142E+1	2.8002E-3	4.5537E+1	5.4952E+1	6.6252E-1	0.0000E+0	8.4119E-1	0.0000E+0	5.6901E-1	-8.0000E+0
5.2000E+1	1.5720E+1	3.9113E+1	3.6771E+1	-4.1285E-1	6.4000E+1	1.2783E-2	2.9694E+1	8.3098E+1	5.7008E-1	1.0000E+0	4.3094E-1	-5.0000E+0	-5.9688E-1	1.8000E+1
5.3000E+1	1.5804E+1	4.6463E+1	3.6724E+1	-1.7473E-1	8.5333E+1	7.2491E-3	4.9806E+1	5.9324E+1	-4.8633E-1	7.0000E+0	-5.9351E-1	7.0000E+0	-8.1708E-1	7.0000E+0
5.4000E+1	1.5081E+1	4.0670E+1	3.6591E+1	-7.4291E-1	7.3142E+1	7.4242E-3	4.0337E+1	4.8699E+1	3.6013E-1	0.0000E+0	5.7982E-1	-9.0000E+0	5.5963E-1	-8.0000E+1
5.7000E+1	1.6644E+1	3.9113E+1	3.6758E+1	-7.6412E-2	6.4000E+1	3.6278E-3	4.4950E+1	7.3201E+1	7.8526E-1	2.0000E+0	5.8410E-1	5.0000E+0	-5.8175E-1	6.3000E+1
5.9000E+1	1.5469E+1	4.1867E+1	3.6768E+1	-3.0182E-1	6.4000E+1	8.2956E-3	3.7588E+1	3.0483E+1	4.8713E-1	-3.0000E+0	8.3662E-1	4.3000E+1	-5.5927E-1	-4.1000E+1
6.0000E+1	1.3515E+1	3.7472E+1	3.6671E+1	-4.7006E-1	7.3142E+1	8.6861E-3	2.3629E+1	8.1416E+1	6.9959E-1	0.0000E+0	8.3925E-1	-5.0000E+0	4.9507E-1	-1.3000E+1
6.1000E+1	1.3037E+1	4.7848E+1	3.6630E+1	-5.0934E-1	5.6888E+1	1.6239E-2	5.4493E+1	7.3881E+1	5.7160E-1	-2.0000E+0	-6.4876E-1	2.7000E+1	-4.6393E-1	2.8000E+1
6.2000E+1	1.3999E+1	3.9829E+1	3.6639E+1	-2.7024E-1	5.1199E+1	6.3426E-3	4.8552E+1	2.3297E+1	6.4914E-1	3.0000E+0	7.3814E-1	-1.0000E+0	3.2092E-1	-9.0000E+0
6.4000E+1	1.5195E+1	4.1979E+1	3.6596E+1	-3.4336E-1	7.3142E+1	7.0180E-3	4.1819E+1	9.1733E+1	8.0888E-1	1.0000E+0	7.5079E-1	-8.0000E+0	-5.5346E-1	1.2000E+1
6.5000E+1	1.5867E+1	4.0162E+1	3.6631E+1	-4.6802E-1	5.6888E+1	9.1669E-3	3.7748E+1	7.5095E+1	7.0141E-1	0.0000E+0	7.7020E-1	-7.0000E+0	6.4069E-1	-6.5000E+1
6.6000E+1	1.4791E+1	3.7417E+1	3.6608E+1	-4.4094E-1	5.1199E+1	9.1311E-3	5.0555E+1	6.4018E+1	7.5797E-1	-2.0000E+0	8.8942E-1	-4.0000E+0	-8.7394E-1	1.6000E+1
6.8000E+1	1.3053E+1	3.7410E+1	3.6776E+1	-4.1524E-1	7.3142E+1	8.3156E-3	2.3297E+1	7.8469E+1	7.5314E-1	-2.0000E+0	8.4313E-1	-9.0000E+0	-6.8097E-1	8.0000E+0
6.9000E+1	1.4151E+1	3.9371E+1	3.6625E+1	-7.8539E-1	6.4000E+1	1.2235E-2	4.8098E+1	8.0418E+1	6.6637E-1	1.0000E+0	8.6176E-1	-4.0000E+0	-7.3478E-1	9.0000E+0
7.0000E+1	1.2464E+1	3.9160E+1	3.6802E+1	-3.7791E-1	9.3090E+1	1.0648E-2	2.8317E+1	1.2453E+2	7.0971E-1	0.0000E+0	8.7055E-1	-1.0000E+1	-5.9735E-1	8.0000E+0
7.1000E+1	1.4866E+1	4.1449E+1	3.6535E+1	-6.1056E-1	6.4000E+1	1.4870E-2	6.3089E+1	9.7639E+1	6.6225E-1	-2.0000E+0	7.8742E-1	-9.0000E+0	-5.8685E-1	3.0000E+0
7.2000E+1	1.2335E+1	3.6044E+1	3.6582E+1	-7.2301E-1	7.3142E+1	1.6051E-2	3.4189E+1	7.2533E+1	7.0759E-1	-2.0000E+0	8.9969E-1	-8.0000E+0	-6.8151E-1	1.1000E+1
Patient: CM	DOB: **24 Jan 1991**													
1.2400E+2	1.4254E+1	3.0699E+1	3.6330E+1	-6.8763E-1	5.1199E+1	4.7800E-3	1.0254E+1	2.3668E+1	3.1950E-1	4.0000E+0	7.8085E-1	-6.0000E+0	-1.2366E+0	3.4000E+2
1.2500E+2	1.6837E+1	3.2905E+1	3.7324E+1	-6.1990E-1	5.1199E+1	7.3565E-3	6.4998E+0	1.9068E+1	6.8235E-1	1.2000E+1	9.5858E-1	-5.0000E+0	-7.1793E-1	5.4000E+1
1.2600E+2	1.1937E+1	2.8366E+1	3.6255E+1	-5.2703E-1	4.6545E+1	9.9979E-3	4.2500E+0	1.5550E+1	6.0039E-1	1.2000E+1	8.1604E-1	-8.0000E+0	5.0611E-1	7.0000E+0
1.2700E+2	1.4180E+1	2.8292E+1	3.6273E+1	-4.6871E-1	6.4000E+1	1.3529E-3	5.3431E+0	1.8205E+1	-7.3602E-1	-2.1900E+2	6.4756E-1	-9.0000E+0	-5.6119E-1	1.2100E+2
1.2900E+2	1.3768E+1	2.5049E+1	3.6078E+1	-1.0086E+0	5.6888E+1	1.0889E-2	1.0141E+1	1.5329E+1	-4.5448E-1	4.4000E+1	5.3896E-1	0.0000E+0	-4.4897E-1	0.0000E+0
1.3000E+2	1.2437E+1	2.2927E+1	3.6175E+1	-6.9597E-1	6.0235E+1	7.8366E-3	6.2320E+0	1.1980E+1	5.1900E-1	-2.1700E+2	6.2675E-1	-6.0000E+0	-5.7425E-1	3.0000E+0
1.3100E+2	1.5735E+1	2.6559E+1	3.6403E+1	-8.5543E-1	1.2800E+2	4.6596E-3	7.1049E+0	1.8368E+1	-4.6775E-1	3.8000E+1	7.1683E-1	-3.0000E+0	4.6018E-1	-2.7000E+1
1.3200E+2	1.4974E+1	2.6403E+1	3.6248E+1	-8.5697E-1	4.6545E+1	2.8385E-3	6.2359E+0	1.5197E+1	5.6207E-1	-6.8000E+1	8.1300E-1	-1.0000E+0	-5.5338E-1	-9.0000E+1
1.3300E+2	1.3191E+1	2.4264E+1	3.6106E+1	-6.1142E-1	5.1199E+1	1.2588E-2	2.6302E+0	1.0273E+1	-5.8218E-1	-4.0000E+0	5.7583E-1	-6.0000E+0	-6.2538E-1	-5.9000E+1
1.3400E+2	1.4045E+1	2.8102E+1	3.6380E+1	-5.5564E-1	5.6888E+1	7.1796E-3	1.0326E+1	1.3564E+1	4.5212E-1	1.0000E+0	-7.7924E-1	-1.4600E+2	7.2264E-1	-1.8600E+2
1.3500E+2	1.2226E+1	2.8720E+1	3.6228E+1	-8.3546E-1	5.1199E+1	6.4126E-3	8.5387E+0	1.8387E+1	2.6484E-1	3.0000E+0	8.3941E-1	-1.0000E+0	5.4163E-1	-2.1000E+1
1.3600E+2	1.4928E+1	2.5253E+1	3.6479E+1	-5.8916E-1	7.3142E+1	5.6153E-3	4.4455E+0	1.5156E+1	-4.8463E-1	3.7000E+1	6.6510E-1	-8.0000E+0	-6.9750E-1	1.0100E+2
1.3700E+2	1.2683E+1	2.4614E+1	3.6394E+1	-7.3474E-1	5.6888E+1	5.7294E-3	6.2864E+0	1.4100E+1	-5.5652E-1	2.8000E+2	6.3585E-1	-1.3500E+2	-4.0678E-1	-7.9000E+1
1.3800E+2	1.4177E+1	2.3769E+1	3.6324E+1	-5.3593E-1	5.1199E+1	3.2600E-3	5.6233E+0	1.4099E+1	5.7444E-1	2.1000E+1	4.8423E-1	-1.1000E+1	-4.5408E-1	-1.1000E+1
1.4300E+2	1.3151E+1	2.5357E+1	3.6349E+1	-1.0503E+0	5.6888E+1	7.7756E-3	5.9515E+0	1.0772E+1	3.9339E-1	1.0000E+1	7.7487E-1	-4.0000E+0	-6.4576E-1	2.0000E+1
1.4500E+2	1.1746E+1	2.5826E+1	3.6452E+1	-7.1710E-1	5.1199E+1	5.5200E-3	6.7464E+0	1.0302E+1	5.9580E-1	1.9000E+1	-6.5356E-1	-7.7000E+1	-4.6345E-1	-1.7000E+1

Age (days)	Median environment temperature (°C)	Median breathing rate (BPM)	Median rectal temperature (°C)	Rectal temperature drop (°C)	Oscillation period (mins)	Power rectal temp oscillations (°C^2)	Power MBR oscillations (BPM^2)	Power IQBR oscillations (BPM^2)	d/dt rectal temp ⊗ IQBR R	d/dt rectal temp ⊗ IQBR Delay (mins)	Rectal temp ⊗ abdo temp R	Rectal temp ⊗ abdo temp Delay (mins)	Rectal temp ⊗ shin temp R	Rectal temp ⊗ shin temp Delay (mins)
Patient: SG	**DOB: 2 May 1991**													
3.5000E+1	1.5682E+1	2.7903E+1	3.7047E+1	-3.3781E-1	6.4000E+1	1.9610E-3	5.4590E+0	1.7440E+1	6.1923E-1	0.0000E+0	7.5747E-1	-2.0000E+0	4.4221E-1	1.0000E+0
3.6000E+1	1.4647E+1	2.8790E+1	3.7154E+1	-1.6536E-1	6.4000E+1	3.8955E-3	8.9003E+0	1.5966E+1	8.2259E-1	0.0000E+0	9.2741E-1	0.0000E+0	7.4633E-1	-9.0000E+0
3.8000E+1	1.4574E+1	2.7136E+1	3.7087E+1	-2.6616E-1	5.6888E+1	4.5939E-3	3.6816E+0	1.0154E+1	7.9812E-1	1.0000E+0	6.8272E-1	9.0000E+0	4.9646E-1	0.0000E+0
3.9000E+1	1.3866E+1	2.7060E+1	3.7142E+1	-1.5621E-1	5.1199E+1	1.8140E-3	2.8684E+0	3.6172E+0	6.8016E-1	-2.0000E+0	6.8715E-1	1.0000E+0	6.1860E-1	3.7000E+1
4.0000E+1	1.4786E+1	2.7006E+1	3.7297E+1	-6.9000E-2	5.1199E+1	1.6183E-3	8.0371E+0	1.9575E+1	6.6125E-1	-2.0000E+0	6.9707E-1	3.0000E+0	2.5619E-1	1.7000E+1
4.1000E+1	1.3747E+1	2.6366E+1	3.7059E+1	-1.2896E-1	7.3142E+1	5.1365E-4	3.9145E+0	1.2742E+1	5.7944E-1	-4.0000E+0	5.7839E-1	-1.0000E+0	-8.8141E-1	-1.8000E+2
Patient: AL	**DOB: 10 Sep 1991**													
1.3300E+2	1.9247E+1	2.4383E+1	3.6902E+1	-8.6524E-1	5.1199E+1	6.4386E-3	1.2204E+0	7.5658E+0	6.2127E-1	1.0000E+0	5.9144E-1	-1.0000E+0	9.3991E-1	-2.4700E+2
1.3400E+2	2.0079E+1	2.3048E+1	3.6918E+1	-7.6920E-1	5.3894E+1	5.0502E-3	1.5440E+0	6.8857E+0	8.1986E-1	2.0000E+0	7.0848E-1	-5.0000E+0	5.9411E-1	-1.3400E+2
1.3500E+2	2.1181E+1	2.4072E+1	3.6814E+1	-8.1812E-1	5.1199E+1	4.8734E-3	1.1410E+0	9.5039E+0	8.7835E-1	-2.0000E+0	1.0618E+0	-2.0000E+2	-5.7967E-1	-7.0000E+0
1.3600E+2	1.6825E+1	2.2891E+1	3.6800E+1	-9.2660E-1	5.6888E+1	9.2324E-3	1.4108E+0	1.0988E+1	7.5631E-1	1.0000E+0	7.6901E-1	-1.0000E+0	6.7685E-1	1.4300E+2
1.3800E+2	2.2198E+1	2.4019E+1	3.6929E+1	-1.3003E+0	4.8761E+1	4.4574E-3	2.2738E+0	8.8087E+0	7.2964E-1	-1.0000E+0	5.7472E-1	-1.0000E+1	-6.5658E-1	0.0000E+0
1.3900E+2	2.3307E+1	2.6060E+1	3.6904E+1	-1.0079E+0	5.6888E+1	7.2889E-3	3.9634E+0	1.0187E+1	7.5753E-1	-4.0000E+0	-6.2489E-1	6.0000E+0	-6.3299E-1	5.0000E+0
1.4100E+2	2.2647E+1	2.4549E+1	3.6991E+1	-7.9464E-1	7.3142E+1	6.1356E-3	3.6915E+0	1.3403E+1	7.8356E-1	-1.0000E+0	7.0405E-1	1.5400E+2	-7.3165E-1	1.6700E+2
1.4200E+2	2.2717E+1	2.4747E+1	3.7039E+1	-6.1351E-1	5.6888E+1	8.2767E-3	3.5724E+1	9.5042E+0	7.4873E-1	0.0000E+0	4.8616E-1	-2.7000E+1	-5.8087E-1	0.0000E+0
1.4300E+2	1.9121E+1	2.4103E+1	3.6896E+1	-9.4625E-1	5.1199E+1	8.0886E-3	2.3049E+0	5.9228E+0	6.4816E-1	-2.0000E+0	6.2558E-1	-1.0000E+1	-6.6050E-1	6.0000E+0
1.4400E+2	1.7924E+1	2.3395E+1	3.6904E+1	-5.8531E-1	7.3142E+1	6.3160E-3	2.1635E+0	8.4851E+0	7.0152E-1	-1.0000E+0	-7.6610E-1	-1.0400E+2	-7.3840E-1	1.0000E+0
1.4600E+2	2.2744E+1	2.4215E+1	3.6916E+1	-8.7150E-1	5.6888E+1	1.0169E-2	1.3899E+0	8.0404E+0	7.4125E-1	-1.0000E+0	-4.6674E-1	-7.9000E+1	-6.8091E-1	7.0000E+0
Patient: CS	**DOB: 14 Sep 1991**													
4.7000E+1	1.7703E+1	3.7324E+1	3.7668E+1	-5.0619E-1	5.6888E+1	1.6006E-3	2.1094E+1	1.9405E+1	6.6399E-1	4.0000E+0	7.6062E-1	3.0000E+0	-7.2673E-1	-2.9000E+1
4.8000E+1	1.9192E+1	3.5873E+1	3.7757E+1	-5.6744E-1	6.4000E+1	3.3436E-3	1.8834E+1	3.2010E+1	7.8182E-1	1.0000E+0	9.0604E-1	1.0000E+0	-7.3511E-1	9.8000E+1
5.0000E+1	1.5804E+1	3.5223E+1	3.7634E+1	-1.2815E-1	6.4000E+1	7.6952E-3	1.5254E+1	1.9893E+1	6.2031E-1	0.0000E+0	8.1472E-1	-5.0000E+0	6.7723E-1	7.0000E+0
5.2000E+1	1.4713E+1	3.4425E+1	3.7416E+1	-3.5919E-1	5.1199E+1	2.7951E-3	9.8984E+0	1.1405E+1	5.8390E-1	-1.0000E+0	5.9945E-1	-1.2600E+2	-4.4457E-1	-1.0600E+2
5.3000E+1	1.5905E+1	3.4373E+1	3.7442E+1	-5.7310E-1	5.3894E+1	3.2496E-3	1.1128E+1	1.6660E+1	7.5974E-1	0.0000E+0	7.8860E-1	-1.0000E+1	5.4870E-1	-1.1000E+1
5.5000E+1	1.6898E+1	3.5544E+1	3.7419E+1	-4.6650E-1	5.6888E+1	2.3287E-3	1.8922E+1	2.2061E+1	8.3664E-1	4.0000E+0	7.4856E-1	0.0000E+0	5.3665E-1	-1.0000E+0
5.6000E+1	1.8491E+1	3.4573E+1	3.7495E+1	-3.7635E-1	6.4000E+1	4.3031E-3	1.2395E+1	1.2195E+1	5.9679E-1	4.0000E+0	7.4656E-1	2.0000E+0	5.8408E-1	5.1000E+1
5.8000E+1	1.4861E+1	3.6381E+1	3.7500E+1	-1.2898E-1	5.6888E+1	5.4540E-3	1.5087E+1	2.3673E+1	7.4173E-1	-3.0000E+0	6.6649E-1	-1.0000E+1	-9.5338E-1	1.7600E+2
5.9000E+1	1.5672E+1	3.5283E+1	3.7578E+1	-3.6009E-1	4.6545E+1	6.5981E-3	1.3151E+1	1.5165E+1	7.2217E-1	-1.0000E+0	2.8275E-1	3.0000E+0	-5.2278E-1	8.8000E+1
6.0000E+1	1.6098E+1	3.4231E+1	3.7330E+1	-5.7427E-1	5.6888E+1	4.7397E-3	1.1829E+1	1.0820E+1	6.1955E-1	-1.0000E+0	7.8432E-1	-6.0000E+0	4.6548E-1	-5.0000E+0

Age (days)	Median environment temperature (°C)	Median breathing rate (BPM)	Median rectal temperature (°C)	Rectal temperature drop (°C)	Oscillation period (mins)	Power rectal temp oscillations (°C^2)	Power MBR oscillations (BPM^2)	Power IQBR oscillations (BPM^2)	d/dt rectal temp ⊗ IQBR R	d/dt rectal temp ⊗ IQBR Delay (mins)	Rectal temp ⊗ abdo temp R	Rectal temp ⊗ abdo temp Delay (mins)	Rectal temp ⊗ shin temp R	Rectal temp ⊗ shin temp Delay (mins)
Patient: NT	**DOB: 27 Mar 1991**													
3.0000E+1	2.0844E+1	3.5157E+1	3.6716E+1	-3.4304E-1	8.5333E+1	3.2603E-3	2.1362E+1	1.0518E+2	4.8600E-1	0.0000E+0	6.4570E-1	-3.0000E+0	4.2408E-1	-1.1000E+1
3.1000E+1	2.0161E+1	3.5439E+1	3.6792E+1	-1.7380E-1	8.5333E+1	2.1222E-3	1.1777E+1	8.6436E+1	-5.2545E-1	3.7000E+1	6.4897E-1	0.0000E+0	-7.0500E-1	4.0000E+0
3.2000E+1	2.0034E+1	3.6222E+1	3.6824E+1	-2.6319E-1	1.0239E+2	2.3800E-3	2.3208E+1	7.0204E+1	4.3216E-1	1.1000E+1	6.4022E-1	1.2000E+1	6.1466E-1	1.3300E+2
3.3000E+1	2.0680E+1	3.5699E+1	3.6868E+1	-1.0700E-1	8.5333E+1	2.2337E-3	1.9025E+1	7.2531E+1	-5.1676E-1	3.8000E+1	7.9454E-1	-8.0000E+0	-4.7457E-1	2.1000E+1
3.4000E+1	2.0952E+1	3.7117E+1	3.6849E+1	-3.5679E-1	8.5333E+1	3.0463E-3	8.7070E+0	9.4571E+1	-4.8642E-1	5.1000E+1	8.7527E-1	0.0000E+0	-8.3627E-1	4.0000E+0
3.5000E+1	2.1529E+1	3.6773E+1	3.6830E+1	0.0000E+0	6.4000E+1	3.7137E-3	1.6523E+1	1.1290E+2	-5.5543E-1	1.5000E+1	4.9329E-1	-9.0000E+0	-5.5601E-1	-2.0000E+0
3.6000E+1	2.3393E+1	3.7880E+1	3.6984E+1	-1.5202E-1	8.5333E+1	1.8405E-3	2.7219E+1	1.1204E+2	5.3284E-1	-2.3000E+1	8.1297E-1	-4.0000E+0	-4.9976E-1	1.0000E+1
3.7000E+1	2.0348E+1	3.8279E+1	3.6822E+1	0.0000E+0	1.0239E+2	1.9301E-3	1.2745E+1	7.9357E+1	3.9510E-1	4.0000E+0	6.3042E-1	0.0000E+0	-5.3213E-1	3.0000E+0
3.8000E+1	2.0811E+1	3.4256E+1	3.6807E+1	-4.8011E-1	1.0239E+2	3.1559E-3	1.1619E+1	6.6885E+1	-3.6626E-1	-4.7000E+1	7.0450E-1	7.0000E+0	-4.4718E-1	1.4200E+2
3.9000E+1	2.0663E+1	3.6279E+1	3.6924E+1	-1.1393E-1	1.0239E+2	2.6739E-3	1.3251E+1	4.9558E+1	6.5511E-1	-3.0000E+0	4.0446E-1	5.0000E+0	-5.5045E-1	5.0000E+0
4.0000E+1	1.7524E+1	3.7333E+1	3.6779E+1	-3.2176E-2	8.5333E+1	1.6897E-3	1.6717E+1	5.8305E+1	6.0330E-1	0.0000E+0	6.2517E-1	-9.0000E+0	5.6874E-1	-1.3000E+1
4.1000E+1	2.0288E+1	3.7059E+1	3.6875E+1	-2.5026E-1	1.0239E+2	4.0820E-3	1.6861E+1	5.5038E+1	-3.9019E-1	5.3000E+1	6.7322E-1	1.1000E+1	-7.4500E-1	4.0000E+0
4.2000E+1	1.7199E+1	4.0546E+1	3.7382E+1	-2.5001E-1	1.0239E+2	3.4495E-3	2.4561E+1	6.4025E+1	4.3597E-1	9.0000E+0	8.0607E-1	0.0000E+0	3.6859E-1	-1.7000E+1
4.3000E+1	1.9272E+1	3.2558E+1	3.6709E+1	-3.7000E-1	6.4000E+1	2.2551E-3	1.0090E+1	5.0730E+1	-5.7442E-1	3.3000E+1	-5.4124E-1	8.0000E+0	-7.8373E-1	6.0000E+0
4.4000E+1	2.0705E+1	3.7464E+1	3.6764E+1	-1.3500E-1	7.3142E+1	4.3924E-3	1.2040E+1	6.4460E+1	3.8815E-1	-2.0000E+0	7.6696E-1	-1.0000E+0	-5.9335E-1	-1.2100E+2
4.5000E+1	1.8897E+1	3.5379E+1	3.6826E+1	-3.5082E-1	7.3142E+1	4.6110E-3	2.0959E+1	6.1484E+1	-5.1989E-1	-1.7700E+2	5.4875E-1	-1.0000E+0	-4.7974E-1	-1.0900E+2
4.6000E+1	1.9444E+1	3.6226E+1	3.6862E+1	-2.5248E-1	1.0239E+2	4.4048E-3	1.1230E+1	6.2992E+1	-6.4053E-1	3.7000E+1	-6.4817E-1	2.7000E+1	-6.0669E-1	1.4000E+1
4.7000E+1	1.7055E+1	3.5680E+1	3.6821E+1	-3.2828E-1	1.0239E+2	6.6687E-3	1.5311E+1	5.3947E+1	4.5451E-1	1.0000E+0	7.8592E-1	-3.0000E+0	4.5084E-1	-1.2000E+1
4.8000E+1	2.0491E+1	3.4318E+1	3.6909E+1	-4.5215E-1	9.3090E+1	4.1058E-3	2.1569E+1	6.1956E+1	3.8795E-1	-1.4000E+1	7.5716E-1	-3.0000E+0	-3.9865E-1	2.1000E+1
4.9000E+1	2.0164E+1	3.3682E+1	3.6804E+1	-3.5220E-1	8.5333E+1	5.5351E-3	1.6536E+1	6.3470E+1	5.5536E-1	1.0000E+0	5.7850E-1	-2.0000E+0	-3.7203E-1	1.8000E+1
5.0000E+1	2.0494E+1	3.5534E+1	3.6907E+1	0.0000E+0	1.2800E+2	2.8542E-3	2.2474E+1	3.3126E+1	4.0673E-1	-6.0000E+0	-6.5792E-1	-1.7600E+2	-6.4790E-1	-1.8400E+2
Patient: NI	**DOB: 18 Apr 1991**													
6.0000E+1	1.2590E+1	3.1560E+1	3.6799E+1	-2.6000E-1	5.1199E+1	3.6961E-3	1.4204E+1	2.1073E+1	8.0853E-1	-2.0000E+0	6.3305E-1	-3.0000E+0	-7.7738E-1	1.2000E+1
6.1000E+1	1.0498E+1	2.7965E+1	3.6668E+1	-5.7881E-1	7.3142E+1	4.0030E-3	3.5419E+1	1.6426E+1	6.7815E-1	1.0000E+0	5.1902E-1	0.0000E+0	6.6717E-1	-1.1000E+1
6.2000E+1	1.2386E+1	2.4988E+1	3.6650E+1	-4.8953E-1	6.4000E+1	1.5832E-2	1.0542E+1	1.8538E+1	7.7247E-1	1.0000E+0	8.5087E-1	-4.0000E+0	5.1963E-1	-7.0000E+0
6.3000E+1	1.0362E+1	3.0591E+1	3.6837E+1	-6.9842E-1	5.6888E+1	8.0297E-3	1.3360E+1	2.7925E+1	7.0872E-1	4.0000E+0	6.6530E-1	0.0000E+0	8.0413E-1	-8.0000E+0
6.4000E+1	9.4828E+0	2.7448E+1	3.6788E+1	-4.9352E-1	5.6888E+1	2.1687E-3	6.1628E+0	1.1949E+1	5.1943E-1	1.0000E+0	5.6857E-1	4.0000E+0	4.9999E-1	1.0000E+0
6.5000E+1	1.0509E+1	2.8054E+1	3.6880E+1	-4.2231E-1	5.6888E+1	2.7619E-3	6.0340E+0	1.8163E+1	7.3776E-1	3.0000E+0	8.2239E-1	-4.0000E+0	6.0339E-1	-1.5000E+1
6.6000E+1	1.1762E+1	2.8170E+1	3.6823E+1	-5.9477E-1	5.6888E+1	3.8965E-3	1.8673E+1	1.7741E+1	6.2271E-1	3.0000E+0	8.2107E-1	0.0000E+0	7.0659E-1	-9.0000E+0
7.0000E+1	1.0863E+1	2.6731E+1	3.6794E+1	-3.3946E-1	5.6888E+1	1.3818E-2	7.4113E+0	1.4472E+1	7.0286E-1	2.0000E+0	8.5854E-1	-2.0000E+0	6.4773E-1	-1.7000E+1
7.3000E+1	1.1095E+1	2.7105E+1	3.6659E+1	-1.0941E+0	6.4000E+1	4.2280E-3	9.1558E+0	2.1880E+1	6.7141E-1	0.0000E+0	6.6773E-1	-6.0000E+0	-4.4392E-1	2.1000E+1